Groundwaters in wet, temperate, mountainous, sulphide-mining districts: delineation of modern fluid flow and predictive modelling for mine closure (Rosebery, Tasmania).

by

Lee R. Evans B.App.Sci.(Hons)

Submitted in fulfilment of the requirements for the degree of Doctor of Philosophy

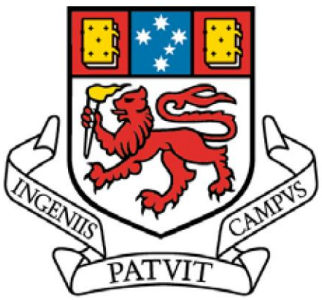

UNIVERSITY OF TASMANIA

September 2009

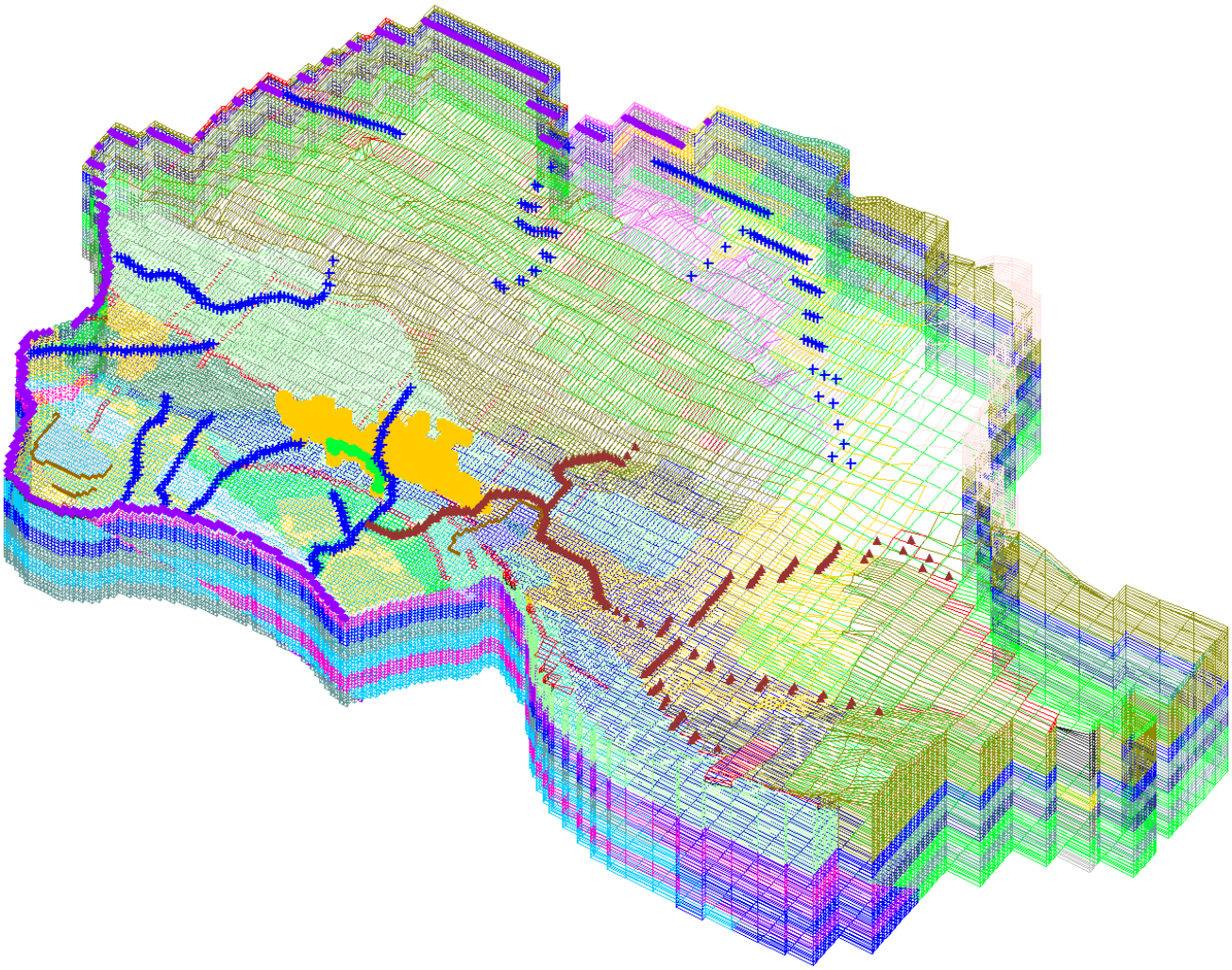

Cover Image: Elevated orthogonal view of the 3D Rosebery groundwater model grid looking towards the northeast.

Declaration

This thesis contains no material that has been accepted for a degree or diploma by the University or any institution, except by way of background information and duly acknowledged in the thesis, and to the best of the candidate's knowledge and beliefs, contains no material previously published or written by another person, except where due acknowledgement is made in the text of the thesis. Three co-authored conference publications written as part of the present study (Evans et al., 2003; Evans et al., 2004a; and Evans et al., 2004b) are provided in Appendix Sixteen.

Lee R. Evans

Date:

This thesis is to be made available for loan or copying in accordance with the *Copyright Act* 1969 from the date this statement was signed.

Lee R. Evans

Date:

Abstract

There are as yet few studies of the hydrogeology of sulphide-mining districts in wet, temperate, mountainous areas of the world. This is despite the importance of understanding the influence of hydrogeology on the evolution and management of environmental issues such as acid mine drainage (AMD). There is a need to determine whether the special climatic and geological features of such districts result in distinct groundwater behaviours and compositions which need to be considered in mining impact studies.

The present study addresses this information gap by broadly delineating the groundwater regime within the temperate Rosebery catchment, western Tasmania, Australia. The mountainous Rosebery catchment contains the large, active, underground, polymetallic Rosebery mine, based on a sulphide deposit hosted in the Cambrian Mount Read Volcanics. Rainfall in the Rosebery region far exceeds evapotranspiration and supports a dense cover of vegetation. The Rosebery groundwater system provides an example of an area in which groundwater management and hydrogeological research is in its infancy, as it is in many regions with similar settings.

Although the area has been glaciated historically, mine data, particularly rock quality designator (RQD) values, provides clear evidence of: (i) a weathering induced increase in permeability within 100 m of the natural ground surface; (ii) an increased permeability associated with shear zones and faults; and (iii) beyond a depth of 100 m, a uniform decrease in permeability with depth below the ground surface. Insights into groundwater flow have been provided by qualitative and quantitative observations of piezometric level in 29 exploration drillholes, 8 piezometers, discharging groundwaters, and surface water flow monitoring points. Together,

piezometric heads, flow rates, and calculated material properties have provided the framework for developing a conceptual model of the groundwater regime within the Rosebery catchment. The groundwater flow system is typified by a deep fractured aquifer (which contain the mine voids), overlain by surficial glacial deposits and weathered material. Significant interaction between surface waters and groundwater was observed throughout the catchment. Geochemistry provided support for conceptual flows and justification of the modelling approaches.

Potential acid-generating and neutralising minerals were identified by examining whole-rock geochemistry. The net acid generation and acid consuming potential of Rosebery materials were quantified. The results indicated that mined materials at Rosebery have the potential to produce a significant volume of acid mine drainage. At the Rosebery mine, metal contaminated waters originate from localised point sources of sulphides, such as tailings dams, waste rock, and mine workings. Waters are contaminated by AMD, resulting in elevated levels of H_2SO_4 as well as the elements Pb, Zn, Cu, Fe, Mn, Mg Cd, Al, and Ca. The Mg content of AMD indicates that neutralisation is occurring, most likely through the dissolution of the hypogene minerals chlorite, ankerite, and dolomite. Although background surface waters and contaminated mine waters are acidic, regionally the groundwaters sampled are near-neutral.

The quantification of the important flows in the conceptual model of the Rosebery catchment allows the construction of a water balance, which provides a reasonable estimation of annual flows. The average precipitation rate across the catchment is estimated at 8.4 m^3/s. The water budget for the Rosebery catchment is: (i) 42% of precipitation runs off to become true surface water flow (including interflow); (ii) 24% of precipitation is lost to evapotranspiration; (iii) 17% of

precipitation becomes groundwater and is discharged as baseflow into creeks and rivers within the catchment; and (iv) 18% remains as groundwater discharging into the regional groundwater system outside of the catchment or into the Pieman River system. The water balance highlights the importance of groundwater in the catchment, with a groundwater to surface water flow rate ratio of 1:1.2. The water balance was applied to three scenarios: (i) a quantification of the contribution of the open pit to underground flows; (ii) the filling of the southern exploration decline; and (iii) the filling of the mine after decommissioning. This work indicated that the open cut makes only a minor contribution to underground water flow and that the mine is expected to fill to a decant point after six years.

A steady-state, 3D numerical groundwater flow MODFLOW model with a geometry representative of the hydrogeologic environment around the Rosebery mine and surrounding catchment was produced. To satisfactorily represent the dual aquifer system, deep fracture flow on a regional scale was represented by a continuum approach to couple with true porous media flow (and shallow fracture flow) in the near surface aquifer. The groundwater model was calibrated to the local observations and water balance to represent the mine whilst in operation. A predictive closure scenario was undertaken using the calibrated model in a non-operational state by eliminating pumping to simulate a flooded mine. Particle tracking was used to plot potential contaminant flow pathways from the mine in the Rosebery catchment. Numerical modelling identified that the potential hydrogeological area of influence of the mine was chiefly controlled by the topography of the host catchment. The topographically-driven western flows off Mount Black are redirected south, primarily by the conduits of the mine workings. Conceptualisation of the groundwater regime improved using computer generated 3D visualisation, and through the numerical

modelling exercise. The numerical modelling suggested that the potential area of discharge for contaminated mine waters is far more limited in extent than was previously believed by mine personnel. This area is limited to: (i) areas along the Stitt River and Rosebery Creeks, which are already experiencing significant acid mine drainage contamination; and (ii) a very limited area south and north of the Pieman River's confluence with the Stitt River. The implications of understanding the area of potential influence are: (i) resources for future monitoring investigations can be focussed in this discrete area; (ii) the scale of future modelling efforts can be restricted to this area, improving detail and limiting computational requirements; and (iii) background monitoring beyond this area can be used to further test the model and provide data for future model calibration and validation.

The present study at Rosebery has wider implications for researching groundwater in wet temperate mountainous sulphide mining terrains. The characteristic feature of such terrains is the local spatial variation in precipitation, evapotranspiration, and therefore recharge. Estimating a representative recharge remains the pivotal quantification for undertaking groundwater investigations in such climates. The significant interaction of surface waters and the groundwater system in wet, temperate, mountainous environments requires modelling to be capable of accounting for this interaction.

Surface water and groundwater interactions present an opportunity to investigate the groundwater regime at the surface and near surface in shallow drillholes. Gauging stream flow for baseflow contribution provides important quantification of groundwater flow where suitable drillhole flow data is scarce, a common state in mined settings. Mine outflows also provide an important quantification of

groundwater flow on a large scale. The present study proposed a method for amalgamating these data which is applicable in other similar environments.

The challenges encountered in the present study provide insight into planning for similar mining projects. Prior to the present study, there was no general knowledge of the groundwater patterns of the region, and no clear idea of whether the Rosebery mine had an influence on the regional groundwater regime. There was no historical information of the type that is usually associated with groundwater resource investigations, and the nature of exploration drillholes meant that some typical groundwater research methodologies were not practical at Rosebery. This resulted in the investigation taking a different research approach compared to that typically used for groundwater evaluation in, for instance, agricultural districts.

Although the present study attempted to endure without standard hydrogeological data, there remains a significant gap in the reliabilty of the modelling. This is a situation that faces most mines nearing closure, when cash flow is likely to be reduced. Time-series piezometric levels, and a larger hydraulic property dataset were the key gaps identified in the present study. Appropriate budgeting for the acquisition of such information should be considered a priority for groundwater investigations of wet, temperate, sulphide-mining districts elsewhere.

Acknowledgements

Firstly I'd like to thank Hannah my wife for all the support and getting me to the end of this. Thanks also to Jack for sitting at my feet and listening to my frustrations for the last few years.

Thanks to all of my peers at UTAS who collectively helped keep an element of sanity in the process. Special thanks to Moose, Stace, Roman, Kieren, Toast, Nik, Kate, Al and of course Gregois. Thanks also to Bec for introducing me to the botanical world.

Thanks must go to my supervisor Garry Davidson for sticking with this work against all odds. Thanks Gaz for all the support and encouragement over all these years, I appreciate it mate. Thanks must also go to David Cooke for his assistance on the geochemical aspects of the work.

The present study was undertaken with the support of an Australian Research Council, strategic partnerships with industry research and training, collaborative research agreement between the University of Tasmania and Pasminco Australia Limited. Thanks to environmental staff, Leon Staude and Greg Doherty, at Pasminco for supporting the project. Special thanks also must go to Andrew McNeill and Craig Archer at Pasminco Exploration, as well as, Charles Carne, Rob Willis, Bronwyn Turner, Cam Graves, Sarah Berg and Peter Edwards at Pasminco Rosebery mine.

Thanks also to all those who provided hydrogeology advice, amongst others: Tammy Weaver; Sarah Tweed; Jed Youngs; Lindsay Campbell; and Neil Milligan. Thanks also go to Mineral Resources Tasmania for providing geochemical analysis of the second round of regional groundwaters and end members. For access to time series data I'd also like to thank Holly Taylor and Mike Connarty at Hydro Tasmania and the Bureau of Meteorology.

Table of Contents

Chapter 1 Introduction

Chapter 2

Chapter 3 Aquifer Observations and Characteristics

4 Acid Mine Drainage and Hydrogeochemistry

5 Conceptual and Mathematical Water Balance and Mine-filling Models

6 Numerical Groundwater Flow Modelling

7 Summary, Synthesis of Conclusions and Recommendations

Index of Figures

Index of Tables

Index of Digital Appendices

Index of Files in Digital Appendices

"We must measure what can be measured, and make measurable what cannot be measured" (Galileo Galilei, 1610).

1 Introduction

1.1 Preamble

Mining activities always impact the environment in some way (Vartanyan 1989; Eggert 1994; Ripley et al., 1996; Lottermosser et al., 1999; Bell et al., 2000; Gabler and Schnieder 2000; Marszalek and Wasik, 2000; and Baba, 2002). Mining results in landscape modification including changes in topography and the introduction of voids. Such changes may result in adverse modification of local hydrogeologic conditions and groundwater flow regimes (Bell et al., 2000; Shevenell, 2000; Baba, 2002; and Hair, 2003). This is a problem of ever increasing significance because the mining industry is striving to reduce its environmental impact and improve its water management procedures, particularly with regards to mine closure (McHaina, 2001; and Hair, 2003). Preparing for mine closure throughout the life of a mine, and understanding the environmental consequences of mine-affected groundwater, are essential factors for minimising the environmental impact of the industry (McHaina, 2001). The Rosebery mine is addressing this with such studies as the present thesis and provides an example for studying relationships between mines and their hydrogeological environments.

Rosebery is a polymetallic (Zn-Pb-Cu-Ag-Au) underground mine situated in the wet, temperate, mountainous, sulphide-mining district of western of Tasmania, Australia (Figure 1.1). The Rosebery mine has been in operation for over one hundred years (Zinifex Limited, 2004). Environmental management practices at the mine site have evolved over time (Pasminco Limited, 2003) and the mine is planning for closure well before decommissioning to ensure that present and future environmental responsibilities are met (*ibid*.). Acid mine drainage (AMD) and

groundwater management has been recognised as an important environmental management focus for the Rosebery mine (Davidson et al., 2000; Hale, 2001; and Carnie 2003).

There has been little research into the long-term effects of mining operations on groundwater systems in the sulphide-mining district of western Tasmania. This is in contrast to mainland Australia where the impact of mining operations on groundwater systems has been a prime consideration (e.g., RUST PPK, 1994; Berry and Armstrong, 1995; Woodward-Clyde, 1995; BHP, 1996; Dundon, 2000; HDMS, 2000; HDMS, 2001; Brown, 2003; Hair, 2003; Johnson and Cormander, 2003; Johnson and Wright, 2003; and Milligan et al., 2003).

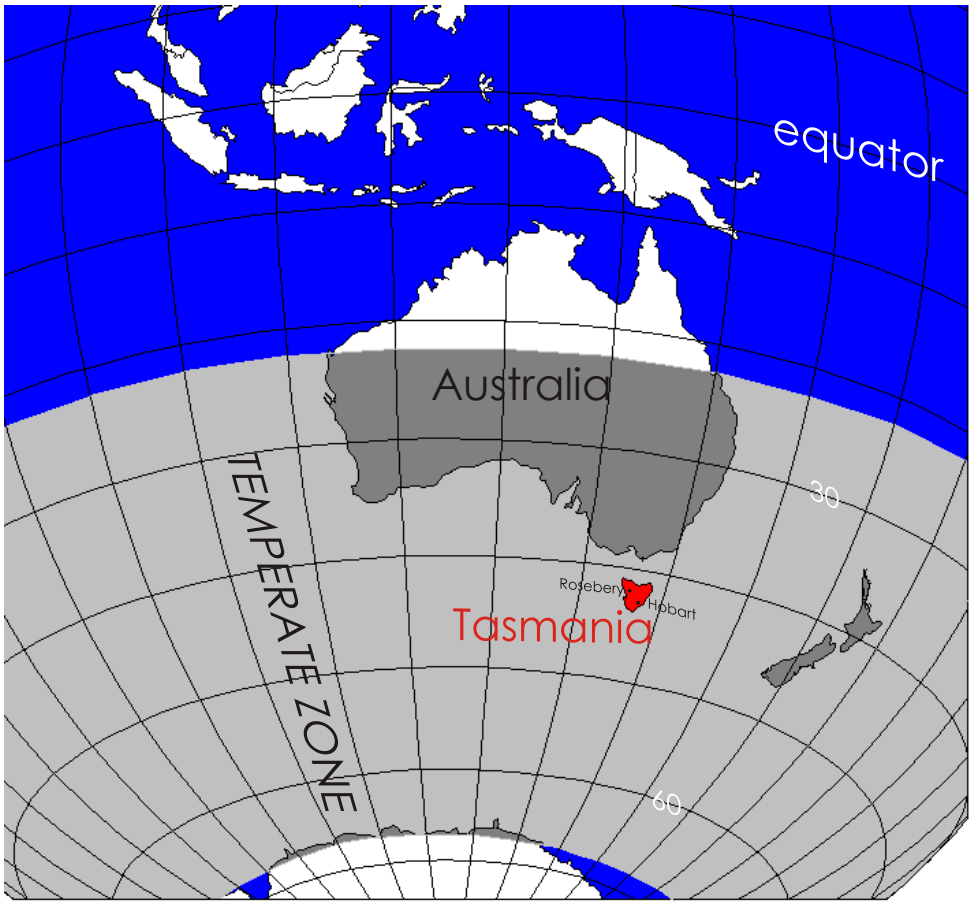

Figure 1.1 Study area location with the southern hemisphere temperate zone (shaded grey), latitude and longitude displayed as a 10 degree grid

1.2 Aims

The principal aims of this PhD study were to: (i) determine the modern existing hydrogeological flow field at and around the Rosebery mine; (ii) assess the impact of AMD on the geochemistry of waters in the Rosebery catchment; (iii) characterise the types and chemical signatures of waters within the Rosebery catchment; (iv) develop a numerical groundwater flow model consistent with the existing conditions; (v) use the numerical model to predict groundwater flow following cessation of mining; and (vi) extrapolate the study findings to outline the challenges and benefits in monitoring and modelling sub-surface fluid behaviour in other wet, temperate, mountainous, sulphide-mining environments.

1.3 Definitions

A „Wet' region, for the purpose of the present study is defined as a region where precipitation exceeds evaporation. Rosebery has a high average annual rainfall receiving over double the rain that it annually loses to evapotranspiration; greater than 2000 mm rainfall and less than 1000 mm evapotranspiration (BOM, 2002).

„Temperate' is a climatic term for the regions between the tropics and polar circles, i.e., the latitudes of 23.5°S to 66.5°S and 23.5°N to 66.5°N. Rosebery (Figure 1.1) is located at 41°47′S inside the temperate region of the Southern Hemisphere.

„Mountainous', for the purpose of the present study, is defined as any area containing large contrasts in relief. The catchment in which Rosebery is contained has relief varying over 1000 m vertically, in less than 1500 m laterally.

In the present study, „sulphide-mining district' are defined as districts in which mining sulphides as the principal ore material including, for example, gold districts hosted within sulphides, but not mining districts containing sulphides as gangue such as coal deposits.

„Acid mine drainage' (AMD) is a natural phenomenon caused by the weathering of sulphide minerals in wet, oxygenated conditions (Stumm and Morgan, 1970, and Lett et al., 1996). Mining severely accelerates this phenomenon by exposing large quantities of sulphide rock and mine waste to the atmosphere (e.g., Gabr et al., 1994; Banks et al., 1997; Bell and Bullock, 1996; and Paulson and Balistrieri, 1999). When sulphides are exposed to oxygen and water they may oxidise rapidly and produce acidic solutions laden with trace metals (e.g., Singer and Stumm, 1970; Nordstrom et al., 1979; and Langmuir, 1997). These solutions can enter surface water and groundwater with potentially damaging environmental effects (e.g., Younger, 1994; Gray, 1997; Stapinsky et al., 1997; and Bell, 2004).

A „Model' is defined as a simplified representation of a real system or process (Hassan, 2003). Three model types are included in the present study: (i) conceptual, the qualitative study of the processes in the system, (ii) mathematical, the quantitative study of the water balance, and (iii) numerical, the computer generated representation of the system. All computer packages used in the present study are referenced in Appendix Four.

„Closure' is defined as "a process which begins during the prefeasibility of a project, and continues through operations to lease relinquishment. It sets clear objectives and guidelines, makes financial provision and establishes effective stakeholder engagement leading to successful relinquishment of lease" (MCA, 2000). Closure is an ongoing process and should not be confused with either: (i) mine decommissioning, which occurs at the cessation of operations; or (ii) relinquishment, which occurs post decommissioning and closure (*ibid*.).

1.4 Environmental Management

Mining companies and government regulatory bodies, driven by the general public, stakeholders, non-government organisations, and more recently shareholders, are placing an ever increasing expectation for improvement of environmental management within the mining industry (EPA, 1995; Kidd, 1997; Donavon and Rose, 2001; McHaina, 2001; and Milnes, 2002). Environmental management and mine closure are now routinely incorporated into the economic and engineering planning of mining projects (Morin and Hutt, 1997; McHaina, 2001; and Rio Tinto, 2007). Although environmental management and mine closure covers many disciplines, the management of AMD and groundwater are the focus of the present study.

1.4.1 Acid mine drainage

The largest and most costly environmental management issue within the mining industry is the management of AMD (e.g., Evangelou, 1995; Dold and Fontbote, 2002; Harris et al., 2003; and Lottermoser, 2003). For example, in Canada, the AMD liability is estimated to be between C$2 billion and C$5 billion (Feasby and Tremblay, 1995). The industry has recognised that significant financial, social and environmental benefits can be gained by incorporating the management of AMD into mine planning, development and operation (Robertson, 1999).

Groundwater has long been recognised as a major contaminant pathway for AMD in sulphide mining districts (e.g., Klusman and Edwards, 1977; and Stapinsky et al., 1997). In mining operations below natural water table levels, there are almost always interactions between mining operations, groundwater and surface waters (Milnes, 2002). Understanding these interactions and their influence on the environment has been recognised as an area requiring further research (Davidson et al., 2000).

AMD management research has received a significant amount of attention in the sulphide mining district of western Tasmania (e.g., Chilcott et al., 1991; Koehnken,

1992; Ladiges, 1995; Renison, 1995; ABM, 1996; EGI, 1996; Giudici et al., 1996; Lawrence, 1996; Miedecke, 1996; PRM, 1996; ABM, 1997; Environment Australia, 1997; HGM, 1997; Koehnken, 1997; Parr, 1997; CMT, 1998; Dellar, 1998; Meskanen, 1998; Oosting, 1998; SEMF, 1998a and 1998b; PRM, 1998; Smith, 1998; Taylor, 1998; East, 1999; ESPL, 1999; WMRL, 1999 and 2000; Hale, 2001; Thompson, 2001; Gurung, 2002, Miedecke, 2002; Carnie, 2003; Gilbert et al., 2003; Gurung, 2003; and Wallace, 2002). Much of this work, however, has concentrated on surface water flows, with little work on groundwater interaction and mine closure.

Gurung (2002 and 2003) summarised the extent of AMD management research in Tasmania and concluded that, along with further surface water investigation, more extensive groundwater sampling and analysis needed to be carried out. Gurung (2003) found that, due to the State's steep topography and high rainfall, the risk to water quality in the receiving environments is significant. Gurung (2003) also determined that base metal mineralised host rocks in the western Tasmanian mining district were "dominantly potential acid forming types and therefore the majority of abandoned mines are acid producers". Gurung's (2003) work attributed the high incidence of AMD in the western Tasmanian catchments to: (i) high sulphide content of the ore rocks; (ii) restricted availability of neutralising materials; (iii) the mountainous physical setting; and (iv) wet climate.

1.4.2 Groundwater management

Much of the groundwater management in Australia has concentrated on water supply resource studies for population centres (e.g., Appleyard, 1995; Cox et al., 1996; Merrick, 1997; and Tweed et al., 2005) and agricultural regions (e.g., Punthakey et al., 1995; Cook et al., 2004; Hillier et al., 2003; and Khan et al., 2004). Recently groundwater management in these agricultural regions has also incorporated

studies of salinity management requirements (e.g., Bradd et al., 1997; GABCC, 2002; Dawes et al., 2004; Doble et al., 2004; and Cartwright and Weaver, 2005) and groundwater dependent ecosystems (e.g., Hatton and Evans, 1998; SKM, 2001; and NGC, 2004), thus broadening and refining the groundwater knowledge base.

In arid and semi-arid mining districts, groundwater is commonly an essential water source for mining and processing operations (e.g., Berry and Armstrong, 1995; Dundon, 2000; Roache, 2002; Brown, 2003; Gilbert and Fenton, 2003; Hair, 2003; and Johnson and Commander, 2003), as well as refrigeration (Pulles, 1992). The wider community also use these same groundwater resources for agriculture and potable water supply (e.g., Banks et al., 1997; Gallagher and Hair, 2003; Hillier et al., 2003). These combined factors have resulted in historical groundwater resource development and research (e.g., Milligan et al., 2003). Unlike these areas, very little hydrogeological information exists in mountainous terrains. Kahn et al. (2008) attributes the problem of the general lack of water table elevations and aquifer parameters in the mountainous settings, to the lack of wells in these environments.

Scanlon (1990) stated that "groundwater in many ways is an unknown resource" in Tasmania, attributing this to: (i) the lack of investment in a resource that is otherwise free; (ii) the perception of abundance from seasonal rainwater; and (iii) the subsurface, concealed nature of groundwater. Mineral Resources Tasmania (MRT) maintain the Groundwater Quality and Borehole Database, BORIS, which contains information on groundwater research and water bores throughout Tasmania (MRT, 2002d). MRT's Geographical Information System (GIS) based website (MRT, 2002e) demonstrated that hydrogeological evaluation in Tasmania has been concentrated on the water supply reserves of the agricultural regions and population centres (Figure 1.2) and is vital to the economy of many of these settlements and

industries (Stevenson, 1982). Reporting in these areas is relatively comprehensive (e.g., Blake, 1939; Mathews, 1983; Moore, 1977; Nye, 1921; Leaman, 1971; Ezzy, 1999; Ezzy and Latinovic 2005; and Ezzy, 2006). In comparison, very few hydrogeological investigations have been undertaken in the sulphide mining district of western Tasmania (MRT, 2002f; Ezzy and Latinovic 2005; and Ezzy, 2006).

Gurung (2002) determined that Tasmanian groundwater data in general has been primarily from bores drilled on agricultural or urban lands and are therefore unsuitable for the purpose of AMD investigation. It is well recognised there is only limited information available on: (i) groundwater quality and quantity; (ii) the hydrogeological properties associated with groundwater; and (iii) groundwater use in Tasmania (RPDC, 2003). This limited data available is recognised to be restrictive to the accuracy of all aspects of the groundwater data compiled for assessment in Tasmania (NLWRA, 2001; and RPDC, 2003).

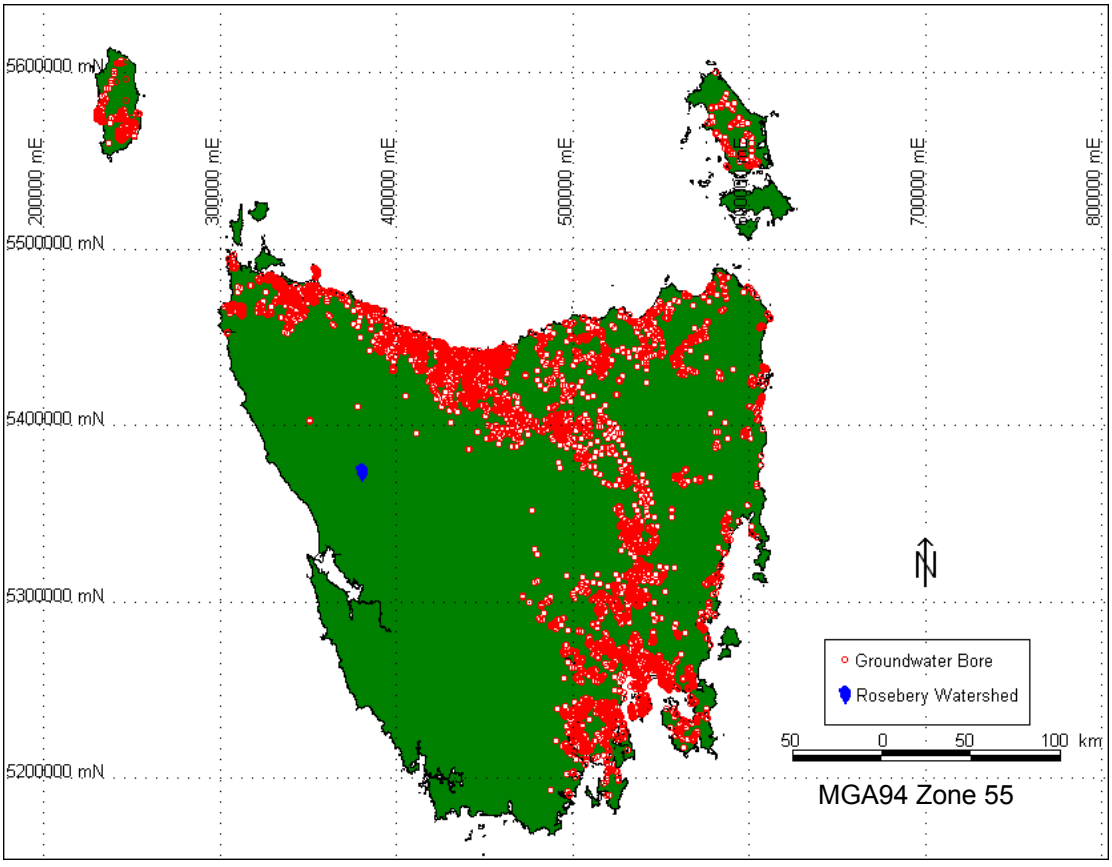

Figure 1.2 Distribution of groundwater monitoring bores in Tasmania (after MRT, 2002e)

1.4.3 Predictive modelling

Environmental management in the mining industry requires an understanding of both: (i) the processes that will occur during the operational phase; and (ii) those that will occur as a legacy well beyond the life of mine (McHaina, 2001). Predictive modelling can be used as a tool for testing and quantifying hypotheses to improve management decisions, which can result in substantial cost savings (Middlemis, 1997). Kidd (1997) stated that predictive modelling is increasingly being required at the project planning stage of mining projects (e.g., BHP, 1996; HDMS, 2000; and HDMS, 2001); as well as throughout operations and closure stages of mining projects (Johnson and Wright, 2003).

Historical examples and research in geochemical modelling provided information on the potential for AMD of reactions to occur, and their likely longevity (e.g., Perkins et al., 1995; Wood et al., 1999; Donovan et al., 2003; and Skousen et al., 2003). With much research previously undertaken on the geochemical modelling of AMD generation, this project focused on modelling the physical transport and fate of AMD-affected waters in the Rosebery groundwater system.

The Rosebery groundwater system provided an example of an area where groundwater management is in its infancy. Prior to the present study there was no general knowledge of the groundwater patterns of the region (Hale, 2001). There was also no clear idea of whether the Rosebery mine has an influence on the regional groundwater regime (*ibid*.). The present study has sought to address these issues, however, without the historical information usually associated with resource investigations, and the impracticality of some typical groundwater research methodologies (for instance large scale multiple well pumping tests and single well packer tests), the investigation required a different research approach compared to those typically used in agricultural and populated areas of Australia. Other setting

related factors also provided challenges to a conventional modelling approach. These included the dramatic topography of western Tasmania and the densely vegetated areas of the catchment which constricted access. The high rainfall and low evaporation also meant that traditional calculations developed for arid and semi-arid environments (e.g., Scanlon et al., 2002) are less definitive in the wet environment.

1.5 Thesis Structure

The first chapter introduces the project, provides some key definitions, and outlines the significance of the study. The chapter also identifies the aims of the study.

Chapter Two defines the study area bounds and limits of the catchment containing the surrounding sub-catchments influencing the local groundwater regime. It provides the background on the Rosebery mine, as well as the geology, vegetation, climate and hydrology of the catchment.

The third chapter describes the field observations and aquifer characteristics. It also introduces a new concept in the analysis of mine geotechnical data as input for hydrogeological modelling.

The geochemistry of acid mine drainage is the focus of the fourth chapter. It examines both new and existing data on the chemistry of local waters and rocks within the study area.

A water balance and the important environmental factors affecting the local system are presented in Chapter Five. A mathematical model created from local data outlines the water budgets for the important factors of the total water balance. A mathematical model to describe the mine filling is also presented in this chapter.

The design, construction and calibration of the numerical models are presented in Chapter Six. This chapter discusses the collection of physical data and their use in the

numerical models to represent the hydrogeological system. Chapter Six also discusses the simulation of the numerical model and generation of particle flow paths representing an area of influence of the Rosebery mine.

The final chapter draws the conclusions together, places the results in a global context, and makes recommendations based on the project's findings.

The appendices are provided in a digital format on a DVD contained in the final sleeve of the bound thesis. The motivation to produce digital appendices was that the data and models contained within the appendices are not in a format that can be readily displayed in print form without impractical volumes of appendices. The hope that the data and models presented will be further used is an additional motivation for the appendices to remain digital, in the most useful format for such information.

"Rosebery: a tale of despair" (Blainey, 1954).

2 Physical Setting

2.1 Study Area

The focal point of the study was the Rosebery mine in the sulphide-mining district of wet, temperate western Tasmania. The study area covered a *c.* 89 square kilometre catchment within the Pieman River catchment, ranging from 375000mE to 386000mE and 5365000mN to 5380000mN in Zone 55 of the 1994 map grid of Australian (MGA) (red area in Figure 2.1). Rosebery is located 305 km, by road, north-west of Hobart (Insert on Figure 2.1).

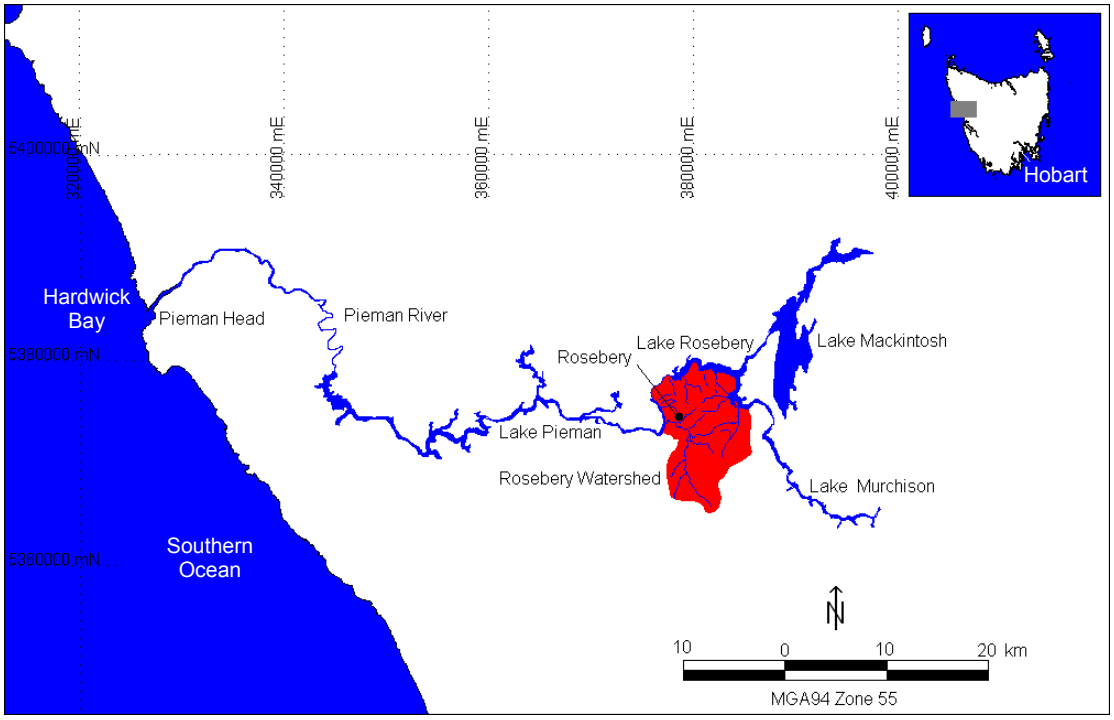

Figure 2.1 Study area location map

2.2 The Rosebery Mine

2.2.1 Resource/reserves

The total resource at Rosebery in 2006 was 34.0 Mt @ 13.8 % Zn, 4.1 % Pb, 0.57 % Cu, 143 g/t Ag, and 2.2 g/t Au (Zinifex Limited, 2006). The estimated economic reserves in 2007 were 3.8 Mt @ 11.9 % Zn, 3.2 % Pb, 0.36 % Cu, 115 g/t Ag and 1.7 g/t Au (Zinifex Limited, 2007) with current production at 0.7-0.8 Mt/year. The mine

life of the Rosebery mine is predicted to 2011, however, the orebody was not closed off and exploration has been ongoing, with the aim of increasing the estimated mine life to at least 2013 (Zinifex Limited, 2004) and potentially to 2021 (Zinifex Limited, 2005).

2.2.2 Mining method

Production at Rosebery occurs by underground bench and open stoping, and cut and fill mining methods. Historically, alimak stoping and open pit mining methods have also been used at Rosebery. Since 2003, ore is trucked to a surface ore handling facility and concentrator via a decline. Prior to the decline, the mine utilised a combination of shaft and rail based locomotion for ore handling. There were more than 25 kilometres of accessible drives underground reaching a depth of approximately 1600 metres below the surface ingress (PRM, 2003a) (Figure 2.2).

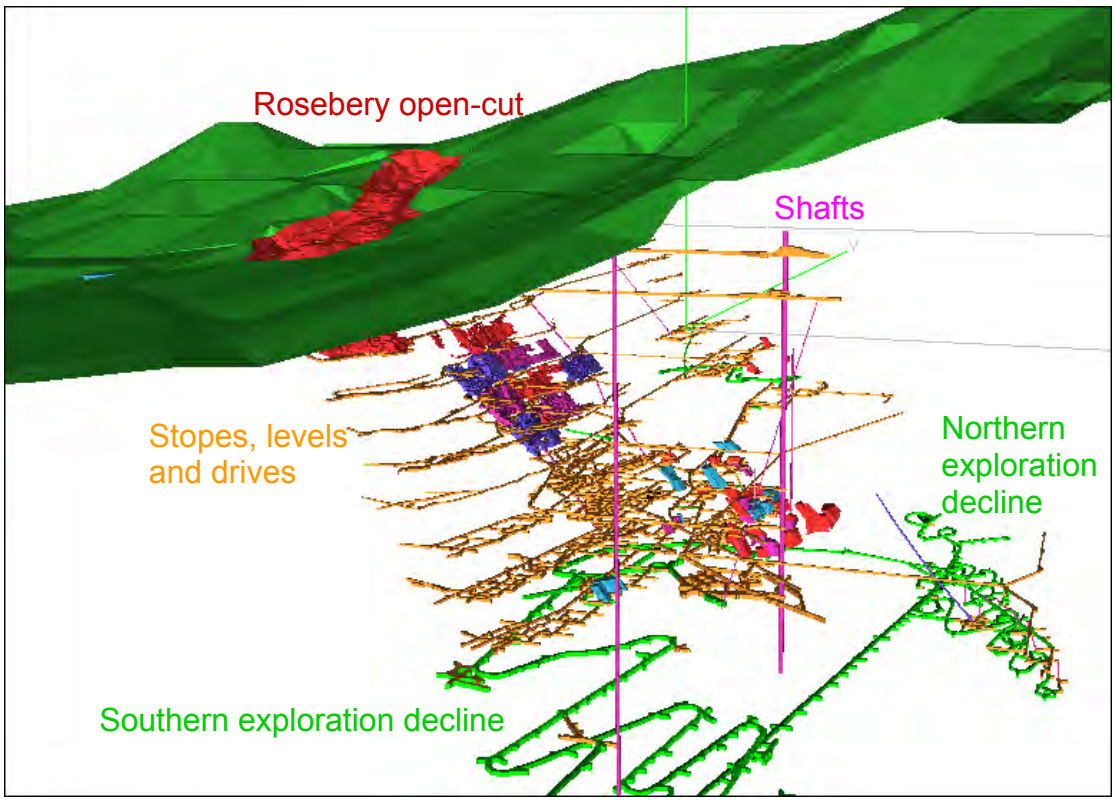

Figure 2.2 Example oblique view (not to scale) of the Rosebery Datamine mine void model looking north-west showing the open pit, shafts, declines, stopes, levels and dives (after PRM, 2003a)

2.2.3 Mine features

The mine features influencing water flow, and potentially AMD, include: (i) the extensive network of underground workings - declines, level development (drives), vertical development (shafts), partially filled stopes; (ii) the open cut void (Figure 2.2, Figure 2.3); (iii) a waste dump, with a storage capacity of 4.3 Mt, located in the Assay Creek valley above the mill and office site (Thompson and Brett, 1998); (iv) three decommissioned tailings dams *c.* 2 km to the south (no.s 1, 2 and 5); and (v) the operational tailings facility, situated on the Bobadil Plain *c.* 1 km to the north-west (Figure 2.3). In total, 7 Mt of tailings are contained in these dams (Atkins, 1998). Field investigations undertaken in the present study also identified that roads and landfill in the townships of Primrose and Rosebery (Figure 2.3) contain sulphide-bearing crushed rock from the mine, and as a result many point sources of potentially acid producing rock are located beyond the confines of the mine area.

2.2.4 Mining history

The history of the Rosebery deposit was reviewed by Kostoglou (2000) using historical reports (e.g., Harcourt Smith, 1898; Waller, 1902; Loftus Hills, 1915; and Finucane, 1932). The discovery of the Rosebery ore body was credited to Cecil Thomas McDonald who traced alluvial gold and sulphide boulders to the Rosebery gossan in 1893 (Kostoglou, 2000).

Since discovery, the orebody was mined intermittently by several companies including the Tasmanian Mining Company, Primrose Mining Company, Tasmanian Metals Extraction Company (TME), Electrolytic Zinc Company of Australia (EZ), Pasminco Rosebery Mining (PRM), and from April 2004, Zinifex Limited (Blainey, 1954; and Kostoglou, 2000). In September 2001, during the initiation of this research, Pasminco Limited, thus Pasminco Rosebery mine, went into voluntary administration. Zinifex Limited acquired the assets of Pasminco Limited in 2004 and

is currently the owner/operator of the Rosebery mine (Zinifex Limited, 2004). With this acquisition came the legacy of environmental responsibility and closure at the Rosebery mine (Zinifex Limited, 2004). In July 2008, Zinifex Limited became OZ Minerals after a merger with Oxiana Limited (OZ Minerals, 2008).

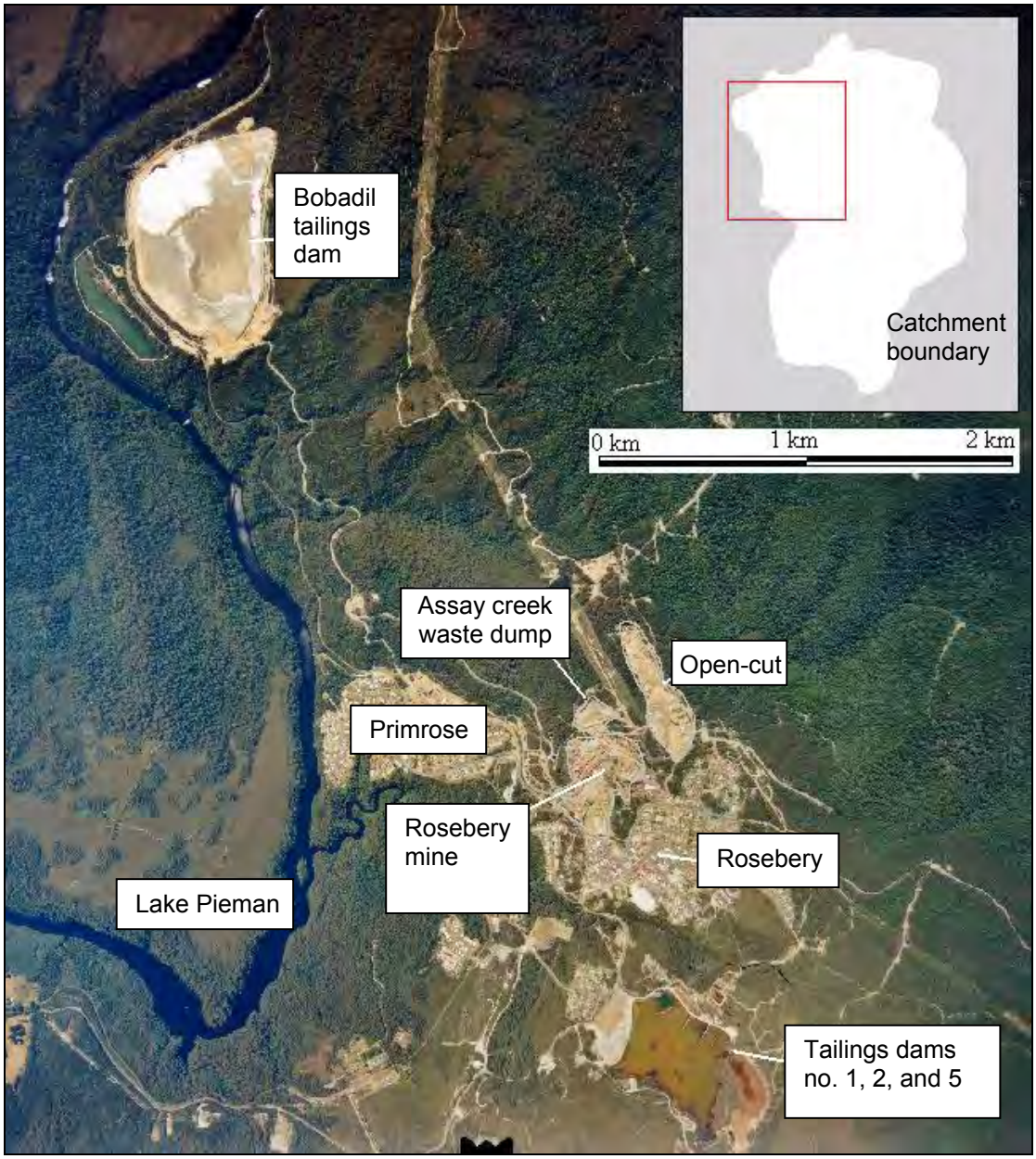

Figure 2.3 Town and mine features; open cut, waste dump and tailings dams (after Evans et al., 2004; aerial photograph provided by Pasminco, 2003)

2.2.5 Regional mining

Gurung (2002) classified 681 sites throughout Tasmania as sulphide mines. Of these, fourteen relatively small abandoned mines and prospects were found within the

study area catchment (Figure 2.4), and many more within the sulphide mining district of western Tasmania. The majority of metallic ore deposits of the sulphide mining district of western Tasmania can be divided into three broad classifications: (i) volcanic-hosted massive sulphide deposits, for example, Que River, Rosebery, Chester, and Mount Lyell; (ii) carbonate replacement tin deposits, such as, Mount Bischoff, Renison Bell, Queen Hill at Zeehan and Cleveland (Solomon, 1981; Reid and Meares, 1981; and Khin Zaw, 1991); and (iii) vein and replacement style, for example, Sterling Valley, Comstock lode Zeehan (Davidson, pers. comm., 2006).

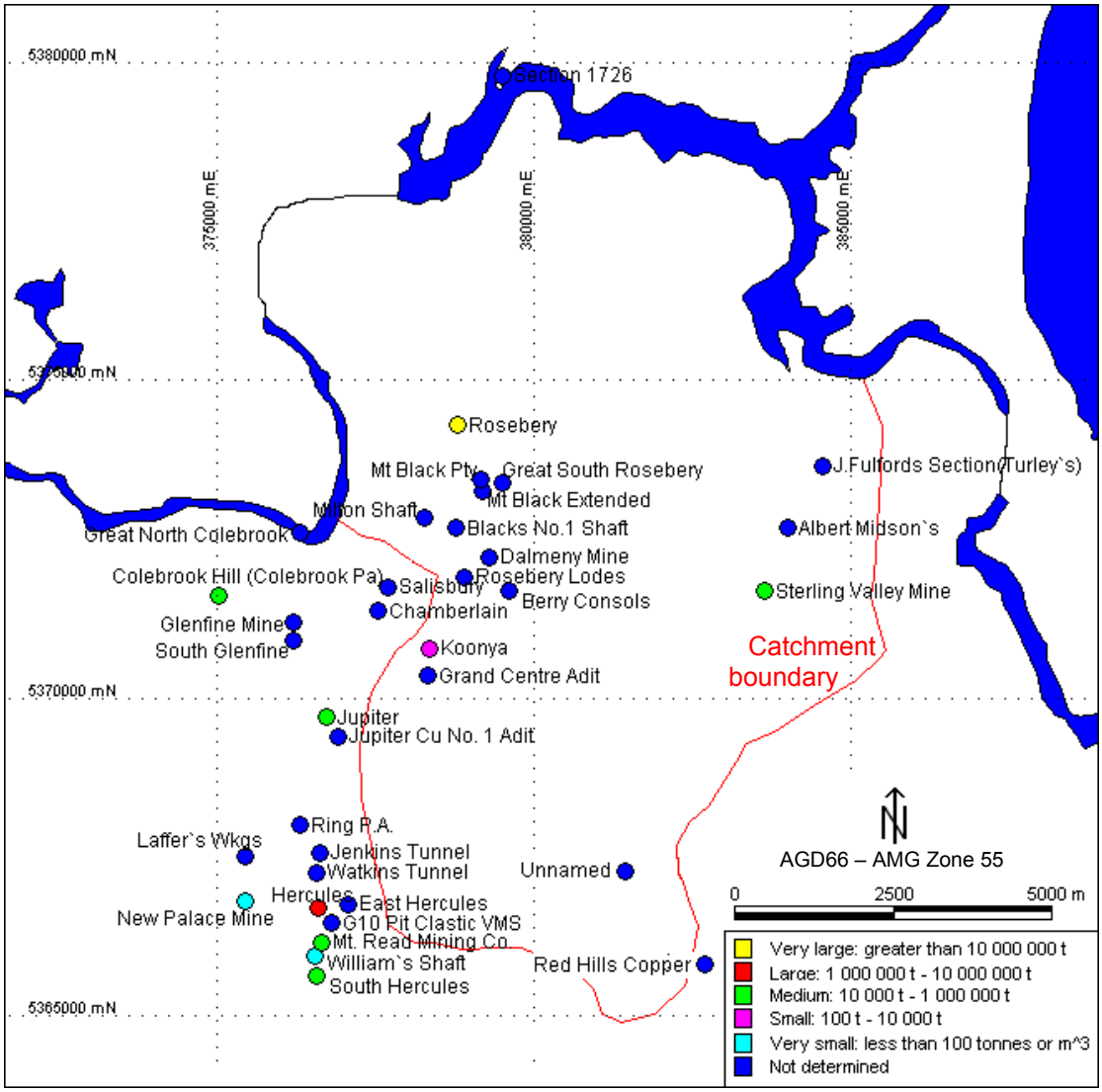

Figure 2.4 Historical mines and prospects in the study area (after MRT, 2002a)

2.3 Geology

2.3.1 Regional geology

The regional geology of western Tasmania consists primarily of the volcano-sedimentary sequences of the Dundas Trough and Mount Read Volcanics placed between two Precambrian blocks (Khin Zaw, 1991): (i) the Precambrian Tyennan Region to the east; and (ii) the Precambrian Rocky Cape Region to the northwest (Insert on Figure 2.5). The Mount Read Volcanics, which dominate the bedrock geology of the study area (Figure 2.5), were deposited along the eastern margin of the Late Proterozoic to Cambrian deposits of the Dundas Trough (Corbett and Lees, 1987; and Corbett et al., 1989).

The geology of the study area catchment is represented as a generalised schematic in Figure 2.6. Glacial and fluvioglacial deposits of Pleistocene-Holocene age overlie bedrock in much of the low-lying areas of the Stitt, Sterling and Pieman Valleys (Corbett and McNeill, 1986). The Rosebery deposit is hosted within the Middle Cambrian Central Volcanic Complex (CVC), an element of the Mount Read Volcanics (Campania and King, 1963; Corbett, 2002b; Corbett, 2004; and Martin, 2004). Gifkins (2001) divided the CVC at Rosebery into four formations: (i) the Hercules Pumice Formation; (ii) the Kershaw Pumice Formation; (iii) the Mount Black Formation; and (iv) the Sterling Valley Formation. The Mount Read Volcanics in the Rosebery area also include correlates of the Tyndall Group, Eastern Quartz-Phyric Sequence, and Western volcano-sedimentary sequence (Corbett, 2002b).

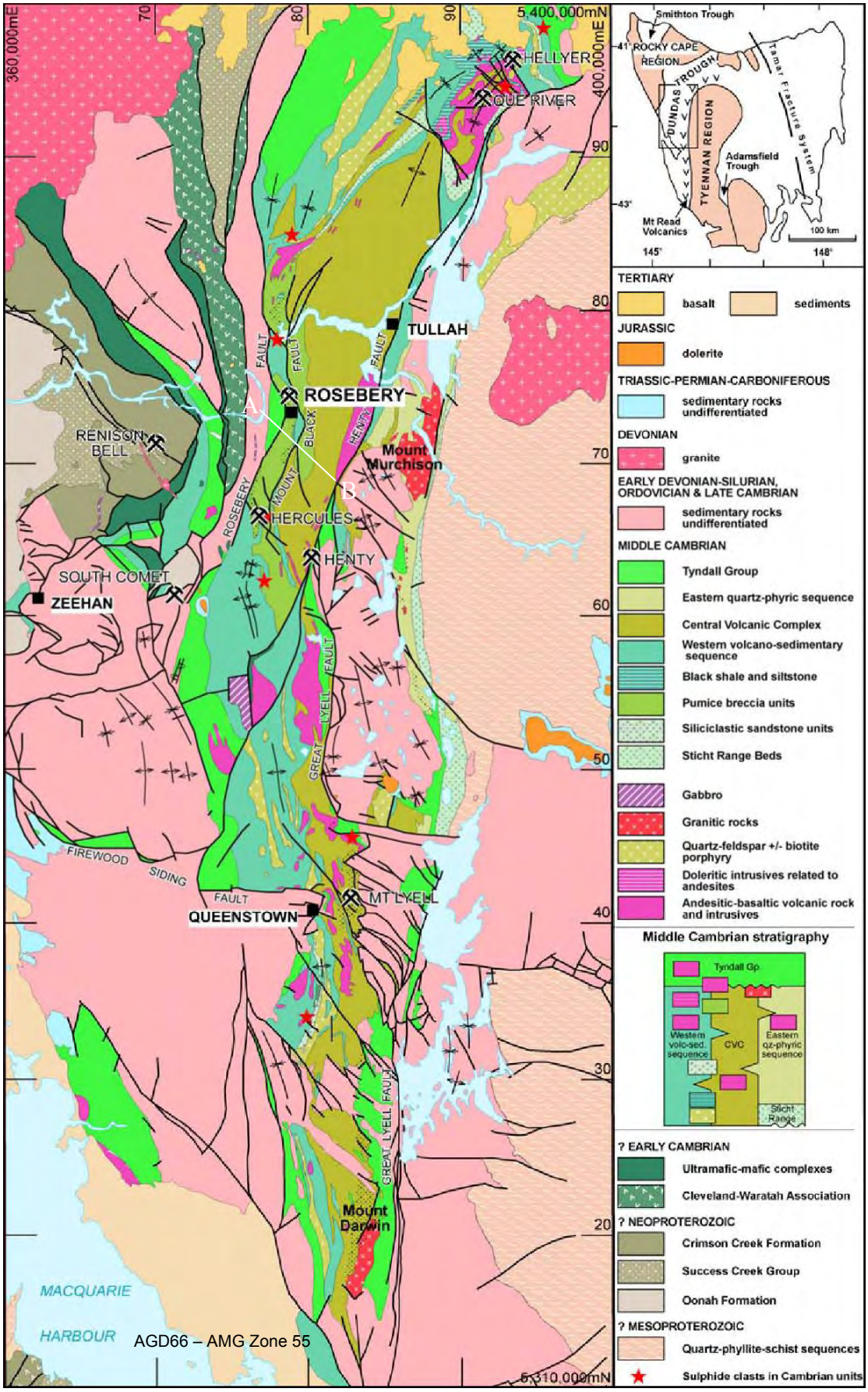

Figure 2.5 Bedrock Geology of the central Mount Read Volcanics (from: Martin, 2004; and after Corbett, 2002a)

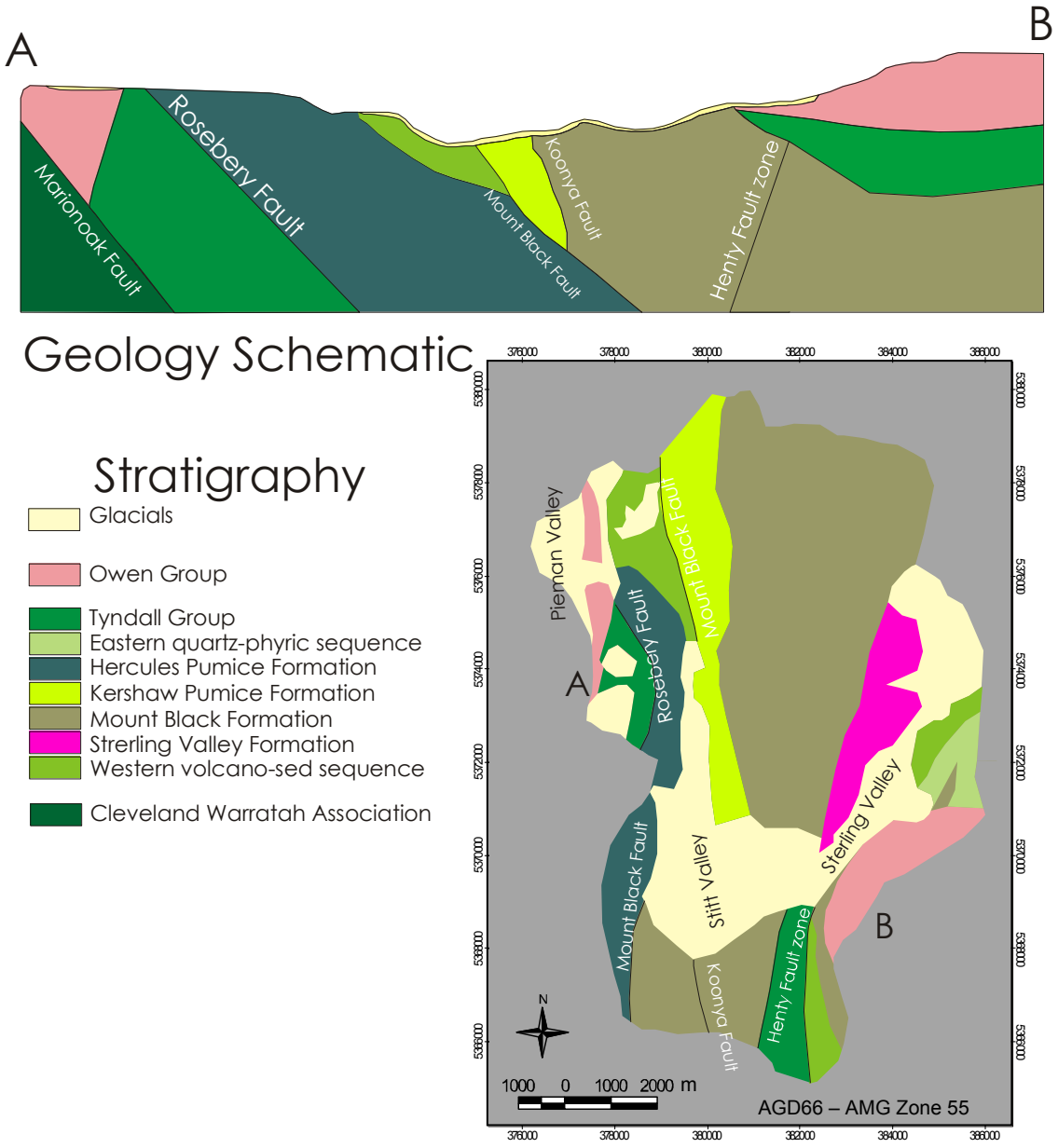

Figure 2.6 Stratigraphy, generalised geological schematic, and layer one model input of the surface geology (simplified after: Corbett and McNeill, 1986; Gifkins, 2001; Corbett, 2002a; and Martin, 2004)

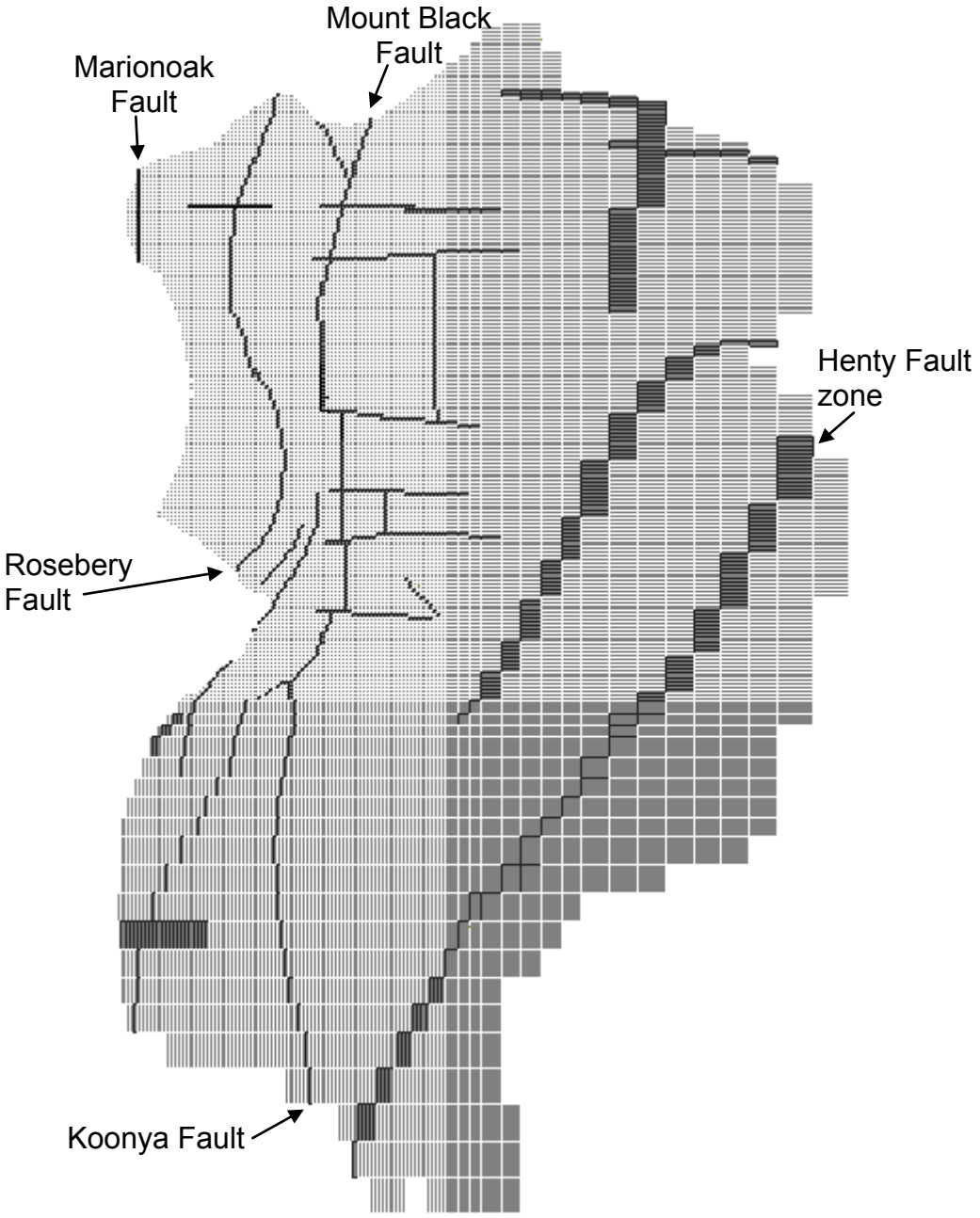

Figure 2.7 Example of layer two hydrogeological model faults in black (after: Corbett and McNeill, 1986; Gifkins, 2001; Corbett, 2002a; and Martin, 2004)

2.3.2 Structural features

The major structural features in the area include: (i) the sub-parallel northerly striking, easterly dipping major thrust faults, being the Marionoak, Rosebery, and Mount Black Faults (Figure 2.6; Figure 2.7); and (ii) the N to NE trending westerly dipping Henty Fault zone and an associated un-named NE trending normal fault in the Sterling Valley (Corbett and Lees, 1987; Berry, 1993; Pasminco Exploration et al.,

2002, Gifkins, 2001; Figure 2.5; and Figure 2.7). The Koonya Fault and a splay off the Mount Black Fault cross cut the northerly striking and easterly dipping structures at acute angles (Figure 2.6; and Figure 2.7). Several east-west striking faults offset the Rosebery and Mount Black faults (Berry, 1993; and Gifkins, 2001). Martin (2004) also recognised post-Devonian brittle faults up to 2 m thick in the Rosebery area.

Berry (1993) and Martin (2004) considered that there was no evidence to suggest that the Rosebery or Mount Black faults were Cambrian structures, although, there is evidence that the Henty Fault zone was active in the Cambrian. Berry (1993) suggested that the geometry of the fault structures requires a 50% shortening of the Mount Read Volcanics due to their reactivation in the Devonian.

Hydrothermal fluids associated with reactivation of faults in the Devonian have resulted in significant silicification and the creation of several quartz vein-associated base metal deposits (Corbett and Lees, 1987). In other hydrogeological settings, faults containing gouge fill and extensive silicification are commonly considered to act as effective hydrologic barriers (e.g., Rojstaczer, 1987; Andersen and Woessner, 1992; Allen and Michel, 1999; and Bense and Person, 2006), however, in the Rosebery area such fault zones, and associated shearing, fracturing and cleavage, resulted in an observed higher effective permeability than the surrounding crystalline rock mass.

The Rosebery Fault contains a 1 m thick gouge-filled zone, and a surrounding zone (ten's of metres thick), of strongly developed slaty cleavage (Corbett and Lees, 1987; and Gifkins, 2001). Corbett and Lees (1987) identified the Rosebery Fault in outcrop north of the Pieman River. Here, the Rosebery Fault and associated fracture zones were observed in the present study to act as conduits for modern day fluid flow

(Figure 2.8). In drilling around the Rosebery mine, the Rosebery Fault has been observed to be a zone of <10 m of increased cleavage and alteration around a narrow 1-2 m thick quartz–tourmaline zone, with thin pyritic intervals (PRM, 2003b; and McNeill, pers. comm., 2006).

The Mount Black Fault is a <1-10 m zone of intense shearing, brecciation, veining and silicification (PRM, 2003b; and McNeill, pers. comm., 2006). The Henty Fault zone is an extensive deformation zone up to 1 km wide (Corbett and Lees, 1987) comprising intensely broken, sheared quartz-veined rock within a strong zone of silicification (Gifkins, 2001). The extent of deformation in the Henty Fault zone is quite variable, from intense to weak (McNeill, pers. comm., 2006).

All faults in the area are likely to have a higher hydraulic conductivity associated to them than that of the surrounding crystalline rock mass (*ibid*.). The observation of central silification and surrounding damage indicates that fluids are likely to partition into the damage zone, rather than the central zone of displacement.

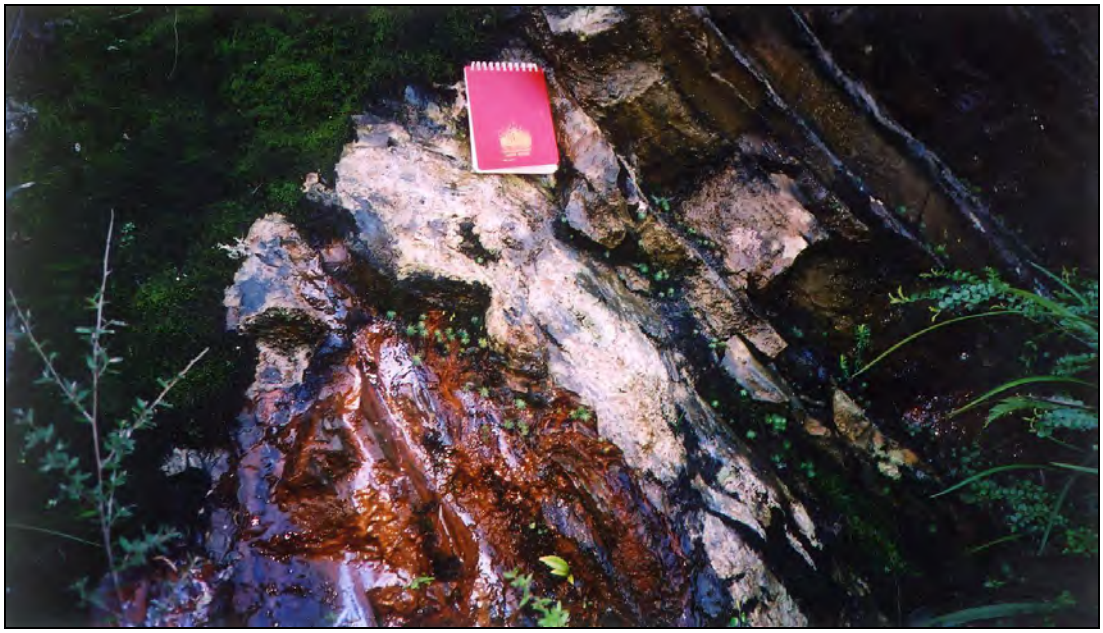

Figure 2.8 Rosebery Fault in outcrop north of the Pieman River downstream of the Bastyan Dam at 377600, 5378640 (AMG 94, Zone 55) showing preferential fluid flow presenting as a spring parallel to the fault plane dipping at *c.* 45º to the east, A6 notepad for scale

2.3.3 Rock unit descriptions

Classification and nomenclature of the mine sequence at Rosebery has varied and developed with ongoing research and increased understanding (e.g., Hall et al., 1965; Braithwaite, 1972; Sainty, 1986; Berry et al., 1998; Gifkins, 2001; Corbett, 2002b; and Corbett, 2004). The present study uses nomenclature consistent with that of Corbett (2004).

From a hydrogeological perspective, it must be noted that all rock nomenclature refers to the relic rock type at deposition prior to diagenesis, deformation, metamorphism and metasomatism. Rock nomenclature, at Rosebery and in this thesis, is therefore not necessarily a description of the present form of the rock mass, particularly from a hydrogeological perspective. This qualification is important as, for example, the unsuspecting hydrogeologist reading this thesis might wrongly assume that pumice, sandstone or tuff could be highly permeable due to primary porosity. Other than the Pleistocene to Recent glacials, all units have been extensively altered and metamorphosed (Pwa et al., 1992; Khin Zaw, 1991; Green, 1983; Berry et al., 1998; and Gifkins, 2001) resulting in a crystalline rock mass which appeared to have little or no effective primary porosity in the unweathered state.

Preferential weathering of relic pumice clasts was observed at surface, with signs of porosity re-developing. This appeared to be limited to the upper regolith zone, within < 5 m of the surface. In addition, in many areas of the study area, the regolith zone is poorly developed and earlier (pre-Quaternary) regolith appears to have been removed by recent glaciation. The rock units of the study area are described below in some detail.

2.3.3.1 Cleveland/Waratah Association

The Cleveland-Waratah Association comprises quartzose feldspathic greywacke, pillowed basalt, mafic intrusives, red-brown shale and bedded chert (Williams 1989;

and Turner and Bottrill, 2001). The Cleveland-Waratah Association does not appear as outcrop within the study area, however, a mafic greywacke sequence of the Cleveland-Waratah Association outcrops on Colebrook Hill *c.* 4 km west of the study area (Corbett, 2002b). Using a 3D geological model (Pasminco Exploration et al., 2002) the Cleveland-Waratah Association is interpreted to occur at depth in west of the model domain.

2.3.3.2 Central Volcanic Complex

The Hercules Pumice Formation of the CVC contains both: (i) the transitional stratified volcaniclastics (hereafter referred to as the „host rocks'); and (ii) the footwall volcanics (hereafter referred to as „footwall').

The host and footwall material are the most extensively studied materials in the area (e.g., Braithwaite, 1969 and 1972; Green et al., 1981; Green, 1983; Naschwitz, 1985; Corbett and Lees, 1987; Green, 1990; Lees et al., 1990; Khin Zaw, 1991; Pwa et al., 1992; and Martin, 2004). Gifkins and Allen (2001) described the footwall as a massive to weakly graded, feldspar-phyric pumice breccia. The footwall contains massive and disseminated ore at its top (*ibid*.). The footwall alteration zone also contains minor carbonate, tourmaline, pyrite and chalcopyrite (Green et al., 1981) as well as carbonate, and sericite, replacement of plagioclase phenocrysts in footwall rocks (Green, 1983).

The host-rock of the Rosebery deposit comprises: (i) transitional stratified volcaniclastics (interbedded crystal-lithic sandstone, siltstone and black mudstone); (ii) quartz-feldspar-biotite-phyric dacite sills; (iii) pumice breccia and sandstone; and (iv) massive sulphide mineralisation (Gifkins and Allen, 2001). Pwa et al. (1992) described the host-rock as containing disseminated pyrite, and being commonly siliceous, sericitic and chloritic; it is normally overlain by pyritic black slate. Martin

(2004) stated that the "majority of the gangue material in the sulphide ore comprises sericite, quartz, carbonate, barite, chlorite and minor rutile" and went on to say "that in ore affected by Devonian metasomatism, there may also be tourmaline, magnetite, haematite, garnet, fluorite and helvite present".

The Kershaw Pumice Formation comprises primarily pumice breccia, pumice-rich sandstone and shard rich siltstone (Gifkins, 2001). The Kershaw Pumice Formation conformably overlies the Mount Black Formation above the Mount Black Fault (McNeill, pers. comm., 2006).

The Mount Black Formation is dominated by dacitic lava overlain by rhyolitic lavas, pumice breccia, shard-rich sandstone and siltstone, pumiceous breccia, and crystal-rich sandstone (Gifkins and Allen, 2001). Pwa et al. (1992) describe the Mount Black Volcanics as mainly composed of weakly sericitised and chloritised dacitic to andesitic lavas. In the mine area they are in fault contact (Mount Black fault) with the host rocks and to the east, they conformably overlie the Sterling Valley Formation (Gifkins and Allen, 2001).

The Sterling Valley Formation is composed of andesitic to basaltic lavas and volcaniclastics units (Gifkins and Allen, 2001). The Sterling Valley Volcanics are exposed in only a few exploration holes due to their distal location relative to the Rosebery Deposit. The Sterling Valley Volcanics outcrop along the Murchison Highway and a small section of the upper Stitt River (Gifkins, 2001).

2.3.3.3 Western volcano-sedimentary sequence

The Western volcano-sedimentary sequence is comprised primarily of interbedded tuffaceous mass flow deposits, turbiditic sandstone, shard-rich tuffaceous mudstone, micaceous siltstone and graphitic black shale (Martin, 2004). The Western volcano-sedimentary sequence is taken to include the Farrell slates, and the White Spur

Formation (Martin, 2004). The White Spur Formation includes both the Hangingwall Volcaniclastics (hereafter referred to as the 'hangingwall') and what is referred to locally as the „black slate' (a graphitic black shale). The hangingwall rocks are classified as sericitic quartz-feldspar-phyric epiclastic rocks (Corbett and Lees, 1987; Lees et al., 1990).

2.3.3.4 Tyndall Group

The Tyndall Group is composed primarily of crystal rich sandstone, volcanic breccia and volcanic conglomerate (Corbett and McNeill, 1986; and White and McPhie, 1996). The youngest part of the Mount Read Volcanic sequence (Corbett and McNeill, 1986), the Tyndall Group is conformably overlain by the Owen Group within the study area (Martin, 2004). The Tyndall Group outcrops in both: (i) the area down gradient of the mine; and (ii) at the southern extremity of the catchment (Figure 2.6).

2.3.3.5 Owen Group

The Owen Group outcrops in both the east and west of the catchment. The western Owen, the Stitt Quartzite, is composed mostly of massive quartzite and shale (McNeill, pers. comm., 2006). The eastern Owen is composed of terrestrial to shallow marine siltstone, conglomerate and sandstone (*ibid*.). In the east of the study area the Owen group meta-sediments outcrop as the dramatic 500 m high cliffs tht form the drainage divide at Mount Murchison on the West Coast Range (Figure 2.9).

2.3.3.6 Murchison Granite

The Cambrian Murchison Granite is an intrusive feature outcropping as close as *c.* 500 m to the east of the study area. Further-a-field is the Devonian granite pluton of Granite Tor, *c.* 8 km north east of Mount Murchison. The Murchison Granite varies from diorite to granite in composition (Polya et al., 1986). As the granites were

strictly beyond the catchment boundary, they were excluded from the hydrogeological model.

Figure 2.9 Mount Murchison. Looking north-west at the outcropping Owen Group; for scale, the tarn in the foreground is at an elevation of 750 m and the peak of Mount Murchison, slightly out of shot, is at 1275 m

2.3.3.7 Glacial deposits

The extent of the glacial deposits across the study area was mapped by Corbett and McNeil (1986). Glacials were observed in the present study to vary in composition from relatively impervious clays of fluvioglacial and lacustrine deposits to what appear to be extremely highly conductive moraine deposits. The glacial deposits are presently best observed in the Rosebery open-cut, rail and road cuttings, and on the Bobadil plain. Observation of drilling and excavations in the tailings dam areas also provided significant insight into the varied nature of the glacial deposits, as did the excellent review of local glacial material at the TME smelter site by East (1999). Although impervious clays are abundant, their lateral extent was observed to be limited. The resulting preferential flow which can be observed in cuttings around

clay layers translates to high flow rates and bulk permeability within the glacial units relative to the fractured rock bedrock.

2.3.4 Rosebery mine stratigraphy

The Rosebery mine stratigraphy does not strictly conform to the classification of Corbett (2004). Table 2.1 summarises the correlation between the STRAT code classification, used in the geological logging of core at the Rosebery mine, and the classification scheme proposed by Corbett (2004).

Mine unit	STRAT code	Stratigraphy (Corbett, 2004)
Fill	FI	N/A
No core	NC	N/A
Fluvial glacials	FG	Glacials
Shear zones	S	N/A
Faults	F	N/A
Chamberlain shale	CS	Western volcano-sed sequence
Black shale	BS	Western volcano-sed sequence
Dundas Group	DG	Western volcano-sed sequence
Natone Volcanics	NV	Western volcano-sed sequence
Hangingwall	HW	Western volcano-sed sequence
Footwall	FW	Hercules Pumice Formation
Mount Black Volcanics	MB	Mount Black Formation
Vein	V	N/A
Host	HO	Hercules Pumice Formation
Transition zone	TZ	Hercules Pumice Formation
Porphyry	PO	Hercules Pumice Formation

Table 2.1 Rosebery mine stratigraphy

2.3.5 Glacial history

The glacial history of the West Coast Range is reflected in its current physiography. Southeast of Rosebery (*c.* 7 km), is the topographic high of Mount Murchison on the West Coast Range, at 1275 m. The jagged cliff faces of Queens Head on Mount Murchison, which appear to have originated as headwalls to hanging glaciers, contrast with the rounded hills and mountains at lower altitude (Figure 2.10). Mount Read at 1124 m, Mount Black at 929 m, Mount Sale at 521 m and Karlsons Knob at 416 m, all have the same distinctive, glacially derived, Roche Moutonnee form (Ward, 1909).

Figure 2.10 'Queens Head' on Mount Murchison from Lake Murchison looking south-west

Figure 2.11 Deeply grooved and chatter marked roche moutonnee exposed at Bastyan Dam site (Augustinus, 1982)

Quaternary glacial ice was thought to have extended back from Rosebery to the Central Plateau and Tyndall Range (Sansom, 1978). Evidence for glaciation, such as striations and chatter marks on bedrock, are clearly visible (Augustinus, 1982). An excellent example is seen in Augustinus' (1982) photograph of the Bastyan Dam

cutting reproduced in Figure 2.11. Such erosive action lead to the removal of much of the regolith from the West Coast Range, resulting in the typically shallow weathering profile observed today in the study area. Shallow weathering profiles observed in the wet, temperate, mountainous environment of western Tasmania contrast with the deep weathering profiles which have developed on much of the Australian continent.

North of Mount Black, the Tullarbardine ice lobe (containing Boco and Bulgobac ice) joined up with Pieman ice lobe (Figure 2.12) resulting in the glacial deposits of the Bobadil Plain (Augustinus, 1982). The Pieman River and former Pieman Glacier path forms the natural topographic low in the study area. Augustinus (1982) stated that unlike its major tributaries, which follow rock strike, this channel was carved independently of structure by glacial action. The present day Pieman River does, however, appear to be structurally controlled by bedrock lineaments, at least locally in the study area. A section of the river is parallel in an arcuate bend with the major fault structures, from the Bobadil Plain to the confluence with the Stitt River and historical ice flows of the Murchison and West Coast Range (Figure 2.5 and Figure 2.12).

Figure 2.12 demonstrates that the glacial deposits found in Snake Gully, and a significant moraine in the south of the study area, indicate that the Murchison ice flowed west to the south of Mount Black over the Sterling Saddle to join the large body of ice that flowed from the West Coast Range over the Moxon Saddle (Augustinus and Colhoun, 1986).

2.3.6 Orebody formation

Genetic models of the Rosebery deposit have developed over a century of mining and research (e.g., Harcourt and Smith, 1898; Twelvetrees, 1901; Waller, 1902; Loftus Hills, 1915; Finucane, 1932; Stillwell, 1934; Hall et al., 1953; Hall and

Figure 2.12 Glacial flow paths over the study area (partially after Augustinus and Colhoun 1986; background image after Google Earth, 2006)

Solomon, 1962; Braithwaite 1969 and 1972; Solomon and Walsh, 1979; Green et al., 1981; Eldridge et al., 1983; Green, 1983; Campbell et al., 1984; McDougall, 1984; Montgomery, 1985; Sainty 1986; Huston, 1988; Huston and Large, 1989; Solomon et al., 1990; Aerden, 1990, 1991, 1992 and 1994; Allen, 1992 and 1993; Large 1992; Solomon and Groves, 1994; and Martin, 2004). Martin (2004) summarised the evidence proposed in these studies, and his own work, concluding that: (i) primary ore formation occurred beneath the Cambrian sea floor; and (ii) the deformation, metamorphism and metasomatism observed at Rosebery was related to the Cambrian

Delamarian Orogeny and Devonian Tabberabberan Orogeny, along with the intrusion of post-tectonic Devonian to Carboniferous granites.

2.3.7 General hydrogeological classification

Simplification and broad grouping of detailed geological units may be required for hydrogeological modelling investigations (Middlemis, 2000). No hydrogeological classification groupings have been proposed by previous studies in the Rosebery area. The geology described in the present study is a simplification of the detailed geological interpretation resulting from extensive previous research (e.g., Stillwell, 1934; Lees et al., 1990; Green et al., 1981; Khin Zaw, 1991; Selley, 1997; Berry et al., 1998; Gifkins, 2001; and Martin, 2004), combined with a significant drill hole database (PRM, 2003b), and a digital 3D model of the Mount Read Volcanics (Pasminco Exploration et al., 2002), and mine geological data (PRM, 2003c).

The simplest hydrogeological classification of the Rosebery system consisted of two units: (i) unconsolidated material overlying; (ii) consolidated bedrock. The final 3D hydrogeological model, however, required further categorisation to account for variation in hydraulic properties within these materials. Hydrogeological classification of geological units, at this scale, was broadly based on the current stratigraphy of Corbett (2004). The geologic units were simplified for use during the process of modelling and areas of high conductivity and artificial conduits were included. The hydrogeological units included: (i) mine workings; (ii) drilling conduits (of varying connectivity); (iii) mine waste; (iv) glacials; (v) faults (varying with depth); and (vi) the consolidated geological units (varying with depth).

2.4 Climate

The rainfall and weather stations considered to represent the study area were in the townships of Rosebery and Tullah, along with a weather station at the summit of

Mount Read (BOM, 2008). Mount Read had current standard weather station information (rainfall; dew point; wind speed; and barometric pressure), and rainfall was collected at Rosebery and Tullah (BOM, 2008). Covering different periods, data from all four stations at Rosebery was treated collectively, as were data from the three stations at Tullah (Table 2.2).

Station name	Latitude	Longitude
Rosebery	-41.7667	145.5333
Rosebery (Gepp Street)	-41.7847	145.5372
Rosebery (HEC substation)	-41.7772	145.5381
Rosebery Station	-41.7903	145.5244
Tullah	-41.7333	145.6167
Tullah (Meridith Street)	-41.7369	145.6122
Tullah Mine Site	-41.7167	145.6333
Mount Read	-41.8444	145.5419
Mount Read (Mount Lyell M.&R.)	-41.9	145.55

Tabl

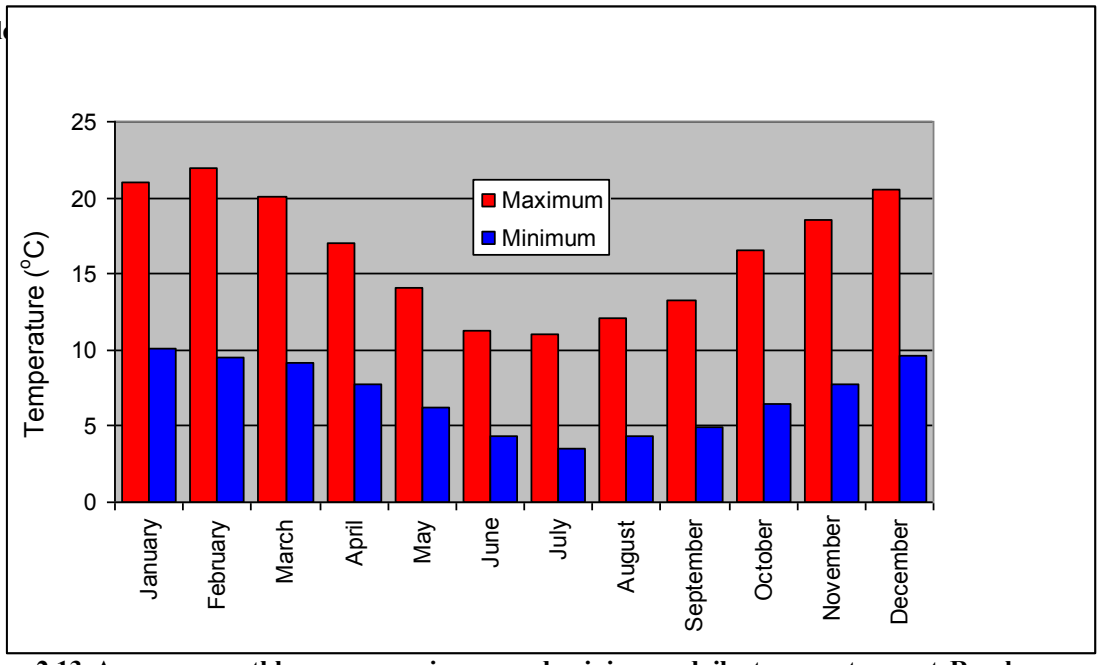

Figure 2.13 Average monthly mean maximum and minimum daily temperatures at Rosebery (after BOM, 2004)

2.4.1 Temperature

The mean monthly minimum temperatures at Rosebery have a range of 3.5-10.1°C and mean monthly maximum temperatures have a range of 11-21.9 °C (BOM, 2004; and Figure 2.13). This can be used as a rough guide to temperatures at higher

elevations using the broad principle that every one hundred metres gained in elevation equates to a loss in one degree Celsius (Tasmap, 1986a).

2.4.2 Precipitation

The interaction of airstream and topography is the main factor governing rainfall in Tasmania (ABS, 2004). Tullah, elevation of 167 m, has an average annual rainfall of 2035 mm based on data recorded from 1968 (BOM, 2002). Rosebery had a similar average annual rainfall to Tullah, 2128 mm based on readings from 1960 (BOM, 2002). The Rosebery mine adits and workings were located near the rainfall stations at an elevation of 165 m. Due to the surrounding rugged terrain, climatic conditions vary considerably with topography, so that rainfall data from Rosebery was not considered representative of much of the study area. The Mount Read weather station at 1119.5 m (i.e., the top of the Stitt River catchment) was used here to gain an insight into the climate change with altitude. The average yearly rainfall for Mt Read is 3723 mm (BOM, 2002), which is *c*. 80% more than the rainfall *c*. 1000 m below (Figure 2.14).

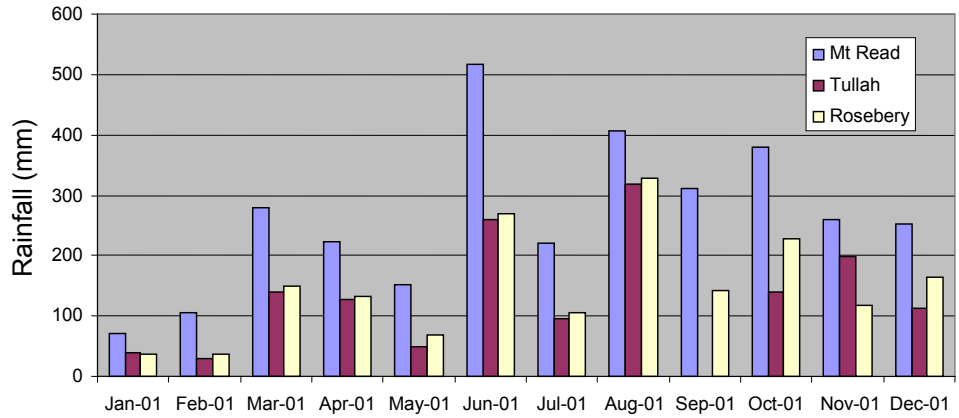

Figure 2.14 Example monthly (2001) rainfall for Tullah, Rosebery and Mount Read (BOM, 2002)

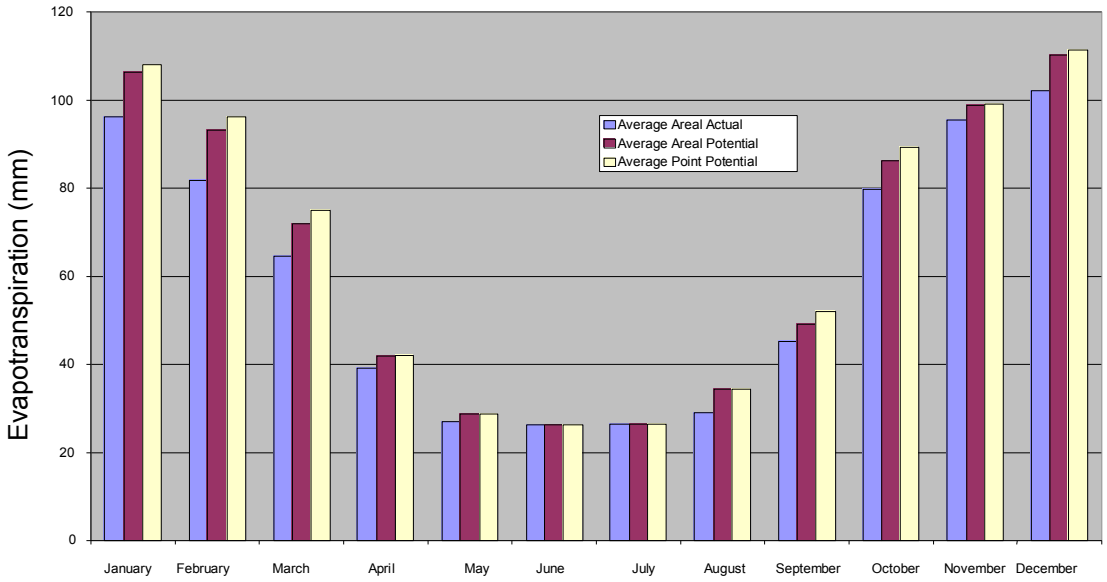

Figure 2.15 Example mean monthly evapotranspiration (mm) at 145.5E 41.7S (after BOM, 2002)

2.4.3 Evapotranspiration

Mean monthly and mean annual evapotranspiration (ET) data at a resolution of 0.1 degrees (latitude/longitude) was provided by BOM (2002) (e.g., Figure 2.15). These mean data are based on the standard 30 year period 1961-1990 (BOM, 2002; and Wang et al., 2002). Three ET values were given: (i) Areal Actual ET; (ii) Areal Potential ET; and (iii) Point Potential ET. Areal Actual ET is defined as the ET that actually takes place, under the condition of existing water supply, from an area so large that the effects of any upwind boundary transitions are negligible and local variations are integrated to an areal average (*ibid*.). The term „areal potential ET' is synonymous with Morton's (1983) „wet-environment ET'. Areal potential ET, is the ET that would take place, under the condition of unlimited water supply, from an area so large that the effects of any upwind boundary transitions are negligible and local variations are integrated to an areal average (BOM, 2002; and Wang et al., 2002). The term „point potential ET' is synonymous with Morton's (1983) „potential ET'. Point potential ET is the ET that would take place, under the condition of unlimited

water supply, from an area so small that the local ET effects do not alter local air mass properties (BOM, 2002).

2.5 Vegetation

Very little catchment scale research on evapotranspiration has been undertaken in Tasmania (Leaman, 2004) and classifying the spatial distribution of vegetation types was considered important in understanding the potential variation in evapotranspiration and therefore groundwater recharge over the study area. As part of the present study, a floral survey was conducted by the author with reference to existing mapping (Tasmap, 1986a; Tasmap, 1986b; Tasmap, 1986c; Tasmap, 1986d; and DPIWE, 2005) and Tasmanian vegetation field guides (e.g., Banks and Kirkpatrick, 1977; Kirkpatrick and Backhouse, 1981; Cameron, 1996; Kirkpatrick, 1997; and Kirkpatrick and Backhouse, 2004). The vegetation types used in the present study were: (i) montane vegetation; (ii) temperate rainforest; (iii) wet sclerophyll; (iv) closed scrub; and (v) sedgeland.

The upper slopes of Mount Murchison (*c.* >900 m) were sparsely vegetated, supporting montane vegetation, including *Athrotaxis selaginoides* (King Billy, King William pine) and *Nothofagus gunnii* (Tanglefoot, Deciduous beech), or no macro-plants at all where steep cliffs and talus slopes provided little or no soil cover. High run-off co-efficients and low evapotranspiration would be expected from such terrain.

In contrast the much lower summit of Mount Black had a low dense rainforest flora, becoming less stunted with a drop in elevation of 100 m. This temperate rainforest contained; *Athrotaxis selaginoides*, *A. cupressoides* (Pencil Pine), *Richea pandanifolia* (Pandani), *Coprosma nitida* (Mountain Currant Bush), *Leptospermum scoparium* (Manuka), *Nothofagus cunninghammii* (Myrtle), *Cyathodes parvifolia* (Mountain Berry), *Anopterus glandulosa* (Native Laurel), *Atherosperma moschatum*

(Sassafras), *Phyllocladus aspleniifolius* (Celery Top Pine), *Gautheria hispida* (Snow Berry), *Cenarrhenes nitida* (Native Plum), *Billardiera longiflora* (Mountain Blue Berry) and *Oleria phlogopappa* (Daisy Bush). Such dense vegetation would be expected to result in large interception of rainfall and evapotranspiration.

At lower elevations the vegetation graded into wet sclerophyll forest containing, at different locations, *Eucalyptus nitida* (Smithton Pepermint) or *E. Obliqua* (Stringybark, Brown-top, Messmate) or *E. delegatesis.* Other species included; *Eucryphia lucida* (Leatherwood), *Acacia mucronata* (Narrow-leaved wattle), *Melaleuca squarrose* (Swamp Melaleuca), *Bauera rubiodes* (Bauera), *Epacris impressa* (Common Heath), *Banksia marginata* (Honeysuckle), and *Gahnia grandis* (Cutting Grass).

The closed scrub, primarily in areas surrounding the mine workings, comprised; *Leptospermum scoparium, L. langinerum* (Woolly Tea Tree), *Phebalium Squameum* (Satinwood), *Acacia melanoxylon* (Blackwood), *A. mucronata, Eucalyptus nitida* and *Anodopetalum biglandulosm* (Horizontal Scrub).

The low-lying areas in Snake Gully (south east of the Rosebery township) and the Pieman Valley have regions of sedgeland dominated by *Gymnoschoenus spaerocephalus* (Button Grass). They also contained; *Melaleuca squarrose* (Scented paper-bark, *Spengelia incarnata* (Pink Swamp Heath), *Leptospermum scoparium* (Manuka), *L. lanigerum* (Wooly tea tree), *Banksia marginate* (Honeysuckle), *Eucalyptus nitida, Restio* spp., *Gleichenia alpina* (Alpine coral-fern), *Epacris impressa*, *E. obtusifolia, E. lanuginosa* (Swamp Heath), *Acacia melanoxylon, Baeckea gunniana* (Alpine baecka), *Allocasurina verticillata* (She Oak) and *Micrantheum hexabdrum.*

Fire is thought to have played a major role in shaping the vegetation over the study area (Banks and Kirkpatrick, 1977). Repeated firing of Tasmanian vegetation has resulted in patchy vegetation on acid peats and skeletal soils (Reid et al., 1988). Other major factors observed include altitude, aspect, variations in geology and soil cover. Variation in vegetation indicate that aspect was important at Rosebery due to rain shadow on northern and eastern faces of land features, and lower level of sunlight on southern faces.

Soil cover was observed in the open pit, in test pits, as well as rail, road and track cuttings. Soils varied significantly over the study area and were grouped into three broad categories: (i) poorly developed thin covers of down-slope transported soil in steep terrain; (ii) clay rich soils of glacial origin; and (iii) organic rich soils or peats developed on montane and sedgeland vegetation. Peats were also observed to occur in the low lying areas in the Rosebery catchment. Acid peats occur in Tasmania from the high mountains and plateaus to sea level (Stace et al., 1968). In creek and river beds at Rosebery, soil and sediment cover was typically entirely absent. This is the combined result of the limited nature of true soil cover observed elsewhere across the Rosebery catchment and the high flow rates of water courses due to the mountainous terrain. The hydrogeologic implication of such conditions is that the watercourses are in contact with the fractured bedrock aquifer. This connection explains the highly responsive baseflow contribution discussed further in Section 5.2.4 and provides justification for surface – groundwater interaction to be included in the modelling. In addition this contact explains how streams could be losing water to bedrock at higher elevations within the catchment.

2.6 Hydrology

2.6.1 Pieman River

The major hydrological feature of the study area is the Pieman River (*c.* 2500 Mm^3/year), which was fed by two major tributaries; the Mackintosh River (*c.* 850 Mm^3/year), and Murchison River (*c.* 1500 Mm^3/year) (Hydstra, 2004; and Figure 2.16). These rivers were dammed in 1980 and 1982, respectively, to form the Murchison and Mackintosh Lakes upstream of the study area (Figure 2.16). Downstream of these lakes within the study area, the Bastyan Dam wall (completed in 1983) formed Lake Rosebery on the Pieman River. Lake Murchison, Lake Mackintosh and Lake Rosebery have been observed to exhibit physical and chemical characteristics typical of temperate lakes (Chapman, 1992; and Koehnken, 1992); dominated by thermal stratification in the summer and thorough mixing during the winter (Denney, 2000).

Tyler and Bowler (1990) stated that before damming, the Pieman River flowed through narrow steep sided, heavily vegetated valleys. The only present day insight to this is observable immediately below the Bastyan Dam (Figure 2.16). Below the Bobadil Plain, the Pieman River gradates into Lake Pieman, becoming seasonally stratified downstream of the Huskisson River (Denney, 2000). Lake Pieman (*c.* 4200 Mm^3/year) (after Hydstra, 2004) is contained by the Reece Dam (completed in 1986), *c.* 50 km downstream of the study area (Figure 2.16). Denney (2000) states "the average residence time of water in Lakes Mackintosh, Pieman, Murchison and Rosebery are: 146 days; 55 days; 23 days; and 19 days, respectively (after Koehnken, 1992)".

Below the Reece Dam, the Pieman River flows west through the Pieman State Reserve before flowing into the Southern Ocean at Pieman Head in Hardwicke Bay (*c.* 6000 Mm^3/year) (Koehnken, 1992). The intermittent and controlled nature of the

discharge water from the Reece, Bastyan, Mackintosh and Murchison power stations have little effect on the river levels due to the deep river bed being below sea level along the final *c.* 38 km length of the Pieman beneath the Reece Dam (Denney, 2000). This tidal estuary has a characteristic salt wedge, the extent of which is dependent on the strength of tides, and discharge from the Reece Dam and rivers discharging into the Pieman below the dam (Koehnken, 1992).

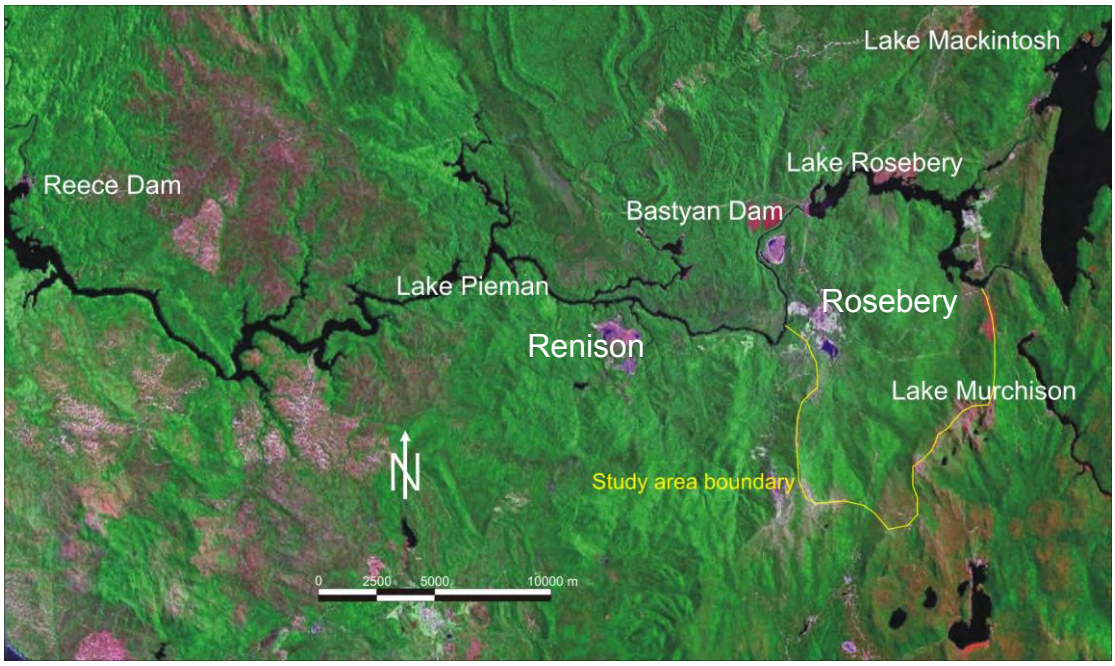

Figure 2.16 Landsat image of the Lake Pieman system (after NASA, 2006)

2.6.2 Stitt River catchment

The major tributary into Lake Pieman within the Rosebery catchment was the Stitt River (*c.* 64 Mm^3/year after Hydstra, 2004). The Stitt River was fed by the Rosebery, Mountain, Saddle, Dalmeny, Koonya and Talune Creeks (combined <10 Mm^3/year *ibid*.; Figure 2.17). Upstream of Rosebery, the Stitt River drained a large catchment of relatively undisturbed grassland, scrub, and rainforest; with Mount Read at the highest point.

2.6.3 Sterling River catchment

Creeks draining the West Coast Range (including Mount Murchison), as well as the Fooks and Bruce Creeks fed the Sterling River (<50 Mm^3/year), which was the

major tributary of Lake Rosebery from the study area (Figure 2.17). Although the Sterling River Catchment contributed to the groundwater regime of the greater catchment, it was beyond the focal area of the Rosebery mine.

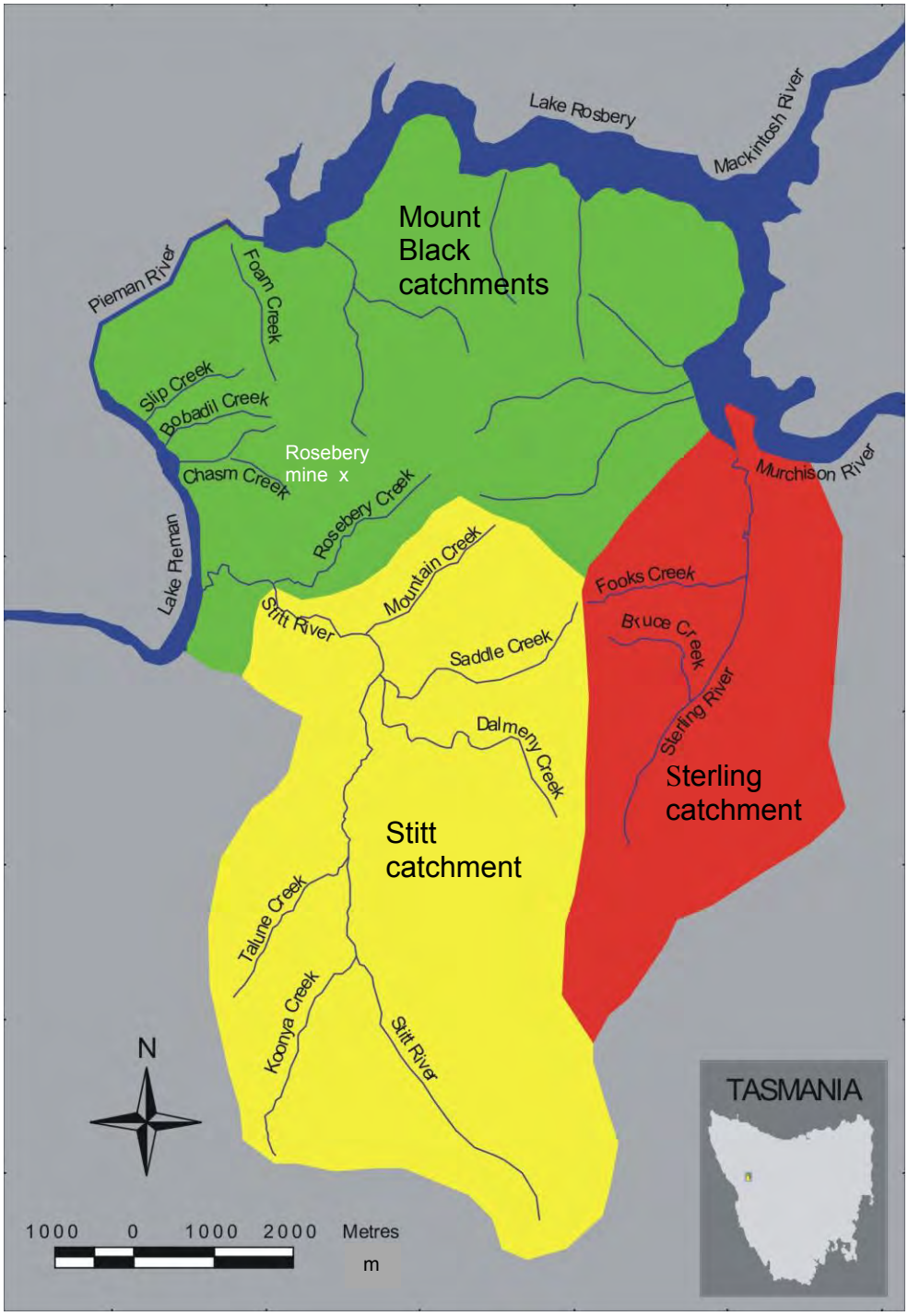

Figure 2.17 Regions of the Rosebery catchment; Mount Black tributaries (green), Sterling River catchment (red) Stitt River above Rosebery Creek (yellow)

2.6.4 Mount Black catchments

The catchments within the study area which did not flow to either the Stitt or Sterling Rivers have been grouped in the Mount Black catchments. The minor tributaries into Lake Pieman from the study area were the Slip, Foam, Bobadil, and Chasm Creeks (combined <5 Mm^3/year); (Figure 2.17). The anthropogenic Bobadil tailings dam discharged at a licensed point directly to the Pieman River (*c.* 6.2 Mm^3/year); (Hydstra, 2004). The minor tributaries into Lake Rosebery were a number of small-unnamed creeks running off Mount Black and Mount Sale (Figure 2.17).

"The uncertainties of lithology, stratigraphy, and structure introduce a level of complexity to geotechnical and hydrogeological analysis that is completely unknown in other engineering disciplines" (Freeze et al., 1990).

3 Aquifer Observations and Characteristics

3.1 Introduction

Key aspects of defining a groundwater system for hydrogeological research are: (i) determining the piezometric surface; and (ii) characterisation of the aquifer hydraulic properties, and representation of their spatial variation (Freeze and Cherry, 1979; Middlemis, 1997; and Fetter, 2001). Groundwater systems, particularly fractured rock aquifers, typically have: (i) a high degree of spatial variability (Cook, 2003); and (ii) sparse data sets that define them (Hill, 1998). In the current chapter, the three major topics of: (i) hydraulic properties; (ii) mine data; and (iii) qualitative observations are addressed. These three topics describe the aquifer observations and characteristics at Rosebery. Due to the diversity of these subjects, each is treated in isolation within the chapter. Unlike other chapters, in the current chapter each topic is deliberately reviewed and discussed sequentially in sections.

Due to the terrain, climate, and land use in the Rosebery area (mountainous, wet, temperate, and sulphide-mining), the lack of a historical emphasis on groundwater as a resource has resulted in an even smaller historical dataset than is available for most groundwater systems (Chapter One). An operating mine, and the nature of current pumping practices, magnified this problem because: (i) the pumping stress resulted in aquifer conditions that differ from that to be predictively modelled; and (ii) there was no fully saturated medium in the immediate vicinity of the mine which could be subjected to hydraulic testing. Adams and Younger (2001) faced this same problem in mines in the United Kingdom stating, "since mine voids are dewatered during mining, their hydraulic properties under flooded conditions cannot

be directly characterised in advance of rebound". Such conditions are expected to be common to all operational mines.

3.2 Hydraulic Properties

Four methods for evaluating the hydraulic properties of the rock mass have been used in the present study: (i) physical measurements; including field observations of the piezometric surface elevation under both „static' and „stressed' conditions to calculate hydraulic conductivity; (ii) classification of geotechnical and geological interpretation of drill core involving a little known experimental approach using fracture density based on the mine's rock quality designator (RQD) database; (iii) qualitative inspection of underground workings and surface seeps; and (iv) calibrated values from a numerical model that attempted to quantify the aquifer system. This chapter describes (i, ii, and iii) of these methods, and Chapter Six describes (iv).

The measurement of piezometric head under 'static' conditions was used to develop a piezometric surface across the study area. The static conditions provided a snapshot of the groundwater regime and were used in: (i) developing the conceptual model; (ii) mathematical model calculations; and (iii) calibrating the numerical model.

The measurements of piezometric heads under „stressed' conditions (pumping and slug tests), and subsequent calculation of rock hydraulic properties such as hydraulic conductivity, were used to characterise the hydrogeologic environment. The hydraulic properties were used in calibrating the numerical model for predictive modelling of how this groundwater regime will respond to changes in stresses on the system.

Measurements of piezometric head taken in water supply bores or purpose built monitoring piezometers are the most common field observation a hydrogeologist is

likely to make (Brassington, 1988). Measurements of piezometric head, excluding GHD's (2001) work in the walls of the tailings dams, had not previously been undertaken within the Rosebery catchment. There were no groundwater supply wells in the district, and prior to the present study, no piezometers, excluding those in tailings dams walls (*ibid*.), were available in the study area.

Due to heterogeneity at different scales, the complete characterisation of any hydrogeologic environment is impossible and partial direct measurement "is at best costly" (CPSMA, 1990). Although the Rosebery mine was both profitable and operating throughout the field component of this research, the anticipated drilling budget was limited by restrictions in company spending emplaced whilst Pasminco was under administration. This had serious consequences for the present study, however, it did produce a situation synonymous with that facing most mines nearing closure, when cash flow is likely to be reduced. Due to budget restrictions, it was not feasible to procure drilling services for pumping and observation drillholes, or to undertake significant (multi-day) pumping tests. Opportunistic use of a drilling rig, nevertheless, resulted in the drilling of three piezometers (Appendix Nine).

Surface mineral exploration drillholes (including angled drillholes), although not ideal, were recognised as an important substitute for piezometers at Rosebery and potentially for other mining districts. Elsewhere within the mining industry, the conversion of exploration drillholes to piezometers at an early stage, and the regular monitoring and analysis of these data, has provided a valuable long term record for later use in groundwater model calibration (e.g., Middlemis, 1997; de Caritat et al., 2005; and Youngs and Milligan, 2006).

3.2.1 Previous Studies

Prior to the present study, relevant hydraulic properties of materials in the study area had not been described. Studies of the local groundwater regime were undertaken at the nearby Renison mine (Coffey Partners, 1979; and GRC, 1985), however, numerical modelling of closure was never considered in these works. Groundwater Resource Consultants (GRC, 1995) assumed an effective porosity of 0.05 for the rock mass at the nearby Renison mine. The Renison mine was closed during 2003 and pumping ceased in December 2003, only to be resumed for reopening in 2004. Although Renison is hosted in a different formation, which is likely to exhibit different fracture behaviour to those in the current study, the Groundwater Resource Consultants (GRC, 1995) study was relevant because the Renison mine is located 8 km south of the study area, with the ingress to the mine at a similar elevation to that of the Rosebery mine (*c.* 200 m) at the foot of the West Coast Range.

Logan and O'Toole (1996) discussed water inflows during construction of a vertical shaft at Rosebery. This large inflow event was considered an extreme event and was unlike flows observed elsewhere within the mine (O'Toole, pers comm., 2008). The major inflow into the shaft (1600 l/min) was attributed to a 48 m section intersecting E-W fault zones, logged as shear zones (Logan and O'Toole, 1996). The remaining 400 l/min was attributed to the surface 160 m weathered regolith and broken bedrock (*ibid.*). These values, based on active area of a vertical drillhole, broadly correlate to a hydraulic conductivity of 12 m/day for the surface 160 m and 160 m/day for the 48 m shear zone. Attributing no water to the bedrock and the entire water inflow to these two zones, overestimated the hydraulic conductivity of the highly conductive zone, and underestimated the hydraulic conductivity of the bedrock. Subsequent grouting in these zones described in Logan and O'Toole (1996)

resulted in the fracture and pore spaces in these zones being cemented. Thus, these values were not directly applied in the groundwater model in the vicinity of the shaft. Such rates from a single HQ (∅ 96.1 mm) drillhole equate to half of the present day inflow rate for the entire mine, hence it would be inappropriate to assign model hydraulic conductivities as high as those above. The highly hydraulically conductive shear zones described in Logan and O'Toole (1996) do, however, provide evidence for highly conductive shear zones and surface regolith material at Rosebery.

Primarily using slug tests, East (1999) investigated the hydraulic properties of the glacials at the TME smelter site, 1 km east of the study area. The hydraulic conductivity of the glacials was found to be extremely variable ranging from *c.* 10 to <0.0001 m/day (*ibid.*). Although outside the catchment, East's (1999) thesis provided useful local information on the variable nature of the hydraulic properties of glacial materials.

The glacial and waste materials in the dams and waste dumps have been investigated by a number of consultants (e.g., SS&B, 1993; Dames and Moore, 1996; Struthers 1996; Dickson 1997; Stephenson EMF Consultants, 1997; Atkins 1998; GHD 2001a and 2001b; Kreigs, 2001; and GHD, 2003). GHD's (2001a and 2001b) work resulted in the installation of piezometers in the tailings dam walls which were made available for the present study, however, no quantification of hydraulic parameters, relevant to the present study, were documented.

3.2.2 Drillhole reconnaissance survey

3.2.2.1 Methodology

Geographical information systems, using both MapInfo and ArcView, incorporating Pasminco's geological drillhole database (PRM, 2003b), were created as part of the present study. Spatial analysis of these data outlined over 250 surface

drillholes within the study area (Figure 3.1). A field survey inspected and assessed whether each of the drillholes was in a condition to act as, or be converted into, simple piezometers.

Low angle drillholes have high friction between the electronic water level meter (dipper) and the footwall of the drillhole. In such cases there was a risk of the tape breakage or stretching upon retrieval of the dipper. In extreme cases standard dippers can not descend down casing due to the aforementioned friction. Subsequently, angled drillholes are not typically used in groundwater investigations. A purpose built *c.* 2 kg *c.* 2 m stainless steel „spear' was constructed to overcome this problem. The spear was constructed to both: (i) attach a dipper; and (ii) act as a bailer to return water samples.

3.2.2.2 Results

Twenty nine „reliable' drillholes were found to be in a usable condition for the present study. Reliable drillholes averaged -79 degrees (from horizontal), with the shallowest angled drillhole considered reliable at -49 degrees. The average total depth of reliable drillholes was 1049 m, with a maximum total depth of 2111 m and a minimum total depth of 60 m. The reconnaissance survey output is provided in Appendix One. Table 3.1 summarises the reconnaissance survey by tabulating the reliable drillholes; Figure 3.1 displays them spatially.

Surface drillholes dated back to 1916 and were part of a number of different drilling campaigns. Inevitably, different drilling programs have differing drilling practices and as a result the drillholes were left in a number of varying conditions. Only recent (<10 years old) drillholes were found due to the presence of a collar above the surface; older drillholes were mainly lost in thick revegetation or covered by later development. More than 70% of the drillholes sought were not found at all.

Very recent drilling (<5 years) in some cases still had vehicular access and revegetation had yet take hold of some drilling sites (e.g., Figure 3.2).

Drillhole Name	AMG66 Easting	AMG66 Northing	Collar RL m (AHD)	Depth to water table (m)	Direction bearing °	Angle °	Piezometric level m (AHD)	Piezometric level m (RMG)
114R	380279.3	5374160	536.29	9	47	-86	527.32	3576.81
120R	379722.2	5375623	626.29	3.38	320	-84	622.94	3672.43
121R	379720.2	5375616	626.29	7.74	248	-87	618.57	3668.06
126R	379718.4	5375618	627.29	7.19	306	-87	620.12	3669.61
128R	379713.7	5376061	506.29	0	248	-78	506.3	3555.79
129R	380028.5	5374687	613.99	15.95	84	-87	598.07	3647.56
132R	379723.6	5375622	626.23	17.94	2	-80	608.57	3658.06
136R	378562.7	5375189	404.69	4.75	90	-85	399.97	3449.46
138R	378577.1	5375110	399.69	10.9	0	-90	388.8	3438.29
141R	378554.8	5375766	538.19	50+	270	-49	500.46	3549.95
230R	379947.2	5373224	211.69	41.75	270	-85	170.11	3219.60
233R	379505.1	5376200	532.39	20.4	265	-80	512.31	3561.80
235R	379506.5	5376201	532.19	50+	84	-87	482.27	3531.76
248R	379905.6	5376590	548.49	50+	270	-75	500.2	3549.69
249R	379906	5376590	548.49	50+	270	-88	498.53	3548.02
250R	378887.4	5377238	351.99	0	80	-87	352	3401.49
256R	378884.6	5377237	351.89	0	270	-55	351.9	3401.39
258R	378628.5	5376987	448.09	6	270	-50	443.5	3492.99
259R	378578.3	5376832	470.49	46.72	90	-87	423.84	3473.33
260R	380296.5	5376523	661.29	50+	90	-90	611.3	3660.79
261R	378664.8	5376616	471.49	50+	270	-70	424.52	3474.01
263R	379506.2	5376199	532.29	50+	265	-68	485.94	3535.43
DP310	379828.6	5372240	154.3	14.4	266	-80	140.13	3189.62
DP317	380088.9	5372820	169.7	17.22	281	-80	152.75	3202.24
DP318	380100	5372525	160	1.8	283	-80	158.24	3207.73
G8P	379200	5372800	150	0.85	180	-90	149.16	3198.65
KP303	378265.9	5370499	474.6	3.5	11	-90	471.11	3520.60
KP308	378230.2	5370726	502.6	27.09	261	-55	480.42	3529.91
KP309	378277.3	5370611	482	0	251	-90	482.01	3531.50
P01	378800	5372780	165	6.76	180	-90	158.25	3207.74
P02	378810	5372785	165	4.4	180	-90	160.61	3210.10
P03	378900	5372750	165	8.84	180	-90	156.17	3205.66
P04	379100.9	5372760	160	6.03	180	-90	153.98	3203.47
P05	376300	5376100	180	13.25	180	-90	166.76	3216.25
P07	376500	5376300	180	10.99	180	-90	169.02	3218.51
P08	376927	5376335	250	1.5	180	-90	248.51	3298.00
P09	376932	5376318	250	1.3	180	-90	248.71	3298.20

Table 3.1 Average elevation of observed piezometric surface (AMG66 refers to the co-ordinate grid, RL refers to Reduced Level, m refers metres, RMG refers to Rosebery Mine Grid, and AHD refers to Australian Height Datum

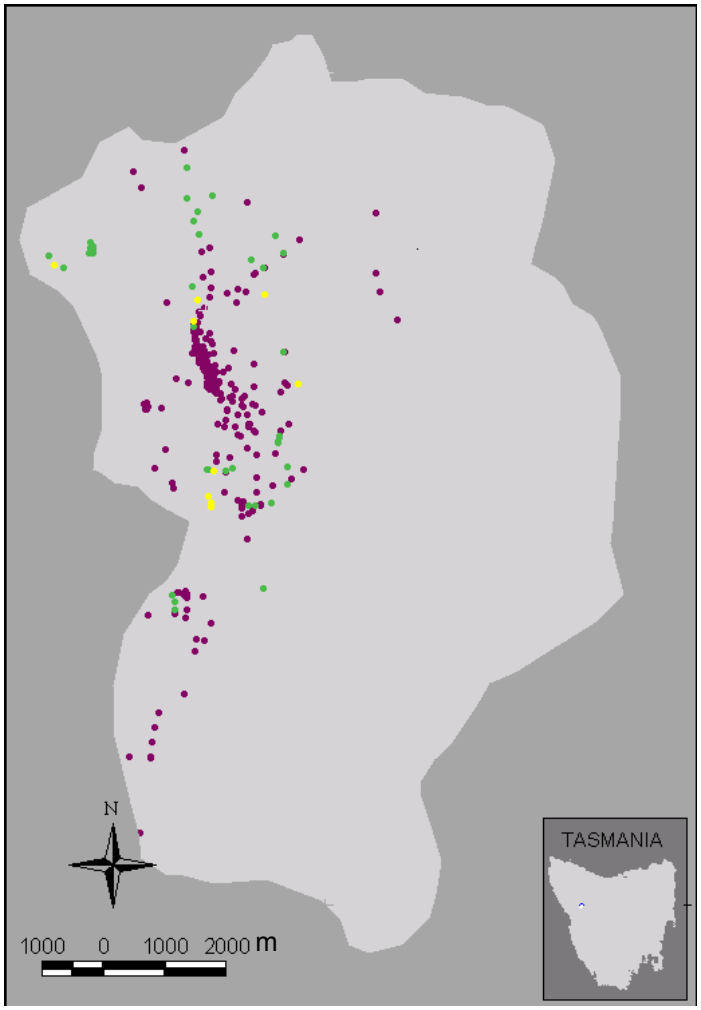

Figure 3.1 Location of surface drillholes throughout the study area (purple), those drillholes that were reliable for measuring piezometric head (green), and those drillholes that were reliable for measuring hydraulic properties (yellow)

3.2.2.3 Discussion: issues of adapting historical exploration infrastructure to hydrogeological investigations

The ideal drillhole for monitoring piezometric head was found to be one that: (i) had easy (vehicular) access; (ii) had an identification tag (for cross reference to the database); (iii) was capped (to prevent blockage); (iv) was vertical (for monitoring ease); and (v) had a collar that extends beyond any incompetent material (so that the drillhole was open to allow monitoring). This condition was rare in the study area as revegetation was rapid in the dense rainforest where much of the drilling at Rosebery has occurred.

Figure 3.2 Recent drilling pad with vehicular access on Mount Black

Drillholes that were cased had far less friction than open drillholes (those without casing). Slotted PVC casing was installed in many drillholes at Rosebery, not for groundwater monitoring, but to permit the use of geophysical logging equipment. In the commonly very deep drillholes, the slots allowed water into the PVC column, equalising the pressure difference between the inside of the PVC and the external groundwater head. This meant that those drillholes cased with slotted PVC for geophysical purposes, or that had PVC installed in them as part of the present study, could be dipped at lower angles than uncased drillholes. The purpose-built spear had a lower friction relative to its weight, compared to a dipper, so that drillholes could be dipped at lower angles than would normally be possible. The present study indicated that exploration drillholes of a lower angle than 45 degrees are at angle that is considered too shallow to be useful in standard hydrogeological investigations. Such lower angle drillholes can still provide valuable information if artesian.

Solid steel casing does allow a drillhole to be dipped, however, without slotted or screened intervals, casing does not allow inflow and water table pressures are only measured from below the casing. The practise at Rosebery was to only install surface

casing as a collar due to the largely competent crystalline rock mass. This means that open drillholes are common, however, they may be caved in at fracture zones. Quite unlike standard piezometers, at Rosebery, it was assumed the entire drillhole was open to inflows. At Rosebery, this includes the unsaturated and saturated sections of drillholes.

Filling drillholes with liquefied cement (grout) after drilling ensures that groundwater and surface inflows do not freely drain into the underground workings. An important finding of the survey was that no surface drillholes were found to be grouted. PRM (2003d) stated that surface exploration drillholes were never routinely grouted. This means that those drillholes not full of grout have the potential act as groundwater conduits. A review resulted in grouting of all new surface drillholes at Rosebery to lower the risk of avoid inrush of water to the underground workings (PRM, 2003d). Completely filling drillholes with grout excludes them from use in future groundwater studies. Only those drillholes that are grouted specifically in the annular outside casing, above the point of water ingress, can act as piezometers.

Many of the roads in the study area had been created specifically for a single drilling pad and have had limited use since. This meant that vehicular access was limited, involving the clearing of existing vegetation and fallen trees. Where road conditions had deteriorated significantly, commonly due to slips and wash outs, access was only possible on foot. Access on foot, in the challenging climatic conditions, was a limit on field productivity. If drillholes were capped tight, they required a number of trips in and out carrying gear; notably the two 36" Stiltsens to open tight capping (Figure 3.3). Brassington's (1998) hydrogeologist tool kit proved impractical where access was only available on foot.

Figure 3.3 Stiltsens (36") re-capping an angled drillhole collar

After the survey, the potential dataset for determining the piezometric surface was lower than anticipated. Drillholes were eliminated from the dataset because: (i) some areas were not accessible due to thickness of the vegetation or rugged terrain; (ii) drillholes were not found on drilling pads or roads and safety constraints limited leaving made tracks in dense vegetation; (iii) were not opened due to excessive rusting, keyless padlocks and welded-on caps (<5%); and (iv) drillholes were caved in or could not be used due to their low angle. In contrast, studies such as Middlemis (1997), de Caritat et al. (2005) and Youngs and Milligan (2006) in: (i) semi-arid tropical north-western Queensland; (ii) semi-arid tropical north-western Western Australian; and (iii) semi-arid temperate western New South Wales, respectively, did not face all such issues. The rapid revegetation, dense existing vegetation, and rugged terrain is the key difference between the present study and the aforementioned studies.

3.2.3 Piezometric surface

3.2.3.1 Methodology

The rudimentary hydraulic test in the field of hydrogeology is the measurement of the piezometric surface (Brassington, 1998). The piezometric head measurement was repeated twice yearly over a two-year period from 2002 to represent summer lows and winter peaks within the groundwater regime. A „dipper' was lowered down the drillhole on a measured tape and when in contact with water, a circuit was completed resulting in both a light and audio alarm being triggered. The down-hole depth to water was then manually measured off the tape (Figure 3.4).

Figure 3.4 Measuring down-hole depths to groundwater

Down-hole depth was converted to actual depth using trigonometry assuming a straight drillhole. The first survey angle of the drillhole from surface was used and any change in the direction of the drillhole was presumed to be negligible for the first fifty metres. Most drillholes were at least HQ in size (∅ 96.1 mm) at this depth; over this short distance, little angle change is possible with such large and rigid drilling rods so the „straight' drillhole assumption was justified. Angles are recorded in the database (PRM, 2003b) to an accuracy of 1 degree. Top of collar surveys were

recorded in the database (PRM, 2003b) to an accuracy of 0.01 m height (z direction). With the measurement of head there was also an associated error of 0.01 m using the tape measure and dipper.

To supplement the drillhole piezometric surface observations, observations of spring seepage and annual creek flows were noted throughout the catchment. Where surface flows were observed to be annual, thus not related to rainfall events or winter interflow, surface points were assigned a piezometric head equal to that of the surface topography. The surface elevation dataset had a large associated error, especially in the dense rainforest. Elevations were extrapolated from the 10 m contour maps and spot heights recorded to an accuracy of 0.01 m.

Mine data used a local grid Rosebery Mine Grid (RMG). RMG is a local grid rotated 11°18'11' from AGD66 – AMG Zone 55. The origin, 0 x, 0 y, 0 z, occurs at 378870.55 mE, 5374181.69 mN and -3049.49 mRL (AGD66 – AMG Zone 55) and accurate conversion to RMG required multiplication by a factor 0.999748 laterally for conversion to AGD66 – AMG Zone 55. All mining related data used the RMG and it was applied throughout the present study to maintain consistency and relevance to the mine. Thus, the conversion from Australian height datum (AHD) to RMG is RMG = AHD + 3049.49 in mRL.

A number of artesian drillholes were encountered (e.g., Figure 3.23). Where artesian conditions were encountered, the value of „depth to water table' was assigned as 0 m. The actual head was not calculated as the artesian conditions were, in all cases: (i) of very low pressure; (ii) had no vehicle access; and (iii) not in a condition to allow infrastructure to be easily altered for measuring artesian heads. Artesian conditions in the catchment did not suggest that areas were under confined conditions and were more likely a result of angular drilling in mountainous terrain (Figure 3.5).

The water levels measured in some drillholes were therefore not believed to represent a true groundwater surface, at the location of the collar.

The condition of the drillholes was also considered to play a large role in the accurate representation of the water table. Where groundwater extraction is the prime use a drillhole, the construction details are commonly well known. For exploration drillholes at Rosebery, this is not generally the case. Typical unknowns included: (i) the extent of the open drillhole; (ii) the degree of drillhole collapse; and (iii) the presence, nature and geometry of the casing materials.

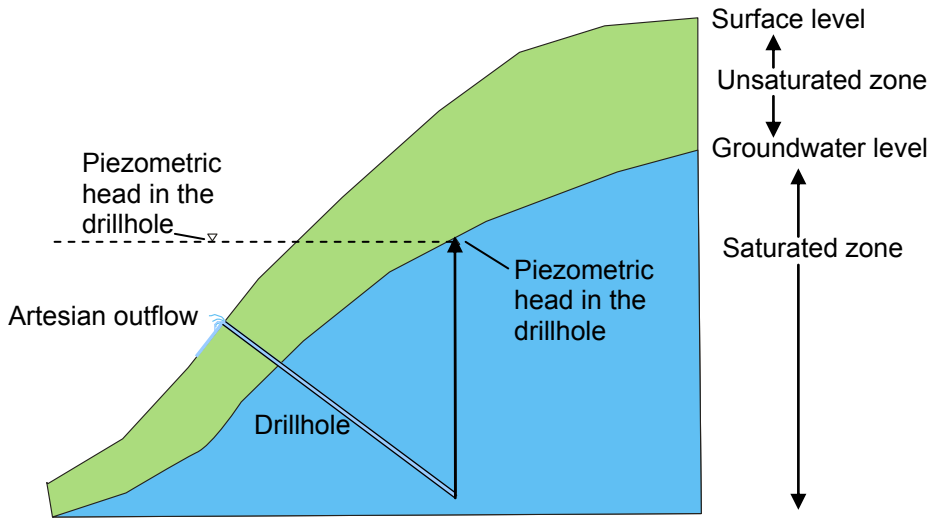

Figure 3.5 Angular un-cased drillholes through crystalline rock in mountainous terrain resulting in artesian conditions by tapping regions that contain heads greater than that of the collar elevation

Some drillholes receive significant surface water inflow due to inadequate collar construction. A sealed drillhole collar extending beyond the height of winter surface water inundation would overcome such issues. Figure 3.6 displays how the lack of a collar results in significant influence to the groundwater regime through the passive injection of surface water.

Some drillholes are also in direct contact with the mine workings, resulting in local groundwater sinks due to mine pumping. One such drillhole (235R) was

considered reliable in the early stages of monitoring and was converted to a standpipe piezometer. Due to ongoing production 235R was encountered by a stope, resulting in an inrush of water and hundreds of meters of PVC casing into the workings. Subsequent monitoring of the drillhole was abandoned, however, the event highlighted the complexities of groundwater monitoring in active mining environments.

Figure 3.6 Drillhole 128R receiving a seasonal influx of winter surface water sheet flow; a sealed drillhole collar extending above the height of inundation would resolve this issue

Numerous problems, principally with access and drillhole configuration, prevented the obtaining of regular winter and summer values each year for all reliable drillholes. Considering such gaps in these data, the term „average elevation of piezometric surface' in the present study reflects either: (i) a subjective interpretation of the most reliable reading of the four seasonal readings; or (ii) in the case of consistent readings, a true arithmetic average of the four values.

3.2.3.2 Results

The average elevations of piezometric surface in drillholes considered reliable are summarised in Table 3.1 and Figure 3.7, with the field results presented in

Appendix One. A head difference of *c.* 500 m was observed throughout the study area due to the mountainous topography. The large head difference complicated the modelling effort (Chapter Six).

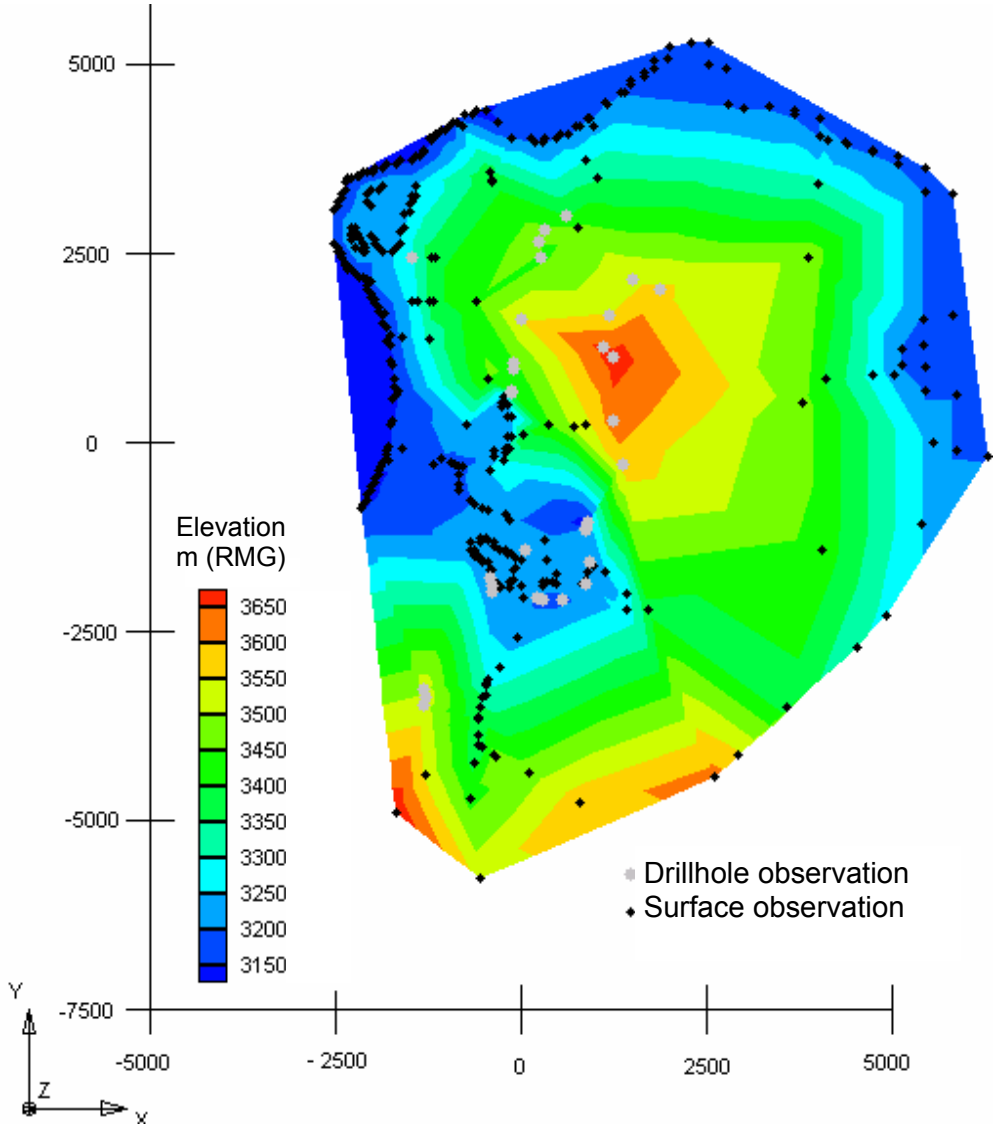

Figure 3.7 Average elevation of piezometric surface from surface and drillhole observations in m (RMG), grid in m (RMG) Contours were constructed using GMS (Groundwater Modelling System) with linear graded triangulations from a duel dataset of the drill observations and perennial surface water expressions.

3.2.3.3 Discussion

The most rudimentary measurement in hydrogeology, that of piezometric head, was problematic and inconsistent in the wet, mountainous, mining environment at Rosebery. Extremely wet conditions resulted in suspect readings in both winter and summer conditions. Standard hydrogeological instruments were not reliable in such

conditions. The retro use of exploration drillholes for the measurement of piezometric head was not ideal, however, it did provide a significant insight into the groundwater configuration which would have otherwise been unavailable.

The average piezometric surface elevations from drillholes provided calibration targets, and were used in the observation coverage of the numerical model (Chapter Six). The surface observations were used in the development of the groundwater contours (Figure 3.7) to aid in areas of the catchment which had no drillhole coverage, but were omitted from the numerical observation coverage. Although valuable for conceptualisation, the surface observations were not considered reliable enough to be treated as true calibration targets. Factors contributing to the unreliability of surface observations were: (i) considerable associated error compared to surface elevation estimation; (ii) potential for the flow to not be associated to true groundwater flow, especially in such a wet environment; and (iii) potential for an unsaturated rock mass to exist beneath the observed site due to the low permeability of the rock mass (i.e., perched aquifers or loosing streams).

These data from the two years of winter and summer readings were considered too limited for comparison of seasonal variation, or the development of temporal trends. Although rainfall at Rosebery is perennial, a marked seasonal variation in rainfall is still apparent. Winter rainfall is significantly higher than summer rainfall (Section 2.4.2) at Rosebery. The trend in precipitation is also evident in groundwater levels over the study area (as well as in stream flow as discussed in Section 5.2.5). The seasonal variation observed in depth to groundwater drillholes over the study area were observed to be between 0.04 and 13 m with a mean value of 3.6 m from 21 samples (Appendix One). The use of down-hole pressure loggers may have overcome the uncertainties associated with the piezometric level fluctuation, however, these

were beyond the budgetary scope of the present study. Such logging instruments would be recommended for obtaining a future dataset to augment the development of a transient groundwater model.

3.2.4 Pumping tests

Procedures for conducting pumping and slug tests for calculation of hydraulic properties are well documented (e.g., Stallman, 1971; Driscoll, 1986; Australian Standards, 1990; Osborne, 1993; EPA, 1995; Halford, 1997; Hvilshoj, 1998; Fetter, 2001; Röhrich and WHI, 2001). Hvilshoj (1998) summarised this topic with a PhD thesis titled "Estimation of Ground Water Hydraulic Parameters".

I envisaged that larger scale pumping tests on exploration drillholes could be used to estimate the larger scale hydraulic properties of the rock mass as part of the present study. Pumping tests were attempted where a number of exploration drillholes had been drilled in close proximity. In each case the tests were unsuccessful due to very low conductivity material. Unfortunately there was a lack of infrastructure and investment to perform accurate, large-scale, low-flow pumping tests. This represented a serious drawback in defining the hydraulic properties of the region and alternate methods were investigated in an attempt to substitute for this shortcoming.

3.2.4.1 Slug test methodology

A total of ten rising head slug tests or bail tests were successfully performed on reliable exploration drillholes and piezometers over the study area. Three methods of analysis were considered for the slug tests: (i) the Hvorslev (1951) method; (ii) the Cooper et al. (1967) method; and (iii) the Bouwer and Rice (1967) methods. Only the Hvorslev method was considered appropriate, given the aquifer conditions and available drillhole configuration data.

The Hvorslev recovery test method was used to estimate the hydraulic conductivity of the rock mass. The Hvorslev test required the following: (i) an understanding of the piezometer construction and geometry; (ii) the ability to remove a „slug' of water from the piezometer; and (iii) observations of piezometric head (beginning at time zero) as the aquifer recovered the volume of water removed in the „slug'. Drillhole geometries were entered into Aquifer Test and hydraulic conductivity calculations were automated using the Hvorslev (1951) methodology referred to in Röhrich and Waterloo Hydrologic Inc (2001). Piezometric head recovery was measured with a precision of 0.01 m with the aid of an audio recording device to provide temporal context to readings and increase the frequency of readings. Slug tests were completed to full recovery, however, in some cases the frequency of head measurements was decreased as tests approached full recovery and static conditions.

The Hvorslev bail test has the following assumptions: (i) the aquifer was homogeneous; (ii) the water table was horizontal and the piezometer was vertical; (iii) the withdrawal of a volume of water was instantaneous and resulted in an instantaneous change in water level; (iv) inertia of the water column and non-linear well losses were negligible; (v) the drillhole was considered to be of an infinitesimal width; and (vi) flow was horizontal towards the well. Although these ideal conditions were not available in the field the method provided an established means of calculating hydraulic conductivity values. Considering these assumptions, field hydraulic conductivity values were intended for use as a guide to the material properties for the numerical modelling at Rosebery (Chapter Six).

Multi-level packer tests, within individual drillholes, can provide information on the vertical distribution of horizontal hydraulic conductivity (e.g., Widdowson et al.,

1990). Multi-level packer tests at Rosebery were not possible due to the lack of infrastructure and investment in the current project, however, they should be considered for any further work.

3.2.4.2 Results

The duration of a slug test is relatively short (theoretically instantaneous although the response is longer) compared to pumping tests (typically hours to days) and the estimated hydraulic conductivity is only representative of the aquifer material close to the well screen (Ferris et al., 1962). The computer program Aquifer Test was used as an aid to interpret the data and an example of its output is seen in Figure 3.8. Table 3.2 summarises the findings of field hydraulic conductivity tests over the study area. Raw data for all slug tests are provided in Appendix One.

Drillhole Name	Conductivity m/day	Stratigraphic Unit	Screen length
P1	2.00E-02	Mine Waste Tailings	4 m
P7	1.45E-02	Mine Waste Tailings	6 m
P13	1.09E-04	Hercules Pumice Formation	3 m
P14	4.04E-03	Hercules Pumice Formation	4 m
P14	1.55E-03	Hercules Pumice Formation	4 m
210R	4.31E-03	Hercules Pumice Formation	34.4 m
210R	9.33E-03	Hercules Pumice Formation	34.4 m
P15	1.37E-02	White Spur Formation	3 m
114R	2.82E-01	Mount Black Formation	200 m
128R	4.20E-04	Kershaw Pumice Formation	1194 m

Table 3.2 Calculations of hydraulic conductivity using the Hsorvlev method

3.2.4.3 Discussion

At Rosebery, the values provided by the Hvorslev test were applicable to modelling as they provided an average, equivalent porous medium, hydraulic conductivity for lengths of open or screened drillhole. The hydraulic conductivity values spanned 4 orders of magnitude displaying the variability of hydraulic conductivity within the fractured rock mass (Hercules Pumice Formation, White Spur Formation, Mount Black Formation and Kershaw Pumice Formation).

Repeat tests on drillholes P14 and 210R (Table 3.2) displayed variation in hydraulic conductivity, in both cases by a factor of *c.* 2. This variation could be attributed to: (i) differing seasonal aquifer conditions (starting heads); (ii) inconsistencies in bailing techniques; or (iii) changing drillhole condition over time (i.e. clogging if values were lower).

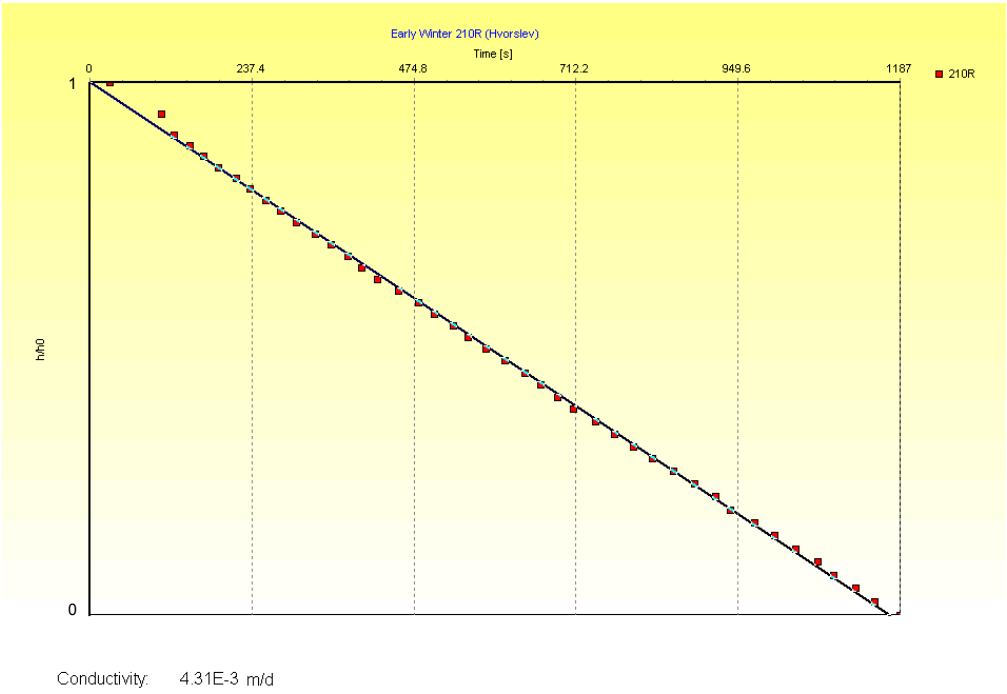

Figure 3.8 Example Aquifer Test output; Hsorvlev test results graph

Gathering data from old diamond drillholes was problematic due to the difference in casing of each of the drillholes (Appendix One) and lack of documentation of down-hole casing configuration. At Rosebery, reliable drillhole configuration consisted of any of: (i) PVC casing; (ii) slotted PVC casing; or (iii) HW steel collar. Casing had an effect on hydraulic tests, as well as hydraulic conditions in the drillhole. The data requirements for the Hsorvlev test necessitated the geometry (size, position and extent of casing) of a drillhole to be documented upon construction. Not documenting construction details resulted in well constructed drillholes not being able to be used for hydraulic testing. Where possible this was overcome with the installation of new PVC casing.

The great depth of exploration drillholes at Rosebery provided an advantage over shallow groundwater wells (typically with discrete screened intervals) that are used in classical groundwater studies. The large extent of the aquifer which was tested in the open exploration drillhole slug tests provided estimates of average properties of the aquifer over the length of that drillhole. This was appropriate when applied to the Rosebery numerical groundwater flow model parameters, which were applied at similar scales (Chapter Six). It is recognised that there may be a significant error associated to situations where only a small fraction of the total bore volume can be removed in the slug test.

3.3 Mine Data

3.3.1 Application of mine data to estimation of hydraulic properties

In the present study, the ability to obtain extensive and standard representative aquifer property values in the field was limited. This is also expected to be the case with many other groundwater studies in mountainous, wet, temperate, sulphide-mining environments. The main limiting factors were lack of infrastructure, access, funds and field time (which also required funding). Plagued by a lack of traditional data, to expand the understanding of the aquifer characteristics I sought to use the special conditions and data that are available in mining environments. The nature of the study site, as a mining environment, offered a different means of determining aquifer characteristics. The geotechnical properties of the rock mass in mining environments are commonly well understood through the rigorous collecting of information on rock and fracture properties for engineering purposes. The present study investigated the possibility of using this information for the purpose of groundwater studies.

3.3.2 Previous work

RQD is a technical measurement of the sum of all competent sticks of core greater than 0.10 m in length (x), multiplied by 100 and divided by the total length (L) of a core run (Deere and Deere, 1964 and 1988). RQD is therefore a value ranging from 0 to 100, 100 being competent with fracture frequency greater than 0.10 m.

$$\mathrm{RQD} = 100 \sum_{i=1}^{n} \frac{x_i}{L} \qquad \textbf{(3.1)}$$

During the geological logging of the core, the geotechnical parameter RQD is recorded for lengths of core. The principle of using RQD assumes that all core is theoretical subject to the same rigours; when a driller's offsider breaks core deliberately (to get it out of the barrel or fit it in the tray) they are routinely expected to mark this and the discontinuity is omitted from the RQD calculation. RQD is a widely used parameter (Choi and Park, 2004) that has been applied to rock engineering for decades (Lui et al., 1999), however, its use to date in groundwater studies has been minimal. The present study investigated how such high density RQD datasets can be used to model geotechnical domains, thus inferring areas of potential fracture porosity. For this approach to be valid, it is understood that permeability due to porous flow is negligible, as it is observed to be in much of the Rosebery catchment bedrock below the weathered zone.

Sen (1996) provided the theoretical framework for the relationship between hydraulic conductivity and fracture porosity to RQD. The fracture density of a rock mass relates closely to the apparent hydraulic conductivity that is due to fracturing (*ibid*.). Singhal and Gupta (1999) state, "although RQD is mainly used in assessing the geomechanical properties of rocks, it is also considered to be an important parameter in assessing relative permeability".

Lui et al. (1999) coupled RQD with hydraulic conductivity, stating "when RQD approaches zero, the rock mass is highly fractured, and fracture permeability will be relatively high; when RQD approaches 100, the degree of fracturing is minimal, and secondary porosity and secondary permeability will be low." Aiken (2003) also displayed that low RQD values correlated with higher hydraulic conductivity, despite the fact that RQD does not directly measure connectivity of fractures.

El-Naqa (2001) correlated hydraulic conductivity with a range of geotechnical indices, including RQD and Bieniawski's (1973) Rock Mass Rating (RMR) system. He also showed how the mean value of hydraulic conductivity could be estimated using the mean value of RQD and RMR obtained from the drillhole and field mapping. The RMR system (Bieniawski, 1973), like RQD, is used to predict the quality of the jointed rock masses. Much more complex than RQD, RMR is based upon six parameters: (i) uniaxial compression strength; (ii) RQD; (iii) fracture spacing; (iv) condition of fractures; (v) groundwater condition of fractures; and (vi) orientation of fractures. Although RMR is far more complex than RQD, El-Naqa (2001) concluded "the obtained relationships between hydraulic conductivity and RQD and RMR are more or less the same for both fracture field mapping and borehole data".

Barton et al. (1974) developed a geotechnical index (Q) for evaluation of rock competency in tunnel design. The method described six fracture characteristics of the rock mass: (i) rock quality designation (RQD); (ii) joint number (J(n)); (iii) joint roughness (J(r)); (iv) joint hydraulic conductivity (J(k)); (v) joint aperture factor (J(af)); and (vi) joint water factor (J(w)), and assigned a numerical value from reference tables based on their fracture properties. Gates (1997) modified this to form the equation for the hydro-potential value (HP):

$$HP = (RQD/J(n))\ (J(r)/(J(k))(J(af)))\ (J(w)) \quad (3.2)$$

Although Q values are not routinely gathered at Rosebery, they are widely used in the mining industry (DME, 1999). Routine conversion of these Q values into HP values could prove valuable in characterising the spatial variation in hydraulic properties in mining environments.

3.3.3 RQD at Rosebery

At Rosebery, RQD was a visual estimate and a single value was given for sections of core that have a similar competency at scales of 0.1 m or larger (Willis et al., 2003). Unlike Rosebery, elsewhere other methods of recording RQD take a physical measurement every metre or every core run recovered from drilling.

The large RQD dataset at Rosebery contained some 239,386 RQD values (PRM, 2003b). Managing such a spatial dataset required the use of mining software, in this case, Datamine studio. Observations were reported at the 0.1 m scale so that the observation dataset was expanded to a „composite' dataset, in which every 0.1 m of core was assigned a RQD value based on the observation for that stretch of core. The resultant drillhole dataset was 768 MB, representing some 8,448,501 data points. This dataset was compared spatially and statistically to a more manageable 1 m dataset. The differences were insignificant for the purposes of our models, so the 1 m dataset was adopted as input for the later block modelling. Many RQD block models were created, however, the model that was found to be most representative involved an inverse squared 25 m spherical search ellipse, on all RQD data points with the study area, using the 1 m dataset (Appendix Six). A 25 m search from a centre within a 50 m block represents the majority of the block. 50 m blocks were appropriate as this was considered the lower limit of the hydrogeological models discretisation.

3.3.4 Results

The result of the work on RQD was the generation of a 3D digital block model for the Rosebery mine area (Appendix Six). The block model can be visualised using the package Datamine studio. A single snapshot of a Rosebery RQD block model is provided in Figure 3.9.

Figure 3.10 reveals that RQD in Rosebery core has a bimodal distribution, skewed strongly to high RQD values. Nine percent of all observations (3% of the core by length) were given an RQD of zero. A further 63% of the observations (67% of the core by length) had an RQD equal to or greater than 90, representing crystalline and competent core.

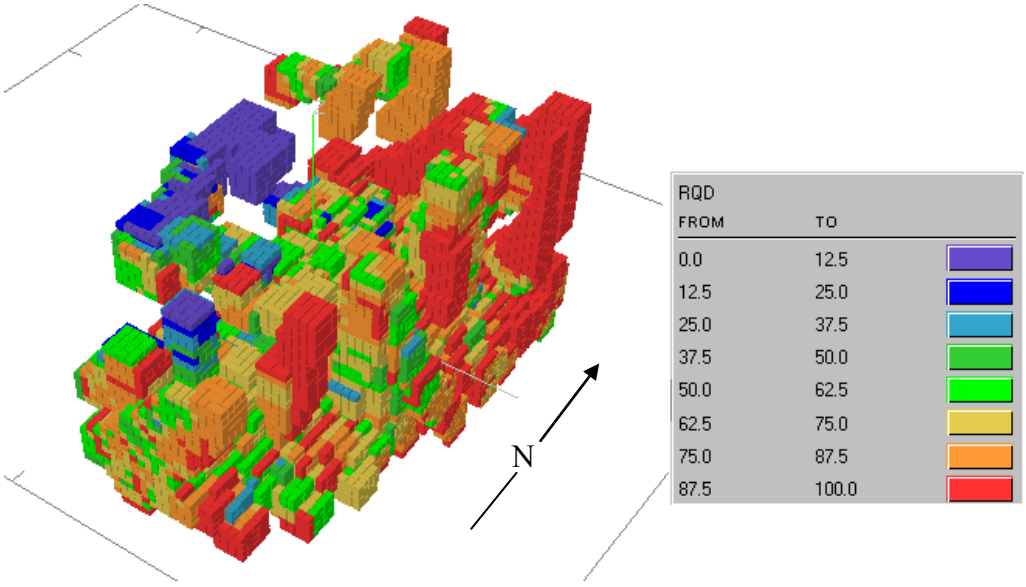

Figure 3.9 Example visualisation of the Rosebery RQD block models using Datamine studio, looking north-east from above (not to scale)

3.3.4.1 RQD observations

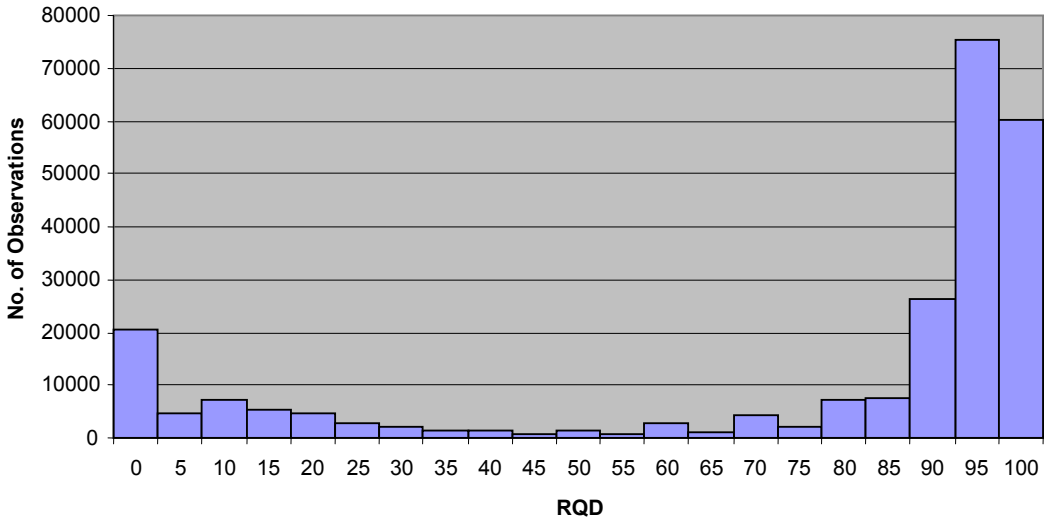

Figure 3.10 Observations of RQD at Rosebery (data from PRM, 2003b)

3.3.4.2 RQD variation with absolute height

The RQD dataset and block model were also examined to provide insight into the rock mass as a whole. Analysis of the model displayed a decrease in RQD with height above sea level (Figure 3.11). At absolute heights deeper than 100 m below the surface adit level of 3225 m (RMG), the trend in the mean RQD displayed an average increase of 0.01 RQD/m, which indicates a total change in mean RQD of 16 from the top of the mine to its deepest point.

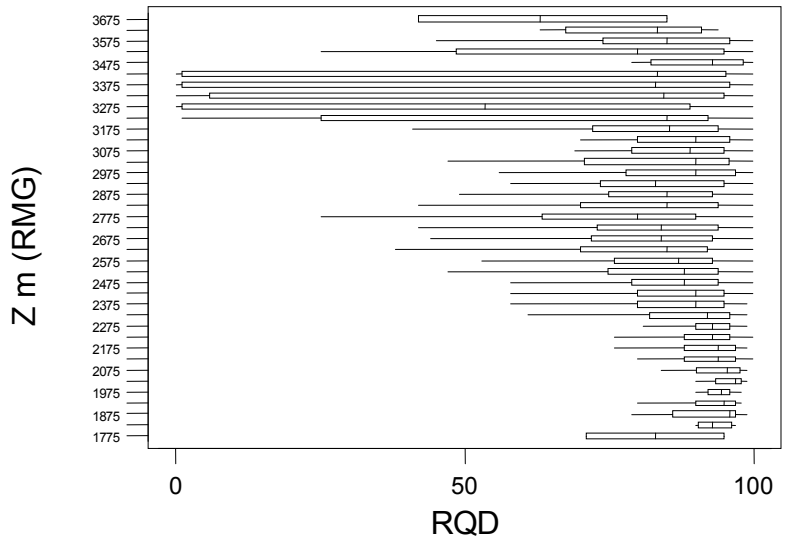

Figure 3.11 Boxplot of RQD versus absolute height (Z) m (RMG)

3.3.4.3 RQD variation with depth

Unlike environments with extensive regolith, pre-collars using non-core drilling were not routinely adopted at Rosebery. With core beginning at or near surface, the regolith or weathering zone was further delineated by plotting the RQD model data against depth beneath the topographic surface using a boxplot of RQD versus depth below surface (Figure 3.12). A dramatic increase in RQD was observed at depths greater than 100 m.

The same linear average increase (0.01 RQD/m) with depth was observed at depths greater than 125 m. Using the first consistently competent mean RQD value beneath this zone, of 75, this trend indicated that at a depth of roughly 2500 m below surface, the mean RQD values should approach 100, representing little flow or groundwater conduits.

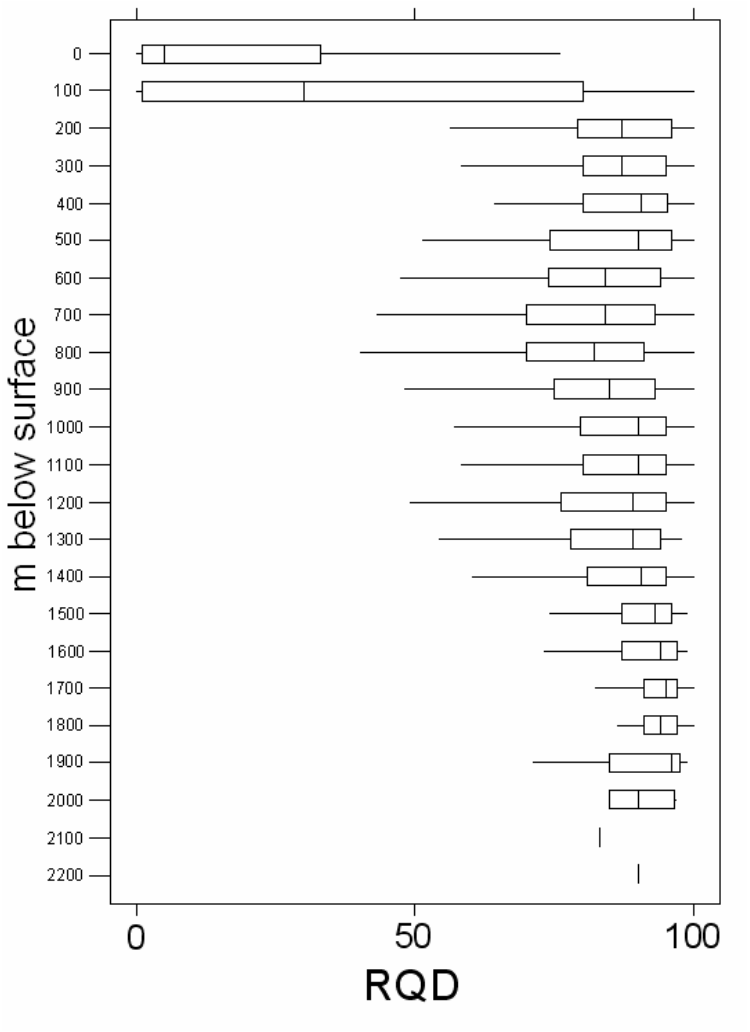

Figure 3.12 Boxplot of RQD versus depth below surface.

3.3.4.4 RQD variation with rock type

Dramatic differences in RQD were observed between different stratigraphic elements at Rosebery. Stratigraphy, the term used loosely in the database (PRM, 2003b) to describe rock type, was logged by Rosebery geologists and given a STRAT code. Based on the mean RQD for each STRAT code, the relative competency (and inversely, hydraulic conductivity) can be assigned. Table 3.4 demonstrates that the mean RQD and hence competency of FI NC FG < F S < CS BS DG NV < HW FW MB < V HO TZ < PO.

Unit	CODE	n	Arithmetic mean RQD	SD
Fill	FI	188	2.06	9.51
No core	NC	165	15.25	30.96
Fluvial glacials	FG	65	34.94	42.03
Shear zones	S	459	43.48	43.68
Faults	F	2395	45.65	39.91
Chamberlain Shale	CS	25	56.24	42.14
Black Shale	BS	3156	58.52	39.90
Dundas Group	DG	329	59.53	39.80
Natone Volcanics	NV	52	67.77	38.19
Hangingwall	HW	4312	70.16	36.41
Footwall	FW	54743	70.62	37.22
Mount Black Volcanics	MB	4451	70.92	35.14
Vein	V	357	76.25	34.76
Host	HO	157230	76.56	32.56
Transition Zone	TZ	1912	77.23	35.41
Porphyry	PO	6095	83.47	29.44

Table 3.3 Rosebery mine stratigraphic unit codes and arithmetic mean RQD and standard deviation

These STRAT types can be divided into three major groups based on their geotechnical properties. Group 1 represented non-competent material such as fill (FI), fluvial glacials (FG), and regolith, which was characterised by the STRAT code for no core (NC). The code NC is also used where sections of core are lost, thus for example, if a section core is lost within the drilling process and an RQD value is assigned for a larger section of core containing the lost core, the zone with the code NC is incorrectly assigned the RQD of the greater section. This results in NC having an RQD incorrectly higher that its true theoretical value of 0. Group 2 represented competent material that had undergone significant physical fracturing such as sheared (S) or faulted (F) material. Group 3 represented competent crystalline rock. The raw RQD data was examined with respect to these groups and the relationship of RQD in Group 1 < Group 2 < Group 3 is presented in Figure 3.13. Each of the rock types in Group 3 is represented in a similar manner in Figure 3.10. The STRAT types were further grouped into (i) CS BS DG; (ii) NV HW FW MB (iii) V HO TZ; and (iv) PO based on their average RQD.

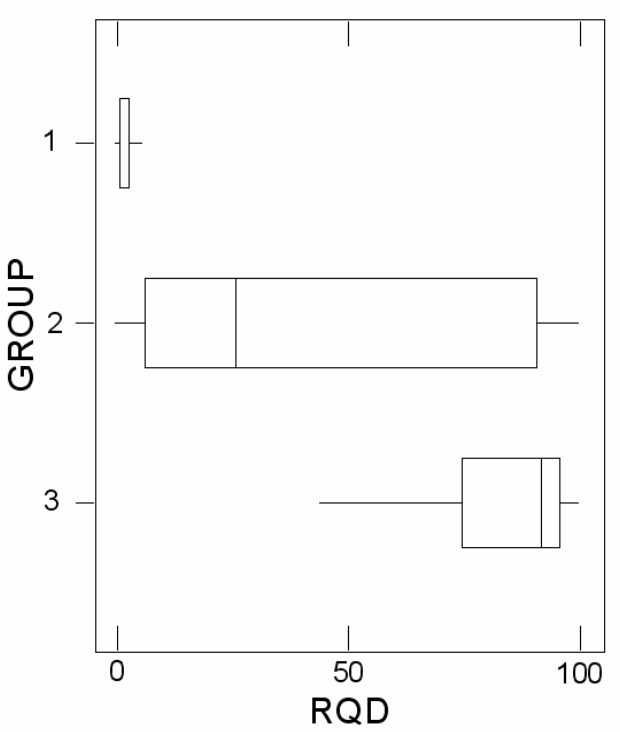

Figure 3.13 Boxplot of RQD versus stratigraphy groups

3.3.5 Discussion

There is no direct conversion of RQD to permeability or hydraulic conductivity. Where correlations have been made (Lui et al., 1999; El-Naqa, 2001; Aiken, 2003; GHD, 2007; and Surette et al., 2008) it is recognised that these correlations are site specific. Although subjectively quantitative for rock mechanics, RQD only provides a qualitative relative estimate of water flows within the rock mass.

Surrette et al. (2008) discuss a similar approach to that applied here in assigning relative potential hydraulic properties using a hydrostructural domain approach. Likewise, GHD (2007) based their hydrogeological modelling approach on geotechnical domains defined using RQD as a broad indicator for identifying geological features.

One reason the value of RQD for groundwater modelling may have been commonly overlooked could be that it does not take fracture orientation into account.

Fracture orientation is an important factor in that it indicates the connectivity of fracture networks in a rock mass. Extensive resource drilling leaves behind a network of large conduits connecting fracture zones, so connectivity exists within the drillhole void, provided they are not grouted. Examination of the block models and drilling records at Rosebery indicate an extensive distribution of zero RQD values, so it was not unreasonable to assume ample connectivity in the mine area.

The differences in RQD that were observed between rock types provided justification for hydraulic conductivity qualifiers to be assigned for modelling to each rock type. The RQD values, like hydraulic conductivity, would be expected to differ dramatically between incompetent surficial material and fracture zone material. The fact that this was the case, justified the proposed approach that RQD values can proxy for hydraulic conductivity values qualitatively and quantitatively but with an unknown accuracy (correlating RQD to hydraulic conductivity is discussed further in Section 6.10.9 and 7.4.3).

The zero RQD values (Figure 3.10) represented two populations: (i) a weathered zone or surface deposit at the start of drillhole; and (ii) discontinuities such as fractures, shears or faults. The extremely low RQD values at depths less than 50 m, and low RQD values less than 100 m (Figure 3.12), provide justification for two higher conductivity surface zones to be included in the groundwater model (Chapter Six).

The decrease in fracture density with depth provide justification for decreasing hydraulic conductivity with depth in the numerical groundwater flow model (Figure 3.11 and Figure 3.12). Using this trend, the depth at which RQD approached 100 (*c.* 2500 m) coincided with and justified the maximum depths within the numerical groundwater flow model.

Although subjectively obtained, the approach used to collect RQD at Rosebery highlights the location of potentially conductive faults and discontinuities. Recognised faults and discontinuities were found to correlate with relatively short sections of low RQD values. It also defined large sections of non-conductive competent material, making this method effective at identifying potential partitioned groundwater flow locally.

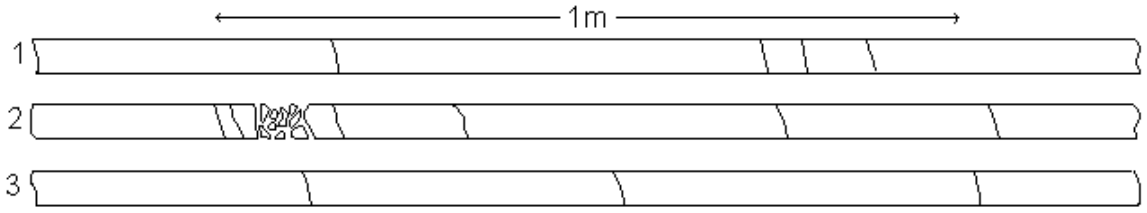

Figure 3.14 RQD: Rosebery Method and Standard Method
Standard Measurement Method Run 1: RQD=90, Run 2: RQD=90, Run 3: RQD=100
Rosebery Method Run 1: RQD=90, Run 2: RQD=100, 0, 100, Run 3: RQD=100

Three methods exist for obtaining RQD: (i) the original proposed by Deere and Deere (1964) that involves a calculation of RQD for every core run; (ii) a widely adopted variation (Scott, pers. comm., 2008) that calculates an RQD value for every metre of core drilled; and (iii) the estimation adopted at Rosebery. These three methods were compared for theoretical sections of core. Figure 3.14 shows an example of three runs of core and highlights the difference in RQD values between the two methods. Using both methods for run 1, RQD equals 90. For run no. 3, both methods give a RQD equal to 100. For run no. 2 however, the two methods yield a different result where there is a potential water conduit. The Rosebery method recognises the conduit with a 0 value for RQD, in between two 100 values. The standard method would yield an RQD of 90 for run no. 2, not distinguishing it from run no 1, which has a much lower potential for water flow. Such analysis provided evidence that the estimation method at Rosebery was not only robust, but sensitive to

local permeability contrasts. This is important, because measurements of hydraulic conductivity in fractured rocks are strongly influenced by individual fracture zones (Cook, 2003).

3.4 Qualitative field observations of water flows

The mine workings and extensive drilling provided a 3D insight into the post mining aquifer system that is not available in most groundwater studies. Observation of other water flows within the catchment also provided insight into the groundwater regime. Upon oxygenation, groundwater presenting at the surface as seeps can result in the deposition of mineral precipitates (Tolman, 1937). In the case of AMD, iron oxy-hydroxides, commonly called ochre or yellow-boy (Harris et al., 2003) precipitate (e.g., Figure 3.15, Figure 3.17, and Figure 3.19). Application of this theory allowed the visual recognition of some types of groundwater discharge in the Rosebery mine environment (See Chapter 2 for observations spatial context).

3.4.1 Previous work

Hale (2001) described the flow pathways for water within the underground Rosebery mine. Her (2001) work also correlated a seasonal variation in rainfall with discharge underground and total mine dewatering rates. Hale's (2001) study summarised the groundwater regime around the Rosebery mine as a fractured rock aquifer influenced by secondary permeability that has resulted from mine workings, drillholes and water bearing faults. This provided the framework for the conceptual model used in the present study. Hale (2001) discussed in detail the generation of AMD at depth within the Rosebery mine. Hale (2001) documented the abundance of precipitates from mine water in the underground workings. My observations made in the underground workings were consistent with Hale's (2001) findings.

Carnie (2003) proposed that the main source of water entry to the Rosebery underground workings was the open-cut, however, provided no volumetric justification. A water balance completed since, as part of the present study, demonstrated that: (i) much of the surface drainage was diverted out of the open-cut; (ii) there was little groundwater intercepted by the open-cut; (iii) and due its small surface area the open-cut receives little recharge from precipitation (for further detail, see Chapter Five).

Both Hale (2001) and Carnie (2003) proposed an intimate relationship between flow in the fault-bounded Rosebery Creek, and water flow in the underground workings. The relationship was based on observations in the upper workings and the decline by both Hale (2001) and Carnie (2003). This relationship provided a separate line of evidence supporting the concept that faults in the Rosebery sequence have higher hydraulic conductivities than the competent crystalline rock mass surrounding them.

3.4.1.1 Shallow groundwaters and surface waters

Shallow groundwaters in the present study refer to groundwater located in the upper regolith (<10 m depth below surface). The presence of oxy-hydroxide precipitates on materials in contact with shallow groundwaters and surface waters emanating from surface features on the mine site, indicated that these waters were affected by AMD (e.g., Figure 3.15). Oxy-hydroxide precipitates were associated with shallow groundwaters and surface waters in contact with the waste dumps, mine process areas and the open-cut. Further indications of AMD, beyond the scope of the present study, are a lack of aquatic biodiversity, and a visible stress on vegetation (geochemistry data are discussed in Chapter Four).

Rosebery Creek, up-gradient of the open-cut, appeared uncontaminated and no mineral precipitation was observed within the creek bed. There was visible evidence that rainfall, interflow and shallow groundwater interacted with sulphidic mine waste and mine walls in the exposed open-cut environment at Rosebery. Shallow and surface mine waters (Figure 3.15) then discharged directly from the open-cut area to the receiving environment of Rosebery Creek. This AMD was responsible for the degradation of the creek downstream of the mine workings. Much shallow and surface mine water also infiltrates into the underground mine workings and was visible in the underground workings of the upper levels (e.g., Figure 3.16 and Figure 3.17).

Despite covers and diversion drainage, the waste material in the open-cut and assay creek dump were observed to be highly saturated due to the wet environment. AMD seeps from these stockpiles were observed to flow seasonally over the field study period (2001-2004) (Appendix Two). AMD surface flow from the open-cut was observed to flow continuously over the study period (Figure 3.15). PRM (2004) measured flow rates varying from 17 to 0.04 L/s (Appendix Two) over the field study period.

Figure 3.15 Iron oxy-hydroxide precipitates from surface run-off that drains to Rosebery Creek from the open-cut mine area

Figure 3.16 Mine water floor-flow in the upper level headings at Rosebery. The field of view is *c.* 1000 mm by 500 mm

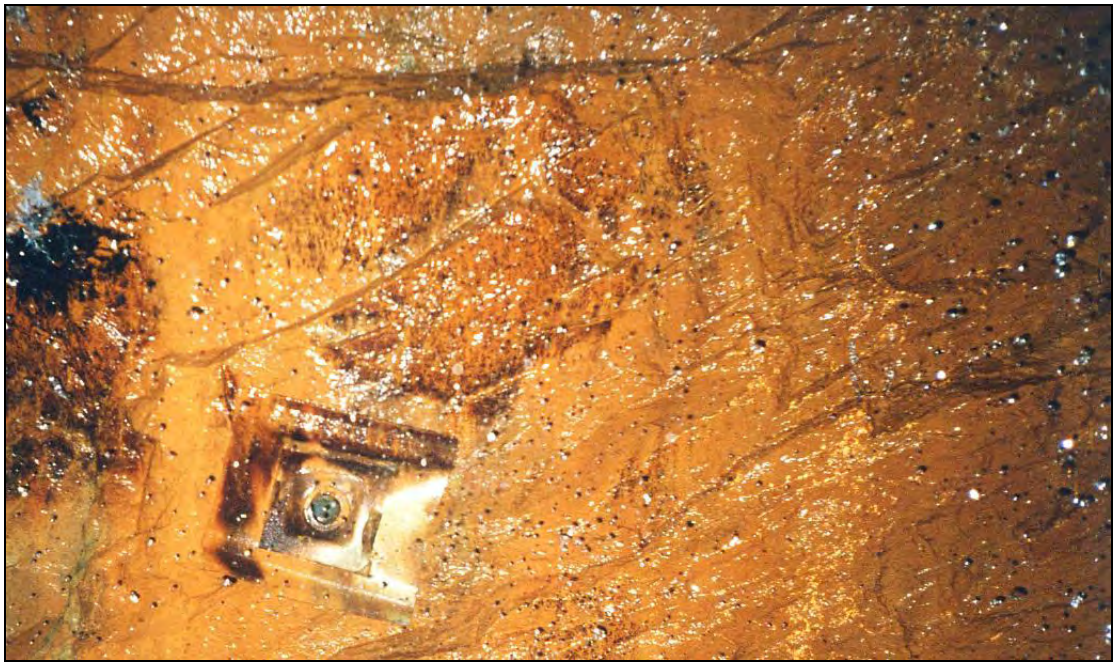

Figure 3.17 Mine water infiltrating the decline in the upper levels at Rosebery. Rock bolt plate (*c*. 250 mm by 300 mm) for scale

Figure 3.18 Groundwater seeps on the Bobadil road *c*. 1 km from the mine workings. Sulphidic rock in the road base was excluded as the source of the precipitates because the plume has extended into a significant area of the undisturbed vegetation up gradient of the road, A6 note pad for scale

Infiltration into the mine is managed via: (i) drains (both 'horizontal' level drains and „vertical' open drillhole drains); and (ii) sump pumping. Ultimately these waters are pumped to the tailings facilities for containment and treatment as AMD. Although pumping theoretically controls groundwater gradients towards the mine, it

is likely that much surface and shallow groundwater exits into the regional groundwater regime due to topographically driven flow.

Down-gradient of the mine workings, the regional groundwater regime is expected to discharge as springs due to a combination of: (i) the preferential flow in the fractured rock and porous aquifers; (ii) the close proximity of the water table to surface; and (iii) the undulating topography of the area. Although much of the area is inaccessible dense rainforest, Fe-precipitates in some road cuttings on the Bobadil road *c.* 1 km from the mine workings, indicate groundwater discharging at surface (e.g., Figure 3.18 and Figure 3.7).

3.4.1.2 Deep Mine Waters

Shallow and surface mine waters were relatively easy to observe and analyse due to their visibility and accessibility. In contrast, deep mine waters, regional groundwaters and waters developing at depth in tailings dams normally require infrastructure (e.g., piezometers or intersecting mine workings) for observations or analyses to be undertaken.

The presence of AMD generated precipitates, down-gradient of sources of disturbed sulphidic material such as stopes and drives, were observable throughout the mine. In the underground mine workings, drilling was observed to act as groundwater conduits, greatly controlling flows, often intentionally in order to manage mine water.

Figure 3.19 Precipitates forming at depth within the southern exploration decline, rock-bolt plate (250 mm by 300 mm) for scale

The southern exploration decline (Figure 2.2) provided an example of where drilling beyond the mine area had intercepted background groundwaters which do not display AMD-based mineral precipitates. Many of the waters infiltrating into the deep mine workings, however, were contaminated by AMD generation at higher mine levels. When deep mine waters were exposed to free oxygen in the mine workings, Fe-precipitates formed on mine surfaces (e.g., Figure 3.19). Like the waters in the upper levels, deep waters which become acidic are managed via drains and sump pumping. These waters are pumped to the tailings facilities for containment and treatment as AMD.

3.4.1.3 Tailings waters

Unoxidised tailings material at Rosebery are a dull grey colour. With the onset of oxidation and generation of AMD, the tailings material changed to the colour of ochre. Although theoretically contained, numerous AMD seeps occur at the foot of the tailings dam walls. Electro-magnetic geophysics (e.g., Wallace, 2002; Andrews and Reid, 2006; and Brown, 2006) supported these observations. In the case of the

tailings dam no. 2 and 5, seeps discharged into: (i) a series of artificial wetlands; (ii) the shallow groundwater regime in the area; and ultimately (iii) the Stitt River. The major seep observed at tailings dam no. 2 (Figure 3.20) flowed into the artificial wetlands and was easily recognisable in the geophysics undertaken by Wallace (2002).

Figure 3.20 Tailings Dam No. 2 Seep, field of view c. 1 m by 0.5 m

Figure 3.21 Water from the Bobadil chimney drain flowing through a v-notch weir

In the case of the Bobadil dam, seeps and waters from retro-fitted chimney drains (Figure 3.21) discharged directly into the polishing pond, and in some cases, to the surrounding shallow groundwater regime or directly to the Pieman River. The presence of secondary Fe-precipitates indicates that the water was contaminated by AMD most likely from the tailings dam. Geophysics undertaken by Brown (2006) displayed extensive electrical conductivity anomalies throughout the walls in the Bobadil dam. Excess water from the Bobadil tailings facility was discharged at a licensed point (BO) directly into the Pieman River.

3.4.1.4 Stitt River

Upstream of the tailings dams, the Stitt River appeared visibly unaffected by AMD. The presence of sulphidic mine materials used on roadways and small scale abandoned mine workings had little observable affect on the catchment. High on the eastern flanks of the Stitt catchment were the small scale abandoned mine workings of Koonya and Grand Central (Figure 2.4). In the upper-southern segment of the Stitt catchment the abandoned Dunkleys tram track, and an unnamed prospect, were the only anthropogenic features (Figure 2.4). A transmission line runs through the catchment from the Rosebery township and the roads servicing this feature were sheeted with mine waste materials, containing visible sulphides.

Surface waters and the shallow groundwater regime in the tailings dams area flowed into the Stitt River, however, this resulted in no apparent visible change in water quality. Rosebery Creek was the most visibly adversely affected natural watercourse in the study area. Downstream of the confluence with Rosebery Creek, the Stitt River changes from what appears to be relatively pristine waters, to a watercourse visibly affected by AMD. The abandoned mine, Blacks P.A. (Figure 2.4), is located on the Stitt River above its confluence with Lake Pieman (Figure

2.16). Dellar (1998) noted that the low flows from Blacks P.A. adit are also affected by AMD.

3.4.1.5 Shallow groundwaters

Discharge of shallow groundwaters (Figure 3.22) was observed at the Bobadil site due to ongoing dam expansion earthworks. Work undertaken by ETS (1996) provided a similar insight into the shallow groundwater regime across the site. Differentiating between shallow groundwater, and interflow, particularly in the very wet winter months was difficult at Rosebery, even with the use of changes in water composition. Intense rainfall resulted in regular seeps appearing out of the surficial covers (Figure 3.24) and fractured rock aquifer (Figure 3.25). Causes of these seeps are either: (i) the groundwater table is recharged to a level which discharges at surface, or (ii) the recharge is retarded at depth by materials with lower hydraulic conductivity resulting in a temporary shallow watertable (or interflow) which discharges at surface. The presence of precipitates favours the former theory, where waters of differing chemistry mix (e.g., Figure 3.24 and Figure 3.25) and the latter where similar waters are involved and no minerals precipitate (e.g., Figure 3.22).

Figure 3.22 Shallow groundwater intersected in a costean 200 m up-gradient of the Bobadil dam site

3.4.1.6 Regional groundwater

Valuable insights into the regional groundwater system were gained where exploration drillholes remained artesian for a considerable time after their drilling (e.g., Figure 3.23). Drillholes may remain artesian as their inclination intersects waters with higher head than the ground level at which they are drilled (Figure 3.5), in addition to conditions of genuine confinement by low permeability overburden. Significant mineral precipitation may occur when a groundwater rich in dissolved minerals is exposed to changes in pH and redox conditions as it: (i) comes in contact with the atmosphere; and/or (ii) mixes with waters of different compositions.

Figure 3.23 Artesian water flowing out of the drillhole 250R at *c*. 1.1 L/s

Figure 3.24 Regular seasonal seepage out of glacial cover 50 m up-gradient of the Bobadil tailings facility. Note the presence of precipitates

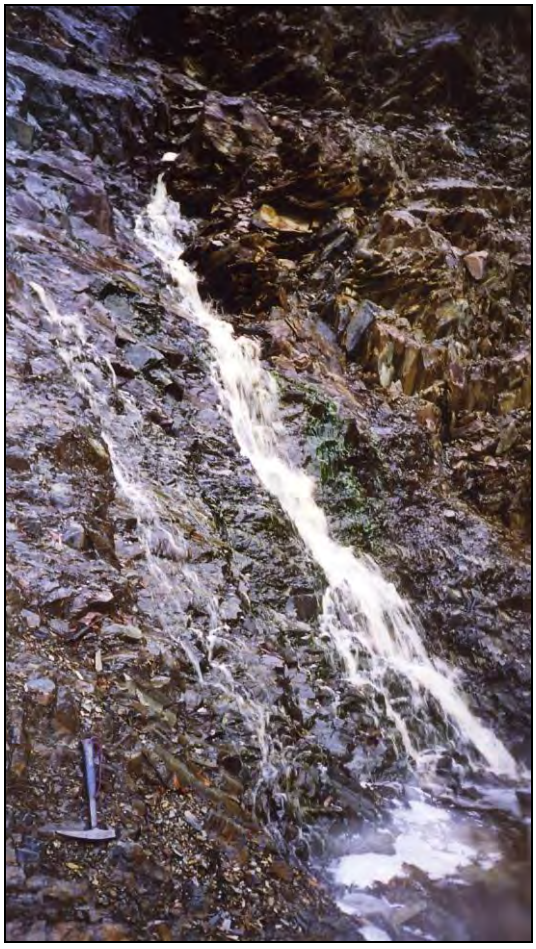

Figure 3.25 A regular winter seep half way up the face of the fractured rock aquifer 50 m up-gradient of the Bobadil tailings facility

3.4.1.7 Pieman River

The deep, high-velocity, Pieman River, with its considerably larger flow than its tributaries in the study area (Hydstra, 2004), appeared visibly unaffected by AMD (Figure 3.26). The waters flowing over the Bastyan Dam, like the waters flowing over the Pieman Dam (Figure 2.10), appear relatively unaffected by AMD. The brown colour is typical of acidic organic rich Tasmanian waters that drain peat-rich forest and button grass catchments (RPDC, 2003).

3.4.1.8 Abandoned mines

Minor flows of AMD-affected waters were observed from the adits of abandoned mines over the study area, as noted previously by Dellar (1998). Iron-rich precipitates from groundwater seepage in the vicinity of the abandoned mines indicated that some degree of the groundwater system was affected locally by AMD from these workings. The small scale nature of these historical operations relative to the current Rosebery mine (Figure 2.4) is evidence that any AMD generated at these workings is likely to be insignificant by comparison.

Figure 3.26 Pieman River beneath the Bastyan Dam

3.5 Summary of observations

The groundwater regime at Rosebery was delineated with observations of piezometric head and the subsequent calculation of hydraulic conductivity values of materials within the Rosebery catchment. Mine data, particularly RQD, provided insight into the spatial variation of local hydraulic properties. There was clear evidence of a weathering induced increase in effective permeability within 100 m of the natural ground surface and an increased effective permeability associated with shear zones and faults. Beyond a depth of 100 m, RQD data also provided clear evidence for a uniform decrease in permeability with depth below the ground surface. Qualitative observation of discharging groundwaters and surface waters throughout the study area provided insight into groundwater flow and surface water interaction within the Rosebery catchment. Together these observations provided the framework for developing a conceptual model of the groundwater regime within the Rosebery catchment.

"In a very real and frightening sense, pollution of the groundwater is pollution of water everywhere" (Carson, 1962).

4 Acid Mine Drainage and Hydrogeochemistry

4.1 Introduction

This chapter reviews geochemical strategies for AMD and hydrogeochemistry research with special emphasis on application to the Rosebery mine and catchment. Geochemical analyses of 36 waters and 75 mine waste materials were undertaken as part of the present study. These new analyses complemented an extensive dataset from previous work in the area (e.g., Finucane, 1932; Braithwaite, 1969 and 1972; Bull, 1977; Green et al. 1981; Green, 1983; Naschwitz, 1985; Corbett and Lees, 1987; Green, 1990; Lees et al., 1990; Khin Zaw, 1991; Pwa et al., 1992; Morrison, 1992 and 1993; ETS, 1996b; Struthers, 1996; Brady, 1997; Atkins, 1998; Blake, 1998; Smith, 1998; Dellar, 1998; East, 1999; Denney, 2000; Hale, 2001; MRT, 2002a, 2002b; 2002c, and 2002d; PRM, 2002; Gurung, 2002; Wallace, 2002; Gurung 2003; and Martin, 2004).

4.1.1 Materials

The aim of geochemical analysis of Rosebery mine materials was to determine their potential to alter the geochemistry of local waters through the processes of AMD generation and neutralisation. Whole-rock and mineral geochemistry from the existing literature (e.g., Finucane, 1932; Braithwaite, 1969 and 1972; Green et al. 1981; Green, 1983; Naschwitz, 1985; Corbett and Lees, 1987; Green, 1990; Lees et al., 1990; Khin Zaw, 1991; Pwa et al., 1992; Blake, 1998; MRT, 2002c; and Martin, 2004) was used to provide information on the potential acid-generating and neutralising minerals, as well as potential contaminants present, whereas new and existing whole-rock acid-base accounting geochemistry (Struthers, 1996; Brady,

1997; and Gurung, 2002 and 2003) provided information on the potential for contamination to occur.

Both economic (ore) and non-economic material (gangue) contribute to AMD. In any underground mining operation a portion of the total ore is either: (i) not extracted due to the mining method, remaining *in situ* and potentially exposed to oxygenated conditions; or (ii) contaminated by gangue due to imperfections in the mining method and is treated as waste material. Depending on the deposit and mining method, a varying proportion of gangue is extracted to access ore and this too is treated as waste material. In an underground operation, waste material may be: (i) returned underground, as ground „fines' or waste rock, into existing voids; (ii) managed as surface waste rock stockpiles; or (iii) managed as ground fines in tailings dams. At Rosebery, waste material is managed with all three of these strategies.

4.1.2 Waters

The aims of geochemical analysis of Rosebery waters were to: (i) provide information on groundwater flow and water-rock interaction; (ii) differentiate between background and contaminated waters; and (iii) determine the quality and maturity of waters. To achieve these, new aqueous geochemical and stable isotope analysis of rain water, mine waters, surface waters and regional groundwaters was undertaken. Both new and existing geochemical data (e.g., Bull, 1977; Morrison, 1992 and 1993; ETS, 1996b; Struthers, 1996; Atkins, 1998; Smith, 1998; Dellar, 1998; East, 1999; Denney, 2000; Hale, 2001; MRT, 2002d; PRM, 2002; Gurung 2002, 2003; and Wallace, 2002) were included in the dataset of the present study.

4.2 Acid Mine Drainage Geochemistry Review

4.2.1 Acid-generating processes

Agricola (1556) first discussed the adverse environmental effects of mine water through the degradation of pyrite to acid and salts, a process that was first recognised by Theophrastus (*ca.* 315 B.C.). Literature references specifically to ‚acid mine drainage' go back to 1913 (Hanna et al., 1963). AMD has recently become a generic term used to describe the generation of acid due to the oxidation of sulphides exposed through mining. Put simply, when sulphides are exposed to oxygen and water, sulphate and sulphuric acid are produced. Using pyrite as an example for all metallic iron sulphides, the chemistry of AMD is typified by Equation 4.1.

$$4FeS_{2\,(s)} + 15O_{2\,(g)} + 2H_2O_{\,(l)} \rightarrow 2Fe_2(SO_4)_{3\,(aq)} + 4H^+_{\,(aq)} + SO_4^{2-}{}_{(aq)} \qquad (4.1)$$

The products of this reaction become the reagents in a series of further reactions, exponentially creating more acid (Mills, 1993). If a stable pH is developed between 2.5 and 3.0, the ferric iron ion (Fe^{3+}) acts as an oxidant (*ibid.*). Ferric iron is hydrolysed to ferric hydroxide above pH 3, and this precipitates as the characteristic rust-coloured stain associated with AMD (*ibid.*). Fe^{3+} is also capable of reacting with many heavy metal sulphides, such as those of lead, copper, zinc, arsenic, cadmium and mercury, through Equation 4.2, where 'M' represents a metal (Dutrizac and MacDonald, 1974).

$$1.5O_{2\,(g)} + H_2O_{\,(l)}\,MS + 2Fe^{3+}{}_{(aq)} \rightarrow M^{2+}{}_{(aq)} + SO_4^{2-}{}_{(aq)} + 2Fe^{2+}{}_{(aq)} + 2H^+_{\,(aq)} \qquad (4.2)$$

AMD generation is greatly accelerated, by up to one million times (Singer and Stumm, 1970), in the presence of bacteria such as the iron oxidising *Thiobacillus ferroxidans*, and the sulphur oxidising *Thiobacillus thioxidans* (Banks et al., 1997). Although biogeochemical processes can be fundamental to AMD generation,

microbiological investigation, geochemical modelling and estimating reactions rates of AMD at Rosebery were beyond the scope of the present study, as the presence of AMD generation was already well established.

4.2.2 Acid-consuming processes

The water quality emerging from mine and waste dumps depends on the chemical behaviour of wall and waste material, and the time dependent balance between the acid-generating oxidation reactions and acid consuming or neutralisation reactions taking place. The neutralisation of potentially acid-generating material is usually associated with calcite, however, many other minerals, for instance feldspar and pyroxene, may play important neutralisation roles (Sherlock et al., 1995). The general formula for the elimination of sulphuric acid by calcite is displayed in Equation 4.3.

$$2H^{+}_{(aq)} + SO_4^{2-}{}_{(aq)} + CaCO_{3\,(s)} \rightarrow Ca^{2+}_{(aq)} + SO_4^{2-}{}_{(aq)} + CO_{2\,(g)} + H_2O_{(l)} \qquad (4.3)$$

Dolomite dissolution is displayed in Equation 4.4 (Shaw and Mills, 1998).

$$CaMg(CO_3)_{2\,(s)} + 4H^{+}_{(aq)} + SO_4^{2-}{}_{(aq)} \rightarrow CaSO_{4\,(aq)} + MgSO_{4\,(aq)} + 2H_2O_{(l)} + CO_{2\,(g)} \qquad (4.4)$$

Chlorite dissolution has been recognised to result in more alkaline conditions through the exchange reaction described by Equation 4.5 (Alpers and Nordstrom, 1990).

$$6H^{+} + Mg_5Al_2Si_3O_{10}(OH)_8 \rightarrow 5Mg^{2+}_{(aq)} + Al_2Si_2O_{5\,(aq)} + 3SiO_{2\,(aq)} + 7H_2O_{(l)} \qquad (4.5)$$

Clay minerals are commonly the products of silicate dissolution. The parent material, reaction conditions (commonly a function of climate), and pH, control whether a montmorillonite group or kaolinite group clay forms (Sherlock et al., 1995). Clay minerals themselves can then result in further neutralisation, as displayed in Equation 4.6 (Lottermoser, 2003).

$$clay\text{-}(Mg^{2+})_{0.5\,(s)} + H^{+}_{(aq)} \rightarrow clay\text{-}(H^{+})_{(s)} + 0.5Mg^{2+}_{(aq)} \qquad (4.6)$$

4.2.3 Acid base accounting

Acid base accounting (ABA) was developed as a means of quantifying the acid-generating and acid consuming potential of materials (Smith and Sobek, 1978). These have been formalised as the „net acid producing potential' (NAPP) and „net acid-generation' (NAG) of a material. ABA is traditionally reported in kg H_2SO_4/tonne or its equivalent kg $CaCO_3$/tonne.

The NAG of a sample is determined by the physical single addition of H_2O_2 to the pulverised material (typically 2.5 g at -75 µm size) under laboratory controlled conditions. This is intended to oxidise any reactive sulphide (AMIRA, 2002). Any net acidity produced is calculated through laboratory titration (Miller et al., 1997; Stewart et al., 2003). A NAG value > 10 kg H_2SO_4/tonne indicates that a sample has a high capacity to form acid, whereas zero indicates that there is no acid forming potential.

The kinetic NAG test is the same as the (single addition) NAG test except that the temperature, pH and EC of the liquor are also recorded over time (AMIRA, 2002). Column leach tests involve the flushing of water over crushed (not pulverised) rock and the product is analysed over time (AMIRA, 2002). Kinetic and column leach tests provide insight into the temporal aspects of AMD, including oxidation rates.

NAPP is calculated using the Maximum Potential Acidity (MPA) and the inherent Acid-neutralising Capacity (ANC) of a material (Equation 4.7).

$$\mathbf{NAPP = MPA - ANC} \qquad \textbf{(4.7)}$$

The ANC of a sample is determined by digesting the pulverised material with 0.1 M HCl and back-titrating with standard 0.1 M NaOH to endpoint pH 7.0 (Sobek et al., 1978; Ferguson and Erickson, 1988; and White et al., 1999). Conversely, MPA is calculated using the percentage of total oxidisable sulphur (TOS), and assuming all

sulphur is present as pyrite using Equation 4.8. Chemical analysis for TOS may use, for example, instrumental neutron activation analysis (INAA) or X-ray fluorescence spectrometry (XRF) (Lapakko, 2002).

$$\mathbf{MPA = TOS \times 30.6} \tag{4.8}$$

The assumption that all sulphur is present as pyrite is not valid for multi-element sulphide deposits where a significant proportion of the sub-grade „ore' material is subject to AMD.

ABA's simplistic approach to acid-generation and consumption has received criticism (e.g., Coastech, 1989; Perkins et al., 1995, Miller et al., 2003; and Stewart et al., 2003). Coastech (1989) and Perkins et al. (1995) discussed the inaccuracies in predicting the net acid production potential and the possibility of improving accuracy by accounting for the mineralogy of samples. Miller et al. (2003) and Stewart et al. (2003) discussed how the single addition NAG test will tend to overestimate acid potential in samples containing high organic matter. However inaccurate, it has become a commonly accepted method of predicting the acid-generating potential of materials within the mining industry (e.g., Lawrence et al., 1988; Lawrence and Wang, 1997; Miller et al., 1997; Price et al., 1997; AMIRA, 2002; Gurung, 2003; and Miller et al., 2003).

Smart and Miller (2005) presented a method for calculating the modified MPA (MMPA), where multiple sulphides are present (Equation 4.9).

$$\mathbf{MMPA} = \sum_{s=1}^{m} \frac{n_s \times 98 \times TOS \times 10}{w_s} \tag{4.9}$$

- n_s is the number of moles sulphuric acid potentially generated from 1 mole of the sulphide mineral s.
- w_s is the molecular weight of the sulphide mineral s.

- m is the number of sulphide species in the sample.
- n_s is determined from NAG reactions of each sulphide mineral.

Application of Equation 4.9 allows theoretical MMPA values to be calculated from whole-rock geochemistry and mineralogical observations.

4.2.4 Aqueous geochemistry

The ANZECC (2000) guidelines provide water quality background values and trigger values for levels at which 95 % of aquatic species in slightly to moderately disturbed freshwater systems are theoretically protected. ANZECC (2000) defined slightly to moderately disturbed systems as "ecosystems in which aquatic biological diversity may have been adversely affected to a relatively small but measurable degree by human activity". These guideline background and trigger values (Table 4.1) form the benchmark for relative toxicity throughout the present study.

Toxicant	Trigger values for freshwater 95 % Species Protection mg/L	Background Australian Freshwater mg/L
Al	0.055	
As (AsIII)	0.024	
As (AsV)	0.013	
Cd	0.0002	0.000001
Cr (CrVI)	0.001	
Cu	0.0014	0.00011
Pb	0.0034	0.00002#
Mn	1.9	0.0015#
Ni	0.011	0.0001
Se	0.011	
Ag	0.00005	
Zn	0.008	0.0009

Table 4.1 Background Australian freshwater concentrations and chemical guidelines of trigger values for toxicants at 95 % species protection levels for slightly to moderately disturbed freshwater systems. # Indicates a world value was used as no Australian value was documented. * Indicates that the low value for New Zealand was used, as no Australian value is documented. (ANZECC, 2000)

Piper (1944) developed a graphical means, now referred to as the Piper diagram, permitting the display of the major cation and anion compositions of many samples on a singular graph. A Piper diagram provides a visual means for deciphering groupings or trends throughout aqueous geochemistry data (Freeze and Cherry, 1979).

Durov (1948) also proposed a graphical representation of natural waters which can be used in a similar manner.

Both Piper and Durov diagrams require the analysis of the major cations (Ca^{2+}, Mg^{2+}, Na^{+} and K^{+}), as well as the major anions (Cl^{-}, SO_4^{2-}, CO_3^{2-} and HCO_3^{-}). Freeze and Cherry (1979) suggested that the major ions generally make up to 90% of natural waters.

Ficklin et al. (1992) developed a graphical means (Ficklin plots) of examining the sum of heavy metal concentrations versus pH of AMD, with the aim of grouping waters into nine categories. Heavy metals included in Ficklin plots are Cd, Co, Cu, Ni, Pb and Zn (Ficklin et al., 1992). Gurung (2002) applied a modified Ficklin classification to Tasmanian waters which also included the metals Fe, Al and Mn as weighting factors due to the relative abundance of these elements in AMD.

4.2.5 Stable isotopic geochemistry

Deuterium and oxygen isotope compositions of water samples provide a useful tool for investigating hydrological processes in surface and groundwater systems (e.g., Dansgaard, 1964; Gat, 1971; Bath et al., 1979; Andrews et al., 1984; Eichinger et al., 1984; Allison and Barnes, 1985; Dutton and Simpkins, 1989; Gat, 1996; Clarke and Fritz 1997; Hoefs, 1997; Seal, 2003; Cartwright and Weaver, 2004; Petrides et al., 2004; Cartwright and Weaver, 2005; and Tweed et al., 2005). In groundwater, the combined δD and $\delta^{18}O$ signatures provide an indication of the climatic conditions under which recharge, and possibly transport, took place (Dansgaard, 1964).

Craig (1961) developed the Global Meteoric Water Line (GMWL), a global averaged relationship between δD and $\delta^{18}O$ which is described in Equation 4.10. Variation from this composition is caused by three principal mechanisms: (i) recharge from areas exposed to evaporation; (ii) recharge that occurred in past periods with

different climates, or (iii) isotope fractionation resulting from water-rock interaction (Gat, 1971).

$$\delta D = 8\,\delta^{18}O + 10 \qquad \textbf{(4.10)}$$

Where the isotopic composition of groundwater is similar to precipitation in the area of recharge, as is typical in temperate and humid climates (Gat, 1971), there is strong evidence for direct recharge to the aquifer (Hoefs, 1997). Recharge from areas exposed to evaporation, such as surface water bodies, is more enriched in δD and $\delta^{18}O$ and plot along an evaporation trajectory with a gradient lower than the meteoric line. Bath et al. (1979), Andrews et al. (1984) and Eichinger et al. (1984) observed lower δD and $\delta^{18}O$ contents in deep groundwaters that formed in colder paleoclimates than more recent shallow groundwaters. Paleo-climatic and seasonal effects can be evaluated by Dansgaard's (1964) empirical temperature scale displayed in Equation 4.11 (which assumes that no oxygen is contributed from other sources).

$$T(^{o}C) = \frac{\delta^{18}O + 13.6‰}{0.695} \qquad \textbf{(4.11)}$$

Equation 4.11 predicts that lighter waters may occur during colder months or during colder periods. Altitude also has a significant effect on the stable isotopic values of waters (Eriksson, 1965 and Stahl et al., 1974), as predicted by departures from meteoric values expected at sea level in Equation 4.12.

$$\delta^{18}O = \frac{-0.2 + 0.4‰}{100\text{ m elevation change}} \qquad \textbf{(4.12)}$$

Variations in deuterium and oxygen isotope compositions from water-rock interactions have also been used in mine settings to differentiate between acid drainage and neutral drainage (Mayo et al., 1992). Mayo et al. (1992) states that acid mine waters have more positive values of $\delta^{18}O$, corresponding to higher temperatures

associated with exothermic acid-generating reactions (e.g., Equation 1). Seal (2003) states "oxygen and hydrogen isotopes in waters can provide insights into {water} budgets at minesites, and the processes that affect the waters."

4.2.6 Climate and topography

Plumlee (1995) established that AMD tends to have lower pH and higher metal contents in dryer, rather than in wetter climates, due to evaporative concentration of acid and metals. Dry climate mine drainage water, with low pH and high metal content may have less environmental impact than a similar water, in a wet climate setting because of the relatively small volume of surface drainage water (*ibid*.). Downstream dilution of AMD by water draining unmineralised areas is much more efficient in wet climates than in dry climates; however, downstream mitigation is enhanced in dry climate settings by the increased buffering offered by solid material in stream beds (*ibid*.).

Quantifying the effect of climate on AMD is difficult because insufficient data are available for any given deposit type in a wide spectrum of climatic and physical settings (Seal and Hammarstrom, 2003). Such multi-parameter "geoenvironmental models" that Seal and Hammarstrom (2003) propose, are beyond the current state of research in western Tasmania, and those developed in wet, temperate, mountainous sulphide-mining districts elsewhere to date.

4.3 Analytical Methods and Sampling Strategies

4.3.1 Acid base accounting

The present study examined 75 samples of mine materials, both outcrop and waste material, within the vicinity of the Rosebery open-cut and waste rock stockpiles (Figure 4.1). This area was chosen as many of the major rock types occur as outcrop in this part of the mine workings, and the waste stockpiles provide a representative

sample of the exposed material that will remain after mine closure. The results were therefore applicable to both the mine workings and the waste piles. Previous local ABA studies at Rosebery (Struthers, 1996) were applied to represent the tailings material.

Sampling methods included: (i) chip sampling from outcrop or open-cut walls (at grade-line where possible); and (ii) grab sampling from waste material (within 2 m channels where possible). Access, geotechnical, and safety constraints compromised the collection of further outcrop samples within the open-cut environment. AMINYA Laboratories in Burnie undertook analysis for the ANC and single addition NAG of the seventy-five 10 kg samples.

At Rosebery, ANC provided a best case scenario that quantified the potential volume of H_2SO_4 that could be consumed by each kg of material. Rosebery ore and gangue contains a combination of many sulphides and sulpho-salts (Martin, 2004) as well as a significant percentage of barite (Finucane, 1932), so determining TOS as part of the ABA was not undertaken. Combined with NAG, ANC provided a valuable tool for determining: (i) the potential that a material has to create acid; and (ii) the potential surrounding materials have to neutralise that acidity.

4.3.2 Whole-rock and mineral geochemistry

New whole-rock and mineral geochemical analyses were not undertaken as part of the present study due to the abundance of existing data (e.g., Finucane, 1932; Braithwaite, 1969 and 1972; Green et al. 1981; Green, 1983; Naschwitz, 1985; Corbett and Lees, 1987; Green, 1990; Lees et al., 1990; Khin Zaw, 1991; Pwa et al., 1992; Blake, 1998; MRT, 2002c; and Martin, 2004). Instead, data from these ore deposit and exploration studies were examined and interpreted from an AMD perspective. In the present study, whole-rock geochemistry provided information on:

(i) the potentially acid-generating sulphide material; and (ii) the potentially acid-neutralising material available. Mineral geochemistry also contributed to the understanding of potential acid-generating and neutralisation reactions. Also, of particular interest were the elevated trace elements in the Rosebery sulphides that had the potential to become contaminants.

4.3.3 Aqueous geochemistry

The environmental impact of AMD can be estimated in a preliminarily way by measuring pH, however, Gurung (2002) found that surface waters in catchments affected by abandoned mine sites across Tasmania display a wide variation in dissolved metals and sulphate concentrations at pH range 2.0 to 9.0. Characterisation of AMD with such wide variation in surface water chemistry requires multi-parameter analysis (Gurung, 2002).

The Rosebery mine, like many operating mines, has undertaken multi-parameter analysis in its routine environmental impact assessment over a number of years (PRM, 2002). The emphasis on water analysis at Rosebery has been on dissolved metal contents rather than on major ion chemistry, other than sulphate (*ibid*.).

The procedure for groundwater monitoring at Rosebery, including the steps needed to collect and analyse a standard groundwater sample, is provided in Appendix Three. Samples for isotopic analysis were taken in a similar manner wherever possible; however, in low flow seeps, the use of medical syringes was adopted to obtain an uncontaminated sample from the specific area of interest. Water sample locations are presented in Figure 4.2.

In May 2002, the first round of 14 samples were obtained across the catchment. Samples were taken from waters: (i) near the mine; (ii) distal to the mine; and (iii) within the mine itself, to characterise the aquatic system and expand the sample sites

within the existing PRM (2002) database. In August 2003 the second round of samples were taken at additional sites with consideration towards delineating end members within the catchment.

The first round of regional hydrogeochemical samples (14 samples) of regional samples was sent to the Pasminco Cockle Creek laboratory for analysis of Al, As, Ca, Cd, Cl, Cr, Cu, F, Fe, K, Mg, Mn, Na, Ni, P, Pb, Si, SO_4^{2-}, and Zn using: flame atomic absorption spectrophotometry (AAS); hydride AAS; I.S.E and; Gravimetric techniques. Of the metals analysed in the initial sampling round (Al, As, Ca, Cd, Cr, Cu, Fe, K, Mg, Mn, Na, Ni, Pb, and Zn), only Al, Ca, Cd, Cu, Fe, Mg, Mn, Pb and Zn were analysed routinely from Rosebery waters according to PRM (2002).

The second round of aqueous geochemical samples (22 samples) was sent to WSL Environmental Services and Mineral Resources Tasmanian (MRT) for analysis. WSL Environmental Services provided analysis of Fe, Mn, Zn, Cu, Pb, Cd, Ca, Mg, As, SO_4^{2-}. Major cations (Na, Ca, K Mg) were analysed using inductively coupled plasma-atomic emission spectroscopy (ICP-AES), trace metals (Fe, Mn, Zn, Cu, Pb, Cd and As) with inductively coupled plasma-mass spectrometry (ICP-MS) and SO_4^{2-} by photometer. MRT provided gravimetric analyses for total dissolved solids (TDS) and SO_4^{2-}, volumetric analysis for CO_3^{2-}, HCO_3^-, Alkalinity and Cl^-, flame AAS for Al^{3+} Na^+, K^+, Ca^{2+} and Mg^{2+}, ISE for F, colour for NO_3^-. Detection limits for all analytes are tabulated in Appendix Three; in some cases multiple detection limits are recorded for the same analyte due to changes in methods and laboratories over time.

Analytes are tabulated throughout the present study as minimum, maximum and mean values for datasets of n (number) of samples. Mean, in the present study refers, to the arithmetic mean of a dataset. The mean calculations in the present study include zero values as well as trace values set to the detection limit as defined in the

dataset. For consistency, analyses are presented in dissolved mg/L where possible throughout the present study. Results (including detection limits as data) are graphically represented spatially and through established methods (e.g., Piper, 1944; and Ficklin et al., 1992).

4.3.4 Stable isotope analysis

Twenty-one water samples were analysed for deuterium and oxygen isotope compositions as part of the present study, to add to the existing data set of 11 analyses undertaken by Hale (2001). The samples were collected at the sample sites used in the second round of aqueous geochemistry sampling (Section 4.3.3). At each site a 10 ml sample was collected in McArtney bottles and sent for analysis. The isotopic compositions of deuterium and oxygen in water were measured and expressed relative to international standards (rel ‰ Vienna Standard Mean Ocean Water (VSMOW)). The Commonwealth Scientific and Industrial Research Organization (CSIRO) Adelaide Laboratory Isotope Analysis Service analysed the samples using a Europa Geo 20-20 gas isotopic ratio mass spectrometer for oxygen, and an on-line H_2O reduction system for deuterium. Analytical errors were 1‰ for δD and 0.15‰ for $\delta^{18}O$, normalised to the SMOW-SLAP scale (CSIRO, 1998). The use of the radioactive ^3H tritium was proposed for the dating of groundwater ages throughout the study area, however, this had to be discarded due to economic constraints.

4.4 Previous Findings

4.4.1 Acid base accounting

Only limited acid base accounting (ABA) had been undertaken at Rosebery prior to the present study (Figure 4.1). Struthers (1996) determined, through ABA of one sample, that the preconditioned Rosebery tailings were strongly acid-forming (Table 4.2). Kinetic column leach testing suggested that preconditioned Rosbery

tailings were likely to become acidic in the medium to long term even with an ANC value of 55.79 kg H_2SO_4/t (Struthers, 1996). Process preconditioning of tailings at Rosebery involved the addition of lime at a rate of 0.2 - 0.3 kg/kL slurry (Struthers, 1996), to act as an acid buffer. The high ANC was enhanced by the addition of lime; fresh tailings direct from the mill will therefore give much stronger acid forming results than those measured after lime addition (Struthers, 1996).

Brady (1997) conducted ABA on 22 samples from the open-cut, determining that all material sampled was potentially acid-forming. Table 4.2 presents the range of results from Brady (1997). Results from Struthers (1996) and Brady (1997) were included in the dataset for this thesis, however, both studies did not describe their sample locations sufficiently, and as a result this previous work could not be represented spatially with confidence.

Gurung (2002) conducted ABA studies across 984 abandoned and operating mines throughout Tasmania. Using the existing databases MIRLOCH (MRT, 2002a), TASGEOL (MRT, 2002b), and ROCKCHEM (MRT, 2002c), Gurung (2002) calculated estimates of NAPP by obtaining average TOS and ANC for each rock type. 43 NAPP values were generated from the database information over the study area (Figure 4.1). Gurung (2002) also undertook ABA studies on 4 samples collected within the Rosebery mine, generating ANC and NAPP values. These data have been included in the geochemical dataset used in the present study and are presented in Appendix Two.

Study	ANC (kg H_2SO_4/t)	NAG (kg H_2SO_4/t)	NAPP (kg H_2SO_4/t)	n
Struthers, 1996	55.79	39.2	230.32	1
Brady, 1997	-8 to 38	3 to 69	6 to 148	22
Gurung, 2002 *	5.06 to 32.34		-28.17 to 122.4	43
Gurung, 2002	0.49 to 24.5		414.13 to 795.11	4

Table 4.2 Ranges of previous ABA results at Rosebery after Struthers (1996), Brady (1997) and Gurung (2002). * Calculated values based on (MRT, 2002a, 2002b and 2002c)

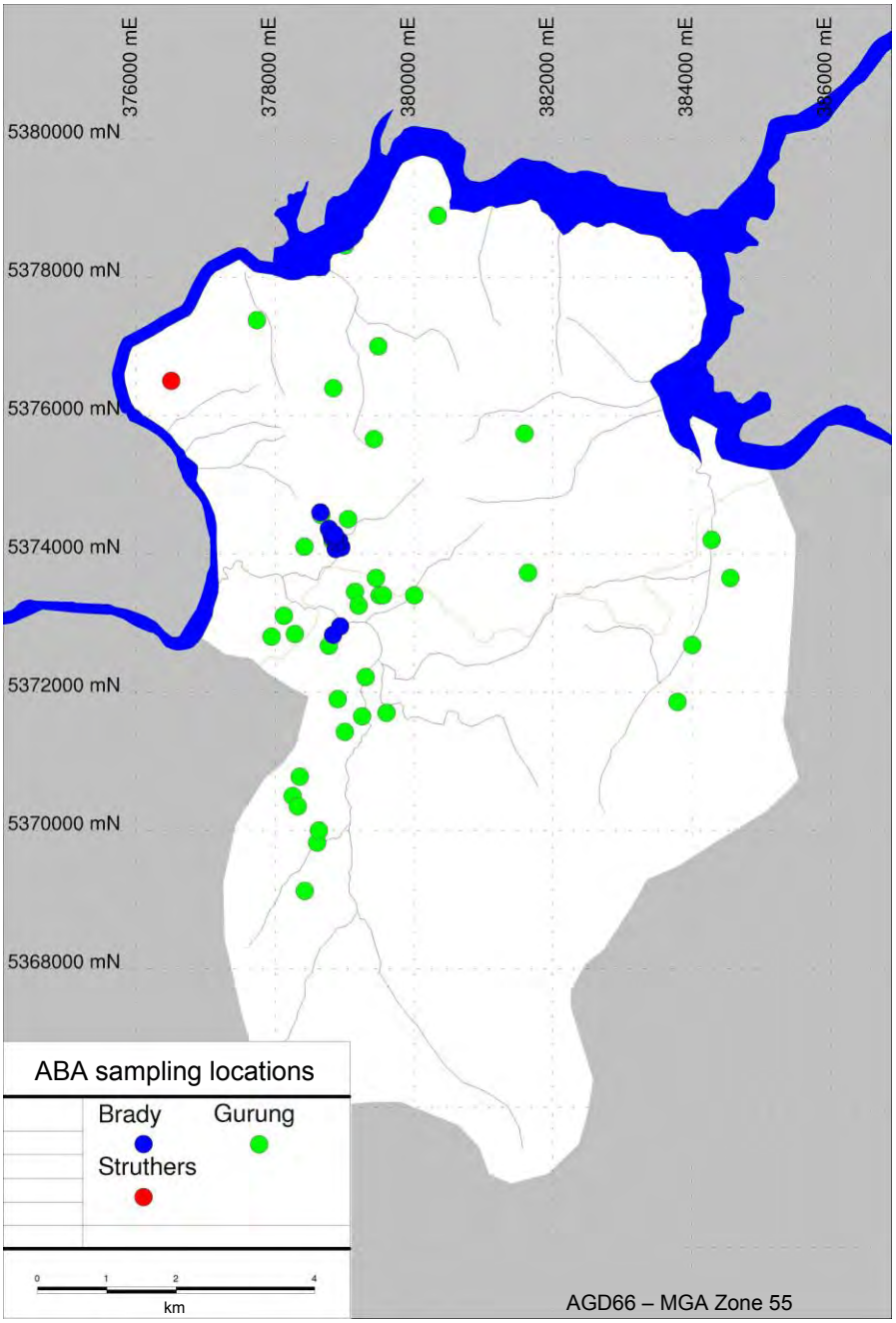

Figure 4.1 ABA sampling locations after Struthers (1996), Brady (1997) and Gurung (2002). Note: Location from Struthers (1996) and Brady (1997) were approximate sample locations based on sample site descriptions

Gurung's (2002) work across Tasmania determined that occurrences of high sulphate and high metal waters were closely associated with abandoned mine sites containing sulphidic materials with high NAPP. Gurung (2002) also determined that many of the volcanic-hosted mineralised metasediments in the West Coast mineral fields, including those from Rosebery, generally have NAPP > 500 kg H_2SO_4/t and

low to negligible acid-neutralising capacity (ANC). Thirty-five of the 47 NAPP values generated over the study area (Gurung, 2002) were positive, indicating the potential for acid-generation to occur. Most rock types over the study area, including those in the mineralised zone, had theoretical ANC values below 30.6 kg H_2SO_4/t, indicating that any materials containing a sulphur content >1% would have a positive NAPP.

4.4.2 Whole-rock and mineral geochemistry

4.4.2.1 Host rocks

Finucane (1932) first defined the average mineralogical composition of metallic and non-metallic minerals within Rosbery ore (Table 4.3). Since this work, the geochemistry of the Rosebery deposit has been studied extensively since (e.g., Braithwaite, 1969 and 1972; Green et al., 1981; Green, 1983; Nmaschwitz, 1985; Corbett and Lees, 1987; Huston and Large, 1988; Green, 1990; Lees et al., 1990; Khin Zaw, 1991; Smith and Huston, 1992; Pwa et al., 1992; Struthers, 1996 and Martin, 2004). Martin (2004) sumarised that the majority of the gangue material in the sulphide ore is sericite, quartz, carbonate, barite, chlorite and minor rutile. Tourmaline, magnetite, haematite, garnet, fluorite and helvite can also be present in ore affected by Devonian metasomatism (*ibid*.).

Metallic minerals	Percent	Non-metallic minerals	Percent
Sphalerite	35.2	Quartz	7.8
Pyrite	31	Sericite and aluminous silicates	6.7
Galena	7.3	Barite	2.5
Chalcopyrite	0.9	Rhodochrosite	2.2
Arsenopyrite	0.7	Dolomite, calcite and ankerite	3.2
Tetrahedrite and bournonite	0.25-0.40	Orthoclase and albite	1.6
Magnetite and ilmenite	0.5		
Total	76		24

Table 4.3 Average mineralogical composition of ore at Rosebery (Finucane, 1932)

The host rock is characterised by enrichment of TiO_2, Al_2O_3, Fe_2O_3, MgO, K_2O CaO, MnO, P_2O_5, Pb, Zn, Rb, Ba and Tl, and depletion of SiO_2, Na_2O, Cu and Sr. (Pwa et al., 1992). Smith and Huston (1992) stated that elements concentrated in the upper portions of the orebody and in the adjacent hangingwall rocks include Pb, Zn, Au, Cd and Sb, whereas Pwa et al. (1992) also identified Ba, As, Sb and Ag. Elements concentrated in the lower portions of the orebody and adjacent footwall rocks include Cu, Bi, As, and Fe (Smith and Huston, 1992). Smith and Huston (1992) presented a summary of the the variation of mineral abundances between the three ore types at Rosebery (Table 4.4).

The footwall alteration zone is characterised by enrichment of Si, K, Cu, Rb Mn, Fe, Mg, S and H_2O and depletion of TiO_2, Al_2O_3, CaO, Na_2O, P_2O_5, Sr, Ba, Tl, Zr, Y and Nb (Green et al., 1981; Naschwitz, 1985; Naschwitz and van Moort, 1991; and Pwa et al., 1992). Smith and Hudson (1992) stated that Hg was also dispersed well outside zones of strong mineralisation at Rosebery in the footwall alteration zone.

4.4.2.2 Country rocks

Collectively the uneconomic rocks including the footwall, hangingwall and black slate were referred to in the present study as the „œountry rocks' as opposed to the „host rocks', which is used to refer to economic ore bearing rocks. Whole-rock geochemistry beyond the Rosebery mine area was contained in the databases MRCHEM (Blake, 1998) and ROCKCHEM (MRT, 2002c) and Gurung (2002). Smith and Huston (1992) tabulated background concentrations of selected elements in the Rosebery area, examining three rock types: (i) felsic volcanics (ii) hangingwall epiclastics; and (iii) shales and siltsones. Samples from the hangingwall epiclastics were not enriched in any of the elements studied (Smith and Huston, 1992). Results of the two other rock types are presented in Table 4.5.

Mineral	Pyrite-chalcopyrite ore (vol %)	Sphalerite-galena-pyrite ore (vol %)	Barite ore (vol %)
Pyrite	30-80	10-30	0-10
Chalcopyrite	2-10	0.5-2	0-1
Sphalerite	1-5	20-60	0-40
Galena	0-2	5-20	0-15
Arsenopyrite	0-1	0-1	Nil
Tetrahedrite -tennantite	0-0.5	0.2-1	0.2-3
Magnetite	0-0.2	0-0.2	Nil
Pyrrhotite	0-0.1	Nil	Nil
Kobellite	0-0.1	Nil	Nil
Cosalite	0-0.1	Nil	Nil
Bismuth	Trace	Nil	Nil
Electrum	Trace	Trace	Trace
Bournonite	Nil	Nil	Trace
Argentite	Nil	Trace	Nil
Quartz	0-7	2-10	1-5
Sericite	1-5	1-5	1-5
Chlorite	2-10	2-10	0-0.5
Carbonate	1-5	1-5	2-7
Barite	Nil	0-2	5-80
Albite	Nil	0-2	1-5

Table 4.4 Variation of mineral abundances (vol %) between ore types, Rosebery deposit (Smith and Huston, 1992 after data from: Braithwaite (1969 and 1974); Green et al. (1981); and Huston and Large (1992))

	Global		Mount Read Volcanics	
Element	Felsic volcanics	Shales and siltstones	Felsic volcanic	Shales and siltstones
Pb	9-29	18-28	13±19	10-42
Zn	33-500	46-197	74±116	45-145
Cu	3.3-25	21-67	12±16	6-65
Ag	0.02-0.09	0.11-0.43	0.02-0.32	0.26-0.70
Au	0.0007-0.005	0.0025-0.0039	0.0001-0.0028	0.0006-0.0001
Bi	0.02-0.22	0.1-2.1		
As	0.5-5.9	3.2-14	0.5-5.7	4-11
Sb	0.1-0.6	0.2-3	0.5-1.8	<1-1
Cd	0.05-0.48	<0.3-8.4		0.3-0.36
Tl	0.7-3.2	0.3-1.6	0.7-1.4	0.49-0.97

Table 4.5 Background concentrations (ppm) of selected elements in the Rosebery area after Smith and Huston (1992)

Russell and Van Moort (1981) conducted a comparative study of element distribution in soils and plants in the White Spur area near Rosebery. Russell and Van Moort's (1981) work determined that Cu, Pb, Zn, Fe, Ni, Ba, Mn and Cd were preferentially concentrated in the wood bark and leaves of trees. Thus, the local

surficial peats could be enriched in these elements, which may be released on contact with AMD.

4.4.2.3 Tailings material

Struthers (1996) investigated the geochemistry of Rosebery tailings, determining that elements with levels raised significantly above crustal averages include Fe, Mn, Ba, Cu, Pb, S, Zn, and Ag. Struthers (1996) also identified other "environmentally significant elements" (As, Bi, Cd and Sb) as being significantly above crustal averages. Table 4.6 and Table 4.7 provide a summary of the average geochemistry of Rosebery tailings.

Fe %	S %	CaO %	MgO %	SiO_2 %	Al_20_3 %	MnO %	K_2O %
12.23	12.95	1.26	1.57	46.63	8.46	2.1	2.15

Table 4.6 Average volume percentage of gangue minerals in Rosebery tailings after Struthers (1996)

As %	Cd %	Pb %	Zn %	Cu %	Ni %	Sb %	Ba %	Bi %	Co %	Ag g/t	Au g/t
0.07	0.005	0.5	1.33	0.11	0.01	0.0041	1.11	0.0016	0.02	19.68	0.78

Table 4.7 Average percentage (unless otherwise stated) of trace elements in Rosebery tailings after Struthers (1996)

4.4.3 Sulphide mineralogy and geochemistry

Some trace elements in the Rosebery sulphides have the potential to become mobile contaminants when the sulphides oxidise or are exposed to AMD. The elements identified through past micro-analytical geochemistry provided constraints on the interpretation of aqueous geochemistry of the study area (Section 4.4.4).

Montgomery (1895) described the occurrence of Zn, Pb, Cu, Au and Ag ores as well as pyritic schist at Rosebery. Over the last century of mining and exploration in the district, sulphide, mineralogy and trace element geochemistry at Rosebery have been studied extensively (e.g., Stillwell, 1934; Loftus-Hills et al., 1967; Groves and Loftus-Hills, 1968; Loftus-Hills, 1968; Braithwaite, 1969 and 1972; Smith, 1975;

Henley and Stevenson, 1978; Green et al., 1981; Green, 1983 and 1990; Khin Zaw, 1991; Smith and Huston, 1992; Huston et al., 1993; Huston et al., 1995; Khin Zaw and Large, 1996; Vallerine, 2000; and Martin, 2004). Table 4.8 summarises the research into the trace element chemistry of sulphides at Rosebery.

Martin (2004) conducted a comprehensive review of sulphide trace element contents at Rosebery. His major findings have been tabulated and are presented in Table 4.9 to Table 4.12. Table 4.9 summarises Martin's (2004) observations of the major sulphide phases, the occurrence of each sulphide, and the type of mineralisation it is physically associated with.

Martin (2004), using an LA-ICPMS method with spot sizes ranging from 20-100 μm and an electron microprobe, investigated the composition of Rosebery sulphides, building on work from Huston et al. (1993). Table 4.10 summarises Martin's (2004) trace element findings for Rosebery sulphides.

Sulphide	Trace Element	Reference
Pyrite	Multi Element	Loftus-Hills and Solomon (1967), Loftus-Hills (1968), Henley and Stevenson(1978), Huston et al. (1993, 1995), Martin (2004)
	Co & Ni	Green et al. (1981), Green (1983)
	Se	Huston et al. (1995)
Sphalerite	Multi Element	Henley and Stevenson (1978), Huston et al. (1993, 1995), Green et al. (1981), Green (1983) and Martin (2004)
	Cd	Groves and Loftus-Hills (1968), Khin Zaw (1991), Khin Zaw and Large (1996)
	Mn & Fe	Khin Zaw and Large (1996)
Chalcopyrite	Multi Element	Huston et al. (1993); Huston et al. (1995) and Martin (2004)
Tetrahedrite Tennantite	Multi Element	Smith (1975), Henley and Stevenson (1978), Vallerine (2000), Martin (2004)
Sulpho-salts	Multi Element	Stillwell (1934), Williams (1960), Martin (2004)

Table 4.8 Previous sulphide trace element research

Table 4.11 sumarises Martin's (2004) observations of inclusions and the resultant additional trace elements within the three major sulphide phases at Rosebery: pyrite, sphalerite, and galena.

Trace elements occur as (i) inclusions, or (ii) replacements within the crystal lattice of the sulphide mineral at Rosebery. Table 4.12 sumarises Martin's (2004) research on elemental replacement within the sulphide lattice of the three major sulphide phases at Rosebery.

Occurrence	Pyrite	Arseno-pyrite	Sphalerite	Galena	Chalco-pyrite	Tennantite tetrahedrite	Sulpho-salts
Fine disseminations	MS						MS
Disseminations	MS, MB		MS	MS	MS		
Coalesced masses			MS	MS	MS		
Grains		MS	MS	MS	MS	MS, MB	
Bands	MS, MB		MS	MS	MS		
Alteration	DM	HO, DM	DM	DM	DM		
Veins	MS, MB, SPD, DM	SPD, DM	MS, SPM, DM	MS, SPM, DM	MS, SPM, DM	SPD, DM	SPD
Faults	SPD		SPD	SPD	SPD		
Lens	MS, MB						

Table 4.9 Summary of sulphide occurrence and association at Rosebery after Martin (2004). Where MS refers to massive sulphide, MB to massive barite, DM to Devonian metasomatism and SPD refers to syn- to post-deformation

Analysis Method	n	Electron microprobe	n	LA-ICPMS
Pyrite	373	As	366	Co, Bi, Mn, Ni, As, Ag, Au, Pb, Sb, Tl, Sn
Sphalerite	294	Fe, Mn, Cd	366	Ag, Mn, Sn, Sb, Cu, Pd, Bi
Tennantite & Tetrahedrite	79	Ag, Cu, As, Sb, Fe, Te, Zn	9	Mn, Sn, Bi
Galena	81	Ag, Zn, Sb	0	-
Arsenopyrite	25	-	10	Co, Ni, Sb, Au, Pb, Bi, Ag, Tl
Chalcopyrite	93	As, Ag, Au	42	Ag, Sn, Zn, As, Sb, Pb, Bi
Pyrrhotite	9	As	0	-

Table 4.10 Rosebery sulphide trace element chemistry after Martin (2004)

Sulphide	Inclusions (Trace Elements)
Pyrite	Galena (Pb, Sb, Ag, Bi), sulpho-salts (Cu, As, Sb, Ag, Bi, Sb, Pb, Tl, Hg), electrum (Au, Ag, Hg), arsenopyrite (As), sphalerite (Zn, Mn, Cd), chalcopyrite (Cu)
Sphalerite	Galena (Pb, Sg, Ag, Bi), sulpho-salts (Sb, Ag, Bi, Pb, Cu), electrum (Au, Ag, Hg) and chalcopyrite (Cu)
Galena	Sphalerite (Zn)

Table 4.11 Inclusions and trace elements within Rosebery sulphides after Martin (2004)

Sulphide	Element replaced	Replacement elements
Pyrite	Fe	Co, Ni, As, Sb, Mn, Sn, Mo, (possible low Au, Ag, Cu, Tl)
Sphalerite	Zn	Cd, Fe, Mn, As, Co, Sn
Galena	Pb	Ag, Sb

Table 4.12 Elemental replacement within the sulphide lattice (after Martin, 2004)

4.4.4 Aqueous geochemistry

Bull (1977) was the first to examine and document the chemical properties of Rosebery tailings water, though one sample only was studied. Routine multi-element surface water geochemistry sampling has become standard practice on the Rosebery Mining Lease since 1990 (ETS, 1996a and 2001). Originally sampling was only at the Bobadil outlet into the Pieman River, however, it has now been extended to cover 47 sample points (Figure 4.2). Environmental staff at the Rosebery mine maintained an aqueous geochemical database (PRM, 2002) containing over 4000 multi-element sample results. Although most samples were taken from surface waters, many were representative of recently emerged groundwater or surface waters, influenced by groundwater interaction.

Although extensive, the primary purpose of routine water monitoring was to determine if discharges exceeded regulatory limits. Very little interpretation of the results has been documented. The present study identified numerous errors in the database, PRM (2002). This cast doubt on the integrity of the remaining data and its format. Typically historical data available from mine sites are not within the control of current practises of quality assurance and control. As part of the present study, all results were checked back to the original lab sheets and the database was corrected, verified and returned to PRM. The corrected surface water monitoring database, PRM (2004) provided the bulk of the hydrogeochemistry dataset. The present study extended monitoring to cover regional, shallow, and surface discharging groundwaters and incorporated them into PRM (2004).

Koehnken (1992) examined waters of the Pieman and Stitt Rivers concluding them to be adversely affected by AMD. Morrison (1992) undertook sampling and detailed trace element geochemistry of streams throughout Tasmania, including Mt Black's Mountain Creek (Figure 4.2). Table 4.13 lists the mean values for some of the relevant metals from the present study.

	Fe	Zn	Cu	As	Sn	Se	Co	Mn	Ni	Cd	Cr	Pb
Maximum (ppb)	189.1	16.7	6.6	1.6	0.5	3.1	0.2	17.3	0.5	8.6	1.1	6.7
Mean (ppb)	132.0	4.8	1.8	0.9	0.4	1.0	0.1	7.3	0.4	4.7	0.7	1.4
Minimum (ppb)	101.3	1.6	0.2	0.4	0.2	0.3	0.1	0.9	0.1	1.7	0.2	0.0

Table 4.13 Selected Mountain Creek trace element concentrations in ppb (after Morrison, 1992)

Morrison (1993) undertook further sampling of waters away from the mining environment draining over the footwall sequence, Mount Black Formation and White Spur Formation. This work identified that drainage on the White Spur Formation was characterised by high Cd (as well as, Cr, Fe, Co, Ni and Pb). Morrison (1993) also found that drainage on the Mount Black Formation was characterised by low Cd and drainage on the footwall sequence by low Zn.

Environmental and Technical Services (ETS, 1996b) undertook a shallow groundwater quality investigation for Pasminco Mine Rosebery. This study contained analyses of 17 samples within the study area, 12 of which were groundwater. These samples, all taken down gradient of mine features, were analysed for metals and major ions and indicated that shallow groundwater and surface runoff were also contaminated by AMD at the mine and tailings dam areas (ETS, 1996).

Atkins (1998) conducted an investigation of groundwater seepage from the tailings dams and an evaluation of a wetland treatment system (Figure 4.2). 15 samples were analysed for trace elements and major ions and the results indicated that the wetlands were not improving acid water seepage from tailings dam no. 2 sufficiently for discharge into the Stitt River (Atkins, 1998).

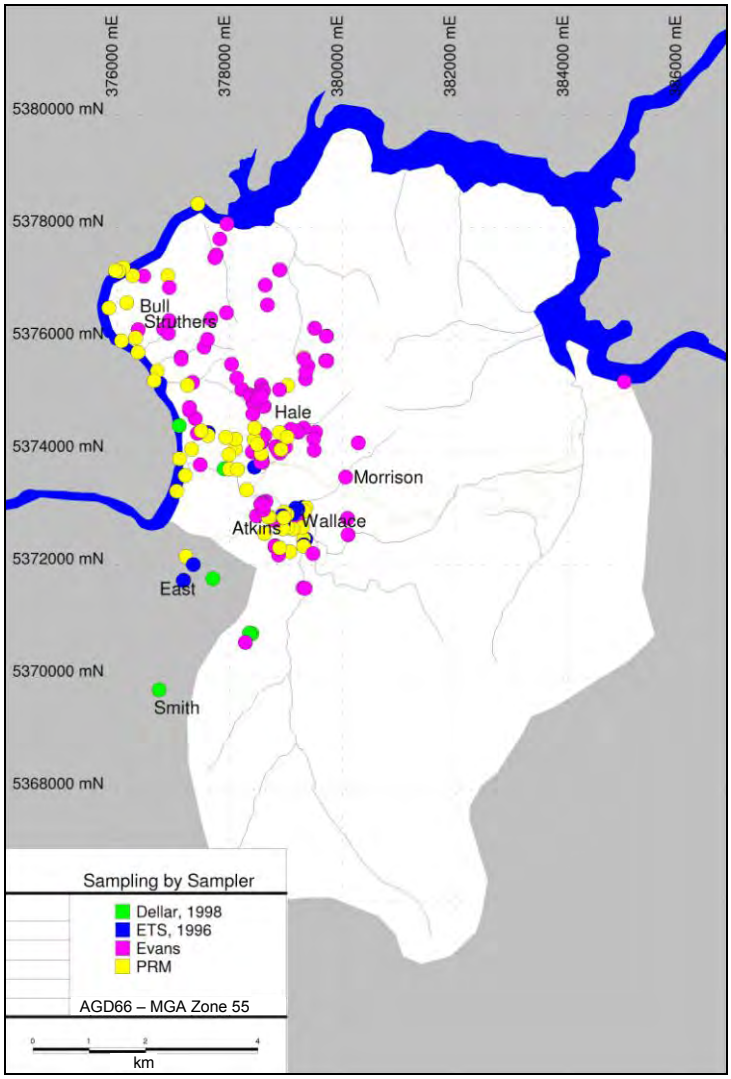

Figure 4.2 Aqueous geochemistry sample locations (after Bull, 1977; Morrison, 1992; ETS, 1996b; Struthers, 1996; Atkins, 1998; Smith, 1998; Dellar, 1998; East, 1999; Hale, 2001; PRM, 2002; and Wallace, 2002). The approximate location of the study areas of Bull, 1977; Morrison, 1992; Struthers, 1996; Atkins, 1998; Smith, 1998; East, 1999; Hale, 2001; and Wallace, 2002 are denoted by the authors name; Evans refers to the present study

Abandoned small-scale mine workings are present throughout the Rosebery district (Section 2.2.5, Figure 2.4). Small-scale mines provide closure analogies for the Rosebery mine, and indicate the potential for long term AMD generation. Waters from abandoned mines throughout the study area were examined by Dellar (1998). Nineteen water samples from her study area were analysed for trace elements and major ions. The abandoned workings of Blacks P.A., Jupiter, Koonya, and Salisbury (Figure 2.4) proved to be discharging acidic drainage in the area (Dellar, 1998). AMD from the abandoned Hercules mine, south of the study area was studied by

Smith (1998) and ETS (2001) (Figure 4.2). East (1999) collected 22 groundwater samples at the TME smelter site *c.* 1 km east of the study area (Figure 4.2). Analyses of metals, trace elements and major ions indicated the TME smelter site was discharging AMD into the downstream environment (*ibid*.). East (1999) indicated that locally, sulphate alone could be used to determine the extent of AMD contamination.

Denney (2000) investigated metal speciation in the Pieman River including three sample sites within the study area: (i) on the Pieman above Bobadil; (ii) the Sterling River; and (iii) Stitt River. Denney's (2000) work concluded that metal ion complexation, speciation and hence bioavailability of these metals was found to be highly variable within the Pieman River catchment. Eighty percent of the total Cu concentration in Lake Pieman waters was accounted for by complexation of Cu associated primarily with dissolved organic material (*ibid*.). Zinc concentrations within Lake Pieman typically exceeded potential complexation capacity. Labile Zn concentrations exceeded water quality criteria (Denney, 2000). Denney's (2000) work suggests that a significant proportion of the dissolved Cd and Zn, in the Stitt River is bioavailabile.

Hale (2001) investigated aspects of acid mine drainage at the Rosebery mine and provided insights into the geochemistry of mine waters in the area. Hale (2001) collected a total of 28 water samples which were analysed for trace elements and major ions. An additional 145 pH and electrical conductivity readings and 111 flow measurements were taken within the mine. At Rosebery, uncontaminated groundwaters entering the mine were observed to become strongly acidic (pH 2 to 3) two years after mining occurred (*ibid*.). Hale (2001) determined that mine waters were contaminated with Cu, Fe, Mn, Mg, Pb and Zn at Rosebery.

Wallace (2002) conducted a study of 28 water sample sites to quantify the amount and extent of AMD emanating from the tailings dam no. 1, 2 and 5 area (Figure 4.2). Wallace (2002) found that major cations (Al, Ca, Fe, K, Mg, Mn, Na and Si), anions (Cl^- and SO_4^{2-}), and trace metals (As, Cd, Co, Cr, Cu, Mo, Ni, Pb, and Zn) were all concentrated within and at the foot of no. 2 dam wall in AMD. Apart from Sn, all concentrations of dissolved constituents decreased with distance from the point source (*ibid*.). Wallace (2002) determined that due to high flow relative to surface area, the wetlands were unable to sufficiently treat their input to an acceptable level.

Of particular interest in Wallace's (2002) study was the dissolved trace element work on 70 samples, as his study achieved lower detection limits than previous studies. Wallace's (2002) work returned Ni concentrations up to 0.055 ppm-well above background and *c.* 5 times the ANZECC (2000) 95% trigger values. The highest As value recorded was 0.16 ppm which was an order of magnitude higher than the ANZECC (2000) 95% trigger level. High Ni values were significant as they had not been investigated in AMD at Rosebery previously. The highest Cr concentration was 0.223 ppm, significantly higher than the ANZECC (2000) 95% trigger level. Mo analysis gave results up to 0.442 ppm. Co samples with values up to 0.31 ppm were identified. Wallace (2002) did not consider the waters to be contaminated by Sn, with most of the Sn values reported as 0.000 ppm.

Gurung (2002 and 2003) examined acid drainage impacted waters throughout Tasmania; his results are summarised in Table 4.14. Gurung (2003) determined that major metal pollutants of concern in AMD impacted waters were Al, As, Cd, Cu, Pb and Zn. Gurung (2003) also found that surface waters in AMD impacted catchments displayed high concentrations of dissolved metals over a wide pH range. Both

sulphate and dissolved metal distributions were found to be equally expressive in depicting acid drainage characteristics in surface waters affected by abandoned mine sites and like East (1999), Gurung (2003) suggests that sulphate could be used as a cost effective analysis for identifying AMD in the absence of costly metal analysis.

Parameter	No. of samples	Minimum	Maximum	Mean
pH	850	2.00	9.0	5.45
EC (dS/m)	776	0.001	5.8	1.0
Acidity (mg CaCO3/L)	377	0.02	10000	254
Alkalinity (mg CaCO3/L)	418	0.03	8100	117
SO_4^{2-} (mg/L)	592	0.20	13900	557
Al (mg/L)	532	0.0001	880	12.4
As (mg/L)	448	0.001	43.91	0.41
Cd (mg/L)	606	0.001	3.71	0.03
Cu (mg/L)	654	0.001	180	2.52
Fe (mg/L)	631	0.001	2230	34.5
Mn (mg/L)	604	0.001	274	4.4
Pb (mg/L)	650	0.001	27.4	0.21
Zn (mg/L)	672	0.001	728	7.45

Table 4.14 Average surface water quality in catchments impacted by abandoned mines across Tasmania (after Gurung, 2003)

All data from previous studies at Rosebery and the monitoring database (PRM, 2004) have been included in the dataset used in this thesis (Appendix 2). The many and varied sampling regimes have resulted in a number of different detection limits reported for individual elements. Reporting of these in the database (PRM, 2004) also varies; in most cases if the sample was below detection limit, the detection limit is included in the graphical output presented in the following section (and in Table 4.14). This is particularly obvious where a large number of samples plot at a specific value (e.g., at 0.005 mg/L in Figure 4.21).

4.4.4.1 Background surface waters metals

The ANZECC (2000) background levels for Australian freshwaters waters (Table 4.1) may not be directly applicable to mining districts due to potentially higher natural „background' conditions. ETS (1996) suggested the following background

limits for surface waters at Rosebery (Table 4.15), however, made no mention of their justification or to the earlier relevant work of Morrison (1992) (Table 4.13).

	pH	Cond µS/cm	Cu mg/L	Pb mg/L	Zn mg/L	Cd mg/L	Fe mg/L	Mn mg/L	SO_4^{2-} mg/L	Cl mg/L
Surface Waters	5.0-6.5	50-100	0.002	0.002	0.05	0.0005	0.1	0.05	1	5-10

Table 4.15 Suggested background levels for surface waters at Rosebery (ETS, 1996a)

Morrison (1992) undertook sampling and detailed trace element geochemistry of surface waters at one site in the study area, Mountain Creek (Figure 4.2). At this point the only material Mountain Creek drains was the barren Mount Black Formation. The sample point was at the same location as the Rosebery town water supply intake (Figure 4.3).

Figure 4.3 Mountain Creek sample point at peak during winter

No mine workings were presumed to be drained by Mountain Creek by Morrison (1992). This presumes the surface water has no interaction with contaminated groundwater, which was a reasonable assumption in this location. There was little mining interacting within the upstream catchment, other than a dozed road and drill pad, in the barren Mount Black Formation. The pad was created for

drillhole 114R which was drilled in 1990. Groundwater sampling of this drillhole (GW014) displayed a near neutral pH and low metal content (Appendix 2). Due to its high location in the catchment on Mount Black, and because of the lack of known AMD sources in the Mountain Creek catchment above this point, these data obtained by Morrison (1992) were valuable as they can be considered background for Rosebery surface waters.

ANZECC (2000) suggested a background level of 0.000001 mg/L for Cd in Australian freshwaters waters. Mountain Creek with a mean Cd level of 0.0047 mg/L (Morrison, 1992) exceeds by an order of magnitude: (i) the ANZECC (2000) guideline trigger level of 0.0002 mg/L for the protection of 95% of species in slightly-moderately disturbed freshwater systems; (ii) the interim limit of 0.0005 mg/L set by ETS (1996a); and (iii) ETS (2001), the mine's environmental management plan (EMP).

Morrison's (1992) work also examined four other Tasmanian streams with similar catchments; all bar one were largely isolated from human activity. Mean Cd levels in these streams were all above those found in Mountain Creek, suggesting that both the mine's EMP and ANZECC (2000) guidelines levels were too low for comparison of Cd levels at Rosebery and throughout Tasmanian streams.

The source of the majority of Cd at Rosebery is elemental replacement of Zn in the Sphalerite crystal lattice (Martin, 2004). A source of Cd in Mountain Creek could be the water contained in open drillholes such as 114R, which form conduits to the orebody and mine area. Russell and van Moort's (1981) work could explain elevated metal levels through the rotting of vegetation. Fallout from zinc processing and mining particulates also provides a potential explanation for high Cd in all Tasmanian streams examined by Morrison (1992). Cd is of concern in AMD studies, because the

solubility of dissolved cadmium increases with decreasing pH and alkalinity (French, 1986).

Gurung (2002) found that the mean concentration of Cd in 606 surface water samples of catchments impacted by abandoned mines across Tasmania was 0.03 mg/L. The maximum Cd level encountered by Gurung's (2002) review was 3.71 mg/L.

The mean Cu concentrations in Mountain Creek at 0.0018 mg/L (Morrison, 1992) also exceed the ANZECC (2000) guideline trigger level of 0.0014 mg/L for the protection of 95% of species in slightly-moderately disturbed freshwater systems. The maximum recorded Cu concentration exceed the ANZECC (2000) guideline by a factor of *c.* 5 and the ETS (1996a) suggested level by a factor of *c.* 3. Morrison's (1992) work on the other Tasmania streams, also found some mean Cu concentrations higher than Mountain Creek. Like Cd, this suggested both the mine's EMP and ANZECC (2000) guidelines levels were too low for comparison of Cu levels at both Rosebery and throughout Tasmanian streams. This was also the case for Cr, which in some cases exceed the guideline slightly (*c.* 10%) in Mountain Creek.

4.4.4.2 Background groundwaters metals

ETS (1996a) suggested the following background limits for groundwaters at Rosebery (Table 4.16). The major differences from the suggested surface water background limits were an order of magnitude increase in the concentrations of Cu, Pb, Cd, Fe, and sulphate. Groundwater background levels Cl increased by 5 mg/L, maximum electrical conductivity by a factor of 2.5 and Mn by a factor of 20, from surface water background levels.

Hale classified groundwater inflowing into unmineralised areas as background (Hale, 2001). This assumption was valid in some cases but generally flawed, as it

assumes no prior interaction with contaminants higher in the mine workings, in drillholes or within the groundwater system.

pH	Cond µS/cm	Cu mg/L	Pb mg/L	Zn mg/L	Cd mg/L	Fe mg/L	Mn mg/L	SO_4^{2-} mg/L	Cl mg/L
5.0-6.0	50-250	0.02	0.02	0.05	0.005	1	1	10	10-15

Table 4.16 Suggested background levels for groundwaters at Rosebery (ETS, 1996a)

4.4.5 Stable isotope geochemistry

Hale (2001) used CSIRO's Adelaide laboratory isotope analysis service to analyse 11 samples for stable isotopic composition of oxygen ($\delta^{18}O$) and deuterium (δD). Using isotopic signatures, Hale (2001) divided the mine waters into three distinct groups, including a surface water group and a groundwater group. The same lab and methods were adopted for the current study. Data from Hale (2001) included in the dataset is presented in (Figure 4.40).

4.5 Results

4.5.1 Acid base accounting

Table 4.17 is a summary of the NAG classifications of samples at Rosebery. Table 4.18 is a summary of the ANC at Rosebery. A summary of the range of results for ABA undertaken as part of the present study is presented in Table 4.19 and Figure 4.4. Figure 4.5 displays the distribution of NAG and ANC sampling around the open-cut and waste dumps at Rosebery. The complete results are tabulated in Appendix 2.

NAG kg H_2SO_4/tonne	Acid forming potential	n
0	None	30
<10	Low	31
>10	High	37

Table 4.17 Net acid-generation results for Rosebery including Brady (1997), Struthers (1996)

ANC kg H_2SO_4/tonne	Acid consuming potential	n
0	None	10
<10	Low	39
>10	High	31

Table 4.18 Acid-neutralising capacity results at Rosebery including Struthers (1996) and Gurung (2002); this excludes Gurung's (2002) theoretically calculated acid consuming potential samples

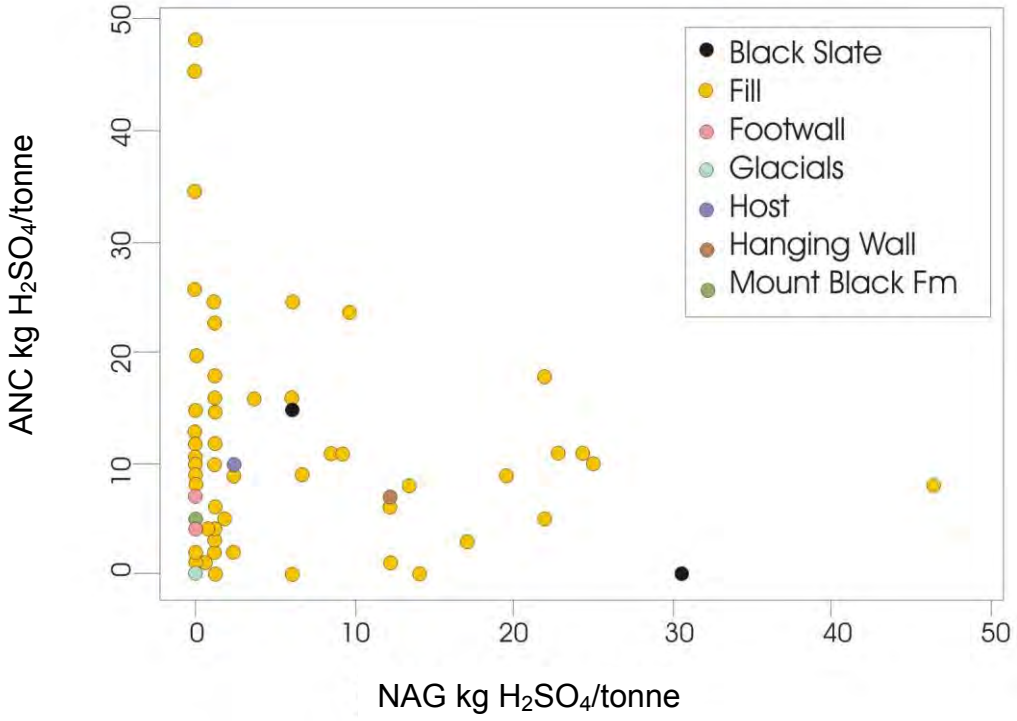

Figure 4.4 Acid-neutralising capacity (ANC) versus net acid-generation (NAG) at Rosebery. Fill refers to mine waste material of various Rosebery rock types (mullock)

Sample	Easting (AMG66)	Northing (AMG66)	ANC kg H_2SO_4/t	NAG kg H_2SO_4/t
RNAG24	378756	5375147	4.9	0.0
RNAG25	378743	5375140	7.8	0.0
RNAG26	378605	5375084	6.9	12.3
RNAG27	378592	5375015	0.0	30.6
RNAG28	378589	5374996	11.8	0.0
RNAG29	378658	5374763	0.0	0.0
RNAG30	378701	5374671	10.8	23.0
RNAG31	378536	5374972	14.7	6.1
RNAG32	378537	5375038	6.9	0.0
RNAG33	378489	5374956	4.9	1.8
RNAG34	378475	5374933	0.0	6.1
RNAG35	378404	5374666	14.7	0.0
RNAG36	378473	5374310	19.6	0.0
RNAG37	378426	5374366	3.9	0.0
RNAG38	378457	5374317	2.0	0.0
RNAG39	378428	5374288	15.7	1.2
RNAG40	378536	5374279	2.9	1.2
RNAG41	378440	5374230	10.8	9.2
RNAG42	378474	5374252	3.9	0.6
RNAG43	378492	5374259	0.0	1.2
RNAG44	378424	5374207	1.0	0.6
RNAG45	378461	5374228	11.8	0.0
RNAG46	378479	5374235	0.0	0.0
RNAG47	378503	5374242	2.0	1.2
RNAG48	378414	5374197	8.8	6.7
RNAG49	378439	5374210	0.0	0.0
RNAG50	378462	5374219	0.0	1.2
RNAG51	378496	5374231	2.0	2.5
RNAG52	378446	5374184	3.9	0.0
RNAG53	378484	5374194	9.8	2.5
RNAG54	378480	5374211	8.8	0.0
RNAG55	378497	5374214	4.9	0.0
RNAG56	378676	5374628	9.8	0.0
RNAG57	378696	5374587	15.7	6.1
RNAG58	378710	5374593	0.0	14.1
RNAG59	378729	5374573	4.9	0.0
RNAG60	378666	5374626	1.0	0.0
RNAG61	378648	5374582	25.5	0.0
RNAG62	378655	5374575	9.8	0.0
RNAG63	378681	5374538	5.9	1.2
RNAG64	378689	5374523	3.9	1.2

continued.

Sample	Easting (AMG66)	Northing (AMG66)	ANC kg H_2SO_4/t	NAG kg H_2SO_4/t
RNAG65	378731	5374458	4.9	0.0
RNAG66	378687	5374495	8.8	19.6
RNAG67	378717	5374451	8.8	2.5
RNAG68	378704	5374438	14.7	1.2
RNAG69	378773	5374384	4.9	22.1
RNAG70	378744	5374423	22.5	1.2
RNAG71	378735	5374374	24.5	1.2
RNAG72	378788	5374353	23.5	9.8
RNAG73	378801	5374331	1.0	12.3
RNAG74	378841	5374327	2.9	17.2
RNAG75	378852	5374079	17.6	22.1
RNAG76	378872	5374090	11.8	1.2
RNAG77	378932	5374083	10.8	24.5
RNAG78	378898	5374072	7.8	13.5
RNAG79	378894	5374087	10.8	8.6
RNAG80	378806	5374229	15.7	3.7
RNAG81	378801	5374233	24.5	6.1
RNAG82	378781	5374255	17.6	1.2
RNAG83	378761	5374279	9.8	1.2
RNAG84	378764	5374274	45.1	0.0
RNAG85	378766	5374254	12.7	0.0
RNAG86	378796	5374132	9.8	2.5
RNAG87	378807	5374119	14.7	0.0
RNAG88	378861	5374155	11.8	1.2
RNAG89	378916	5374153	14.7	0.0
RNAG90	378908	5374192	9.8	25.1
RNAG91	378901	5374203	0.0	1.2
RNAG92	378865	5374218	5.9	12.3
RNAG93	378807	5374270	7.8	46.6
RNAG94	378860	5374308	6.9	0.0
RNAG95	378796	5374299	8.8	0.0
RNAG96	378772	5374310	10.8	0.0
RNAG97	378753	5374321	34.3	0.0
RNAG98	378743	5374328	48.0	0.0
n			75	75
Maximum			0	0
Minimum			48.02	46.55
Mean			10.07	5.18

Table 4.19 Acid base accounting of Rosebery materials undertaken as part of the present study; all units in kg H_2SO_4/t; ANC refers to acid-neutralising capacity; NAG refers to net acid-generation; and locations are given in Australian Map Grid 1966 (AMG66) in Zone 55.

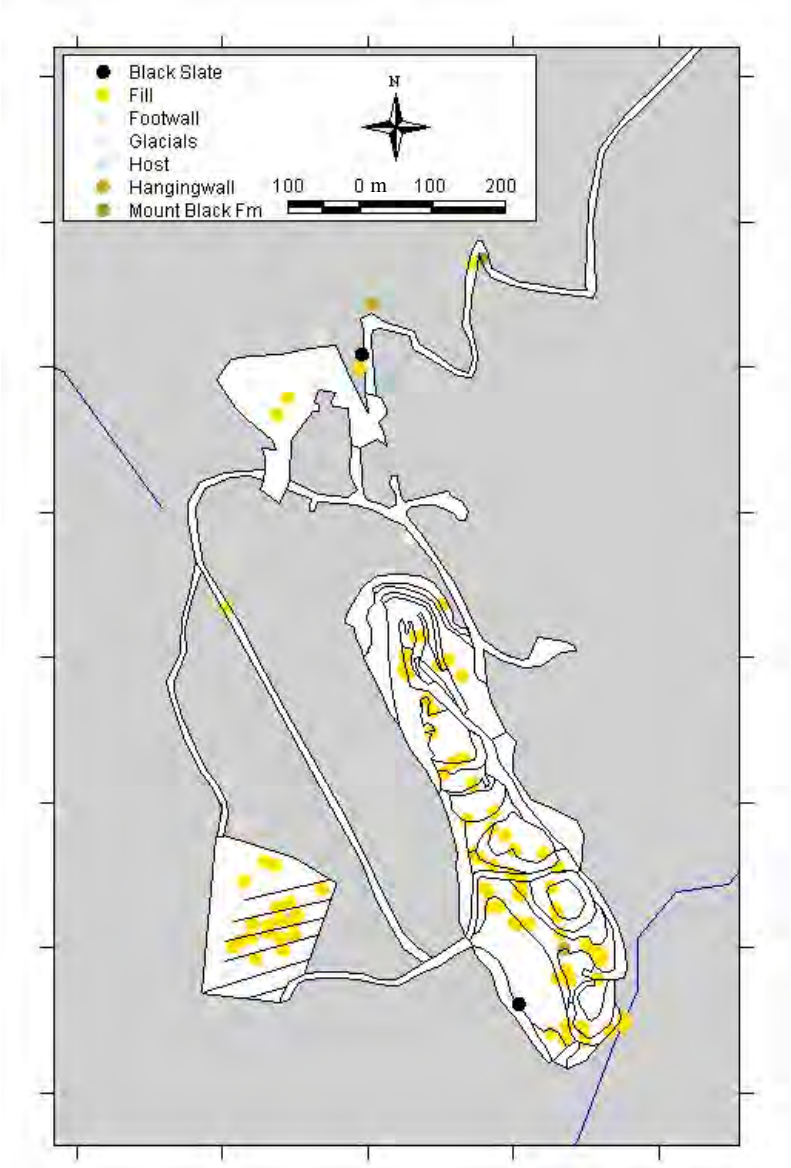

Figure 4.5 Acid base accounting sample locations of the present study at the assay creek waste dump and Rosebery open-cut (mine infrastructure in white)

4.5.1 Rock and mineral geochemistry

No additional numerical rock and mineral geochemistry results were obtained as part of the present study.

4.5.2 Aqueous geochemistry

Based on source location, each sample was given the classifier of deep groundwater (DGW), shallow groundwater (SGW) or surface water (SW). Figure 4.6 displays the spatial distribution of these water types. Deep ground water samples were obtained from within mine workings and exploration drillholes. Throughout the

present thesis, „shallow groundwaters' refers to groundwaters near surface (<10 m) which were thought to be influenced by interflow and surface waters. Shallow groundwater samples were obtained from: (i) seeps; (ii) through holes drilled for the current study; and (iii) from excavations. Surface waters were sampled from surface water bodies including, dams, lakes, rivers, creeks and streams throughout the study area.

Half of the *c.* 4000 total surface water data set from PRM (2004) refer to three sample sites grouped as „process waters' (PW) which are not naturally derived waters, rather the output from the flotation processing plant. PW sites include: (BO) the Bobadil outflow – discharge from the tailings dams polishing pond; (BL) the discharge from the Bobadil dam to the polishing pond; and (BF) Bobadil flume - being the process water being delivered to Bobadil dam from the processing plant (Figure 4.6). To avoid bias from PW samples, these results have been omitted from the dataset where appropriate.

4.5.2.1 pH and temperature results

Figure 4.7 displays the study area surface drainage and pH variation in groundwaters, surface waters and mine waters. Recorded pH values varied from 2.2 to 14.4 over the study area (Table 4.20). Table 4.20 summarises the pH variation within each of the water classifications. Table 4.21 summarises the pH variation within various water bodies over the study area.

pH	n	Minimum	Maximum	Mean
Total	4522	2.2	14.4	6.8
Deep groundwater	53	2.3	8.9	5.9
Shallow groundwater	374	2.2	8.6	4.8
Surface water	1770	2.65	11	5.4
Process water	2325	3.53	14.4	8.0

Table 4.20 Summary of pH variation in the water classes

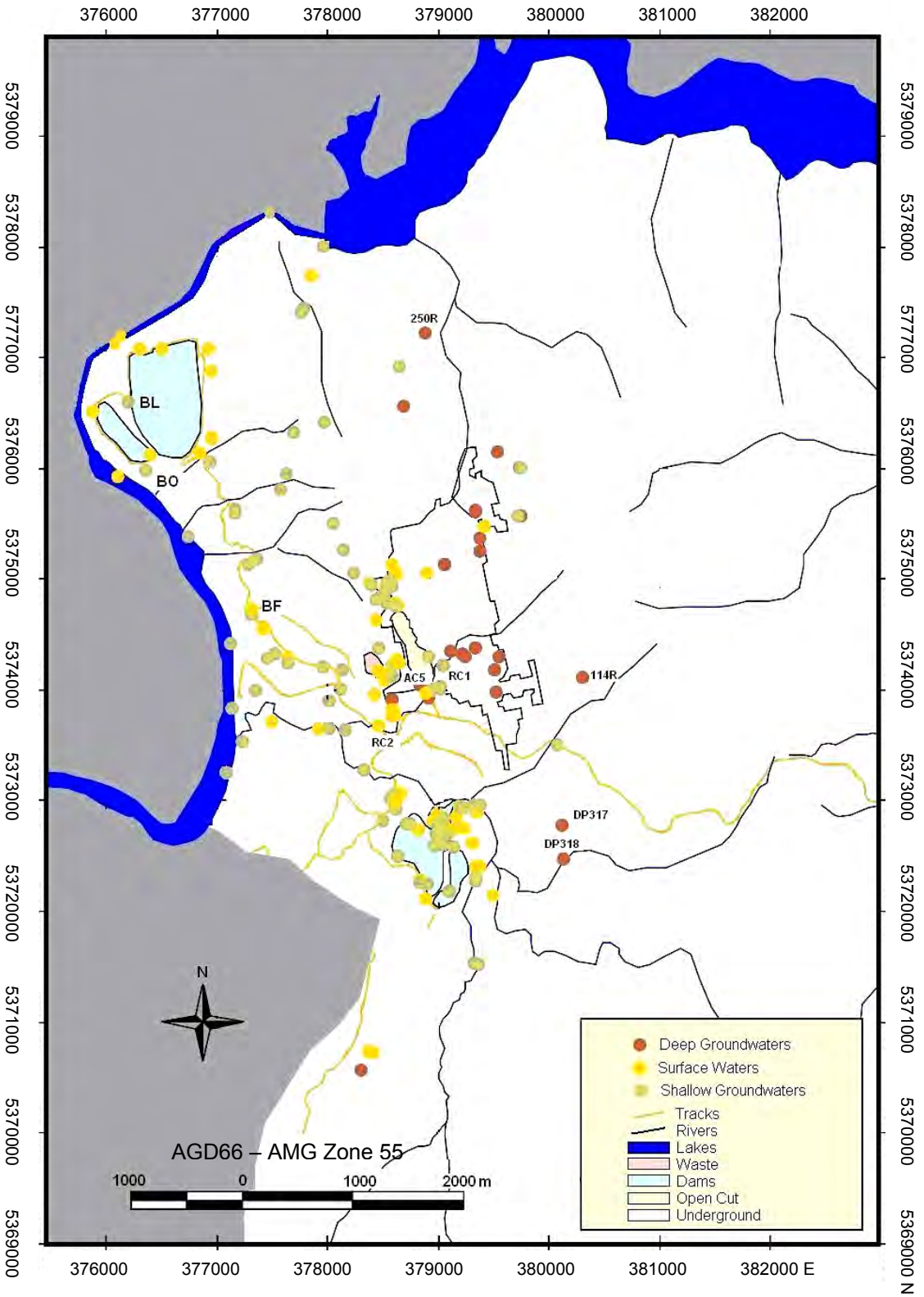

Figure 4.6 Water sampling locations and classification (including PRM, 2004); drillhole locations are marked for DP318, DP317, 114R and 250R; locations are marked for the sample points titled AC5, RC1, RC2, BF, BO and BL.

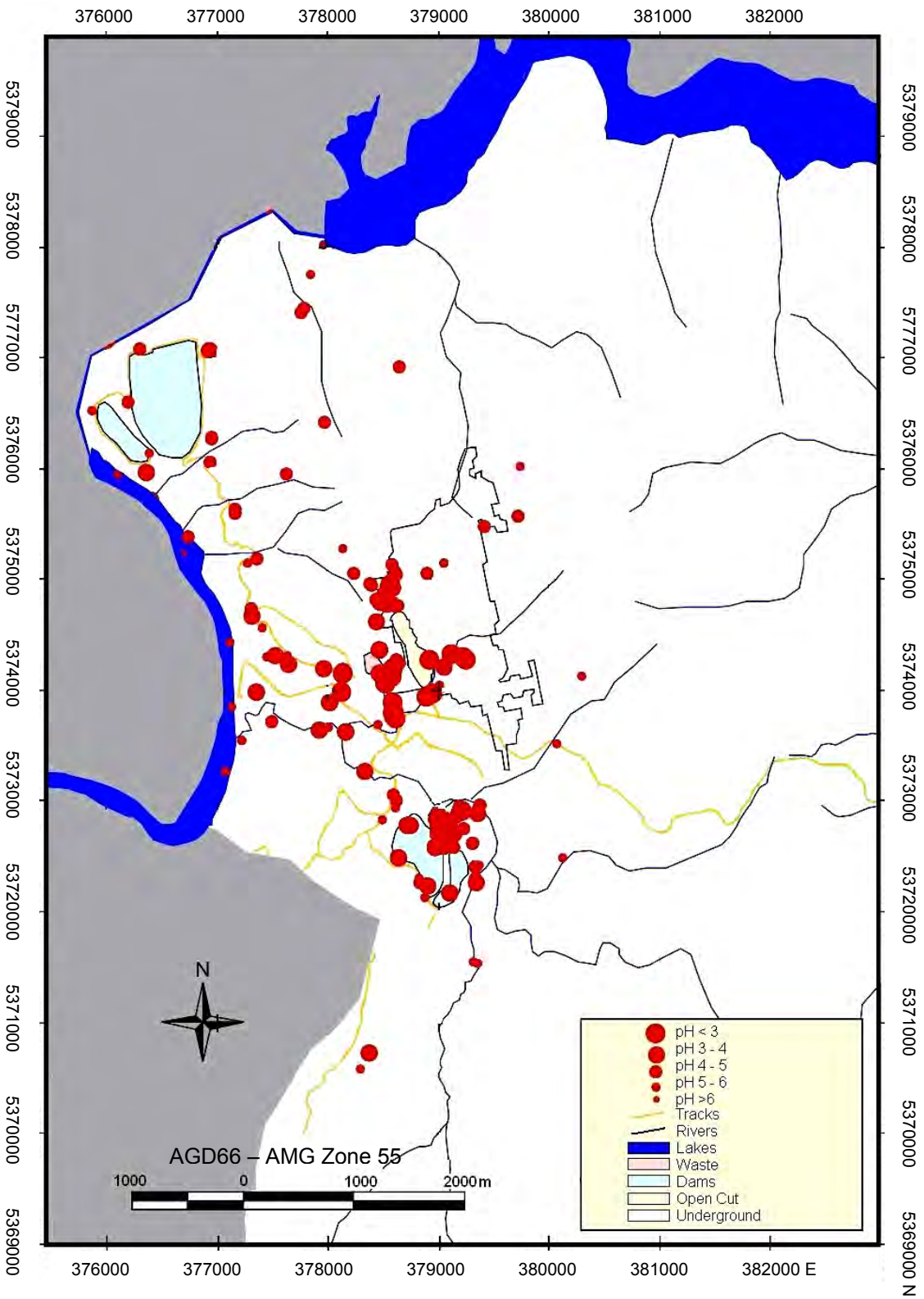

Figure 4.7 Surface hydrology features and pH variation over the study area

	n	Minimum pH	Maximum pH	Mean pH
Rainfall	1	5.8	5.8	5.80
Lake Rosebery	1	5.4	5.4	5.40
Lake Pieman	718	3.2	8.58	5.99
Drillholes groundwater	23	4.36	7.67	6.24
Stitt River	132	3.83	9.16	6.01
Rosebery Creek	64	3.53	9.04	5.07
Assay creek	193	2.2	4.74	3.50
Open-cut	53	2.86	8.74	4.69
Underground	36	2.3	8.87	5.63
Primrose creek	77	2.75	7.8	4.48
Filter plant creek	94	3.3	8.76	5.05
Miscellaneous creeks	21	3.97	7.3	5.18
Tailings dams No. 2&5	253	3.18	11	5.78
Wetlands	175	2.84	7.8	4.36
Seepage @ dams 2&5	166	3.1	8.4	4.87
Flume	423	5.27	14.4	10.54
Polishing pond	431	4.96	11.42	7.95
Bobadil outflow	1432	3.53	11.9	7.19
Bobadil seepage	62	3.46	8.6	6.40
Abandoned mine workings	19	3.18	7.75	4.59

Table 4.21 Variation of pH over the study area

The temperature of waters was monitored over the study area and the results are presented in Figure 4.8 to Figure 4.13 and summarised in Table 4.22. When examining the entire temperature dataset (Figure 4.8) against pH, trends are difficult to decipher, however, when examining a single temporal snapshot or single water-body trends become more apparent (Figure 4.9 to Figure 4.12).

All temperatures are plotted against pH (Figure 4.8) for all samples other than process water for spring 2003 as a snapshot (Figure 4.9). Despite scatter there is a general trend that lower pH values have higher temperatures. The temperature of all samples at Rosebery is plotted over time and shows a strong seasonal correlation in all samples other than assay creek (Figure 4.10), which is associated with AMD. The natural seasonal correlation is further displayed in Figure 4.11, showing all samples from the Pieman River. Rosebery Creek is used as an example to display the temperature variation in a surface water course (Figure 4.12), using data from two

sample sites RC1 and RC2 (Figure 4.6). RC2 generally has higher temperatures and lower pH than RC1. Figure 4.13 shows elevated temperatures are not just related to the underground workings but also the tailings dams and mine infrastructure.

	n	Minimum temp °C	Maximum temp °C	Mean temp °C
Rainfall	1	7	7	7.00
Lake Rosebery	1	10.2	10.2	10.20
Lake Pieman	687	7.3	22.2	12.14
Drillholes groundwater	22	6.65	40.1	10.83
Stitt River	132	6.3	22.6	11.94
Rosebery Creek	62	6.7	20.1	12.14
Assay creek	193	6.7	28.4	13.52
Open-cut	53	7.8	22.6	14.09
Underground*	20	10.6	30	19.45
Primrose creek	77	5.5	22.6	14.13
Filter plant creek	92	8.7	28.6	16.02
Miscellaneous creeks	18	5.9	10.3	7.81
Tailings dams No. 2&5	253	6.1	27.6	15.60
Wetlands	175	6.1	24.2	14.20
Seepage @ dams 2&5	166	7.5	26.1	13.45
Flume	386	10	25.1	17.05
Polishing pond	399	6.4	30	14.80
Bobadil outflow	1136	6	29.6	15.04
Bobadil seepage	60	6.8	20.1	11.90
Abandoned mine workings	19	6.8	17.8	10.50

Table 4.22 Variation of Temperature over the study area; results in degrees Celsius

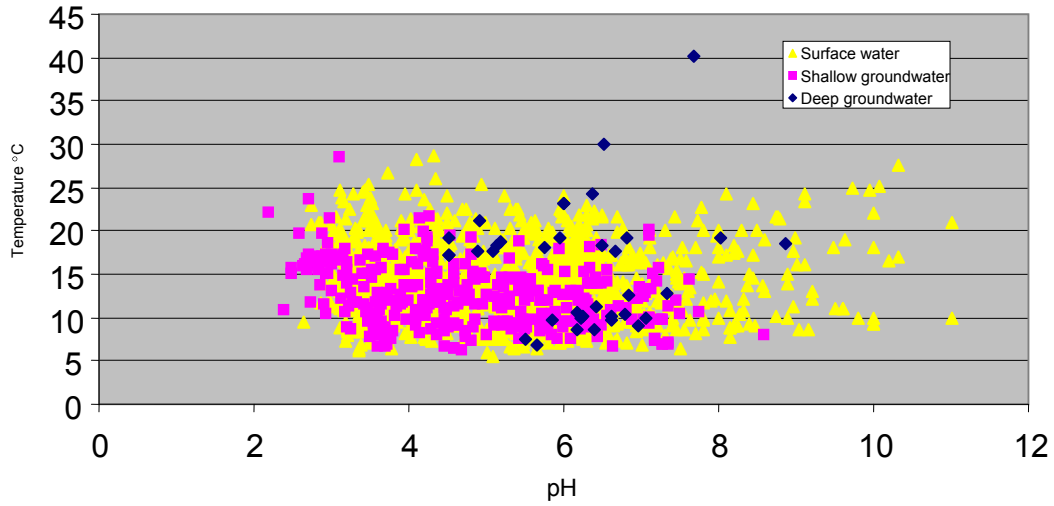

Figure 4.8 Temperature in degrees Celsius versus pH for Rosebery waters (excluding process water)

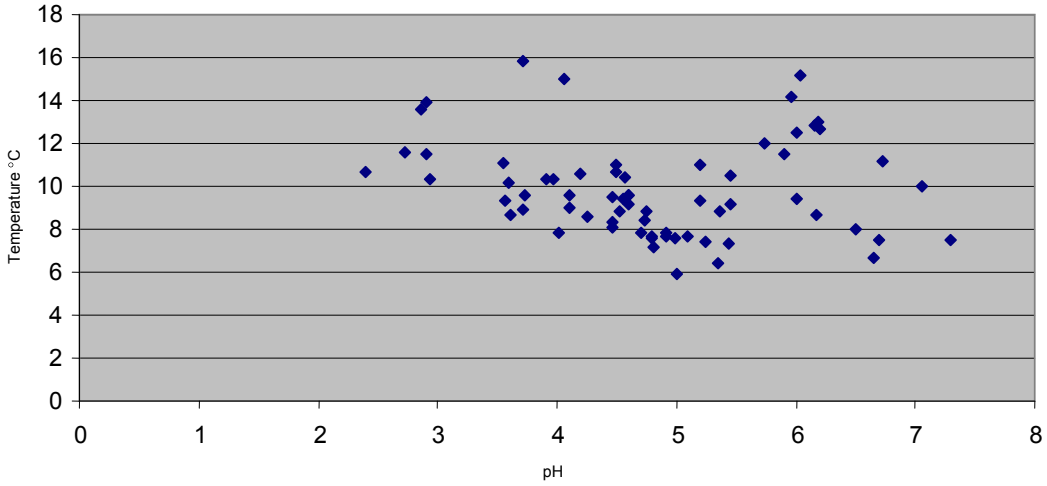

Figure 4.9 Temperature in degrees Celsius versus pH snapshot survey for Rosebery waters 22-25/09/2003

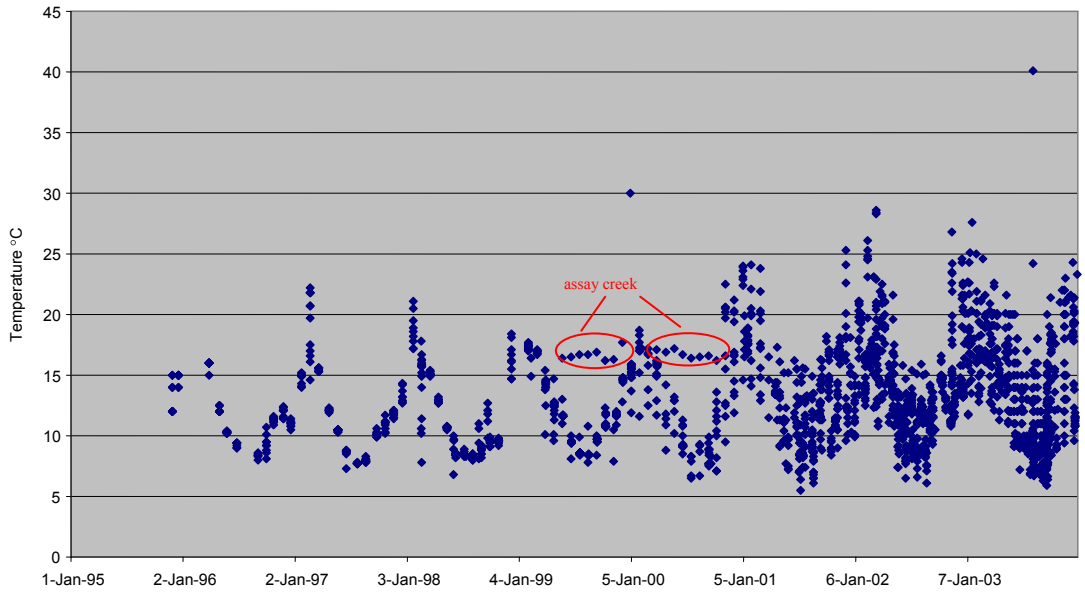

Figure 4.10 Temperature dataset over time; results in degrees Celsius

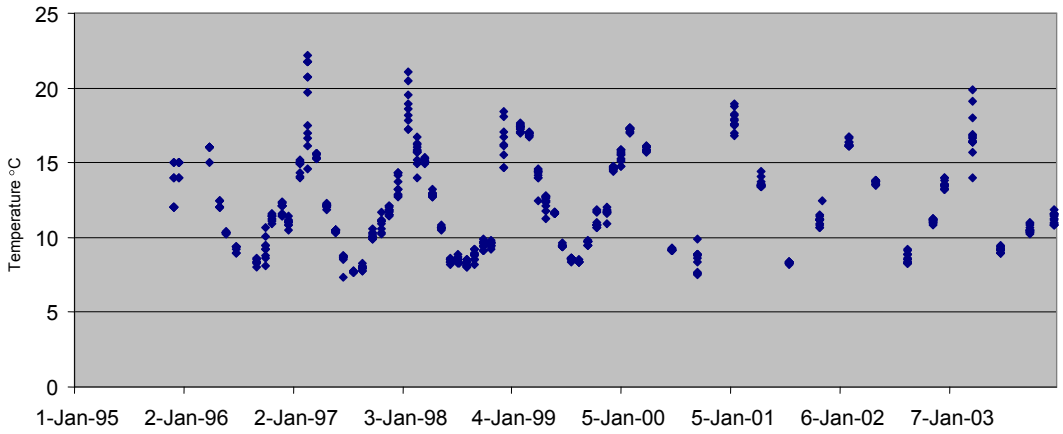

Figure 4.11 Pieman River natural seasonal temperature variation; results in degrees Celsius

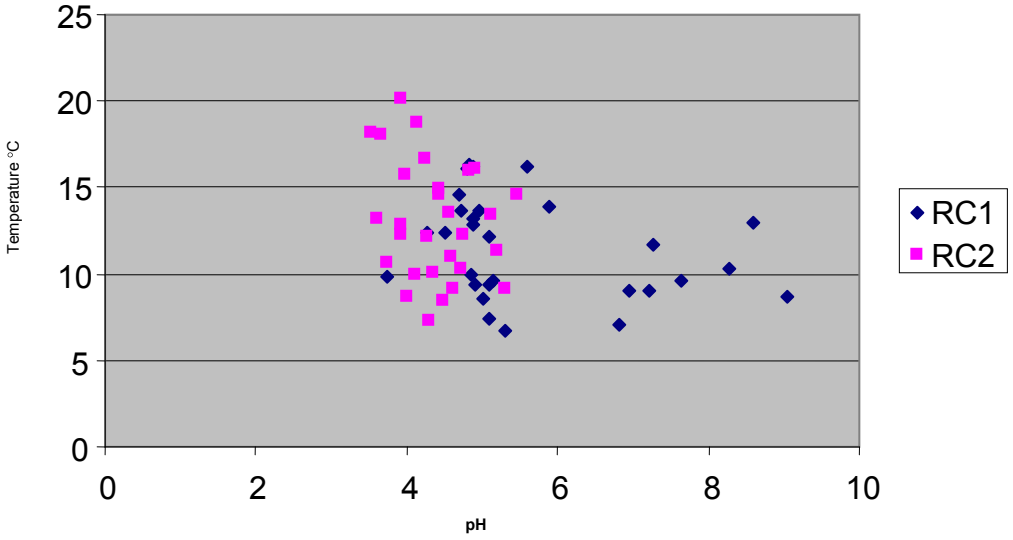

Figure 4.12 Temperature in degrees Celsius verses pH, over the same period (July 2001 to December 2003) in Rosebery Creek; RC1 was up-gradient of the mine workings; consequently these data were useful for setting the local surface water background. RC2 has AMD directly reporting to it (Figure 4.6)

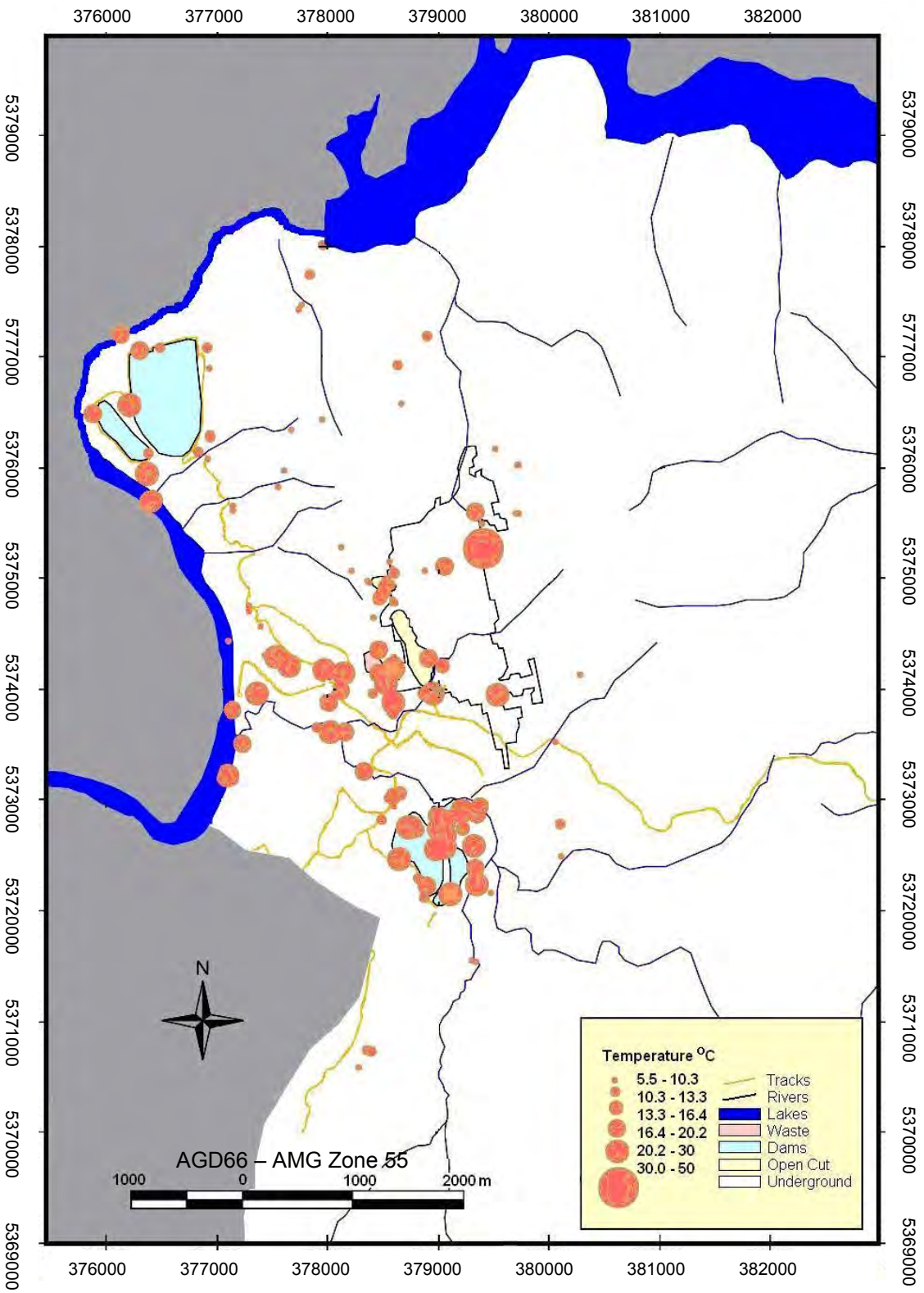

Figure 4.13 Temperature of all waters over the study area

4.5.3 Major and trace element results

4.5.3.1 Metals

Analytical results for samples undertaken as part of the present study, together with the complete pre-existing metals data set, including PRM (2004), for Rosebery waters are provided in Appendix Two.

AMD waters are enriched with metals due to the influence of acid on metal solubility (Mills, 1995). The presence of anomalously high concentrations of dissolved heavy metals in waters was used as a link to point sources of AMD and provided insight into the subsurface flow field.

The most distinct trend in these data was the increase in most metal concentrations with decrease in pH. Using zinc as an example, Figure 4.14 displays this trend for all waters at Rosebery. Lead did not display the same proportional increase, however, did increase in concentration with acidity (Figure 4.15). Other metals (Mn, Mg, Fe, Cu, Al, and Cd) exhibited a similar trend to zinc, with metal content increasing with acidity (Figure 4.16 to Figure 4.21). Calcium, however, does not display this trend at all (Figure 4.22).

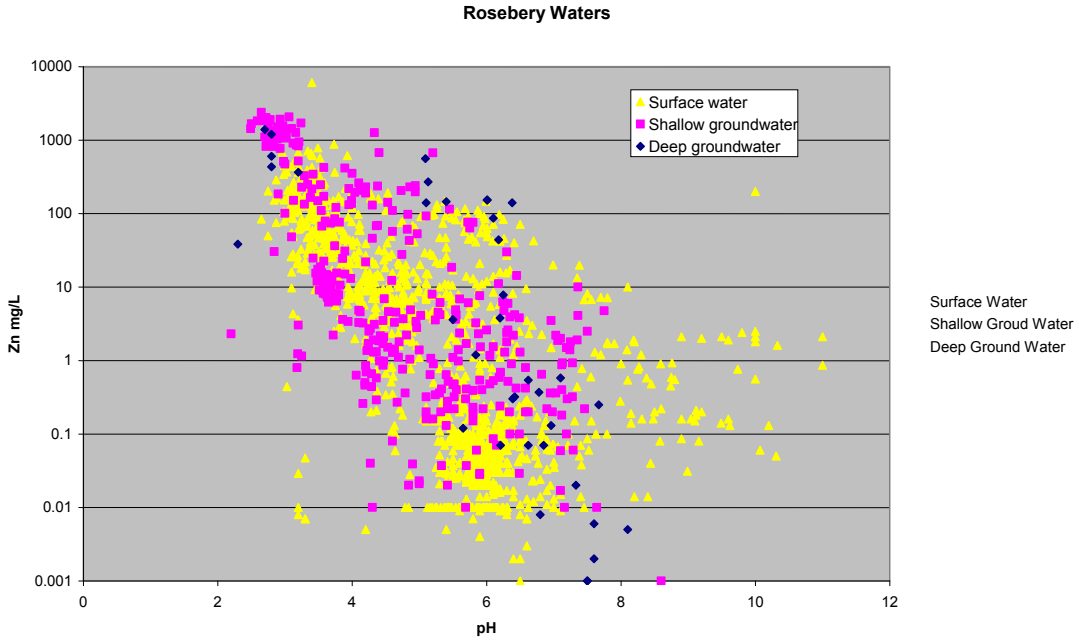

Figure 4.14 Zinc concentrations versus pH for Rosebery waters (excluding process water)

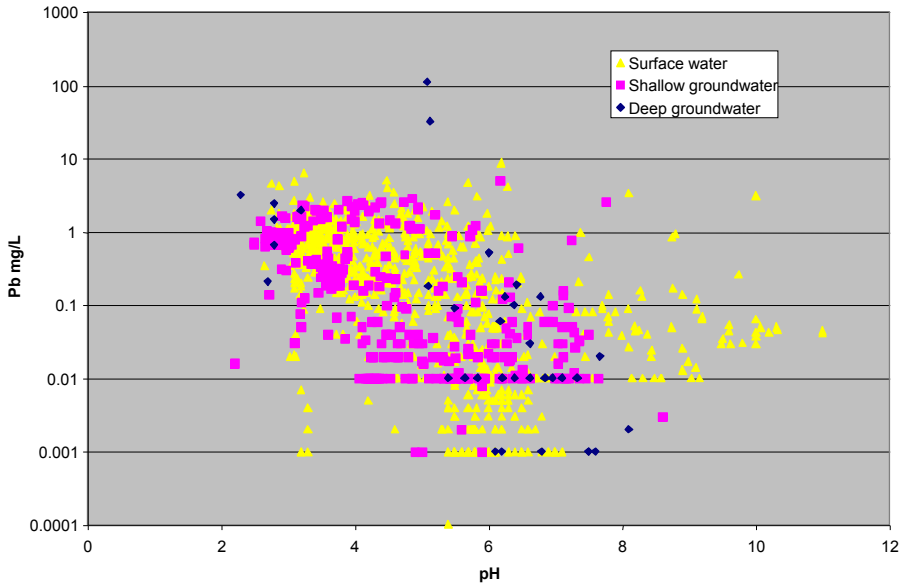

Figure 4.15 Lead concentrations versus pH for Rosebery waters (excluding process water)

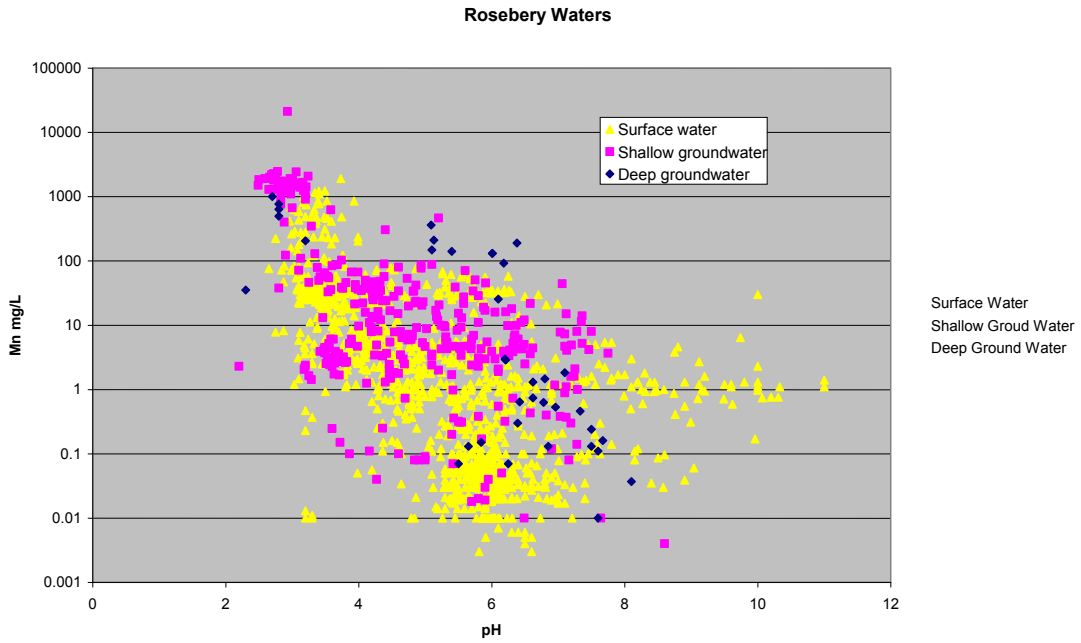

Figure 4.16 Manganese concentrations versus pH for Rosebery waters (excluding process water)

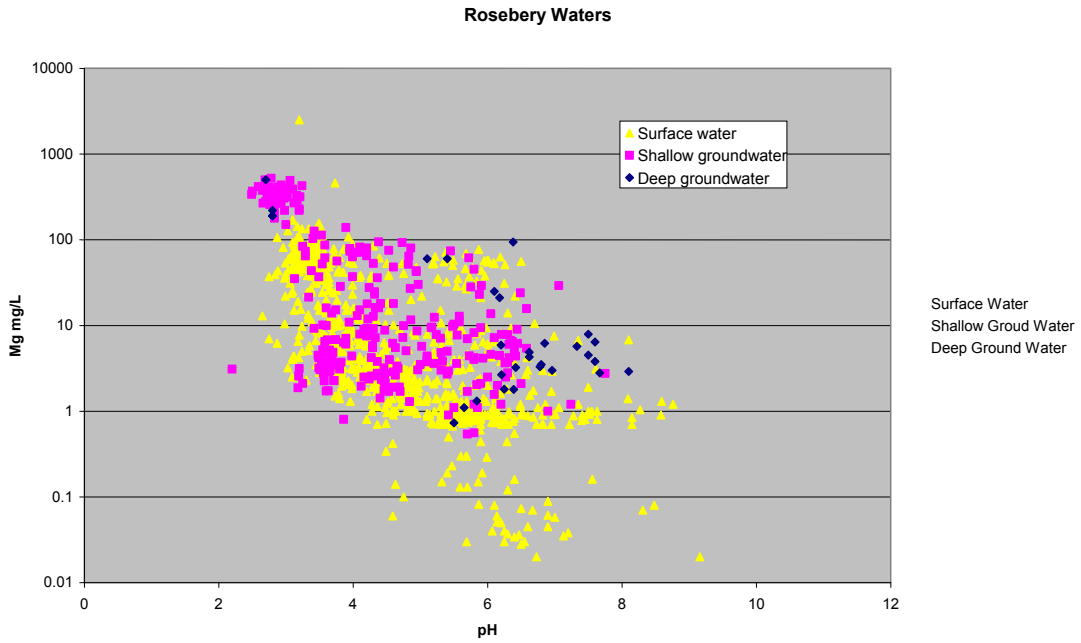

Figure 4.17 Magnesium concentrations versus pH for Rosebery waters (excluding process water)

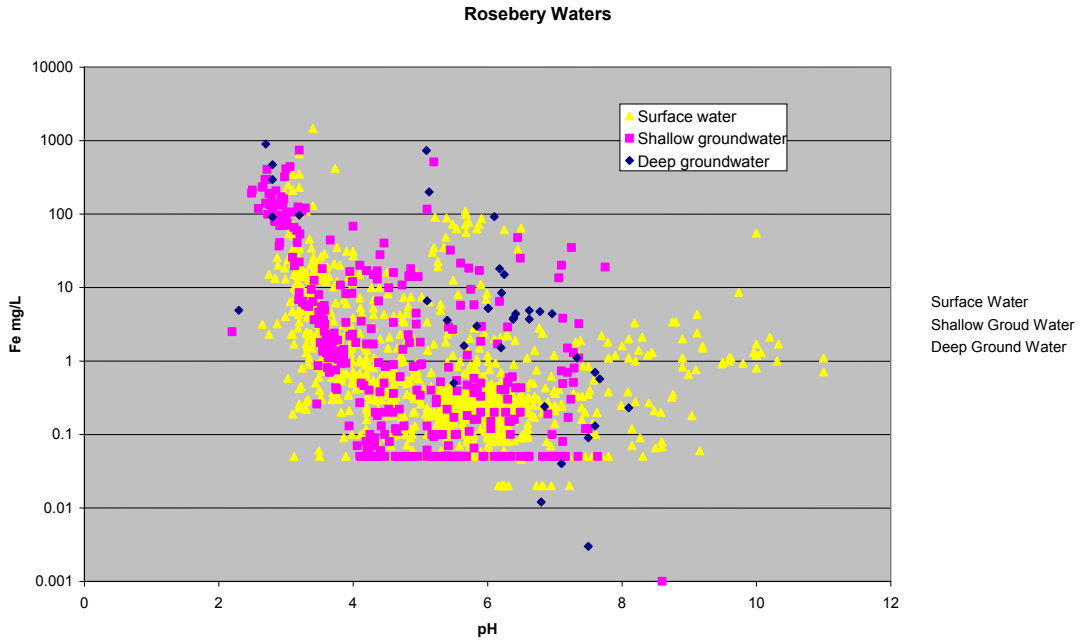

Figure 4.18 Iron concentrations versus pH for Rosebery waters (excluding process water)

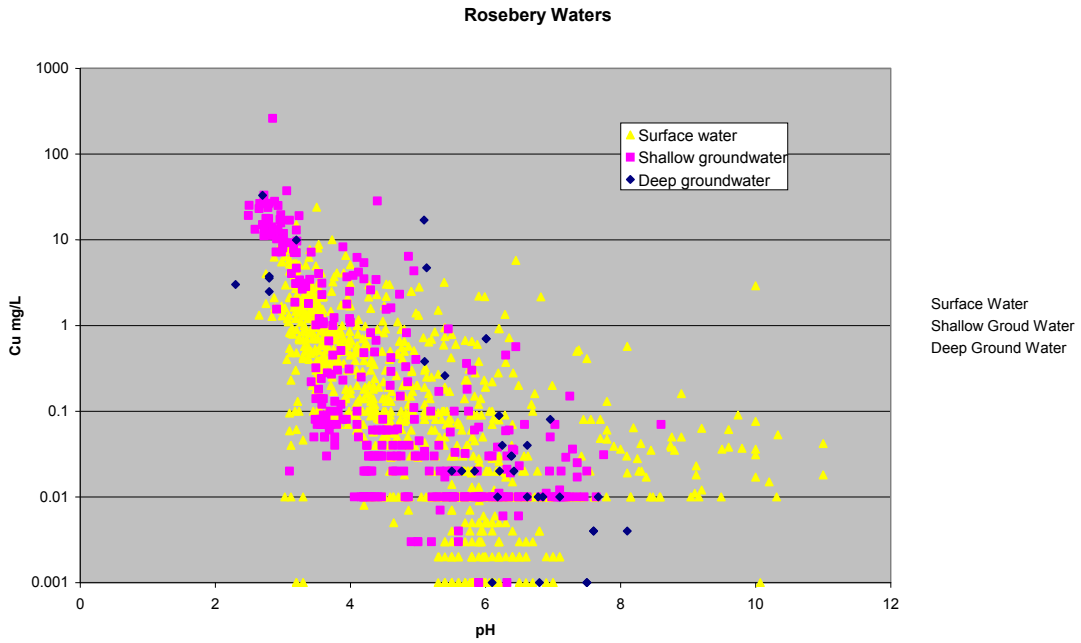

Figure 4.19 Copper concentrations versus pH for Rosebery waters (excluding process water)

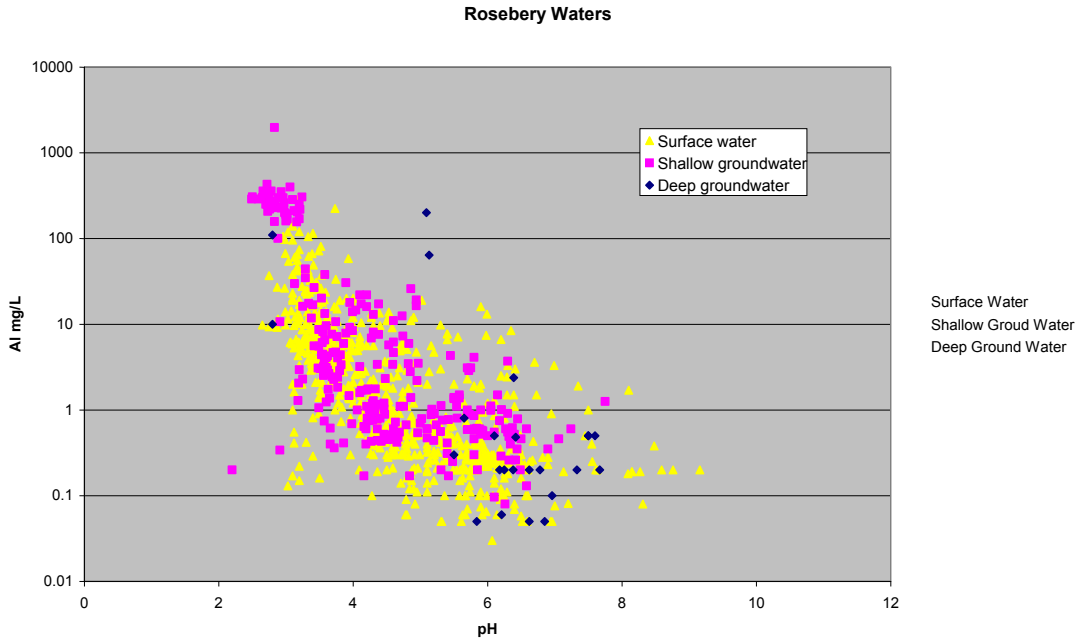

Figure 4.20 Aluminium concentrations versus pH for Rosebery waters (excluding process water)

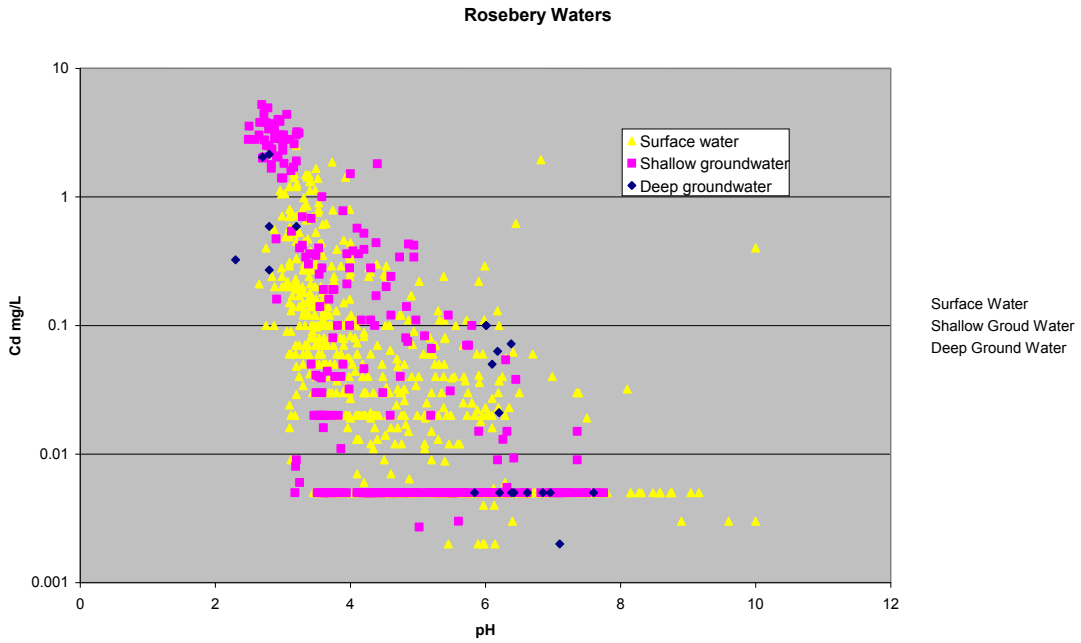

Figure 4.21 Cadmium concentrations versus pH for Rosebery waters (excluding process water)

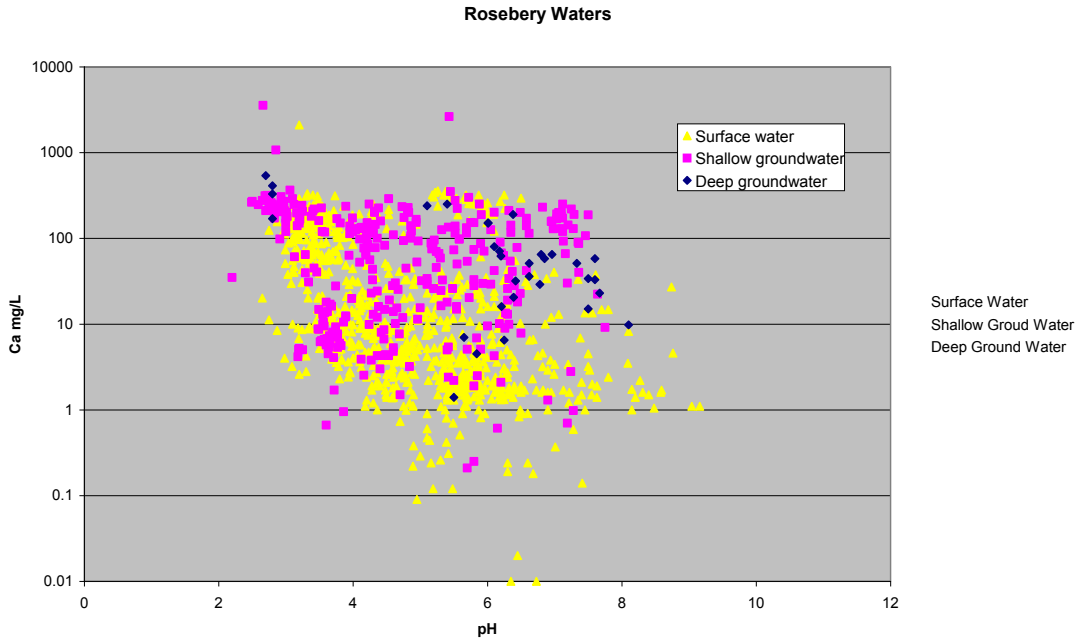

Figure 4.22 Calcium concentrations versus pH for Rosebery waters (excluding process water)

Both electrical conductivity (Figure 4.23) and sulphate (Figure 4.24), plotted against pH, follow the same trend as metals in Rosebery waters. In the present study, modifications omitting Co and Ni were made to the Ficklin et al. (1992) and Gurung (2002) approach due to: (i) lack of abundance in the sample; and (ii) lack of analyses of these elements in historical data. This resulted in the creation of modified Ficklin

and Gurung plots with some 1577 data points from the Rosebery data (Figure 4.25 and Figure 4.26). Modified Ficklin and Gurung plots (Figure 4.25 and Figure 4.26) display metal concentrations plotted against pH for all Rosebery waters.

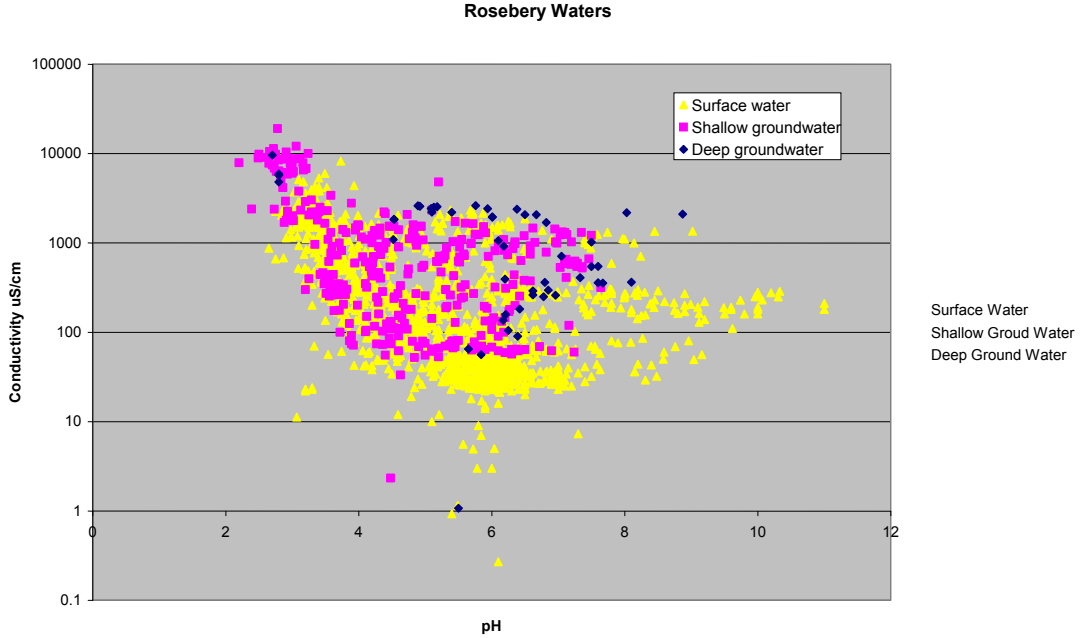

Figure 4.23 Electrical conductivity versus pH for Rosebery waters (excluding process water)

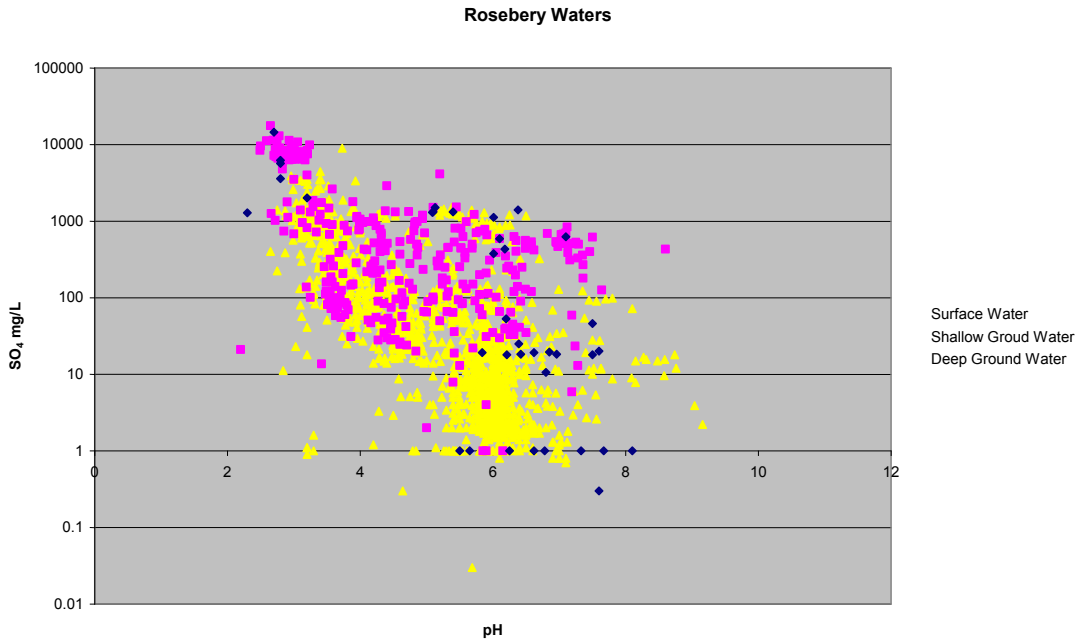

Figure 4.24 Sulphate versus pH for Rosebery waters (excluding process water)

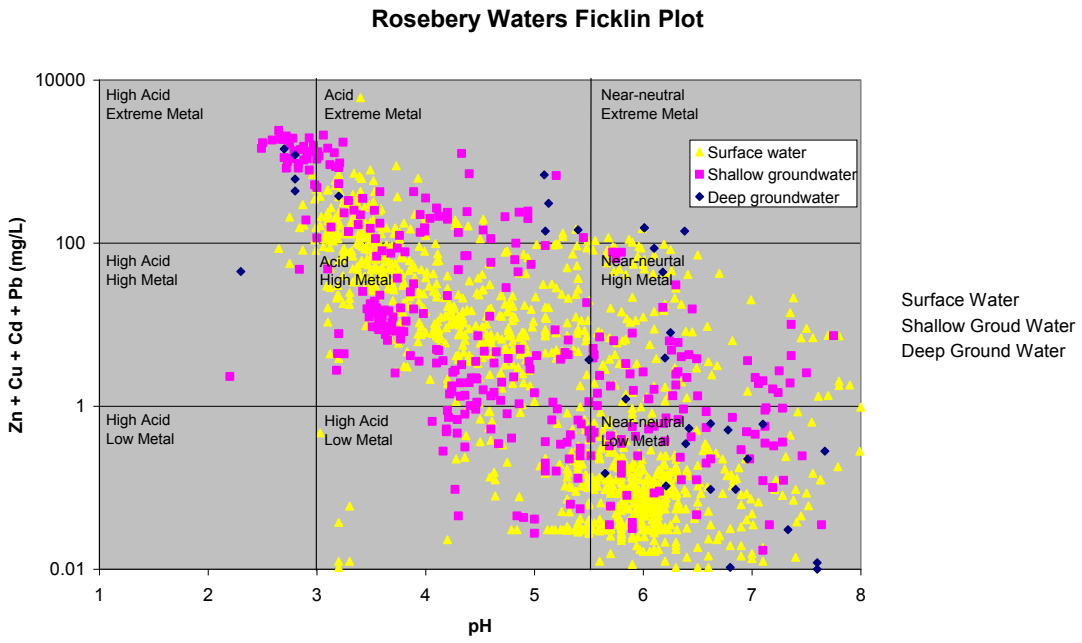

Figure 4.25 Ficklin plot for Rosebery waters

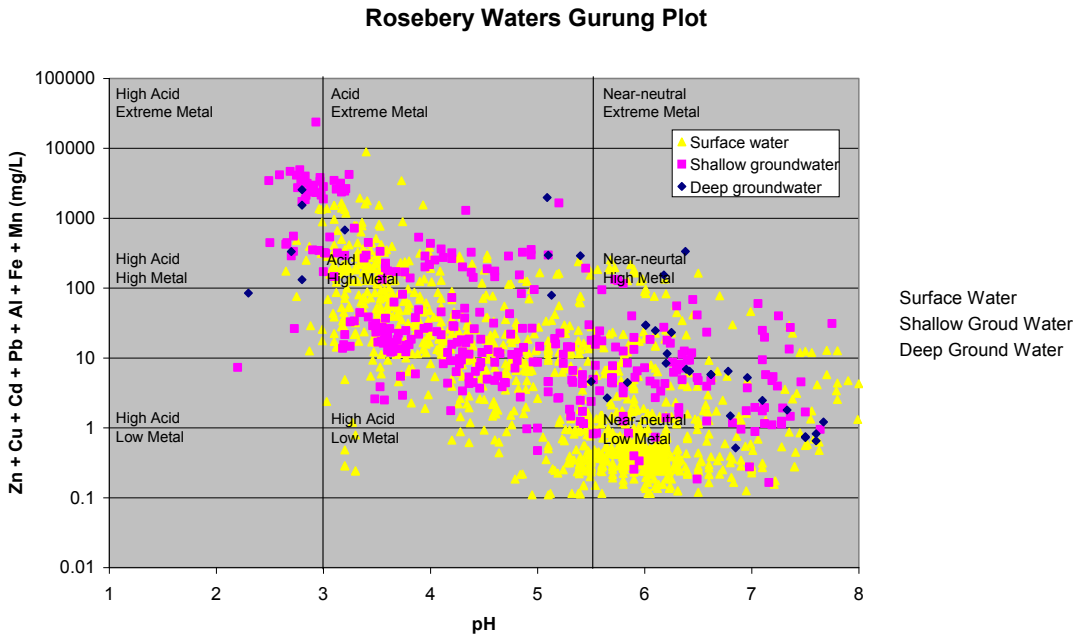

Figure 4.26 Gurung plot for Rosebery waters

Rosebery waters were distributed over all classifications on Ficklin and Gurung plots (Figure 4.25 and Figure 4.26), displaying a range from uncontaminated waters, to water where AMD was well developed. Both groundwaters and surface waters were found in the high acid-extreme metal section of the plots.

4.5.3.2 AMD contamination

The highest contamination recorded within the study area occurred at the sample site AC5 (Figure 4.6). Assay creek is therefore considered the end member representing severe AMD generation at Rosebery. AC5 sampled shallow groundwater near the foot of the assay creek waste dump. It was a unique sample point constructed using an open vertical cement pipe which allows a sample to be collected and flow observed at the base of the waste dump.

Figure 4.27 displays the spatial distribution and concentrations for Zn in waters over the study area. These spatial representations, like the spatial representations of pH and temperature (Figure 4.7 and Figure 4.13), demonstrate that all recorded contamination in groundwater was proximal to an obvious point source of AMD. These point sources include the underground and surface mine workings, waste rock piles, processing areas, tailings dams, as well as contaminated surface water draining from such sources.

The highest value for Zn (Figure 4.14; Figure 4.27; Table 4.23) occurs within AMD from the open-cut followed by process waters and the assay creek waste dump (AC5). Zn values recorded in Rosebery waters were up to six orders of magnitude greater than the ANZECC (2000) trigger values.

The highest values for dissolved Pb over the study area (Table 4.24; Figure 4.15) relate to process water (not necessarily AMD) and mine discharge. Concentrations of Pb associated with AMD at Rosebery were up to five orders of magnitude higher than the ANZECC (2000) trigger values.

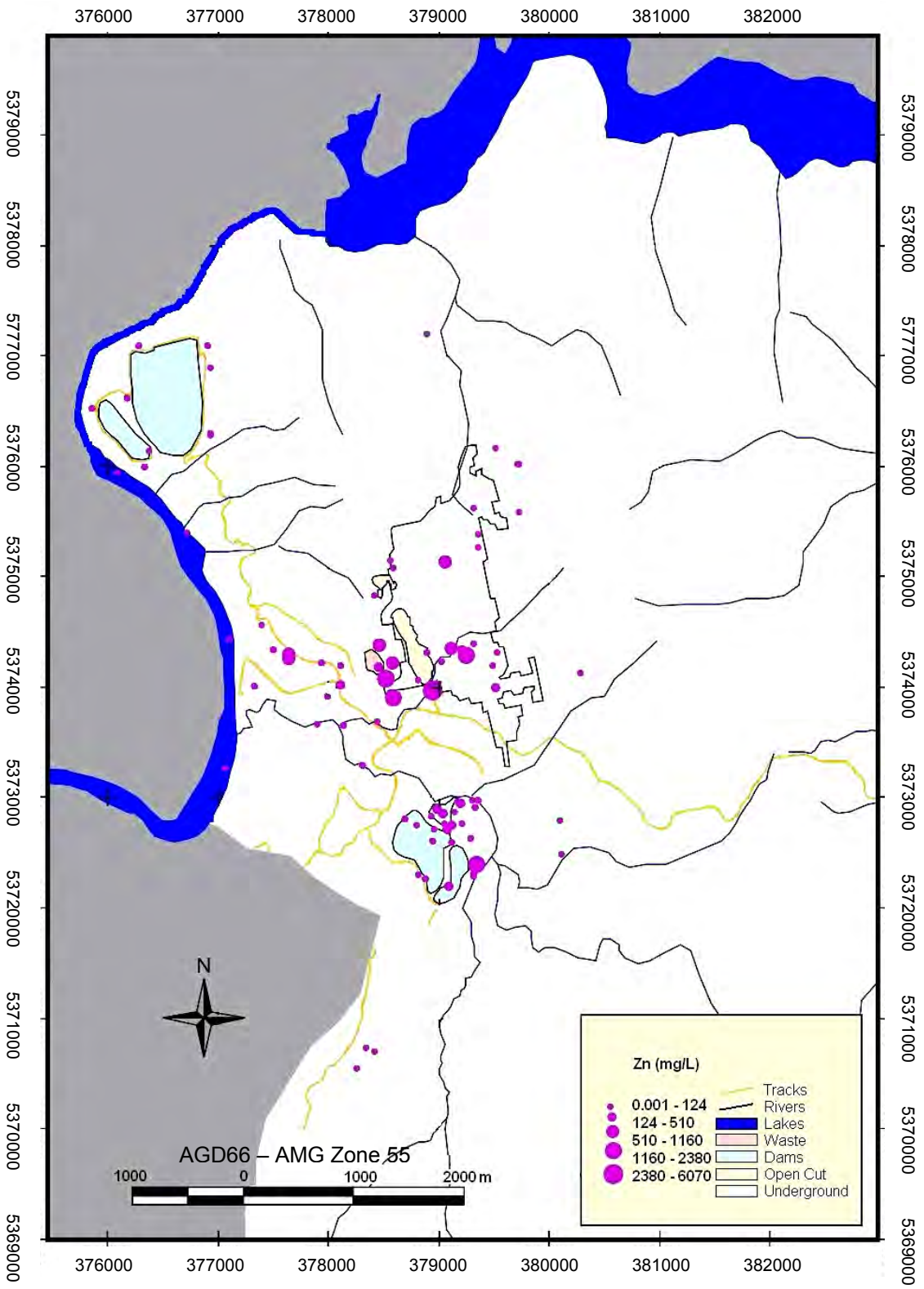

Figure 4.27 Concentration of Zn in Rosebery waters (total dataset)

	n	Minimum Zn mg/L	Maximum Zn mg/L	Mean Zn mg/L
Rainfall	-	-	-	-
Lake Rosebery	-	-	-	-
Lake Pieman	441	0.001	2.7	0.09
Drillholes groundwater	19	0.001	7.8	0.90
Stitt River	70	0.03	25.7	1.37
Rosebery Creek	56	0.01	26.2	5.86
Assay creek	185	1.8	2380	393.03
Open-cut	51	0.15	6070	166.79
Underground	41	0.001	1390	285.46
Primrose creek	75	1.75	91	25.91
Filter plant creek	88	0.5	85	14.22
Miscellaneous creeks	4	0.005	0.059	0.03
Tailings dams No. 2&5	161	0.01	200	19.26
Wetlands	163	0.086	414	97.43
Seepage @ dams 2&5	112	0.01	1258	66.82
Flume	417	0.001	1300	46.73
Polishing pond	419	0.001	29.4	0.61
Bobadil outflow	1360	0.0005	16	0.64
Bobadil seepage	59	0.001	15.4	1.68
Abandoned mine workings	19	0.801	18.5	7.35

Table 4.23 Variation of Zn over the study area; results in mg/L

	n	Minimum Pb mg/L	Maximum Pb mg/L	Mean Pb mg/L
Lake Pieman	428	0.0001	4.7	0.04
Drillholes groundwater	19	0.001	0.46	0.07
Stitt River	56	0.01	0.83	0.03
Rosebery Creek	54	0.001	2	0.29
Assay creek	185	0.01	2.34	0.53
Open-cut	50	0.01	0.94	0.19
Underground	38	0.001	110	18.14
Primrose creek	75	0.14	6.47	1.10
Filter plant creek	87	0.02	8.8	0.73
Miscellaneous creeks	4	0.005	0.042	0.02
Tailings dams No. 2&5	157	0.01	5.09	0.55
Wetlands	160	0.01	2.54	0.68
Seepage @ dams 2&5	101	0.01	2.9	0.67
Flume	417	0.0001	1190	23.58
Polishing pond	422	0.001	2.52	0.12
Bobadil outflow	1314	0.0005	1.89	0.08
Bobadil seepage	57	0.003	0.76	0.07
Abandoned mine workings	19	0.028	5.1	0.53

Table 4.24 Variation of Pb over the study area; results in mg/L

	n	Minimum Cd mg/L	Maximum Cd mg/L	Mean Cd mg/L
Lake Pieman	423	0.0005	0.13	0.00
Drillholes groundwater	19	0.0005	0.005	0.00
Stitt River	57	0.0005	0.03	0.01
Rosebery Creek	51	0.0005	1.94	0.06
Assay creek	181	0.0005	5.22	0.94
Open-cut	47	0.0005	1.31	0.16
Underground	16	0.0005	2.14	0.40
Primrose creek	73	0.005	0.22	0.05
Filter plant creek	80	0.0005	0.17	0.03
Miscellaneous creeks	4	0.0005	0.005	0.00
Tailings dams No. 2&5	117	0.0005	0.4	0.04
Wetlands	155	0.0005	0.8	0.15
Seepage @ dams 2&5	94	0.0005	0.78	0.12
Flume	413	0.0005	3.5	0.14
Polishing pond	379	0.0005	0.39	0.01
Bobadil outflow	1206	0.0005	1	0.01
Bobadil seepage	50	0.0005	0.02	0.01
Abandoned mine workings	19	0.005	0.11	0.02

Table 4.25 Variation of Cd over the study area; results in mg/L

Results at AC5 display exceptionally high values for Cd. Mean Cd concentration was 2.89 mg/L (n = 47), 14500 times the ANZECC 95% trigger level for aquatic environments. Cd levels were diminishing with time, however, in AC5 waters (Figure 4.28). Similar trends in pH and sulphate for the same period were more difficult to determine (Figure 4.29 and Figure 4.30). With pH values consistently below 4 and frequently below 3 the shallow groundwater migrating through the assay creek waste dump were considered to represent well-developed AMD. Although not abundant in the host rocks, Cd was a focus of the present study due to its association to AMD and its relatively high toxicity. Cd was found at up to 5.22 mg/L (Figure 4.21) in the waters within the assay creek waste dump (AC5). This level, were it reporting to the aquatic environment, is considered highly toxic, with 0.0002 mg/L being the trigger levels for the protection of 95% of species in slightly-moderately disturbed freshwater systems (0.0008 mg/L for 80%) (ANZECC, 2000).

Mean Cd 0.04 mg/L levels entering the Stitt River at Rosebery Creek and 0.009 mg/L from Bobadil outflow report directly to the Pieman River.

Elevated concentrations of Al and Ca (Figure 4.22; Figure 4.20; Table 4.26) were also noted in AMD waters at Rosebery. Al was found at up to 1970 mg/L in assay creek (AC5); the ANZECC (2000) trigger levels for the protection of 95% of species in slightly-moderately disturbed freshwater systems were 0.055 mg/L (0.150 mg/L for 80%).

	n	Minimum Al mg/L	Maximum Al mg/L	Mean Al mg/L
Rainfall	1	0.2	0.2	0.20
Lake Rosebery	1	0.3	0.3	0.30
Lake Pieman	42	0.24	1.5	0.30
Drillholes groundwater	19	0.05	2.38	0.46
Stitt River	75	0.03	8.4	0.52
Rosebery Creek	52	0.05	3.69	1.11
Assay creek	181	0.2	1970	81.98
Open-cut	44	0.05	115	15.41
Underground	26	0.2	200	49.42
Primrose creek	67	0.06	105	5.56
Filter plant creek	78	0.06	14	1.84
Miscellaneous creeks	2	0.2	0.22	0.21
Tailings dams No. 2&5	111	0.074	16	2.19
Wetlands	158	0.06	37.4	6.39
Seepage @ dams 2&5	113	0.13	30.5	4.61
Flume	0	0	0	
Polishing pond	0	0	0	
Bobadil outflow	20	0.15	195	10.38
Bobadil seepage	2	0.6	1.5	1.05
Abandoned mine workings	19	0.08	2.95	0.95

Table 4.26 Variation of Al over the study area; results in mg/L

Mn contamination was up to 4 orders of magnitude greater than the ANZECC (2000) trigger values over the study area. The highest Mn value (Figure 4.16) was recorded in the assay creek waste dump followed by process waters reporting to the Bobadil Dam. The highest concentrations of Mg (Figure 4.17) were in the assay creek waste dump. Rainwater and surface waters end members sampled as part of the present study were four orders of magnitude less than the highest concentration of Mg.

Assay creek (AC5) also resulted in the highest value for Cu occurring over the study area; up to five orders of magnitude greater than the ANZECC (2000) trigger values. Process and mine waters reporting to the Bobadil Tailings dam also have extremely high Cu concentrations.

Iron concentrations were highest in process waters reporting to the Bobadil dam. The highest concentrations in AMD were found in the assay creek waste dump and open-cut mine. Fe concentrations of up to 15000 mg/L were recorded in the PRM (2004) database.

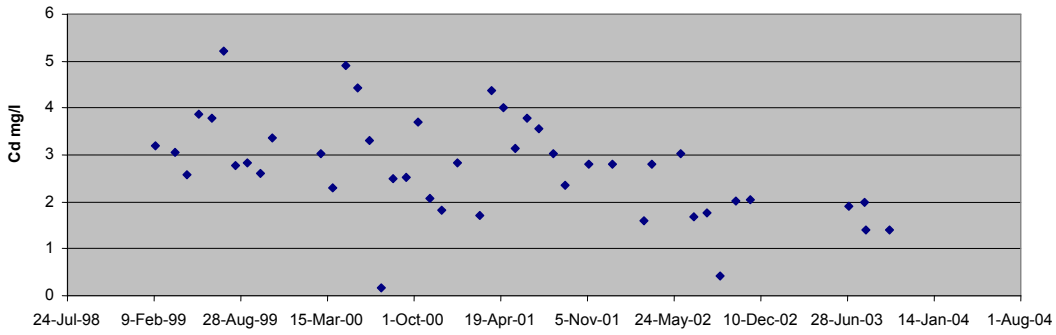

Figure 4.28 Cd concentration of sample point AC5 versus time

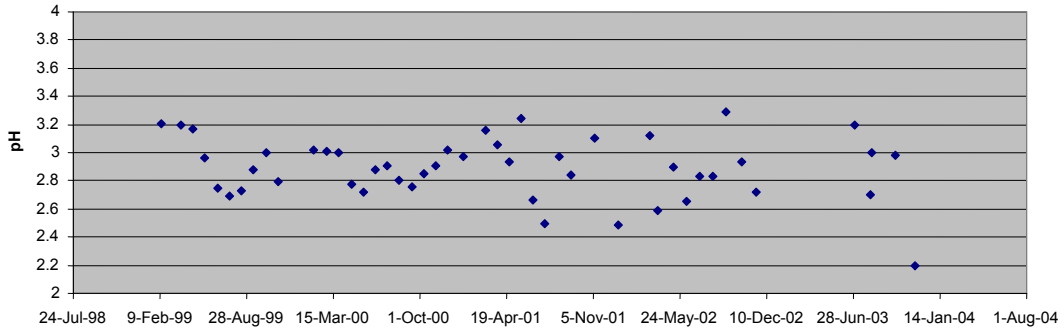

Figure 4.29 pH of sample point AC5 versus time

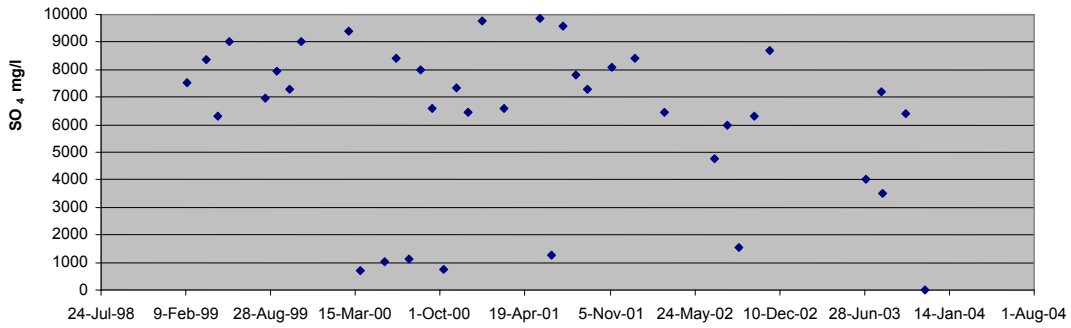

Figure 4.30 Sulphate concentration of sample point AC5 versus time

The metals Ni and Cr were all below detection limit (0.05 mg/L) in the initial sampling and not analysed for in later sampling campaigns within the present study. Arsenic was analysed for in 30 samples within the present study with only 2 samples having recordable limits (> 0.001 mg/L), the highest of which was 0.083 mg/L *c.* 4 times the ANZECC (2000) 95% trigger level. 104 analyses of Bi from the dataset returned results below detection limits of 0.1 mg/L and 0.01 mg/L (where more than one detection limit is stated, data has come from numerous sources, see Appendix Three). All analyses for Sb in 211 water samples gave results below detection limits which ranged from 0.1 to 0.001 mg/L (Appendix Three).

4.5.3.3 Major ions

Sulphate analyses confirmed the theory expressed in Chapter Three, that Rosebery Creek is contaminated downstream of the Rosebery mine. Figure 4.31 displays a definitive increase in sulphate between the upstream sample point RC1 and the downstream sample point RC2 (over a *c.* 1 km length of the creek; Figure 4.6) indicating the source of the contamination is AMD originating from the Rosebery mine.

Surface waters (SW), groundwaters (GW) and acidic drainage (AD) represent the three dominant water groups at the Rosebery mine. Figure 4.32 and also Table

4.27 display the water chemistry for rainwater (RW), together with three samples chosen to represent end-members for each group.

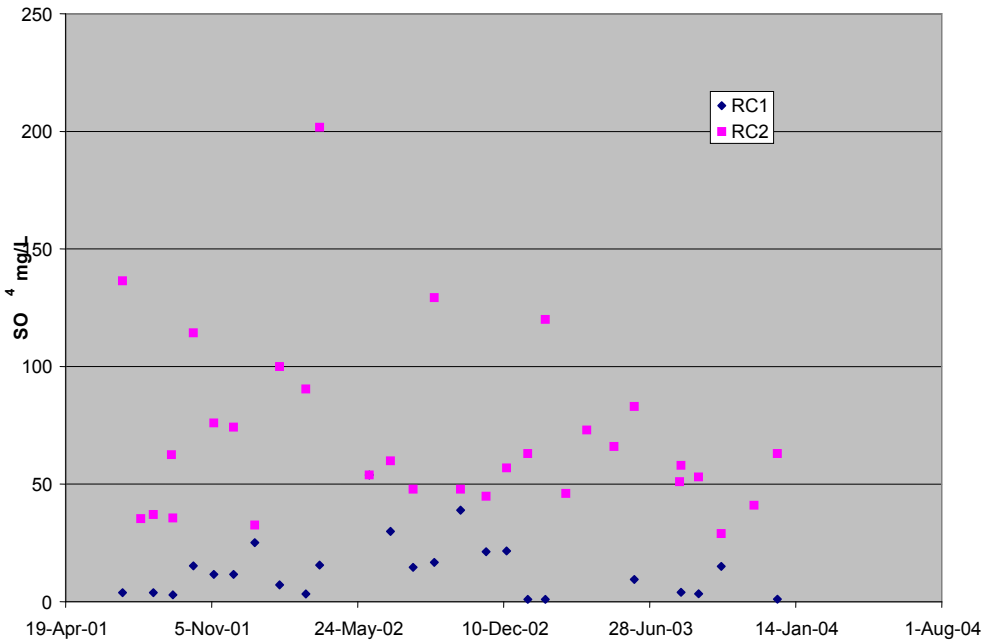

Figure 4.31 Sulphate over time in Rosebery Creek; RC1 was up-gradient of the mine workings; consequently these data were useful for setting the local surface water background for sulphate. RC2 has AMD directly reporting to it (Figure 4.6)

Sample RW was taken from Rosebery rainwater in Beech Road and SW was uncontaminated surface water taken from Mountain Creek during peak flow (Figure 4.3). Peak flow conditions were sampled to ensure the relative proportion of baseflow contributing to the stream flow was at a minimum, thus representing the end-member for surface water flow. GW was obtained from a deep artesian drillhole (250R) and is representative of the deep groundwaters that have undergone extensive interaction with both mine sequence rocks and country rocks. AD was taken from AC5 and is representative of groundwaters severely affected by AMD. Sampling for major ions in 2003 enabled the plotting of 20 samples on a Piper diagram (e.g., Figure 4.32). To display relative contamination loads on piper diagrams, a thematic colour approach was developed where the colour of the sample was varied with concentration of a specific analyte using the same 20 samples displayed in Figure 4.32 (Figure 4.33 to

Figure 4.38). This approach also enabled a visual comparison of the samples chemistry relative to the end members. Combined with existing data (Hale, 2001), a total of 59 samples could be represented on the cation section of a Piper diagram (Figure 4.39).

	Beech Road Rosebery Rainwater (RW)	Surface water end member (SW)	Groundwater end member (GW)	Acid drainage end member (AD)
Ca^{2+} (mg/L)	0.3	0.7	44	175
Mg^{2+} (mg/L)	0.6	0.8	5.4	270
Na^{+} (mg/L)	5.4	7.6	24	5.8
K^{+} (mg/L)	0.3	1.0	0.8	1.4
Cl^{-} (mg/L)	10.5	12.5	16	19.5
CO_3^{2-} (mg/L)	0	0	0	0
HCO_3^{-} (mg/L)	<5.0	<5.0	210	0
SO_4^{2-} (mg/L)	<5.0	<5.0	<5.0	5600
pH	5.8	5.5	7.3	2.7

Table 4.27 End-member water chemistry for August 2003 sampling (all results in mg/L with the exception of pH), note that alkalinity isn't measured at pH < 4.5 (the typical indicator point for carbonate alkalinity)

	n	Minimum sulphate mg/L	Maximum sulphate mg/L	Mean sulphate mg/L
Rainfall	0	0	0	0.00
Lake Rosebery	1	5	5	5.00
Lake Pieman	680	0.03	591	11.0
Drillholes groundwater	19	1	46	14.4
Stitt River	64	0.30	310	23.6
Rosebery Creek	57	1	202	44.4
Assay creek	185	13.7	17659	2355
Open-cut	51	7.78	4430	453
Underground	41	0.3	14500	1767
Primrose creek	75	8.68	540	131
Filter plant creek	87	5	480	74.2
Miscellaneous creeks	3	5	18.9	9.90
Tailings dams No. 2&5	106	1	973	245
Wetlands	163	11.2	1739	832
Seepage @ dams 2&5	109	7.9	1793	500
Flume	416	149	10710	794
Polishing pond	420	97.3	7005	627
Bobadil outflow	1348	270	2244	599
Bobadil seepage	59	1	840	441
Abandoned mine workings	14	31	819	179

Table 4.28 Variation of sulphate analyses over the study area; results in mg/L

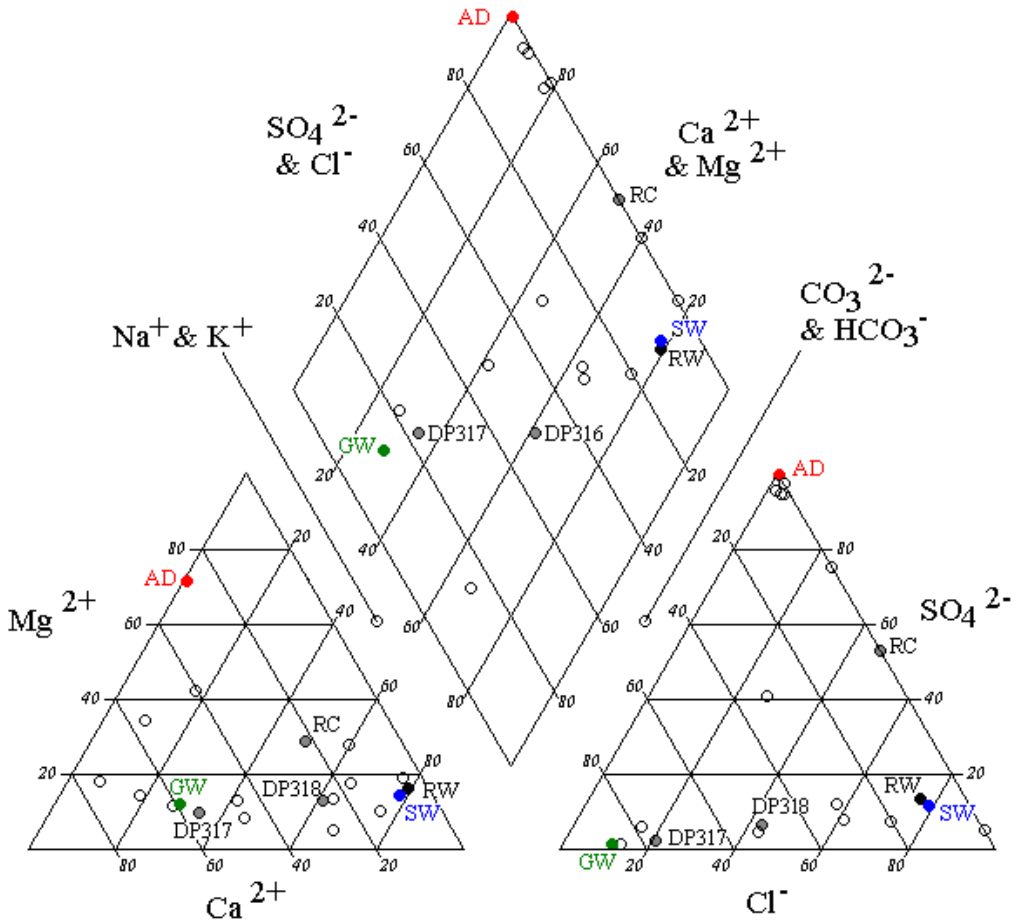

Figure 4.32 Geochemistry of end member and additional 16 waters at Rosebery, August 2003. End members are denoted by SW (surface water), GW (groundwater), RW (rain water) and AD (acid drainage). RC refers to the mine sample point RC2 from Rosebery Creek and DP317 and DP318 are drillholes discussed specifically in the text (Figure 4.6)

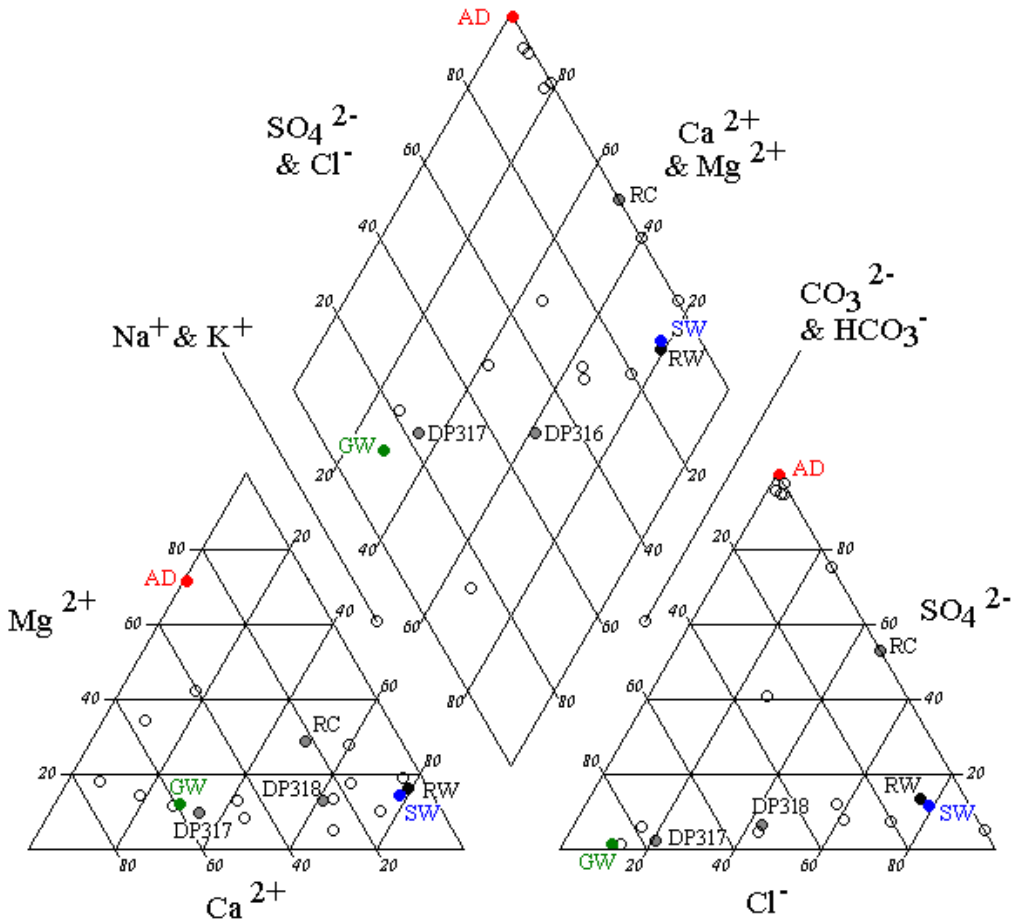

Figure 4.32 Geochemistry of end member and additional 16 waters at Rosebery, August 2003. End members are denoted by SW (surface water), GW (groundwater), RW (rain water) and AD (acid drainage). RC refers to the mine sample point RC2 from Rosebery Creek and DP317 and DP318 are drillholes discussed specifically in the text (Figure 4.6)

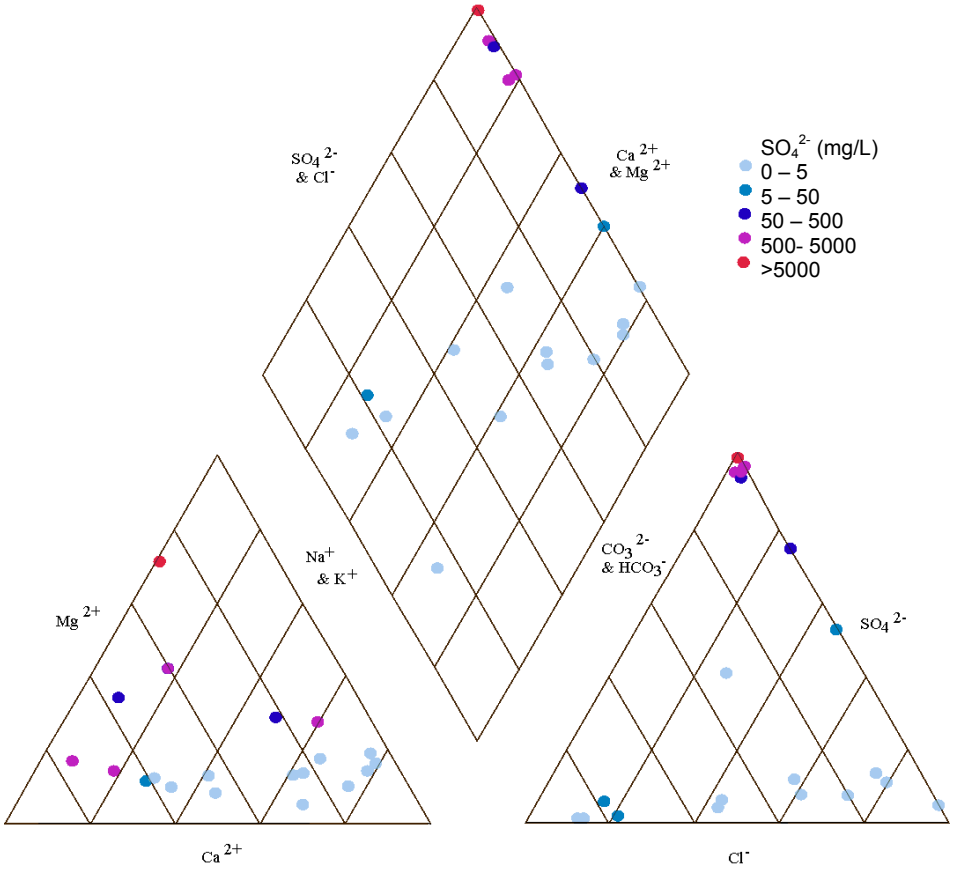

Figure 4.33 Piper diagram with sulphate concentrations

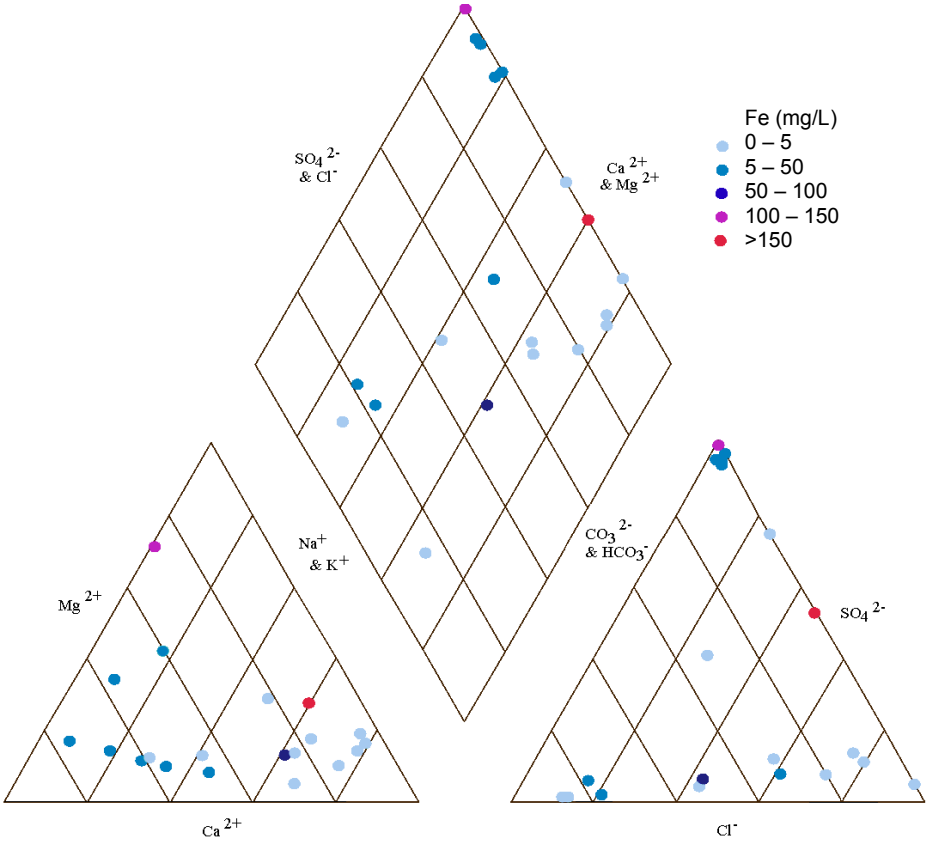

Figure 4.34 Piper diagram with iron concentrations

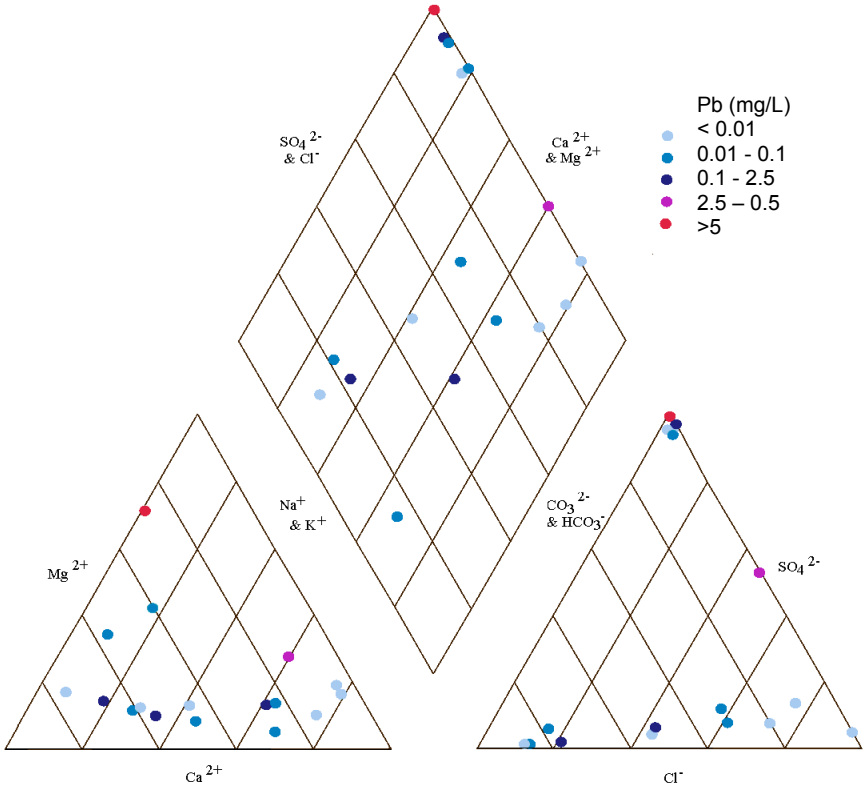

Figure 4.35 Piper diagram with lead concentrations

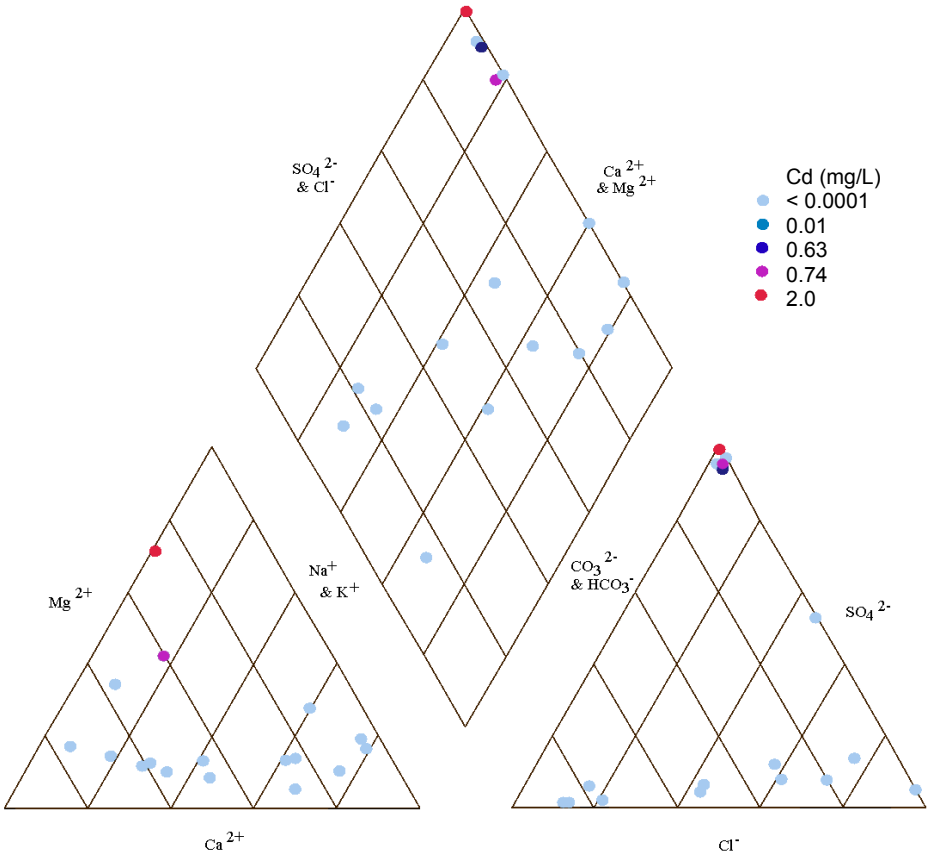

Figure 4.36 Piper diagram with cadmium concentrations

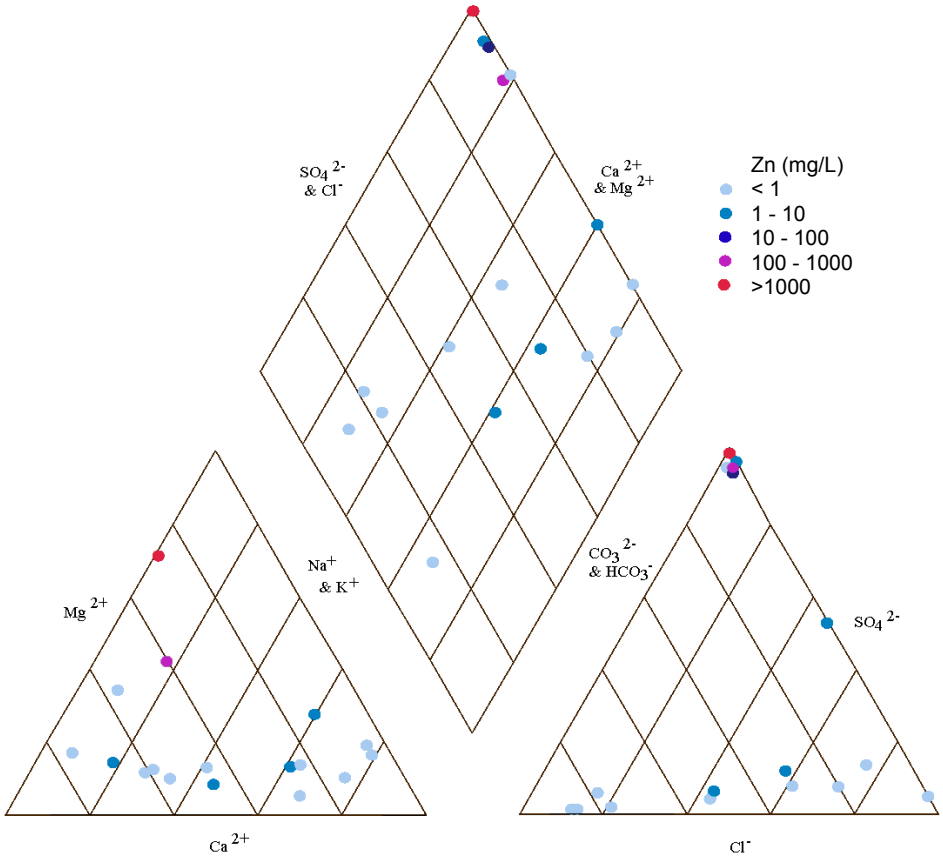

Figure 4.37 Piper diagram with zinc concentrations

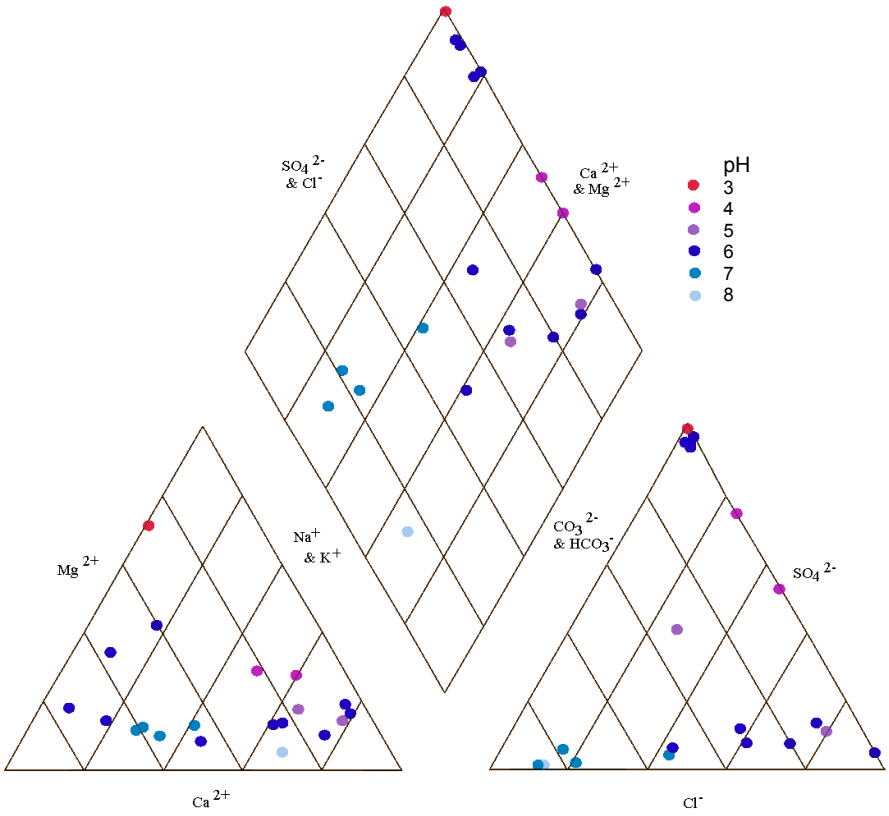

Figure 4.38 Piper diagram with pH

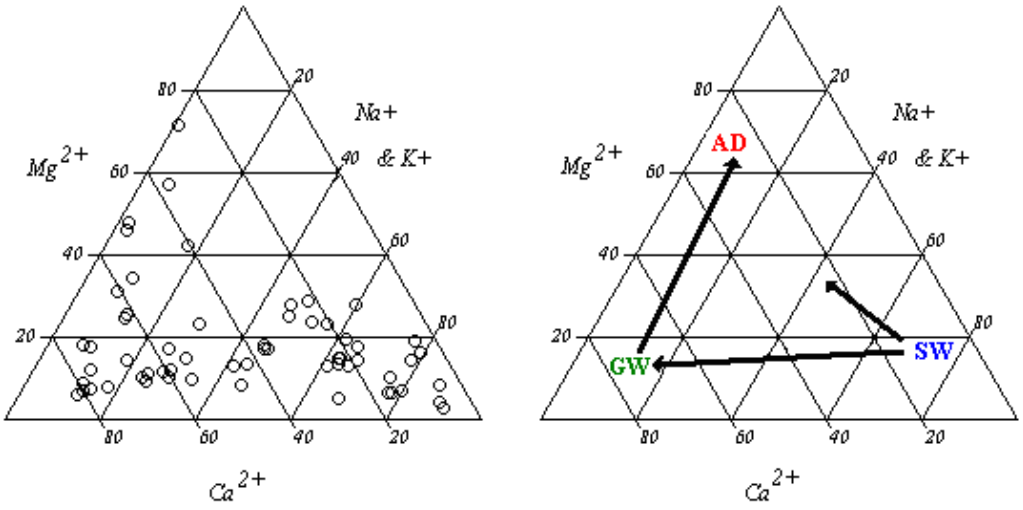

Figure 4.39 Cations in groundwaters and mine waters of the 59 samples at Rosebery. AD = acid drainage end member, GW = groundwater end member, and SW = surface water end member. Arrows represent the development of waters from surface waters, to groundwaters and acid drainage

4.5.4 Stable isotope results

At Rosebery δD and $\delta^{18}O$ contents of waters have been examined to investigate their potential recharge sources with regard to: (i) exposure to evaporation; (ii) climate; (iii) water-rock interaction; and (iv) elevation of precipitation. Table 4.29 lists the results of the new stable isotope research. These data were added to Hale's (2001) results in Figure 4.40.

Both studies (Hale's (2001) study and the present study) provided isotopic analysis of rainwater (Figure 4.40). Theses values form a local meteoric line, along which most data at Rosebery lie. Those data that lie off the local meteoric line lie parallel to an accepted trend for evaporation.

Source	$\delta^{18}O$ ‰SMOW	δD ‰SMOW	pH
DP318 G.W.	-5.4	-30.0	6.3
DP317 G.W.	-5.7	-29.6	6.8
P13 pre-tailings 2P/6	-4.7	-24.7	5.9
P1 tailings 2P/5	-1.3	-9.6	6.5
RW field house	-5.1	-26.2	5.8
250R G.W.	-5.9	-31.2	7.3
250R sump water	-6.5	-34.8	7.0
235R G.W.	-5.7	-29.8	6.6
AC5	-5.9	-32.2	2.7

138R G.W.	-5.5	-26.8	4.5
9 level fault	-5.5	-28.8	6.2
SED mine water	-5.2	-26.9	6.4
DDH NED	-5.9	-29.6	7.7
BD V-notch	-4.8	-25.0	5.9
BD fault	-6.2	-32.7	6.2
114R G.W.	-7.3	-39.2	5.7
KP309 G.W.	-3.5	-19.2	5.5
Mountain Creek	-6.1	-31.5	5.5
Lake Rosebery	-6.1	-33.9	5.4
RC2	-6.5	-34.6	4.0
Beech Rd seep	-5.0	-27.5	6.0

Table 4.29 Stable isotope analyses of $\delta^{18}O$ and δD at Rosebery, analysed in the present study

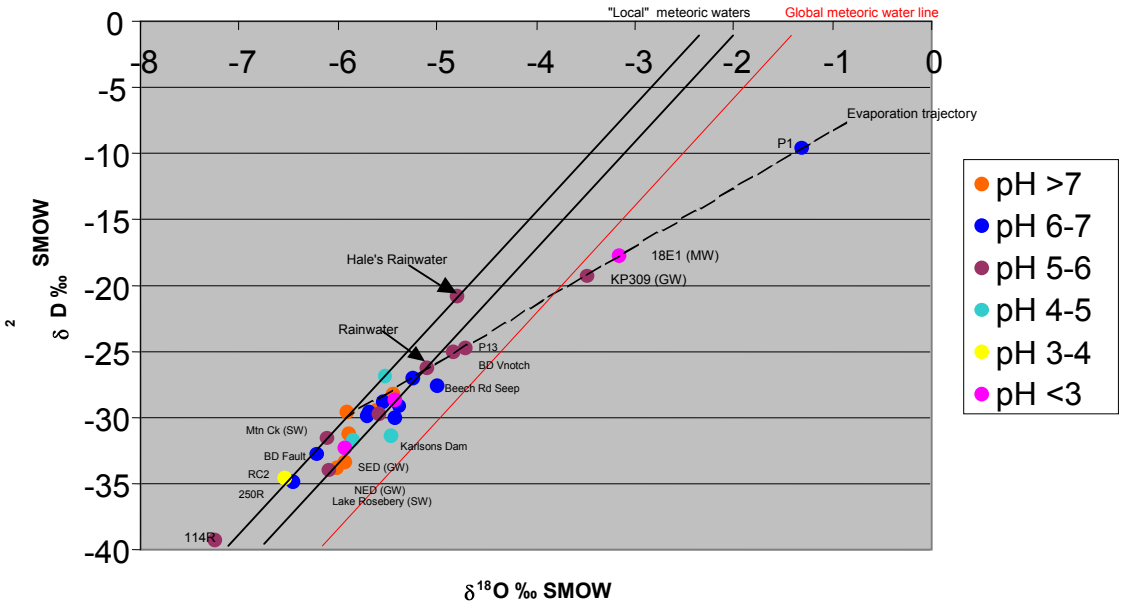

Figure 4.40 Rosebery stable isotopes (11 of the 32 samples after Hale, 2001); local meteoric lines were created parallel to the global meteoric line using the two varying rainwater samples

4.6 Discussion

4.6.1 Acid base accounting

4.6.1.1 Acid-consuming potential

Sampling beyond the open-cut area in the present study highlighted the presence of non acid-forming bedrock material. This material was also identified as having a limited amount of acid-consuming potential (ACP), a combination not identified in

previous studies. Non acid-forming material with a zero NAG result indicated that the material either: (i) contains no sulphide, or (ii) contains more neutralising material than acid-generating sulphides. The presence of materials with zero NAG and positive ANC indicates that some of the material at Rosebery has potential to consume acid. These materials in contact with, and down stream of acid sources, have the potential to neutralise AMD before entering the receiving environment.

The natural material with the highest ANC recorded at Rosebery (48.02 kg H_2SO_4/t) was a sample of oxidised schists and clays taken from the southern open-cut (Table 4.19; Figure 4.1; Appendix 2). By definition of ANC, this material has the potential to neutralise a sample with a NAG of 48.02 kg H_2SO_4/t. This NAG corresponds to a theoretical 1.57% S or *c.* 3% pyrite contained in a material with no acid consuming minerals.

Local materials in general have low ANC relative to NAG values. Pure calcite has a theoretical ANC of 1000 kg H_2SO_4/t (Section 4.2.3) which indicates Rosebery materials with ANC < 50 kg H_2SO_4/t have relatively low ANC. Some *c.* 4 km from the Rosebery mine, the Ordovician Gordon Group Limestone is a potential external source of high ANC material. The use of industrial lime, which is the practice at Rosebery, is a more likely source due to logistics and the inaccessibility of the local limestone deposits.

At Rosebery, neutralisation of metal-rich acidic water was evident from the precipitation of minerals on surfaces in contact with AMD (e.g., Figure 3.14-20; Figure 3.24). When an acid is neutralised, precipitates are removed from solution and coat flow surfaces (e.g., DeNicola and Stapleton, 2002; and Hammarstrom et al., 2003), however, the build up of such precipitates greatly decreases the potential to neutralise additional acid, a process referred to as armouring (Hammarstrom et al.,

2003). The formation of precipitates also has the potential to cement pore and fracture spaces, or dissolve fracture fill, both greatly altering the hydraulic connectivity and fluid flow within a rock mass (Benlahcen, 2003), further lowering the acid consuming capacity of a rock mass.

Although evidence for significant neutralisation has been observed on surface through the porous regolith, glacial and waste pile deposits (e.g., Figure 3.14; Figure 3.17; Figure 3.19), this is expected to be less in the fractured rock aquifer. In a porous material the porosity and resultant surface area available for reaction with AMD is dependent on the grain size and shape, whereas in a fractured material the available surface depends primarily on fracture density (Banks and Robins, 2002). In general, fractured rock aquifers have far less reaction surface and fewer available reactive minerals than granular porous media; the later offers greater potential to attenuate and retard pollutants (*ibid*.). ANC is calculated on crushed fine material with theoretically the entire sample exposed to acid and hence completely neutralised. ANC is an over estimate of the acid consuming capacity for a crystalline fractured rock aquifer such as that observed at Rosebery, however, ANC analyses indicate that the country rocks do have a small but limited capacity to neutralise AMD.

4.6.1.2 Net acid-generation

ABA results (Section 4.5.1) indicated that materials at Rosebery range from non-acid forming to those that have a high capacity to produce acid. These results were consistent with the results of Brady (1997) for material from the Rosebery open-cut area. The NAG analyses of material from waste rock piles and wall-rock within the open-cut indicated that AMD generation will continue to occur into the future. Further kinetic testing is required to quantify the expected longevity of AMD generation at Rosebery.

The tailings material is potentially acid forming, even with the current preconditioning involving the addition of lime (Section 4.4.1). The addition of lime is considered a temporary measure due to the large volumes required to neutralise the sulphide fraction of the tailings material. Assuming a 100% efficient neutralisation, the *c.* 7 Mt of tailings would theoretically require *c.* 2.5 Mt of pure lime, to completely neutralise the tailings potential AMD, at a current cost of *c.* $100/t. The addition of such quantities of lime, at much higher rates than the existing preconditioning (Section 4.4.1), would result in larger volumes of waste material. These volumes would require impractical extensions to the existing tailings dams as well as significant reworking of the existing material, with costs of up to hundreds of millions of dollars.

The results of the tailings, waste rock and wall-rock material NAG analyses were extrapolated to represent the underground mine workings because the workings were both: (i) the original source of these materials; and (ii) the final disposal site of these materials. NAG results indicate that the underground mine workings were therefore also expected to continue to produce AMD into the future, despite a limited amount of ANC from the country rock in the area.

4.6.2 Whole-rock and mineral geochemistry

4.6.2.1 Host rocks

In the present study „host rocks' refer to those capable of containing ore material and „country rocks' refers to those which are considered waste material. Carbonates (rhodochrosite, dolomite, calcite and ankerite) and silicates (sericite, chlorite, albite and orthoclase) provide potential neutralising materials in the host rocks (e.g., equations 4.4 and 4.5) at Rosebery. Of the minerals Finucane (1932) identified in the Rosebery ore, the potentially acid-generating sulphides included; pyrite, sphalerite,

galena, chalcopyrite, arsenopyrite, tetrahedrite, and bournonite. Host rocks at Rosebery were potentially acid-generating material due to the abundance of sulphides, primarily of pyrite. When reviewing theoretical MMPA values obtained for typical ore types using Equation 4.9, pyrite was found to control most of acid-generation from Rosebery ores (Table 4.30). The major improvement of MMPA over MPA at Rosebery is that the sulphur component of barium, having no contribution to the resultant acid-generation, is taken into account.

Minerals	Pyrite-chalcopyrite ore type MMPA kg H_2SO_4 / t		Sphalerite-galena-pyrite ore type MMPA kg H_2SO_4 / t		Barite ore type MMPA kg H_2SO_4 / t	
	Minimum	Maximum	Minimum	Maximum	Minimum	Maximum
Pyrite	490.04	1306.78	163.35	490.04	0.00	163.35
Chalcopyrite	10.68	53.39	2.67	10.68	0.00	5.34
Sphalerite	0.00	0.00	0.00	0.00	0.00	0.00
Galena	0.00	0.00	0.00	0.00	0.00	0.00
Arsenopyrite	0.00	12.04	0.00	12.04	0.00	0.00
Tetrahedrite-tennantite*	0.00	0.21	0.08	0.42	0.08	1.26
Pyrrhotite	0.00	0.30	0.00	0.00	0.00	0.00
Barite	0	0	0	0	0	0
MMPA	500.72	1372.72	166.1	513.18	0.08	169.95
Pyrite % of MMPA	97.87	95.20	98.34	95.49	0.00	96.12

Table 4.30 Ore types contents (after Table 4.4) and the relative contribution to MMPA. All Sb was assumed to be present as Tetrahedrite, all Cu as Chalcopyrite, all As in the form of Arsenopyrite, and trace sulphides as well as sulpho-salt content was assumed as 0

4.6.2.2 Country rocks

As in the host rocks, pyrite in the country rocks was the principle acid-generating mineral at Rosebery. Carbonates, sericite and chlorite in the footwall have the potential to act as the major neutralising minerals at Rosebery (e.g., Equation 4.4 and Equation 4.5). In addition, the significant clay fraction observed in waste stockpiles was thought to play a major neutralisation and potential attenuation role in containing contaminants. Clay minerals observed in the glacial cover may also contribute to the neutralisation (e.g., Equation 4.6) and were not expected to contribute to generation of acid.

4.6.2.3 Tailings material

Tailings material at Rosebery is made up of finely ground material created as a by-product from the flotation process. The significant fraction of gangue in the host rock, including sulphides, which are not removed by flotation are delivered by a flume to the tailings facilities. For practical purposes it was reasonable to assume that the material was essentially identical to that processed as ore minus a fraction of lead, zinc, copper, silver and gold that was extracted. The major addition was lime which was intended to provide some buffering capacity to the tailings material. Like the ore material, it was pyrite in the tailings which has the greatest contribution to acid-generation. The tailings average sulphur content of 12.95 wt % (Table 4.31) indicates an MPA of 396 kg H_2SO_4/t and a back-calculated MMPA of 361 kg H_2SO_4/t (Table 4.31).

Tailings	wt%	wt% S	kg H_2SO_4/t
Pyrite	21.89	11.71	358
Chalcopyrite	0.32	0.11	1.70
Sphalerite	1.98	0.65	0.00
Galena	0.58	0.08	0.00
Arsenopyrite	0.15	0.03	1.83
Tetrahedrite -tennantite	0.02	0.00	0.01
Barite	2.70	0.37	0.00
MMPA			361

Table 4.31 Tailings contents (after Table 4.7) and the relative contribution to MPA when applying Equation 4.9. All Sb was assumed to be present as Tetrahedrite, all Cu as Chalcopyrite, all As as Arsenopyrite, and trace sulphides as well as sulpho-salt content was assumed as 0

4.6.3 Sulphide mineralogy and geochemistry

Of particular interest were the elevated trace elements in the Rosebery sulphides that have the potential to become contaminants. Although the main sulphide phase generating AMD at Rosebery was likely to be pyrite (Equation 4.1), under the acidic conditions generated, all sulphides present will contribute to the contaminant load (Equation 4.2). Metal contaminants; Fe, Zn, Pb, Cu, As and Sb were all primary elements of the major sulphides present in Rosebery host rocks; pyrite, sphalerite,

lead, chalcopyrite, arsenopyrite and tennantite - tetrahedrite respectively. Of these, all but Sb were found to be mobilised and concentrated in AMD at Rosebery. Although tetrahedrite was anomalously high at Rosebery, up to 3% in the barite ore, Sb has not been detected in Rosebery waters, however, only limited analysis has investigated Sb.

Martin (2004) showed the sulphides at Rosebery to have elevated levels of Ag, As, Au, Bi, Cd, Co, Cu, Fe, Ni, Mn, Pb, Pd, Sb, Sn, Te, Tl and Zn. The trace element concentrations within neutralising materials could also contribute to the contaminant load of AMD at Rosebery. Further analysis at Rosebery was considered beyond the scope of the present study, however, it is recognised that trace elements from rock and plant material not yet investigated may also contribute to contaminants related to AMD.

4.6.4 Aqueous geochemistry discussion

4.6.4.1 pH

Waters with very low pH (2-4), could in all cases be associated with a local up-gradient point source of AMD at Rosebery (Figure 4.7; Figure 4.29; and Figure 4.38). Local vegetation in Tasmania contributes to decreased pH (4 to 6) in surface waters due to organic acids in the soils (RPDC, 2003). Waters considered uncontaminated by AMD have background pH values as low as 4 in the Rosebery area. Because background surface waters were quite acidic, early detection of the onset of acid mine drainage development at Rosebery required further chemical analysis and could not rely on pH alone.

Regionally, deep groundwaters had near-neutral pH (6 to 8); (Table 4.21; Figure 4.14 to Figure 4.26. The only deep groundwaters which had low pH values were within the vicinity of the operating mine. This demonstrated that either: (i) limited monitoring has not detected the deep migration of acidic water; (ii) acidic waters have

not migrated regionally; (iii) acidic waters have been diluted and neutralised by groundwaters; (iv) the natural buffering capacity of the aquifer has neutralised any acid; or (v) a combination of (iii) and (iv).

4.6.4.2 Temperature

Elevated temperatures were seen within the Bobadil dam, tailings dams no. 2 and 5, underground and open-cut workings, assay creek waste dump, Stitt River, wetlands, filter plant creek, Rosebery Creek and Pieman River (Figure 4.13). All waters with anomalously high temperatures (excluding the Pieman River) have correspondingly low pH values. Consistent with East's (1999) results, the present study identified that low pH (4-7) waters with low temperatures were more likely to be associated with natural acidic conditions than to be related to AMD. The later waters have anomalously higher temperatures. This is displayed in Figure 4.12 where in general, lower temperatures are displayed in the Rosebery Creek at RC1 which is considered to be unaffected by AMD, than RC2 which is known to be contaminated with AMD. Likewise, a snapshot survey displayed a general trend towards higher temperature with decrease in pH, in many, but not all waters at Rosebery (Figure 4.9). Temperatures at AC5 in assay creek clearly displayed a different trend to all other sample sites throughout 1999 and 2000 (Figure 4.10). The constant temperature assay creek displayed could be explained by AMD smoothing out the seasonal variation as a result of exothermic heat generation in the assay creek waste dump. At Rosebery it was apparent that many factors affected the temperature of waters.

The principle AMD reaction is exothermic (Mills, 1995) and can be responsible for increases in the temperature of waters. At Rosebery, temperature variations were also associated with: (i) seasonal surface temperature variations; (ii) depth of the sample; and (iii) mine activities. Mine activities such as the presence of explosives in

water can produce an endothermic reaction e.g., along with fuel, the active ingredient in ANFO is ammonium nitrate; when mixed with water the reaction is endothermic (Kaufman and Ferguson, 1988).

The high temperatures of the Pieman River (Figure 4.11) may be associated with the large lacustrine source upstream of the Bastyan Dam, Lake Rosebery. All temperatures greater than 15 degrees Celsius within the Pieman River occurred between December and March (inclusive) (Figure 4.11); months when Lake Rosebery would be receiving a significant amount of radiant energy. Without a natural influence like solar radiation, groundwaters (shielded by the overlying rock and soil material), and the small mountain creeks and rivers (shielded by dense vegetation) would not be naturally expected to greatly vary in temperature at Rosebery.

Hale (2001) documented the temperature increase in mine waters with depth. The highest encountered water temperature in the present study (Figure 4.10) was 40.1°C in water intersected by a drillhole in the NED at a depth of roughly 600 m below sea level. Considering the sample had a pH of 7.67, 1 mg/L sulphate and was considered a deep groundwater this temperature was more likely to be associated with the elevated geothermal gradient at Rosebery (Jaeger and Sass, 1963) than AMD. It is in the surface waters and shallow groundwaters proximal to point sources of AMD, that anomalous temperature increases are most likely to be associated with this exothermic reaction.

The present study determined that locally, waters associated with AMD have both low pH and anomalously high temperatures. This can be useful in differentiating between naturally acidic waters and AMD waters and was used as a cost saving tool to avoid expensive analysis, provided external factors contributing to temperature change are considered.

4.6.4.3 AMD contamination

Locally to point sources, the down gradient dispersion of AMD was apparent at Rosebery. On a regional scale, however, groundwater indicated no sign of dispersion of metals from AMD within the flow field. This may have been due to: (i) insufficient data due to the limited access to appropriate sub-surface sampling sites; or (ii) the theoretical regional gradient is towards the mine workings due to pumping at present.

Surface waters over the study area displayed wide variations in dissolved metals (Figure 4.14 to Figure 4.26). Waters over the study area displayed a log normal distribution in dissolved metals (Figure 4.14 to Figure 4.26). The concentration of dissolved metals, electrical conductivity and sulphate correlated negatively with pH (e.g., Figure 4.14 to Figure 4.24). The mean surface water quality (Table 4.23 to Table 4.26 and Table 4.28) was generally many times above the background and critical trigger values of the ANZECC (2000) guidelines (Table 4.1 and Section 4.5.3.2).

The present study confirmed Hale's (2001) work that mine waters were contaminated with the metals Pb, Zn, Cu, Fe, Mn and Mg. The present study also displayed that Rosebery waters were also highly enriched in Cd, Al, and Ca. Results indicated that AMD contamination was evident emerging from or within: (i) assay creek; (ii) the Rosebery open-cut mine; (iii) the Rosebery underground mine; (iv) Rosebery Creek; (v) the Stitt River; (vi) Primrose creek; (vii) filter plant creek; (iix) the tailings facilities; (ix) abandoned mine workings; and (x) mine-waste material used as fill throughout the catchment (e.g., Figure 4.7; Figure 4.27; Table 4.21; Table 4.22; Table 4.23; Table 4.24; Table 4.25; Table 4.26; and Table 4.28).

AMD at Rosebery contains elevated levels of the metals Pb, Zn, Cu, Fe, Mn, Mg, Cd, Al, and Ca. These elements are present at Rosebery in: (i) metallic sulphides (Table 4.3) in the case of Pb, Zn, Cu, Fe; and (ii) minerals such as Rhodochrosite, sericite, orthoclase, albite, dolomite, calcite and ankerite in the case of Mn, Mg, Al and Ca (Table 4.3). Such elements are liberated through the chemical reactions (Equation 4.1 to Equation 4.6) or similar. In addition, metals (including Cd) are present within sulphides at Rosebery as: (i) trace element inclusions; or (ii) replacement elements (Table 4.11 and Table 4.12). Trace elements are liberated when the sulphides they are contained in react through Equation 4.1 and Equation 4.2.

The main objective of reviewing the existing geochemical analysis of metals, and conducting further geochemical analysis was to make inferences about AMD sources and groundwater interaction. Elevated metals have clear connection with the minerals present within the Rosebery deposit, and known potential mechanisms for their liberation and transport in solution are provided (Equation 4.1 to Equation 4.6). The geochemistry of metal contamination from AMD generation and transport at Rosebery is complex and could be the focus of extensive further work, however, any more depth is considered beyond the scope of the present study.

Detailed analysis of AMD using trace metals identified in Martin's (2004) sulphide study, could be the focus of further aqueous geochemical work at Rosebery. Little was known about the concentrations of Ag, Pd, Te and Tl within Rosebery waters. In the present study, As, Bi, Cd, Co, Ni, Sb, and Sn analysis would have benefited from using methods with lower detection limits (Appendix Three), as many samples were below detection limit and data at low levels may have provided more insight into AMD contributions. Likewise, methods with lower detection limits could provide additional information on the potential contamination from Ag, As, Bi, Cd,

Co, Cu, Fe, Ni, Mn, Pb, Pd, Sb, Sn, Te, Tl and Zn within the high volume receiving waters such as the Pieman.

4.6.4.4 Major ion chemistry

Determining the extent of interaction between streams and groundwater was a necessary precursor to developing a groundwater flow model for the Rosebery area. Many surface waters have compositions that suggest that they are recently emerged groundwater. Others appear to have not been influenced by groundwater or interflow interaction. Even in such a perennial high rainfall environment, the small creeks on Mount Black were ephemeral, suggesting that they have little base flow contribution. In support of this conclusion, the chemistry of Mountain Creek (SW) was very similar to that of rainwater (RW), indicative of minimal water-rock interaction.

At the Rosebery mine, waters contaminated by AMD plot at extreme sulphate and magnesium dominance (Figure 4.32). It can be further seen that pH is lowered and metal concentrations are distinctively enriched in the AMD trend (Figure 4.33 to Figure 4.38). Figure 4.33 to Figure 4.38 display thematic Piper diagrams for pH, Zn, Pb, Cd, Fe and sulphate. Extreme contamination values correspond to the end member (AD) acid drainage (except extreme Fe and pH where enrichment is due to AMD in the contaminated Rosebery Creek, RC).

Understanding the end member water types and mixing behaviour was important for identifying contamination sources. Contamination in Rosebery Creek (RC) provided the signature of AMD discharging into the surface watercourses in the area (Figure 4.32). Using this, AMD contaminated surface waters are seen to form an important subgroup of waters. Figure 4.32 also highlights the differences between other groundwaters, for example DP317 and DP318. Spatially DP318 was closer to Saddle Creek and chemically it was also closer to surface waters than DP317. This

represented local surface water leakage to the aquifer from Saddle Creek and provides justification of the use of stream, river or general head boundaries in the model to represent this (Chapter Six).

In Figure 4.39, which summarises the observed trends, the vector approaching AD from SW represents contamination of surface waters and immature groundwaters. Water contaminated by AMD approaches the signature of AD. The vector between GW and AD represents mature groundwater that has interacted with mine materials. Increasing contamination of mine water causes enrichment of Mg^{2+}. It is seen that very few intermediate groundwaters evolve towards the AMD end member, and this is attributed to the fact that the Rosebery mine lies in a discharge region of the current regional groundwater flow system.

Figure 4.32 shows that the water chemistry of each end member is distinctive, and also illustrates that hybrid waters form by mixing of the end members. Many of the waters sampled had chemistries that were consistent mixtures of surface water and groundwater. Mature groundwaters, with little surface water mixing, plot to the left side of the charts in Figure 4.39. Mature groundwaters plot close to GW whereas immature groundwaters and surface waters plot closer to SW (Figure 4.39). As uncontaminated surface water interacts with country rock, compositions migrate towards the left on the Ca^{2+} axis, as displayed by the vector from SW to GW. This is an enrichment of Ca, rather than depletion of Na and K (Table 4.27). It is also concluded that groundwaters with low Ca (i.e. plot to the right of all charts in Figure 4.39) have had little time to interact with country rock and resemble rainwater or surface waters.

Waters rapidly became sulphate dominated upon interaction with AMD and plot towards extreme sulphate on a Piper diagram (Figure 4.33). AMD increases the

sulphate contents relative to other ions so greatly that when presented on a piper diagram it dominates the effects of any other chemistry. Chloride is also slightly enriched in AMD waters (Table 4.27 and Figure 4.32). Bicarbonate is absent in AMD water suggesting removal of CO_2 as a gas (e.g., Equation 4.4). The cation graph of the Piper diagrams (Figure 4.39) proved to be more useful for path tracing because: (i) more samples had cation analysis; and (ii) the chemical effects of AMD on the cation concentrations were not as extreme as for the anions. Contaminated waters became more magnesian and the predominant path for acidification of water in the mine was conversion of pure end member groundwater to AMD.

Figure 4.39 illustrates a trend for water at any point in the SW – GW spectrum to move off the evolution trend towards the AMD end member, providing clear evidence that Mg dissolution was a key process resulting from contamination of Rosebery waters. The source of Mg was likely to be chlorite dissolution (Equation 4.5 and Equation 4.6) or carbonate (dolomite and ankerite) dissolution (e.g., Equation 4.4). These reactions (Equation 4.4 to Equation 4.6) consume H^+ ions, and provide chemical evidence that buffering of AMD occurs within the mine and surrounding aquifer. This may explain the ANC of materials observed at Rosebery (Figure 4.4; Table 4.18 and Table 4.19). Further work is required to determine the relative extent of chlorite to carbonate breakdown in acid consuming reactions occurring at Rosebery. It nevertheless provides a line of evidence that both chloritic and carbonaceous lithologies should be considered for AMD remediation works. The removal of CO_2 related to neutralisation of AMD with carbonaceous lithologies (e.g., Equation 4.3; and Equation 4.4) also has greenhouse implications (Davidson, pers. comm., 2008) which, as yet, have not been addressed and documented by the international mining community.

Although no contamination was observed in the subsurface flow field distal from obvious point sources, it was not conclusive that no contamination was occurring. The location of the available monitoring sites was dependent on drillhole locations. Due to the nature of the deposit at Rosebery most drillholes were drilled from the east to intersect the east dipping orebody at right angles. Due to topography, flow was generally west in the mine area. This means that regionally, most potential sub-surface monitoring points were up gradient of potential contamination.

4.6.5 Stable isotope discussion

Based on isotope analysis, Hale (2001) divided the waters into three distinct groups: (i) a mine water; (ii) a surface water; and (iii) a groundwater group. With the additional analysis performed as a result of the present study, these groups became less pronounced. The additional data did give insight into an evaporation trajectory for the Rosebery area and a second rainwater sample gave further insight into the local variation of meteoric waters (Figure 4.40).

The water sample from the 114R drillhole plots lower on the MWL (Figure 4.40). This could be attributed to its recharge occurring: (i) in a colder climate or more likely in this case (ii) occurring at a higher elevation.

P1, a piezometer in tailings dam no. 2, displays the typical high δD and $\delta^{18}O$ content of groundwater recharged by a surface water body subject to evaporation and this was supported by its relatively high Cl content (Appendix Two; 18 mg/L compared to 10.5 mg/L for rainwater). The high pH (6.5) of P1 (Appendix Two and Figure 4.40) may indicate little influence from AMD, however, based on the sulphate content and its location within the tailings dam, the enrichment in δD and $\delta^{18}O$ could also be due to AMD generation which can produce a similar trajectory to evaporation (Mayo et. al., 1992). In contrast, the nearby P13, a piezometer up-gradient of tailings

dam no. 2, plots closer to the LMWL (Figure 4.40). BD v-notch plots near P13 rather than P1 which indicates this Bobadil groundwater has either seen less evaporation or AMD than P1, however, both high Cl and sulphate contents (18 and 840 mg/L respectively) do not support this hypothesis (Figure 4.40).

18E1, a filled stope also produced a sample enriched in δD and $\delta^{18}O$ (Figure 4.40). Backfilled stopes were filled with process waters sourced from the surface water bodies in the area. The lakes do not plot on any evaporation line, which could be due to their large volumes, and hence the relative lack of evaporation in the wet, temperate environment. However, to achieve this, there must be some degree of mixing in the lakes. In the case of 18E1, the enrichment of δD and $\delta^{18}O$ was most likely due to the generation of AMD, and this was supported by high sulphate contents and a very low pH. In contrast, AC5 at the foot of the assay creek waste dump (Figure 4.6), plots on the meteoric line with high sulphate contents and very low pH. This conflicts with the hypothesis of δD and $\delta^{18}O$ enrichment is due to the generation of AMD at Rosebery and that the process moving waters off the meteoric line could be both AMD generation and climatic. Thus it was not possible to assess whether the isotope signature of mature groundwater varied significantly of immature shallow groundwater at Rosebery, nor if the aquifers could be divided into multiple aquifers based alone on the isotopic signature of groundwaters at Rosebery.

4.7 Application to Modelling

The purpose of geochemistry in the present study was to determine the extent of the AMD problem and gain a better understanding of the existing flow field. Point sources of AMD have been identified for particle starting points for MODPATH models. No contamination was encountered up-gradient of obvious point sources, validating the conceptual and model flow directions. Geochemistry has also provided

justification for surface-groundwater interaction and the use of the various stream, river and general head boundaries within the model. It has also established that most AMD generation occurs in groundwaters that are already evolved, confirming that the Rosebery mine groundwaters are in the discharge zone of the regional groundwater system.

Potential heavy metal contaminants were identified and quantified. It was envisaged that this information could be used for contaminant transport modelling using the MT3D code, however, the application of such models to fractured rock aquifers modelled using a continuum approach is considered inappropriate (Cook, 2003) and was therefore not pursued.

4.8 Geochemistry Conclusions

Potential acid-generating and neutralising minerals were identified using whole-rock geochemistry; the NAG and ANC of Rosebery materials were quantified by ABA. NAG and ANC classification provided a predictive management tool to assess the risk of AMD development at Rosebery. The results indicated that exposed materials at Rosebery have the potential to produce a significant volume of AMD. However, the ANC and major ion studies suggest that Mg containing lithologies react with AMD waters and consume hydrogen ions. The most likely reactions at Rosebery are the breakdown of chlorite, dolomite or ankerite. Local lithologies, rich in these minerals may prove useful in the long term management and neutralisation of AMD at Rosebery.

At the Rosebery mine, metal contaminated waters were derived from localised point sources of AMD such as tailings dams, waste rock, and mine workings. Although background surface waters and contaminated mine waters were acidic, regionally, groundwaters sampled were near-neutral. Using only existing up-gradient

exploration drilling at Rosebery to monitor groundwater contamination was inadequate and is further justification for the installation a purpose-built monitoring network of piezometers at Rosebery.

Although a considerable cost for a mine undertaking closure studies, metal and major element water chemistry can provide valuable information on the interaction and development of groundwaters, surface waters, and AMD. Differentiating among waters contributed to the understanding of the regional flow field in the Rosebery area. There was direct application of the geochemical results to validating the conceptual and numerical groundwater flow model results of the Rosebery groundwater system.

"The physiography, surficial geology, topography of a drainage basin, and the vegetation, influence the relationship between precipitation over the basin and water draining from it" (Fetter, 2001).

5 Conceptual and Mathematical Water Balance and Mine-filling Models

The preceding four chapters have provided the background and raw data pertaining to the nature, scale and controls on groundwater flow and quality at the Rosebery mine and in the surrounding catchment. In the following two chapters, the aim is to use this information to model groundwater flows at Rosebery; first conceptually and mathematically in this chapter, and then numerically in Chapter Six. The modelling approach taken should be dependent on the scope of a given project (Middlemis, 2000). In this project, the modelling objective was to examine the impact of the Rosebery mine on the existing flow field and predict groundwater flow following cessation of mining.

Once a scope is defined, the next two steps in model application are the development of: (i) a conceptual model; and (ii) a mathematical model (Anderson and Woessner, 1992). A conceptual model is an idealised summary of the system and characteristics of the aquifer. Development of a conceptual model includes assessing and qualifying: (i) the internal stresses on the system; and (ii) the boundary conditions influencing the groundwater system (Middlemis, 2000). The mathematical model repeats the same information as the conceptual model, however, it is expressed as a set of equations (Bear et al., 1992).

In this chapter the conceptual model is quantified as a water balance, and subsequently two applications of this are presented: (i) testing of an assertion of the degree of water input to the mine that originates in the open-cut; and (ii) testing the assertion that the mine would fill upon decommissioning. The conceptual model, water balance, calculated open-cut inputs and mine filling model presented within this

chapter provided input for the 3D numerical groundwater flow model presented in the following chapter.

5.1 Conceptual Model

The critical importance of the conceptual stage to the success of modelling is well documented (e.g., Bear et al., 1992; Diodato, 1994; Middlemis, 1997; and Reilly, 2001). Bear et al. (1992) defined conceptualisation of a groundwater system as a set of assumptions that "verbally describe the system's composition, the transport processes that take place in it, the mechanisms that govern them, and the relevant medium properties." Producing a viable and robust conceptual model is an ongoing process which requires refinement throughout the study (Environment Agency, 2002). The conceptualisation of the groundwater system and model commonly comprises 30% of any study effort, although can sometimes be up to 60% (Middlemis, 2000).

5.1.1 Flow processes

5.1.1.1 Aquifer characteristics

Both a porous media aquifer and fractured rock aquifer are present within the modelled area (Section 2.3.7). The catchment was typified by porous flow in unconsolidated glacial (< 50m thick) and weathered material (< 100 m thick), underlain by fracture flow in consolidated bedrock. To satisfactorily represent this dual aquifer system, fracture flow on a regional scale was represented by a continuum approach to couple with true porous media flow. This approach is justified in Chapter Six (Section 6.5.3). Geochemical analysis of local groundwaters showed evidence of only a single evolution trend, supporting a case for strong connectivity between these two types of aquifer. This is supported by the fact that the lower boundary of the upper weathered aquifer is transitional into the lower aquifer across a weathering front. This good connectivity between the dual aquifers provided the motivation to

apply a simplistic approach of treating the whole subsurface flow system as a single unconfined aquifer.

Little is known about the water table configuration in mountainous regions (Jamison and Freeze, 1983), however, water tables in regions with high relief are typically relatively deep (Sandford, 2002). In general, water tables are also shallow in wet climates and deep in semi-arid climates, however, depths to the water table can be highly variable across short distances within a given mining district (Plumee, 1995) due to the influence of pumping. Thus at Rosebery we have a highly variable combination: (i) of deep (>50 m) water tables influenced by mining; (ii) deep water tables in areas of high relief; and (iii) shallow water tables (even saturated to surface) due to the wet temperate climate.

5.1.1.2 Boundary conditions

The model boundaries were expanded to encompass the entire surface catchment that included the Rosebery mine and auxiliary mining-related features (Figure 2.3). The external boundaries of the model took advantage of the natural and physical groundwater boundaries (Figure 5.1). The upper boundaries of the Stitt and Sterling catchments were considered to be no flow boundaries within the model; the lower boundaries were the specific head boundaries of Lake Pieman and Lake Rosebery.

5.1.1.3 Stresses

Inputs to the system included precipitation, recharge from streams, and mine production water. Outputs from the system included: (i) runoff; (ii) evapotranspiration; (iii) mine pumping; and (iv) discharge to streams, seeps and lakes. Figure 5.1 illustrates the conceptual groundwater flow regime over the Rosebery study area.

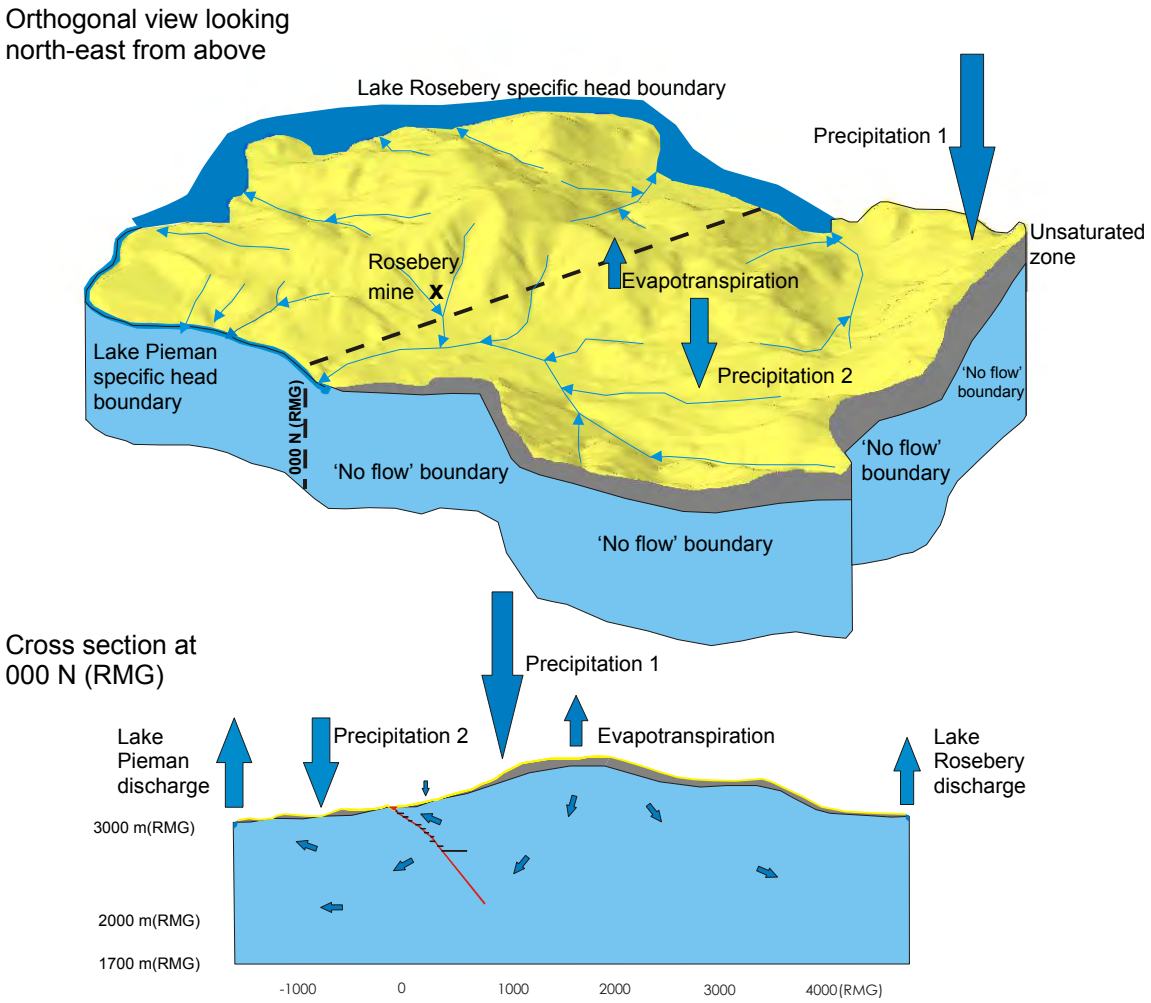

Figure 5.1 3D & 2D conceptual groundwater flow diagram (red line represents the extent of the mine workings)

5.2 Water Balance Mathematical Model

The aim of a mathematical groundwater model is to attempt to represent an actual groundwater system with a mathematical counterpart (Reilly, 2001). The conceptual model in Figure 5.1 was also expressed in a volumetric mathematical model or water balance. Mathematical models offered an inexpensive way to evaluate the physical characteristics of the groundwater system. The water balance for the Rosebery study area utilised Equation 5.1 to estimate recharge; it assumes that on average there was no change in storage (Freeze and Cherry, 1979):

$$r = P - Ro - ET \quad (5.1)$$

where, r = recharge,
P = precipitation,
Ro = runoff,
ET = evapotranspiration.

For the purpose of calculation of the water balance, the Rosebery study area can be divided into three regions: (i) the Sterling River catchment; (ii) Mount Black tributaries; and (iii) the Stitt River catchment upstream of Rosebery Creek – hereafter referred to as the Stitt catchment (Figure 2.13). The three fold division was appropriate as the three catchments in the Rosebery study area were of a broadly comparable size, and only the Stitt catchment has detailed documented stream flow measurements.

Within the Stitt catchment, the average rainfall varied from *c.* 2 to *c.* 3.7 m/year (BOM, 2002), over a total relief of *c.* 1000 m. All vegetation types found in the total Rosebery study area were represented in the catchment and aspect varies in a similar manner to the total catchment. There is no vegetation evidence that suggests the Stitt catchment is not representative of the Rosebery study area. Thus, the Stitt catchment, covering *c.* 37 Mm^2 was considered to be representative of the entire catchment (89 Mm^2) due to its typical range and distribution of rainfall, topography, aspect and vegetation.

Results from the Stitt catchment were extrapolated to the entire Rosebery study area in light of this gap in stream flow data. The water balance was refined for the Stitt catchment and applied to the entire Rosebery study area.

5.2.1 Precipitation

A grided dataset for all of Tasmania derived from 504 Tasmanian rainfall stations has been produced using the BIOCLIM approach (Parks and Wildlife, 1995). This approach uses bioclimatic parameters derived from mean monthly climate estimates,

to approximate energy and water balances at a given location (Nix, 1986). Nunez et al. (1996) and Edgar et al. (1999) discussed how the dataset greatly underestimated precipitation in western Tasmania, as records were based on only a small number of rainfall stations at low altitude. This concern was addressed in the present study. To account for the large relief, and resultant precipitation variation, over the Rosebery study area (Section 2.4.2), a function (Equation 5.2) relating precipitation to elevation was developed from the local data.

$$P = 0.000005x + 5 \quad (5.2)$$

where P = daily precipitation (mm)
and x = height above mean sea level (mm)

Equation 5.2 draws on daily rainfall data from the local Rosebery study area (BOM, 2002) and when combined with the digital elevation model (DEM), attempted to provide a representative rainfall for the Stitt catchment and the entire Rosebery study area. Examples of potential similar settings globally are presented in Chapter 7.

5.2.1.1 Results

When Equation 5.2 was applied to the local 25 m spaced DEM, the total average volume of rainfall for the Stitt catchment was 109.6 Mm^3/year. This volume corresponds to an average precipitation of 2.94 m/year or 8.1 mm/day for the Stitt catchment.

5.2.2 Evapotranspiration

Mean monthly and mean annual ET data at a resolution of 0.1 degrees (latitude/longitude) were provided by (BOM, 2002). These mean data were based on the standard 30 year period 1961-1990 (*ibid*.). Within the vicinity of the Rosebery study area, six values of areal actual ET (*ibid*.) show the ET rate to be in the range of 0.661 to 0.720 m/year in the area. The greater number of evapotranspiration data points compared to rainfall stations, allowed the adoption of a kriging griding method

to the estimation of ET. Using these six data points as input, a 500 m spaced dataset was created to represent spatial variation of evapotranspiration over the Rosebery study area.

5.2.2.1 Results

Using the 500 m spaced ET dataset, the total average volume of evapotranspiration for the Stitt catchment was calculated to be 0.83 m^3/s; i.e., 26.2 Mm^3/year. This volume corresponds to an average ET of 0.703 m/year (Appendix 8) or 1.9 mm/day for the Stitt catchment. Wang et al. (2002) describe sources of error in the ET datasets as: (i) measurement error in the basic input data; (ii) ET means are subject to sampling error due to limited record lengths; (iii) the mapping of ET estimates is affected by the spatial coverage of the climate stations available, and by the interpolation and mapping techniques used; and (iv) model error in deriving the ET estimates. Any error in the ET will affect the outcome of the water balance and the subsequent setup of the model.

5.2.3 Stream flow

Hydro Tasmania's Resource Monitoring and Information Group (RMI) have measured daily stream flow in the Stitt catchment since February 1991. These data were extracted from the Hydstra Time Series data management package (Hydstra, 2004) and analysed to determine annual average flows for the Stitt catchment. Instrument measurement error and the associated error of extrapolating flows across a section of river bed provided sources of uncertainty in the flow data.

5.2.3.1 Results

The Stitt catchment had an average flow of 2.04 m^3/s; 64.4 Mm^3/year. Flow in the Stitt catchment was permanent over the *c.* 13 years of data (Hydstra, 2004). Over this period, daily flows were observed to vary from 5961.6 to 2255040 m^3, and annual

flow was observed to vary from 43.5 to 77.6 Mm^3/year. The Stitt catchment displayed a rapid response to rain events, coupled with a significant baseflow contribution (Figure 5.2). The raw data for stream flow is provided in Appendix Seven. An example year (2003) is presented below in Figure 5.2.

5.2.4 Baseflow

The stream flow data was further analysed to determine the baseflow contribution. Arnold and Allen (1999) and Arnold et al. (1995) published automated methods for filtering stream flow data to estimate baseflow. Using these methods, the Baseflow Filter Program contained in the computer package Soil and Water Assessment Tool (SWAT, 2004) estimated baseflow from the stream flow data. This filter was passed over the stream flow data three times (forward, backwards and forward).

5.2.4.1 Results

Using the daily stream flow values (Hydstra, 2004), daily baseflow estimations were calculated. The *c.* 13 years of data and daily baseflow estimation is presented in Appendix Seven. From these data the annual average baseflow contribution to the Stitt River was calculated at 0.518 m^3/s or 16.3 Mm^3/year. An example year (2003) is presented below (Figure 5.2) and shows that the total runoff is comprised of numerous but hydrologically distinct rainfall events.

5.2.5 Runoff

In the present study, runoff (Ro) included interflow through the unsaturated zone. In the wet climate at Rosebery the division between interflow and true surface flow was difficult to make. Runoff in the Stitt catchment was defined as the stream flow minus the estimated baseflow.

$$\mathbf{Ro = Sf - Bf} \qquad \mathbf{(5.3)}$$

where Sf = Stream flow
and Bf = Estimated baseflow

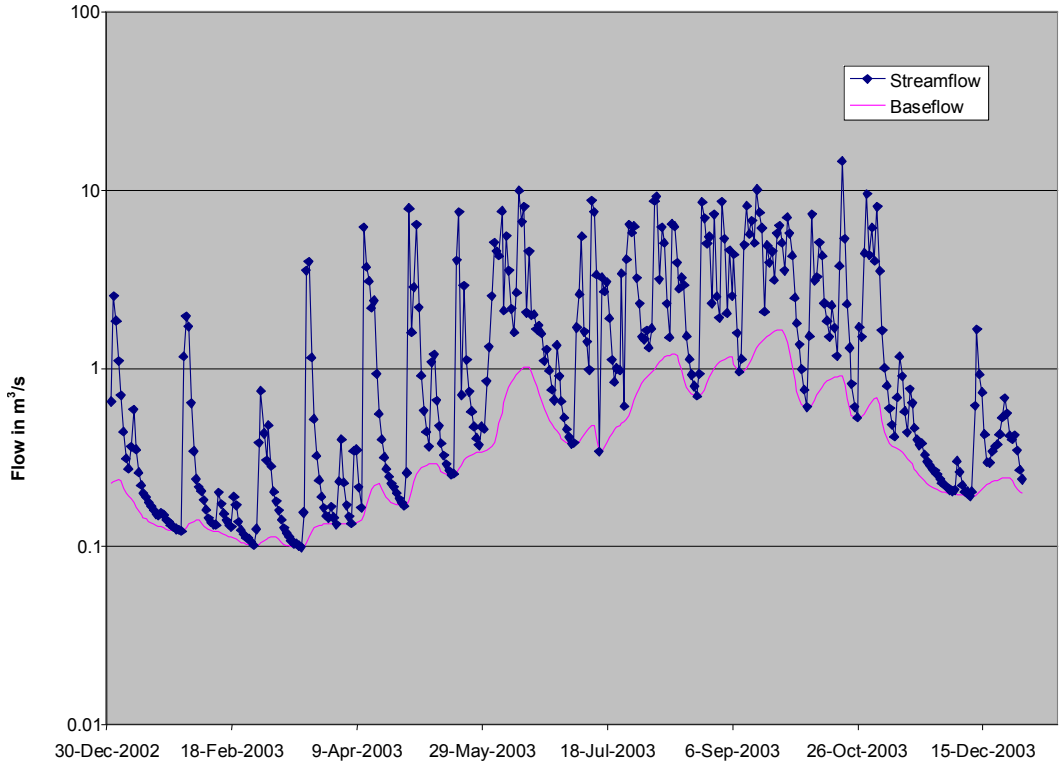

Figure 5.2 Daily stream flow and estimated baseflow for 2003 for the Stitt River below Rosebery

The measure of the runoff of a catchment relative to the precipitation it receives over a year is referred to as the annual runoff co-efficient (Critchley et al., 1991). Edgar et al. (1999) calculated annual runoff coefficients for catchments across Tasmania. The Edgar et al. (1999) method used stream flow (including baseflow) rather than runoff to calculate runoff coefficients, thus, was not appropriate for the water balance estimation. The resultant annual runoff co-efficientfor the Pieman was 0.60, similar to many west coast Tasmanian catchments, however, up to 10 times greater than catchments on the east coast of Tasmania (Edgar et al., 1999).

5.2.5.1 Results

Using a stream flow of 64.4 Mm^3/year (Section 5.2.3.1) and estimated baseflow of 16.3 Mm^3/year (Section 5.2.4.1), the runoff value for the Stitt catchment was 1.522 m^3/s or rounded to 48.0 Mm^3/year. Given a precipitation of 109.6 Mm^3/year (Section

5.2.1.1), the average runoff co-efficient for the Stitt catchment was 0.44. Using the stream flow value for comparison with Edgar et al. (1999) the runoff co-efficient for the Stitt catchment was 0.59.

5.2.6 Recharge

The two standard techniques for estimating regional recharge (Lee et al., 2006) are: (i) applying a water balance model (e.g., Finch, 1998; Simmons and Meyer, 2000; and Chen et al., 2005) with the use of estimations of baseflow to streams (Sandford, 2002); or (ii) parameter-value adjustment of groundwater flow models (e.g., Jyrkama et al. 2002; and McDonald and Harbaugh 2003). A third method of applying a chloride mass balance (Scanlon et al., 2002) is widely used for estimating aquifer recharge (Cook, 2003) in Australia. A fourth method; (iv) involves the use travel time of water to wells based on age determination (Sandford, 2002).

5.2.6.1 Results

Using method (i), Equation 5.1, and the values obtained for P, ET and RO (Section 5.2.1.1, 5.2.2.1 and 5.2.5.1) the average recharge for the Stitt catchment was 1.19 m^3/s or 35.4 Mm^3/year. This value equates to an average recharge of 2.6 mm/day, or 32 % of the precipitation.

5.2.7 Mine water balance

Hale (2001) stated that an average of *c.* 1.89 Mm^3 (60 L/s) was being pumped from the Rosebery mine. Mine usage and production input accounted for *c.* 0.39 Mm^3/year (12.5 L/s). Annually the value for mine water inflow (pumping – input) was *c.* 1.50 Mm^3 (47.5 L/s). A water balance was undertaken, as part of the present study (Table 5.1), to test the finding of Carnie (2003) that the open-cut was the major source of water to the underground mine. Mine inflow data was drawn from Hale (2001), and runoff estimations were from Doherty (2004).

5.2.7.1 Results

Rosebery open-cut water balance	Average flow Mm^3/year	Average flow L/s
Direct Precipitation	0.18	5.73
Diversion and collection (Doherty, pers comm., 2004)	0.09	2.86
Pan evaporation, (BOM, 2002)	0.08	2.60
Evapotranspiration	-	-
Open-cut wall contribution	-	-
Recharge to underground from open-cut	0.01	0.26
Total underground outflow (Hale, 2001)	1.89	60
Underground production water	0.39	12.5
Underground inflow	1.50	47.5

Table 5.1 Water budget average flows deduced for the open-cut and underground mine

Doherty (2004) estimated that half the precipitation within the vicinity of the Rosebery open-cut was diverted and collected as runoff (Section 5.2.7; and Table 5.1). This estimate broadly correlates with the runoff co-efficient calculated for the Stitt catchment (0.44), as a runoff co-efficient for the deforested open-cut would be expected to be higher. Actual values of runoff out of the open-cut, measured over a v-notch weir (PRM, 2004) range from 17 to 0.04 L/s (Section 3.5.1.1) over the 2001 to 2003 period.

Evapotranspiration was assigned a flow rate of zero L/s (Table 5.1) as the open-cut area has been deforested. On this basis, the pan evaporation estimate was considered more appropriate and the Savage River data (BOM, 2002) was used to produce the value in Table 5.1.

The open-cut was believed to be above the water table and any seeps would likely be sourced from interflow. The open-cut wall contribution was assigned a flow rate of zero L/s (Table 5.1) as no seeps were observed in the open-cut.

Mine water studies and void volume calculations were also used in predicting filling times in disused areas of the mine in 2003 (Evans, pers. comm., 2003). Using the mine model (PRM, 2003a), the volume of the Southern exploration decline (SED)

to be filled was estimated at 50,000 m^3. Groundwater inflow was *c*. 11 L/s prior to flooding and remained at *c.* 10-11 L/s in April 2003 post flooding.

5.2.8 Other volumes

Other flows that have been considered as potential inflows to groundwater were: (i) loss or gain from the tailings dams into the system; (ii) municipal water use; and (iii) municipal wastewater disposal. The loss of water from the tailings dam water to the groundwater regime was the focus of a PhD study (Reid, pers. comm., 2004) and an honours (Brown, 2006), both at the University of Tasmania, thus, was considered beyond the scope of the present study. Municipal wastewater was pumped to the tailings dams for treatment, however, historically (pre-2002) it was discharged directly into the Stitt River (Staude, pers. comm., 2002a). Unlike many urban areas, the influence of municipal water use on the groundwater regime in the Rosebery area was considered negligible, because very little water was required for use on gardens in the wet temperate environment.

5.2.9 Summary of the water balance

The Stitt catchment was used as an example for the rest of the Rosebery study area (Figure 5.3; Figure 5.4; Table 5.2; and Table 5.3). Equation 5.2 was applied to the DEM for the modelled catchment to calculate precipitation using the method described in Section 5.2.1. The method described in Section 5.2.2 was used for calculating evapotranspiration of the modelled catchment. The runoff co-efficient (0.44) from the Stitt catchment (Section 5.2.5.1) was applied to the entire catchment area to estimate runoff (inclusive of interflow, and independent of baseflow). To calculate stream flow over the catchment, a baseflow component relative to the Stitt catchment was added to the estimated runoff.

5.2.9.1 Results

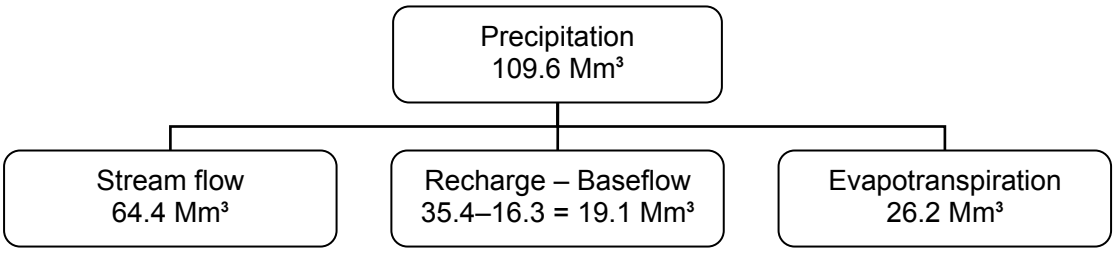

Figure 5.3 Annual water budget summary for the Stitt catchment

Stitt catchment	Annual volume Mm^3	Rate m^3/s	Method	Source of raw data
Precipitation	109.6	3.47	Equation 5.2	BOM, 2002
Stream flow	64.4	2.04	N/A	Hydstra, 2004
Baseflow	16.3	0.518	SWAT, 2004	Hydstra, 2004l
Evapotranspiration	26.2	0.83	Morton, 1983	BOM, 2002
Recharge	35.4	1.19	Equation 5.1	BOM, 2002; Hydstra, 2004

Table 5.2 Annual water budget summary for the Stitt catchment

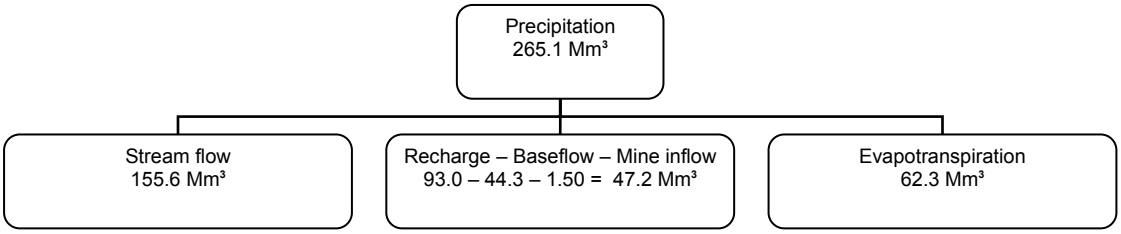

Figure 5.4 Annual water budget summary for the total modelled Rosebery study area

Total Catchment	Annual volume Mm^3	Rate m^3/s	Method	Source of raw data
Precipitation	265.1	8.40	Equation 5.2	BOM, 2002
Stream Flow	155.6	4.93	N/A	Hydstra, 2004
Baseflow	44.3	1.40	SWAT, 2004	Hydstra, 2004
Evapotranspiration	62.3	1.97	Morton, 1983	BOM, 2002
Mine Inflow	1.50	0.05	N/A	Hale, 2001
Recharge	93.0	2.95	Equation 5.1	BOM, 2002; Hydstra, 2004

Table 5.3 Annual water budget summary for the total modelled Rosebery study area

While all volumes are of interest in balancing the groundwater model, it is the estimated value of groundwater discharging from the catchment that is the key unknown. For the Stitt catchment above Rosebery, this value is 19.1 Mm^3 and for the total modelled Rosebery study area, 47.2 Mm^3. This figure refers to all groundwater

discharging into the regional groundwater system outside of the catchment and all groundwater discharging into the Pieman River (including Lake Rosebery and Lake Pieman). In summary, the water budget (rounded to the nearest whole number percentage value) is: (i) 42% of precipitation runs off to becomes true surface water flow (including interflow); (ii) 24% of precipitation is lost to evapotranspiration; (iii) 17% of precipitation becomes groundwater and is discharged as baseflow into creeks and rivers within the catchment; and (iv) 18% remains as groundwater discharging into the regional groundwater system outside of the catchment or into the Pieman River system.

5.3 Predictive Mine-filling Mathematical Model

5.3.1 Background

Following the closure of deep mines, cessation of pumping generally results in groundwater rebound and mine flooding (Henton, 1981). Gradually the mine voids and surrounding strata fill up to the level of a decant point (Adams and Younger, 2001).

Flow in large open voids is often turbulent (Adams and Younger, 2001) so the mine filling models: (i) GRAM (Groundwater rebound in abandoned mine-workings) (Sherwood, 1993); and (ii) MIFIM (The mine water filling model) (Banks, 2001), were examined to model the initial filling of the mine upon decommissioning.

The pond based mine filling model GRAM has been successfully applied to many mine water rebound scenarios (e.g., Sherwood and Younger, 1994; Sherwood and Younger, 1997; Younger, 1998; Walker, 1998; Younger and Adams, 1999; Adams and Younger, 2001; and Dumpleton et al., 2001). Although GRAM has been used successfully in rebound modelling, its major drawbacks, as defined by Banks (2001), made it unsuitable at Rosebery. These drawbacks include the assumptions

that recharge to a given mine is from surficial sources, and is head-independent. At Rosebery, inflow varied with water level because part of the inflow is derived from groundwater in fracture systems, rather than totally from directly infiltrating rainfall (Hale, 2001). Inflow will reduce as water level rises above inflow horizons, due to decreasing head gradients (Banks, 2001). As mine waters rise they may become outflow to an aquifer system and GRAM does not allow for interaction with groundwater systems, nor does it account for variations in void volume with depth (Banks, 2001).

To overcome the aforementioned problems, Banks (2001) developed the MIFIM. Banks (2001) stated that "MIFIM is applicable to relatively dry mines in low permeability strata, with a limited number of discrete water inflow features (fractures, exploration boreholes, permeable strata of limited thickness)". This makes MIFIM ideal for use at the Rosebery mine. The Rosebery mine is located in a wet, temperate, mountainous, sulphide-mining district, however, the low permeability of the crystalline bedrock (Chapter Three) controls inflow, and the mine itself was considered relatively dry due to ongoing dewatering. MIFIM was used to examine the 'filling' of the mine to a steady state condition of discharging at a decant point.

5.3.2 Methodology

The two inputs required for MIFIM are: (i) vertical distribution of the mine; and (ii) vertical distribution of flow inputs. Data points, created from the mine model (PRM, 2003a), were examined to assign percentage volumes to depth levels (50 m layers) within the mine. This means that all horizontal development (including waste drives), production stopes and shafts are accounted for in the model. The incomplete nature of the wireframes within the mine model (PRM, 2003a) rendered it inappropriate for use in precise volume calculation, however, they provide scope for

further refinement as the mine model improves. The total void volume was instead calculated using bulk densities (Willis, 1999) and materials (including waste) mined figures (Edwards, 2003). As part of the present the study, the information Hale (2002) provided on mine inflows, was expanded through underground inspection, and through ongoing monitoring undertaken by Doherty (2004).

The total volume was calculated at 8000000 m^3 and the vertical distribution applied to MIFIM modelling is applied summarised in Table 5.4. The overflow level was set at 3225 mRMG, the level of the main Rosebery adit. At time zero, the water level was set at 2175 m the static water level at the deepest point of the mine at the time of modelling in 2003. A head-independent inflow of 25 L/s was assigned to represent the water inflows in the upper levels (above 8 Level). Head-dependent flows totalling 22.5 L/s were assigned to the MIFIM model based on observations of Hale (2001), Doherty (2004) and the present study. The total underground inflows of 47.5 L/s correspond to the value expressed in the water balance (Table 5.1).

Head-dependent inflow L/s	Elevation of inflow m (RMG)	Estimated head of inflow m (RMG)	Description
5	3224	3225	8 level flow
5	3100	3200	14 level fault
10	2500	3200	Southern exploration decline
2.5	2175	3600	Exploration drill holes

Table 5.4 Head-dependent inflow (after Hale, 2001)

5.3.3 Results

The input – output files for MIFIM predictions are provided in Appendix 10. The output of MIFIM is a chart representing mine filling (Figure 5.5). In above-drainage mines, as at Rosebery, the mine was likely to discharge at the lowest adit level (3225 m RMG). MIFIM represented the water level in steady state at the Rosebery mine at 3225 m (Figure 5.5).

Level	% volume	Volume in interval (m^3)
3225	100	
3175	93	585915
3125	86	540845
3075	80	458216
3025	71	721127
2975	63	615962
2925	58	439437
2875	50	657277
2825	42	646009
2775	37	386854
2725	32	371831
2675	29	232864
2625	26	262911
2575	21	386854
2525	16	413146
2475	12	356808
2425	7.6	319249
2375	4.5	247887
2325	2.3	176526
2275	0.89	108920
2225	0.28	48826
2175	0	22535

Table 5.5 Model levels, percentage volumes and volume in interval used within the mine filling model

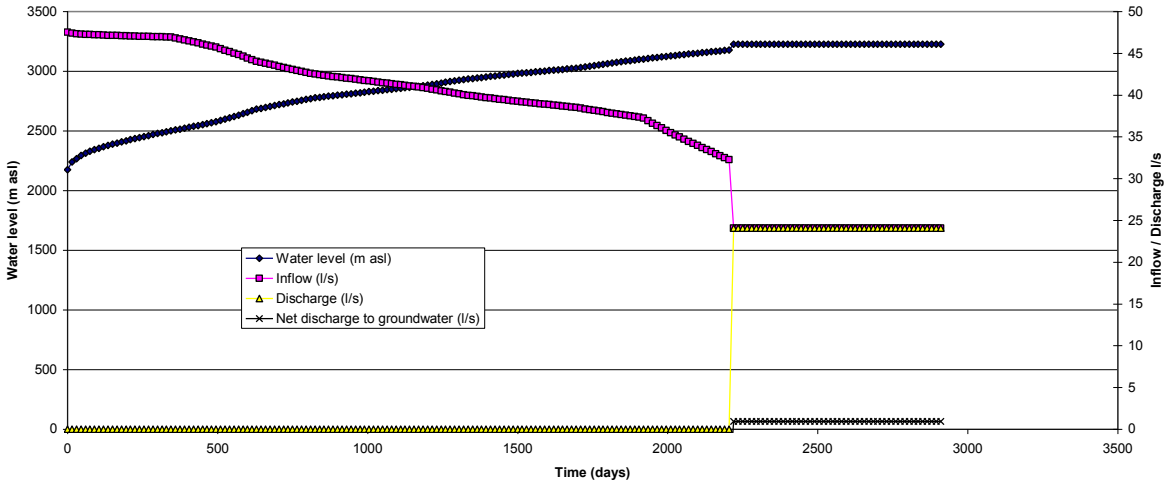

Figure 5.5 The mine water filling model (Banks, 2001) output for the Rosebery mine decommissioning. Note a full mine steady state condition is achieved after 2200 days once the water level reaches an elevation of 3225 m and decants.

5.4 Discussion

5.4.1 Conceptual model discussion

Simplifications and assumptions are required to describe a complex real-world hydrogeologic environment (Middlemis, 2000). Thus, no groundwater system can be modelled with a unique solution that exactly defines the hydrogeologic environment (Bear et al., 1992). Varying assumptions will result in different models, each approximating the groundwater system in differing ways (*ibid*.).

The major assumptions of the Rosebery conceptual model included: (i) that the major surface water divides and groundwater divides coincided; (ii) that there was on average no change in groundwater storage; and (iii) that the catchment was large enough that fractured rock and porous media can be modelled using an equivalent porous medium continuum approach. Some justifications for these assumptions are argued below and further in Chapter Six.

Whether all groundwater from the catchment either: (i) discharged north, or (ii) reached no-flow boundaries at the surface water bodies, was the key unknown in the system. The no-flow boundary assumed that no flow-through occurs from the catchment into the groundwater system north of the Pieman. It was likely that the surface water and groundwater divides coincided in the catchment because: (i) the dramatic topography of the West Coast Range occurs at the upper boundaries, which would be expected to result in sharply divergent subsurface hydraulic gradients across watershed boundaries; and (ii) the large volume and permanent state of the surface water bodies at the lower boundaries.

The scale beyond which the hydraulic conductivity of a system of fractures approaches a constant hydraulic conductivity of an equivalent porous medium is referred to as the „representative elementary volume' (REV) (Bear et al., 1992; and Cook, 2003). Justification that the catchment, and hence the model domain, was

much larger than the aquifers REV, was the large regional scale (*c.* 89 km^2) of the catchment. Much literature addresses the concept of the REV (e.g., Chen, 1987; Drogue, 1998; Kulatilake and Panda, 2000; Jackson et al., 2000; Min, 2002; and Wellman, 2006). The least dimension of the REV is at least an order of magnitude larger than the joint spacing (Chen, 1987). Drogue (1998) defined a minimum practical REV stating "if we refer to the different sizes of the interfissural distances normally observed, we note that the representative porosities can probably be reached only for volumes in excess of 10^6 m^3". Wellman (2006) argued the "appropriate "REVs" differ depending on the scale at which model predictions are needed to facilitate decision making". Quantification of the REV for the Rosebery aquifer required detailed fracture geometry, and thus was considered beyond the scope of the present study. The application of a continuum approach for the Rosebery study area at the scale proposed in the present study was well within the justifications of Chen (1987), Drogue (1998), and Wellman (2006).

5.4.2 Water Balance Discussion

5.4.2.1 Precipitation Discussion

The error associated with precipitation calculations in the present study was large due to the contrasts in actual precipitation recorded over the Rosebery study area (Section 5.2.1). Equation 5.2 assumed a linear increase in precipitation with increase in elevation. Equation 5.2 does not account for the important factor of aspect, and was only based on the three local weather stations. Having only three stations, there was little scope for the application a kriging griding method to represent the spatial variation of precipitation over the Rosebery study area. The estimation presented in Equation 5.2 requires testing with additional local stations and a longer history. Equation 5.2 was a logical improvement on using data from one of the rainfall

stations. For instance, if data from only Rosebery was used, at an average of 5.8 mm/day, this would underestimate precipitation for the Rosebery study area; if Mount Read data was substituted (average of 10.2 mm/day), this would overestimate rainfall over the catchment. If the Parks and Wildlife (1999) dataset were used, rainfall over the Rosebery study area would be greatly underestimated, giving a value even lower than for the Rosebery average alone.

5.4.2.2 Evapotranspiration Discussion

The closest comparable evaporation dataset was the Savage River mine, *c.* 40 km NW of Rosebery. Although relevant, these data give little insight into the evapotranspiration occurring at Rosebery, within the West Coast Range. The long term (*c.* 30 year) spatial dataset (BOM, 2002), when applied to the local area in a logical manner, provided a more relevant evapotranspiration estimation (Section 5.2.2).

Evapotranspiration was assumed to vary with the variation in vegetation, as the water consumption for each species and vegetation type differs. Differing aspect was also assumed to have a significant control upon evapotranspiration. It was anticipated that the vegetation study (Section 2.5) could be worked into the calculations for ET over the area, however, insufficient data existed on how ET varies in these native Tasmanian forests (Adams, pers. comm., 2006) for this aim to be fulfilled.

5.4.2.3 Stream flow discussion

The temporal database (Hydstra, 2004) enabled a long term (*c.* 13 years) analysis of the Stitt catchment (Section 5.2.3). Although no such flow data exists for other streams within the catchment, these data allowed me to speculate on the flow regime in other catchments in the Rosebery study area, notably the Sterling River, which was of a comparable size to the Stitt River (Section 2.6). The baseflow

contribution and its separation from true surface flows also provided scope for further analysis of groundwater – surface water interaction.

5.4.2.4 Baseflow discussion

Arnold et al. (1995) proposed that the filter method (Section 5.2.4) was comparable in accuracy to the time consuming manually separated base flow methods (e.g., Meyboom, 1961; and Rorabaugh, 1964). Arnold et al. (1995) displayed that the range of errors averaged 13% between the automated approach and that of manually derived recession constants. Automating the baseflow separation removes some of the subjectivity of manual separation. It was unlikely that the individual rain events of the *c.* 13 years of data would have been manually separated using the methods proposed by Meyboom (1961) and Rorabaugh (1964). By automating the separation, using the SWAT (2004) process, the entire dataset (*c.* 13 years) could be used.

Estimating the baseflow was valuable in quantifying the groundwater – surface water interaction within the Stitt catchment. Baseflow was a key unknown in Equation 5.3, and subsequently Equation 5.1, which allowed for the calculation of recharge. Baseflow excludes an interflow component in the unsaturated zone, which is grouped collectively with true surface flow in the present study to form „runoff'.

5.4.2.5 Runoff discussion

The calculated runoff co-efficient for the Stitt catchment 0.59 (Section 5.2.5) correlates well to the wider Pieman 0.60 catchment (and other western Tasmania catchments) presented by Edgar et al. (1999). The very high runoff co-efficient does reflects the anomalously wet and mountainous terrain of the catchment and wider Rosebery study area. In comparison, runoff co-efficients in arid to semi-arid mainland Australia are commonly less than 10% of the value calculated at Rosebery (IEAust, 1987).

5.4.2.6 Recharge discussion

Method (i) (Section 5.2.6) provided a logical means for estimating recharge for the Stitt catchment. Method (ii) and (iv) (Section 5.2.6) could be applied in future works with further refinement and confidence in hydraulic parameters within the groundwater model. Age determination could provide validation of calculations presented here, however, was considered beyond the scope of the present study.

Method (iii) (Section 5.2.6), was less defined than elsewhere on mainland Australia due to the narrow ranges of Cl concentrations in the wet temperate environment of western Tasmania. The method is valuable when Cl ranges are orders of magnitude greater than the error of analysis. At Rosebery the Cl content of rainwater (10.5 mg/L) was found to be comparable to the Cl content of all waters within the catchment (8.9 to 34 mg/L) (Appendix 2). Given the waters Cl contents were of the same order of magnitude as rainwater, these data imposed large errors when applying method (iii) to calculate recharge. Thus this method was considered inappropriate for the Rosebery area, and other such wet temperate environments.

5.4.2.7 Mine water balance discussion

With all contributions considered (Table 5.1), the open-cut provided less than 0.01 Mm^3 (0.26 L/s) to the underground flow. This was understandable, given that the open-cut makes up only 0.01% (Appendix Ten) of the total wall rock exposed underground in the Rosebery mine. Large inflows observed in the upper levels may be most related to the higher hydraulic conductivities expected closer to the surface (Section 3.3). Thus, the present study does not consider that the open-cut contributes greatly to the mine inflows.

The anticipated time to fill (up to 22 level) was 7.5 weeks based on volume and rate. This correlated well with the observed filling time of 7 weeks, and also

indicated that the inflows were responding to heads greater than the elevation of 22 level.

5.4.2.8 Water balance summary discussion

Using the Stitt catchment as an example for the rest of the Rosebery study area catchments (Section 5.2.9) was considered to be necessary because no other catchments in the Rosebery study area had long term monitoring or the infrastructure to undertake such monitoring. Elsewhere in the Rosebery study area, the groundwater – surface water regime was expected to differ from that of the Stitt catchment. This difference was a source of error within the mathematical model. However, in the absence of data on all catchments in the Rosebery study area, the water balance (Table 5.3) provided a reasonable estimation of annual flows that could be applied to numerical modelling.

The mine inflows represent 1.6% of the total estimated recharge to the Rosebery study area. The estimated recharge value and mine inflows were applied directly as numerical and mathematical model inputs. The estimated baseflow component of the Stitt catchment was used as a calibration tool for the numerical model.

The summary water balance highlights the importance of groundwater in the catchment, with a groundwater (those waters that have been groundwater at some stage i.e. inclusive of baseflow) to surface water (those that have been true surface waters including interflow) flow rate ratio of 1:1.2. The relative amount of surface water to groundwater research ratio does not reflect this on the wet, temperate, mountainous west coast of Tasmania.

5.4.3 Predictive mine-filling mathematical modelling discussion

At the Rosebery mine, the MIFIM model (Section 5.3) was sensitive to the relative allocation of head-independent inflow compared to head dependent inflow.

This is because the mine adit at the Rosebery mine (3225 m RMG) is below the regional water table over much of the mountainous Mount Black. This provides justification for a significant contribution of head-independent inflow in much of the mine. The extreme case, that all flow is head-independent inflow, results in the most rapid filling of the Rosebery mine (1950 days). Based on inflows observed throughout the Rosebery mine, the filling is anticipated to reach the adit level after 2220 days (Figure 5.5). Regardless of the MIFIM model inputs, understanding the flow regime enough to be able to state that mine filling will reach steady state at the adit level within the first decade of decommissioning represents a significant advancement in the understanding of the Rosebery mine water for closure management.

The implications for rates filling of the Rosebery mine are: (i) that management options need to be in place within five years of the cessation of pumping; and (ii) that as flooding is relatively slow (not instantaeous) the environmental impact of sulphidic waste rock placed underground is increased (Perkins et al., 1995). No previous mine filling estimates could be produced by the Rosebery mine, however, the unfounded assumption was voiced that as pumping had been undertaken for a century, rebound would be of a similar magnitude (Carnie, pers. comm., 2002).

With the MIFIM results in mind, there was little benefit in attempting to numerically model the process of mine filling at the Rosebery mine within a package such as MODFLOW. Understanding that mine filling will occur naturally within a decade, or could be artificially filled (relatively instantaneously) was sufficient. The scope of numerical modelling was refined to represent: (i) operating conditions (an empty mine); and (ii) post decommission conditions (a full mine).

5.5 Conclusions and implications for water balance models in wet, temperate, mountainous environments

The characteristic feature of wet, temperate, mountainous environments is the large local spatial variation in precipitation, evapotranspiration, and therefore recharge. Estimating a representative recharge for a catchment or areas within a catchment remains the pivotal quantification for undertaking groundwater investigations in such climates.

The significant interaction of surface waters and the groundwater system in wet, temperate, mountainous environments present an opportunity to investigate the groundwater regime from the surface. Gauging stream flow for baseflow contribution in the current study provided important quantification of groundwater flow where bore flow data was scarce. The mine outflows also provided an important quantification of groundwater flow on a larger scale. The hydrochemical data (Chapter Four) provided evidence that this outflow was only derived from evolved waters that would typify a discharge regime of a flow system.

In the current chapter, a method for amalgamating these data into a water balance for quantification of the important aspects of the groundwater system was presented as an example for use in wet, temperate, mountainous mining districts, elsewhere. It is recognised that errors exist in all stages of the estimation, and that the values presented are not a unique solution, thus further work, refinement and validation of the water balance is recommended. The present study did, however, provide an estimation that surface water flow rates were of a comparable magnitude to groundwater flow rates in the catchment, highlighting the importance and need for hydrogeological research in other wet, temperate, mountainous, mining environments.

" the supreme goal of all theory is to make the irreducible basic elements as simple and as few as possible without having to surrender the adequate representation of a single datum of experience" (Einstein, 1934).

6 Numerical Groundwater Flow Modelling

6.1 Introduction

Numerical groundwater flow models have become increasingly important tools for the analysis of groundwater systems since the 1960s (USGS, 2005). The need for modelling studies is addressed by Middlemis (2000) who maintains that groundwater models are used to investigate the important features of groundwater systems, where these features cannot be directly observed, other than through the construction of bores, along with their pumping and monitoring. Bear et al. (1992) described the use of groundwater models as management tools.

This chapter discusses the design, construction, calibration and sensitivity of the numerical groundwater flow model for the Rosebery catchment. A numerical flow groundwater model is "a computer-based representation of the essential features of a natural hydrological system that uses the laws of science and mathematics" (Middlemis, 2000). The Australian Government (2009) promotes the Middlemis (2000) guidelines as having "comprehensive technical information relating to the different stages of the modelling process such as conceptualisation, calibration, prediction, uncertainty analysis and reporting." and this document is used at present throughout the Australian groundwater modelling community in lieu of any relevant Australian standard. This chapter refers to Middlemis (2000) throughout and describes how the essential features of the Rosebery catchment, and Rosebery mine, were represented in the numerical model. By creating a regional numerical groundwater flow model of the Rosebery catchment, which incorporates the Rosebery mine, the influence of the mine on the groundwater regime could be examined.

6.2 Scope

The key aims of the numerical modelling were to: (i) develop a numerical groundwater flow model that was consistent with the existing conditions at, and around the Rosebery mine; and (ii) use the numerical model to predict groundwater flow following cessation of mining. The numerical simulation of the existing operational conditions, i.e., consistent with those conditions observed and calculated in preceding chapters, was aimed at providing the structure for the numerical simulation of the post-decommissioning state of the flow system (predicted conditions).

The numerical model is a tool to increase the understanding of the system with the aim of improving management decisions regarding mine closure. As such, the Rosebery mine staff and future consultants were the target audience for the numerical model, and it is stressed that as ongoing work and long term monitoring is undertaken, the model should be further validated and revised accordingly.

The ultimate aims of such predictive modelling, beyond the scope of the present study are to: (i) fulfil the closure objective at the Rosebery mine; (ii) prevent or minimise adverse long-term environmental impacts; and (iii) create a self-sustaining natural ecosystem or alternate land use, as set out by the Australian and New Zealand Minerals and Energy Council and Minerals Council of Australia (ANZMEC and MCA, 2000).

The closure scenarios that needed to be considered at the Rosebery mine were: (i) a planned closure; (ii) sudden closure; (iii) temporary closure; and (iv) maintenance and monitoring. With regards to groundwater management and pumping, scenario (iv) was synonymous to operation, whereas scenarios (i), (ii), and (iii) were synonymous to decommissioning.

The present study assumed decommissioning will involve the eventual flooding of the mine to a static level and ongoing management of discharging mine water at that level. The mathematical model presented in Section 5.3 of the present study, indicated this will occur within a decade of decommissioning. The numerical models provided: (i) a present day operational scenario; and (ii) a predictive post decommissioning scenario (Appendix Eleven).

6.3 Model Complexity

Model complexity is defined as the degree to which a model application resembles, or is designed to resemble, the physical hydrogeological system (Middlemis, 2000). The guiding principle in the numerical model development within the present study has been to maintain parsimony while still considering the major elements of the hydrogeologic and mining processes of the catchment.

The model objectives dictate which features should be represented in the model, and their degree of accuracy (Bear et al., 1992). The natural hydrogeologic system at Rosebery was interpreted as a complex combination of heterogeneous fractured rock, glacial material and regolith; all distributed across a large relief. In addition to modelling the natural hydrogeologic system, modelling the total hydrogeologic system at Rosebery involves modelling the anthropogenic influence of mining.

The major features that were important to the natural Rosebery catchment were: (i) the topography; (ii) recharge; (iii) the surface water features; and (iii) the geology (including rock type and fracture systems). The major anthropogenic features were: (i) the introduction of voids (including drill and mine workings); (ii) the practice of pumping; and (iii) the development of surficial and underground waste storage facilities. Representing the scale and extent of the mining operations in the geometry

of the model has resulted in the generation of very complex and deep, multi-layered numerical models.

6.4 Previous Studies

There is a vast literature of application of flow modelling to groundwater behaviour, however, studies of mined environments are more meagre. Numerical flow models have been used to simulate dewatering and recovery of groundwater around: (i) underground mine workings (e.g., Cook, 1982; Winter et al., 1984; Weiss and Razem, 1984; Toran and Bradbury, 1988; Berry and Armstrong, 1995; Zhang and Lerner, 2000; Jakubrick, et al., 2002; Bochenska et al., 2004; and Usher et al., 2003); (ii) underground tunnels (e.g., Merrick, 1997; Kitterod et al., 2000; Molinero et al., 2002; and Kim and Lee, 2003); and (iii) underground waste storage facilities (e.g., Heathcote et al., 1996; Gutmanis et al., 1998; Hassan, 2003; and Boyle et al., 2006). Such studies have historically been primarily focussed on control of water inflow, however, within the last 30 years the focus has included environmental impact (Attanayake and Waterman, 2006). Numerical groundwater flow modelling has also been used specifically in mountainous terrain to determine hydraulic characters and describe flow systems (e.g., Jamieson and Freeze, 1983; Schoeenfeld and Pfaff, 1990; and Forster and Smith, 1998). The previous work, combined, provided the theoretical framework for the numerical modelling in the present study.

6.5 Conceptual Numerical Groundwater Models

6.5.1 Saturated porous media

Numerical groundwater modelling in saturated porous media use: (i) finite-difference models; (ii) finite-element models; (iii) boundary element models; (iv) particle tracking models; and (v) integrated finite-difference models (Bear et al., 1992). The physical processes controlling saturated flow, and associated

mathematical descriptions used within these models are well understood (CPSMA, 1990). Saturated continuum flow models are reliant on the principles of fluid mechanics and laboratory column validation of Darcy's (1856) laws (CPSMA, 1990). Reid (1998) presented the key equations of groundwater modelling using the most common finite-difference and finite-element methods.

Finite-element modelling codes include: e.g., AQUIFEM-N (Wilson et al., 1979); AQUA3D (Vatnaskil, 1994); SUTRA (Voss and Provost 2002); FEMWATER (Yeh and Ward, 1980); and FEFLOW (Diersch, H.J. G, 1998). The finite-difference code MODFLOW (McDonald and Harbaugh, 1984) is regarded worldwide as the most used groundwater modelling package (Osiensky and Williams, 1997; and Modflow, 2006).

6.5.2 Fractured flow

In the 1980s, the hydrogeology of fractured rocks remained to be a "riddle engaging the serious thought of several scientists of eminence in the field" (Briz-Krishore and Bhimasankaram, 1982). Stevenson's (1982) review of fractured rock groundwater studies refers to the „too hard' label for the science in relation to the lack of literature available. Since then, understanding of fractured rock aquifers has advanced by amongst other things, the increased numerical capacity of modern computing. This increase in computing capacity has allowed the generation of a number of fracture flow numerical models described below.

Diodato (1994) presented a compendium of fracture flow numerical models in which he stated "conceptual models that have been invoked to describe fluid flow in fractured porous media include explicit discrete fracture, dual continuum (porosity and/or permeability), discrete fracture network, multiple interacting continua, multipermeability/multiporosity, and single equivalent continuum". Cook (2003)

grouped these models in three classes: (i) the equivalent porous media approach; (ii) the dual porosity approach; and (iii) the discrete fracture network approach (Figure 6.1).

6.5.2.1 Single equivalent continuum

Fractured rock aquifer systems are typically modelled using an approach that represents the system as an equivalent porous medium (Middlemis, 2000; Fetter, 2001) (e.g., Hseih and Neuman, 1985; Toran and Bradbury, 1988; Schwartz and Smith, 1988; Novakoski, 1990; Rehfeldt et al., 1992; Tsang et al., 1996; Gburek et al., 1999; and Pohll et al., 1999). This approach is referred to as the single equivalent continuum approach because the fractured mass is hydraulically equivalent to a porous medium (Domenico and Schwartz, 1997). In the continuum approach, instead of individual fractures being explicitly treated in the model, the heterogeneity of the fractured rock system is modelled (Cook, 2003). This approach is applicable on a regional scale and at scales larger than the representative elementary volume (REV) of the aquifer (*ibid*.; and Section 5.4.1). The successful use of the continuum approach for modelling regional water resources and contaminated sites in fractured rock aquifers is well documented in the literature (e.g. Long et al., 1982; Pankow et al. 1986; Schmelling and Ross, 1989; Berry and Armstrong, 1995; Woodward-Clyde, 1995; Hopkins; Gburek et al., 1999; Jackson et al., 2000; MWH, 2006; Wellman, 2006; and GHD, 2007).

6.5.2.2 Discrete fracture networks

Discrete fracture network models treat flow through each fracture as equivalent to flow between two uniform plates with equivalent separation to that of the fracture (Cook, 2003); (e.g., Long et al., 1985; Shapiro and Andersen, 1985; and Cacus et al., 1990a and 1990b). Modelling fractured rock aquifers as a series of discrete fracture

networks requires a detailed understanding of fracture geometry and connectivity; thus, data acquisition can become onerous where large numbers of fractures occur (Diodato, 1994). Discrete fracture models allow for the explicit representation of fluid potential gradients and fluxes between fractures and porous media (*ibid*.). As the complexity of the model domain increases in a discrete fracture network, by increasing numbers of fractures, the computational burden increases significantly (*ibid*.).

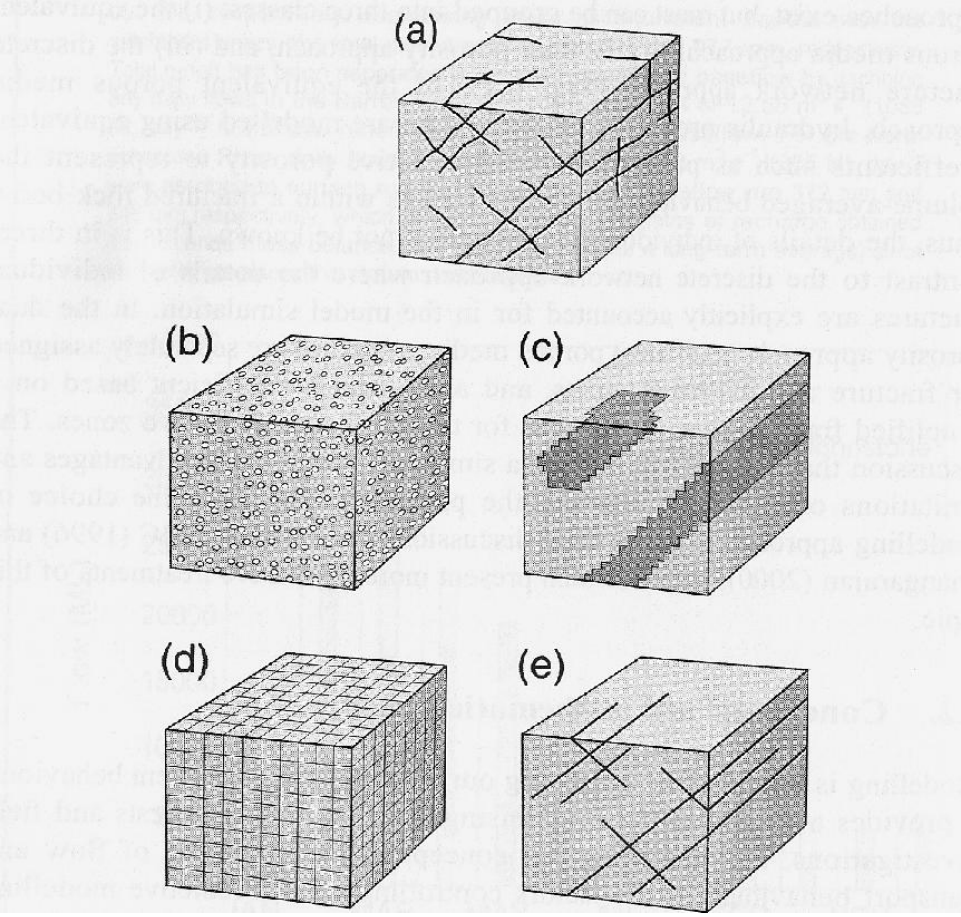

Figure 6.1 Example of different modelling approaches for fractured rock aquifers: (a) Actual fracture network; (b) Equivalent porous media model, using uniform aquifer parameters; (c) Equivalent porous media model in which highly fractured zones are represented by regions of higher hydraulic conductivity; (d) Dual porosity model; (e) Discrete fracture model, in which the major fractures are explicitly modelled. The discrete fracture model may have zero porosity in the matrix, porosity but zero flow, or may allow flow (Cook, 2003)

6.5.2.3 Dual porosity

Dual-continuum strategies model flow through both the: (i) porous media; and (ii) the secondary porosity of fractured rock (Barenblatt et al. 1960; and Warren and Root, 1963). Dual-continuum models are based on an idealised flow medium consisting of a primary porosity and a secondary porosity created by fractures (Warren and Root 1963). The dual-continuum approach can be summarised as a hybrid between the equivalent porous continuum approach and the discrete fracture approach (Diodato, 1994). "The basis of these models is the observation that unfractured rock masses account for much of the porosity (storage) of the medium, but little of the permeability (flow). Conversely, fractures may have negligible storage, but high permeability. The porous medium and the fractures are envisioned as two separate but overlapping continua." (*ibid*.)

6.5.3 Modelling at Rosebery

Detailed fracture information (aperture, length, frequency) was not available for the total Rosebery area catchment due to a lack of sufficient outcrop unaffected by blast damage; nor was it considered obtainable within the scope of the present study. Even at the Rosebery mine scale, the limited detailed fracture descriptions and orientation data which do exist (McDonald, 1984; and PRM, 2003b and 2003c) were insufficient to describe the hydrogeology for such discrete fracture network modelling. Aquifer heterogeneity and anisotropy further complicate such methods. For further discussion on anisotropy see Section 6.8.3.8 and on heterogeneity see Section 6.10.4 The presence of extensive glacial and regolith surface deposits would require the use of a combination of a porous medium model and a discrete fracture network model. An equivalent porous medium approach was considered more appropriate to represent these interconnected aquifers.

The equivalent porous media approach to modelling fractured rock aquifers is usually the least data intensive of all approaches (Cook, 2003). At Rosebery, dual porosity modelling, as with the discrete fracture approach, was also not considered viable due to the lack of oriented fracture data. The scale of such representation of the fracture network was beyond the scope of the present study, however, it should be considered for further work by the mine. The extensive network of underground workings does provide scope for such research to be undertaken. Using existing geological mapping (PRM, 2003c) as a base, fracture information could be expanded to form the input for such modelling. If such information is routinely gathered elsewhere in other mining environments, it could also provide direct input to dual porosity or discrete fracture network modelling.

The model approach used at Rosebery was a single continuum porous volume, coupled above a single equivalent continuum volume approach. This structure attempts to model the porous flow in the surficial deposits and regolith, in addition to the permeability transition that was observed from weathered to un-weathered bedrock at Rosebery. In this approach, flow in the un-weathered fractured rock on a regional scale was represented by an equivalent porous flow. In the model approach used at Rosebery, highly fractured zones, mine workings, and drill holes were represented by regions of higher hydraulic conductivity. The degree to which the hydraulic conductivity was varied was dependent on drill-core based observations indicating the average extent of fracturing that the drilling intersected (Section 3.3). The hydraulic conductivity was decreased with depth to correlate with the local geotechnical data at Rosebery (Section 3.3).

6.6 Graphical User Interface and Code Selection

For simplicity and repeatability in other mining environments, commercially available software was used for groundwater modelling, rather than developing a site-specific package or code. To spatially analyse and prepare the Rosebery data for input into a groundwater modelling package, mine planning data, an environmental and a geological database were linked in a single GIS. Mine planning and exploration data at Rosebery (Pasminco Exploration et al., 2002; and PRM, 2003a; 2003b; and 2003c) existed in each of the major three formats of the three major mine planning and resource definition software packages used throughout Australia: (i) „Vulcan' (Maptek, 2004); (ii) „Surpac' (Gemcom, 2008); and (iii) „Datamine Studio' (MICL, 2003). The environmental database (PRM, 2004) utilised a Microsoft Access interface. None of these packages allow direct data input into commercially available groundwater modelling packages. Exporting mining data and subsequently constructing a groundwater model similar to that described in the present study, is likely to be an issue faced in all mining related groundwater modelling exercises; a solution to this problem is elaborated on below.

6.6.1 Graphical user interface (GUI) selection

A „graphical user interface' GUI is a computer package which in the case of groundwater modelling, enables the user to construct, run and display models with a more visual input rather than writing the input files manually. Both the mining packages: (i) Vulcan; and (ii) Surpac contain simple MODFLOW GUIs, however, these currently require significant improvements to create models with the flexibility offered by purpose built GUIs such as: PMWIN (Chaing and Kinzelbach, 1991 and 2001); MODFLOW-Surfact (Hydrogeologic Inc., 1996); GMS from Engineering Computer Graphics Laboratory (ECGL, 1998); Visual MODFLOW (Waterloo Hydrogeologic, 2000); and Groundwater Vistas (ESI, 1997). As a result, a significant

part of the effort of the study involved drawing together the available data into the same format for import into the GUI.

The program Groundwater Modelling System (GMS) v4.0 (Brigham Young University, 2002), incorporating both MODFLOW and FEMWATER, was chosen as the GUI for constructing the 3D model within the present study. GMS also incorporates MODPATH (Pollock, 1994) which is a particle tracking code used in conjunction with MODFLOW. Data from a variety of sources has been incorporated into GMS as part of the present study (Figure 6.2).

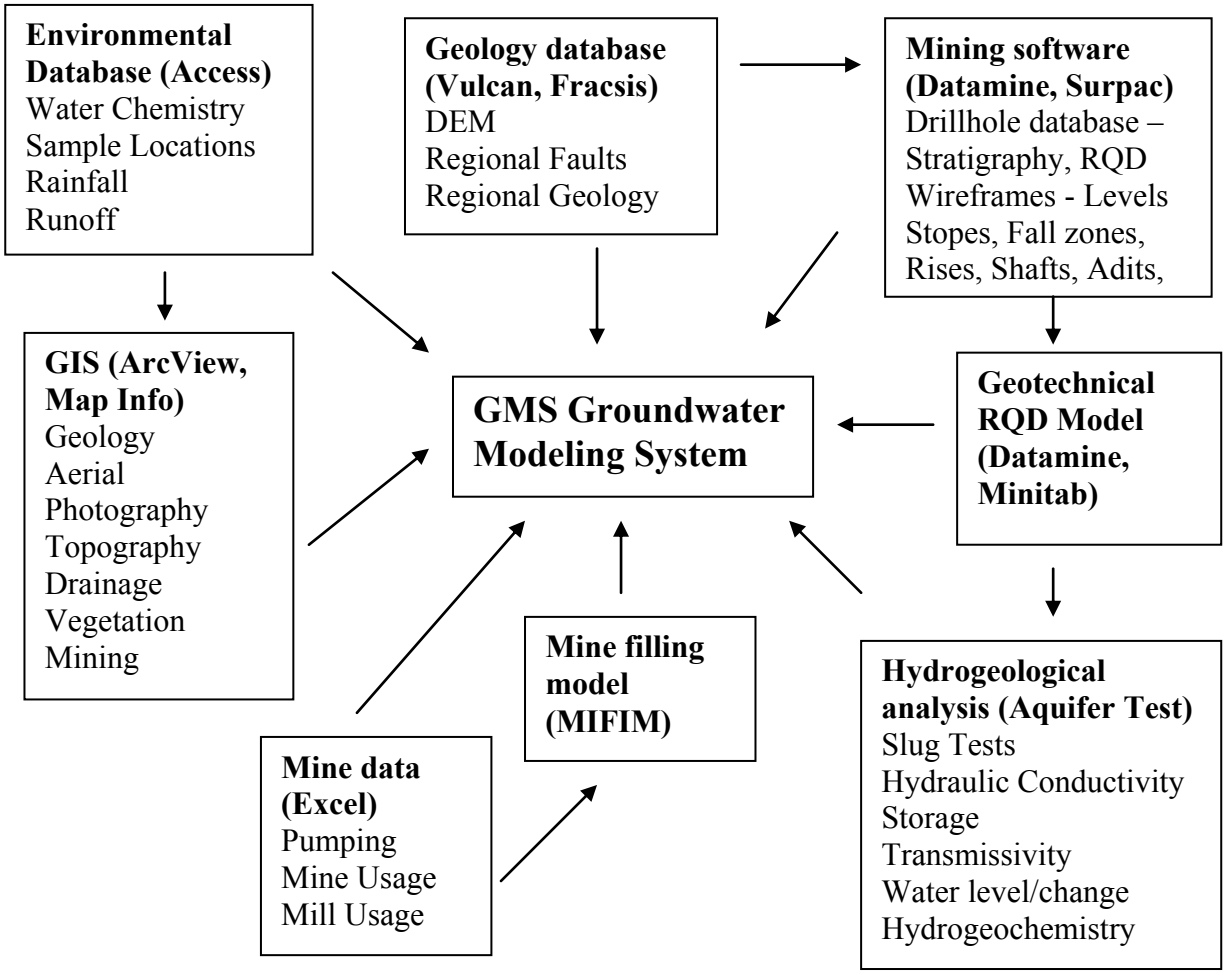

Figure 6.2 Data flow diagram

Visual MODFLOW was also a potential GUI, however, unlike GMS, at the time the work was undertaken did not yet support FEMWATER or all of the new parameter features and analysis capabilities of MODFLOW-2000 (Waterloo

Hydrologic, 2003). The GUIs PMWIN, Groundwater Vistas, and MODFLOW-Surfact did not contain a comprehensive GIS package, which was a major consideration at the conceptual stage of the numerical modelling within the present study.

A demo version of GMS 4.0 (Brigham Young University, 2002) is provided in Appendix Eleven for the reader. The demo package is capable of displaying the two simulations provided in Appendix Eleven and discussed throughout this chapter. The reader is encouraged to refer to models in their 3D digital form throughout the chapter rather than solely relying on the 2D snapshots of the simulations presented in Appendix Twelve. Thus, some familiarity with GMS or similar modelling packages is desirable; otherwise, GMS tutorial files are included (Appendix Eleven).

6.6.2 Code selection

The GMS GUI offers the user a number of groundwater modelling codes. This section describes the decision making process for choosing the particular modelling code that was used in the present study, by elaborating on the two major code choices FEMWATER and MODFLOW.

6.6.2.1 FEMWATER

The finite-element flow code FEMWATER was investigated as an alternative to finite-difference modelling (Yeh and Ward, 1980). The benefits of finite-element modelling can be extensive, particularly with large datasets available from mining operations. One of the major advantages would be the removal of the block modelling stage, described in the present work in Section 3.3. Finite-element modelling has the scope for direct importation of xyz data, without the requirement of thinning the information into a rigid grid, as is required for finite-difference modelling. Such information could include: (i) geological unit wireframes; (ii)

geotechnical data such as RQD observations; (iii) geological variation (i.e. where mineralisation is associated with secondary porosity (Liquid Earth, 2005; and Evans, 2005)); (iv) mine workings geometry; and (v) drillhole strings.

6.6.2.2 MODFLOW

Using the concept of equivalent porous media, MODFLOW can be used to simulate groundwater flow through fractured rock (Middlemis, 2000). The MODFLOW code was developed by the U.S. Geological Survey to simulate groundwater flow through a porous medium by using a finite-difference method. First documented by McDonald and Harbaugh (1984), MODFLOW has since become the most widely used groundwater modelling code in the world (Middlemis, 2000). The present study uses the version „MODFLOW-2000, The U.S. Geological Survey Modular Ground-Water Model' (Harbaugh et al., 2000).

MODFLOW is divided up into packages, and each package simulates a different function within the groundwater problem (Harbaugh et al., 2000). The important hydrologic functions, such as leakage to rivers, recharge and evapotranspiration, are typically included within the ground-water flow equations, and are provided as separate packages in MODFLOW (*ibid*.). Each solution method is also considered to be a package (*ibid*.). Packages may be turned off and on throughout the modelling process. This functionality is important for finding erroneous data within particular packages during model set up and for representing different scenarios throughout the modelling process. MODFLOW is considered to have the best range of stream-aquifer interaction modules (Middlemis, 2000).

6.6.2.3 Final Code Selection

Although the versatile functionality of FEMWATER presented an exciting potential in the present study, the lack of modular packages available for use with

finite-element codes, favoured the use of the finite-difference package MODFLOW. The decision to use MODFLOW was made primarily on the basis of: (i) its widespread application (Osiensky and Williams, 1997); and (ii) its versatile modular nature (Harbaugh et al., 2000). The stream-aquifer interaction capacity made MODFLOW powerful for modelling in the wet, temperate, mountainous environment of western Tasmania where quantifying the interaction between groundwater and surface water was of high importance in the viability of the conceptual model.

6.7 MODFLOW Packages

6.7.1 Global/basic package

Unlike other packages within MODFLOW, the Global/Basic package (BAS) does not solve an equation; rather, it administers and controls the various input data for the model (Harbaugh et al., 2000). The BAS package reads all the data, sets up the simulation and controls the model outputs (Harbaugh et al., 2000; and Brigham Young University, 2002).

6.7.1.1 Run options

Rather than just the forward run process, MODFLOW 2000 within GMS contains three „automated' run options: (i) the Observation Process; (ii) the Sensitivity Process; and (iii) the Parameter Estimation Process (Brigham Young University, 2002). These options were documented by Hill et al. (2000).

A „forward run' applies the MODFLOW simulation and is the standard run option used in the present study. The observation process generates values that the model calculates for comparison with field measurements or observations (Hill et al., 2000).

The sensitivity process calculates the sensitivity of deduced properties such as hydraulic head throughout the model with respect to specified parameters (*ibid*.). The

„sensitivity analysis' option undertakes a „forward run' and quantifies the sensitivity of individual parameters relative to the model solution.

The parameter estimation process adjusts input parameter values automatically to minimize the error between calculated heads and observed heads (*ibid*.). Using the „parameter estimation' run mode, MODFLOW calculates a set of parameters that minimises the residual between observed and simulated heads and flows, and then undertakes a forward run (Brigham Young University, 2002). Automated „parameter estimation' was performed as part of the present study by using manually calibrated values as the starting values.

6.7.1.2 Steady state versus transient simulations

MODFLOW can simulate both steady state and transient model types. Steady state numerical modelling, in the present study, is defined as a model in which the stresses do not change with time. Such modelling removes the seasonal variation and uses average annual inputs to describe the system. Transient numerical modelling, in the present study, is defined as a model in which stresses change over the period of the model run. Average data or actual data may be used to describe the system. The benefit of using temporal numerical modelling is that calibration can be achieved not only to a point in time, but to a response to a change in stress over time. Transient modelling requires considerable temporal data as input. For future work, such temporal data could be obtained through the use of automatic water level loggers. This would involve obtaining measurements over a number of years, observing the seasonal fluctuation in water levels, then coupling this potentiometric surface data with stresses such as pumping, stream flow, and rainfall, as well as finally calibrating to material hydraulic properties. This was considered beyond the scope of the present study, however, it does provide direction for future work.

The two scenarios of: (i) operation; and (ii) post decommissioning, were modelled using the same steady state model, each with different stresses. This variation is not considered transient modelling, in the present study; rather two scenarios of the steady state system. Likewise, particle tracking with the use of MODPATH has a temporal component, however, is not considered a transient model, as the stresses do not vary over time. Rather, the steady state model is run and the particles are given a time component in MODPATH.

6.7.2 Groundwater flow packages

The groundwater flow process solves the partial-differential groundwater flow equation (Equation 6.1) using the finite difference method, in which the groundwater flow system is divided into a grid of cells (McDonald and Harbaugh, 1988).

$$\frac{\partial}{\partial x}\left(K_x \frac{\partial h}{\partial x}\right)+\frac{\partial}{\partial y}\left(K_y \frac{\partial h}{\partial y}\right)+\frac{\partial}{\partial z}\left(K_z \frac{\partial h}{\partial z}\right)=S_S \frac{\partial h}{\partial t} \qquad (6.1)$$

where S_S is the specific storage,

$K_x, K_y K_z$ is hydraulic conductivity in the x, y and z directions,

h is the piezometric head, and t represents time.

There are three variations for solving the groundwater flow equation available in MODFLOW-2000 within GMS v4.0: (i) Layer Property Flow (LPF); (ii) Block Centred Flow (BCF); and (iii) Hydrogeologic Unit Flow (HUF) (Brigham Young University, 2002).

The LPF package was utilised in the initial modelling because: (i) using GMS, the additional run options „sensitivity analysis' and „parameter estimation' are also only available using the LPF package (Brigham Young University, 2002); (ii) the LPF package contains many improvements on the older BCF package (Harbaugh et al., 2000); (iii) unlike the BCF, all input data in the LPF package are independent of cell

dimensions, and due to the mountainous terrain it was important to vary the dimensions of cells at Rosebery; (iv) unlike the BCF package, the LPF package does not require the input of transmissivity; and (v) the HUF package was inappropriate at Rosebery as it assumes that the hydrogeologic units that occur within each model finite-difference cell are virtually horizontal.

6.7.3 Solver packages

The simultaneous equations that are solved at each cell are determined by one of four packages in MODFLOW: (i) the „Strongly Implicit Procedure' (SIP1) (Trescot et al., 1976); (ii) the „Pre-Conditioned Conjugate Gradient' method (PCG2) (Hill, 1990); (iii) the „Slice Successive Over Relaxation' method (SSOR) (McDonald and Harbaugh, 1998); or (iv) the „Link Algebraic Multigrid' method (LMG) (Mehl and Hill, 2001).

During the present study, after attempting to use all available solvers, convergence was consistently more stable using the PCG2 solver. This was a strong motivation in deciding to use PCG2 as the default solver used in the modelling and calibration. The methods vary in: (i) the way they solve simultaneous equations; (ii) the results they produce (Osiensky and Williams, 1997); (iii) the speed in which they solve the equations (Mehl and Hill, 2001; and Fetter, 2001); and (iv) their consistency in converging. The LMG solver is 2-25 times faster than the PCG (Mehl and Hill, 2001), however, it was not available to the author due to a lack of license. The PCG2 solver, unlike SIP and SSOR, allows for the possibility of defining a criterion for the water balance error (Hekman, 2000). SSOR is considered a solution that is only useful for cross sectional models (Fetter, 2001), and, like SIP, is considered relatively slow (*ibid*.).

6.7.4 MODPATH

The particle tracking package MODPATH (Pollock, 1994) is used within MODFLOW to show the relative flow paths for groundwater flow down gradient of the mine voids. Simulations based on the two scenarios (operation and post decommissioning) were performed and compared. MODPATH produces a graphical visualisation of the theoretical particles and their paths.

Additional inputs for the MODPATH package are: (i) starting locations for particles; and (ii) the porosity of materials. Porosity in the present study was a broad estimate and was not considered definitive. Like GRC (1985), the present study assumed an effective porosity of 0.05 for the rock mass and 0.5 was assumed for voids. Cells containing significant sources of AMD, identified in the Chapter Four, are assigned particles. As the time step modelled was 1 day, MODPATH can be run within the MODFLOW solution using, for example, the time periods of 365, 3650, 36500 to represent the time periods, 1 year, 10 years and 100 years, respectively. Alternately MODPATH can track particles to their final destination within the model domain; these are presented as the output for each model scenario in Appendix Twelve.

6.7.5 Grid design

Given that the Rosebery Mine Grid (RMG) was used for the majority of geological and mine planning information available for the present study, this was the format that was imported into GMS.

Initial modelling used a 200 m grid and was subsequently refined to 50 m. The grid was manually thinned significantly in the x and y directions from 50 m in the area of interest to up to 450 m at the headwaters of the model (Figure 6.3, Figure 6.5). In areas where data was sparse in the east and south of the study area, the grid was refined in order to reduce the number of cells and improve processing time.

The grid spacing alteration suggestion of less than 50% (Anderson and Woessner, 1992) or 30% (Fetter, 2001) was not adhered to at the eastern and southern extremities of the model domain, in order to keep block centres at factors of 50 m to aid data entry. The fact that this may provide a source of computational error in the extremes of model is acknowledged, however, keeping the grid centres at multiples of 50 m enabled the input of the mine data produced at that scale. The scale of such errors at the edge of the model was considered insignificant in relation to the lack of data constraints in such areas.

In the main area of interest, the block size was maintained at a constant 50 m (Figure 6.3). In the eastern and southern extremities of the model domain, the 50 m blocks were first expanded to three sets of 150 m, then five sets of 250 m, followed by seven sets of 350 m and two 450 m wide rows in the extreme east of the study area. This resulted in a grid 195x100x54 rather than 279x168x54. Although this manual refinement was extremely time consuming, this refinement greatly improved, not only the computation time, but also the speed at which the model could be further manually altered at the construction stage. The total modelled area (92.5 Mm^2) was greater than the actual catchment area 89 Mm^2 due to cells over-lapping natural boundaries (Table 6.1, and Figure 6.3).

No. of cells	Cell size (m)	Cell size (m)	Area m^2	Area km^2	% of area
9567	50	50	23917500	23.9175	25.84349
696	150	50	5220000	5.22	5.640347
1214	250	50	15175000	15.175	16.39699
1580	350	50	27650000	27.65	29.87655
319	450	50	7177500	7.1775	7.755477
9	150	150	202500	0.2025	0.218807
30	250	150	1125000	1.125	1.215592
42	350	150	2205000	2.205	2.38256
17	450	150	1147500	1.1475	1.239904
25	250	250	1562500	1.5625	1.688322
59	350	250	5162500	5.1625	5.578217
8	450	250	900000	0.9	0.972474
9	350	350	1102500	1.1025	1.19128
13575	Total	Total	92547500	92.5475	100

Table 6.1 Grid design sizes and areas

Grid design should be oriented in line with the principle direction of flow (Waterloo Hydrologic, 2003). Although the grid was essentially designed to fit the RMG and aid data entry, the principle direction of flow essentially follows this rule. Based upon potentiometric surface analysis (Chapter Three), the principle flow direction in the area of interest was transverse to the topographic gradient, flowing along the RMG y axis from the West Coast Range in the south and essentially turning at right angles along the RMG x axis into Lake Pieman at Mount Black (Figure 6.3).

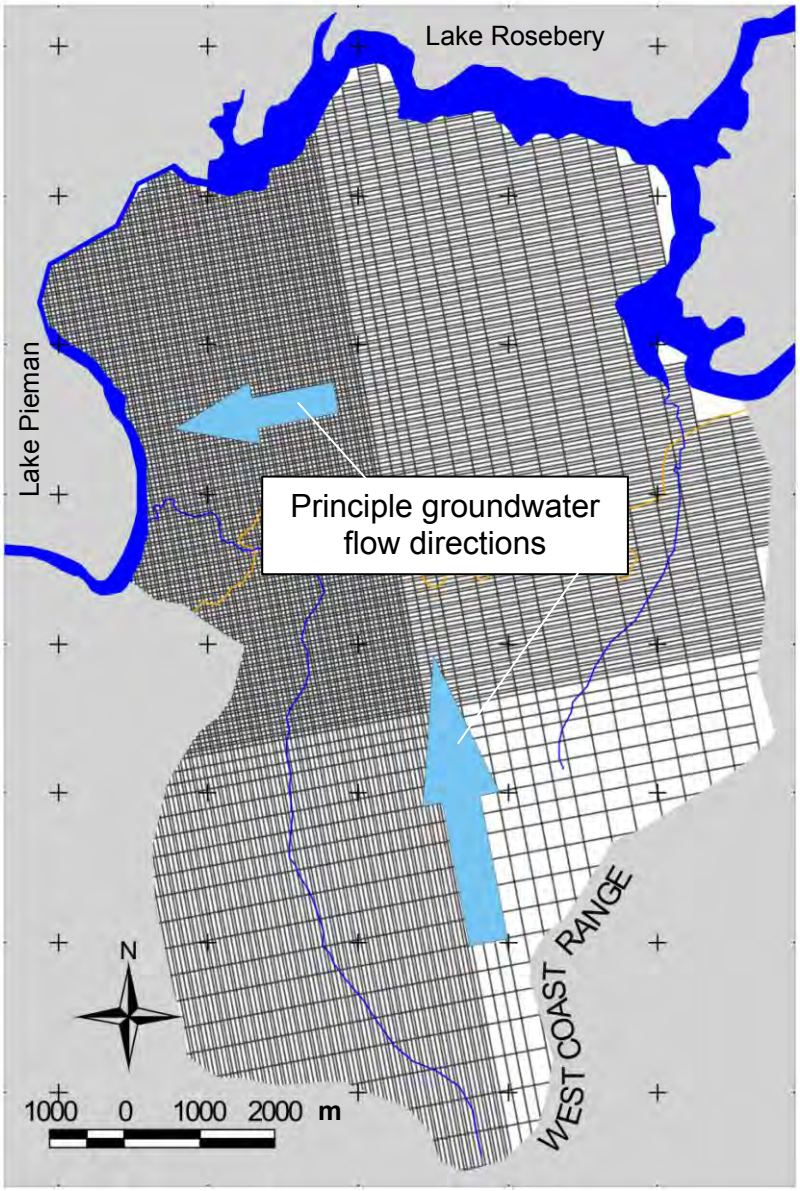

Figure 6.3 Grid in plan layout and principle flow directions

To incorporate the geometry of the mine at depth, and the West Coast Range altitude, a very large vertical component was required in the model. The groundwater model was limited to these extents as: (i) flow in the bedrock deeper than the mine (outside major vertical fracture zones) was assumed to be negligible, which was supported by the RQD data (Section 3.3.4.3); and (ii) the vertical model extent was already very large such that extension significantly below mine level would significantly retard the already cumbersome model computation. Grid size refinement in the z direction is addressed below (Section 6.7.6.2).

6.7.6 Layer data

The two major input data types for the Ground-Water Flow Process (GWF) are: (i) layer data; and (ii) list data. With layer data, a value is required for every cell in one or more horizontal layers of the grid. Layer data inputs include areal recharge flux, starting heads, and material properties such as hydraulic conductivity and porosity. List data refers to any type of data for which values are required for only some of the cells in a grid (Harbaugh et al., 2000).

6.7.6.1 Material properties

Orebody modelling and mine design packages, GISs, statistical packages, and GMS have been used to provide three-dimensional insight into the geology and mine infrastructure within the study area (Figure 6.2, and Figure 6.4). The material properties spatial variation input data followed a hierarchy from the geology of the area, which was then overwritten by major faults, then geotechnical data, mine planning data and finally surface features. Figure 6.4 represents the data hierarchy and the relative importance of the model geometry and features which affected the

groundwater regime. It also shows schematically how the natural hydrogeologic regime becomes pixelated in a hydrogeological model due to the rigid nature of modelling grids.

6.7.6.2 Geological input

Geology data exist as: (i) hardcopy maps (e.g., Corbett and McNeill, 1986; and Corbett, 2002a), (ii) the 3D fault and geology models (Pasminco Exploration et al., 2002); (iii) the Rosebery mine drillhole database (PRM, 2003b); and (iv) the Rosebery mine mapping and cross-sections (PRM, 2003c). Mine based geological data are generally too defined for direct input into hydrogeological modelling software and require simplification.

A regional three dimensional fault model was created for Pasminco Exploration by Fractal Graphics (Pasminco Exploration et al., 2002) and delivered in the Vulcan format. As part of the present study, conversion and projection into mine grid and to a format which could be imported into MODFLOW required a number of steps: (i) the Vulcan (Maptek, 2004) files were converted to Datamine (MICL, 2003); (ii) then to xyz AMG points; (iii) then projected to RMG; before (iv) being reimported into Datamine (MICL, 2003) as wireframed faults; (v) converted into 3D solids; and (vi) a block model of each of the faults created for input into GMS.

The regional geology (Pasminco Exploration et al., 2002) was also in Vulcan format, however, significant problems were encountered with: (i) the un-referenced local grids used; (ii) the complexity of the wireframing; and (iii) the existence of voids, containing no geologic properties between the solids. The geological units defined by this model also required further division into hydrogeological units. Thus, a decision was made to only use this modelling as a guide to creating cross sections rather than direct digital input.

The hardcopy 1:25,000 map (Corbett and McNeill, 1986) of the surface geology was used as the primary input into layer 1 (the upper most layer) of the numerical groundwater flow model. A 50 m cube hydrogeological block model of the surface geology was created using a combination of the hardcopy map (Corbett and McNeill, 1986) and the DEM. The 25 m DEM was used to create a 50 m DEM using Surfer, which acted as spot heights for the top of layer 1. Layer 2 utilised the bedrock geology map (Corbett, 2002a) in a similar manner.

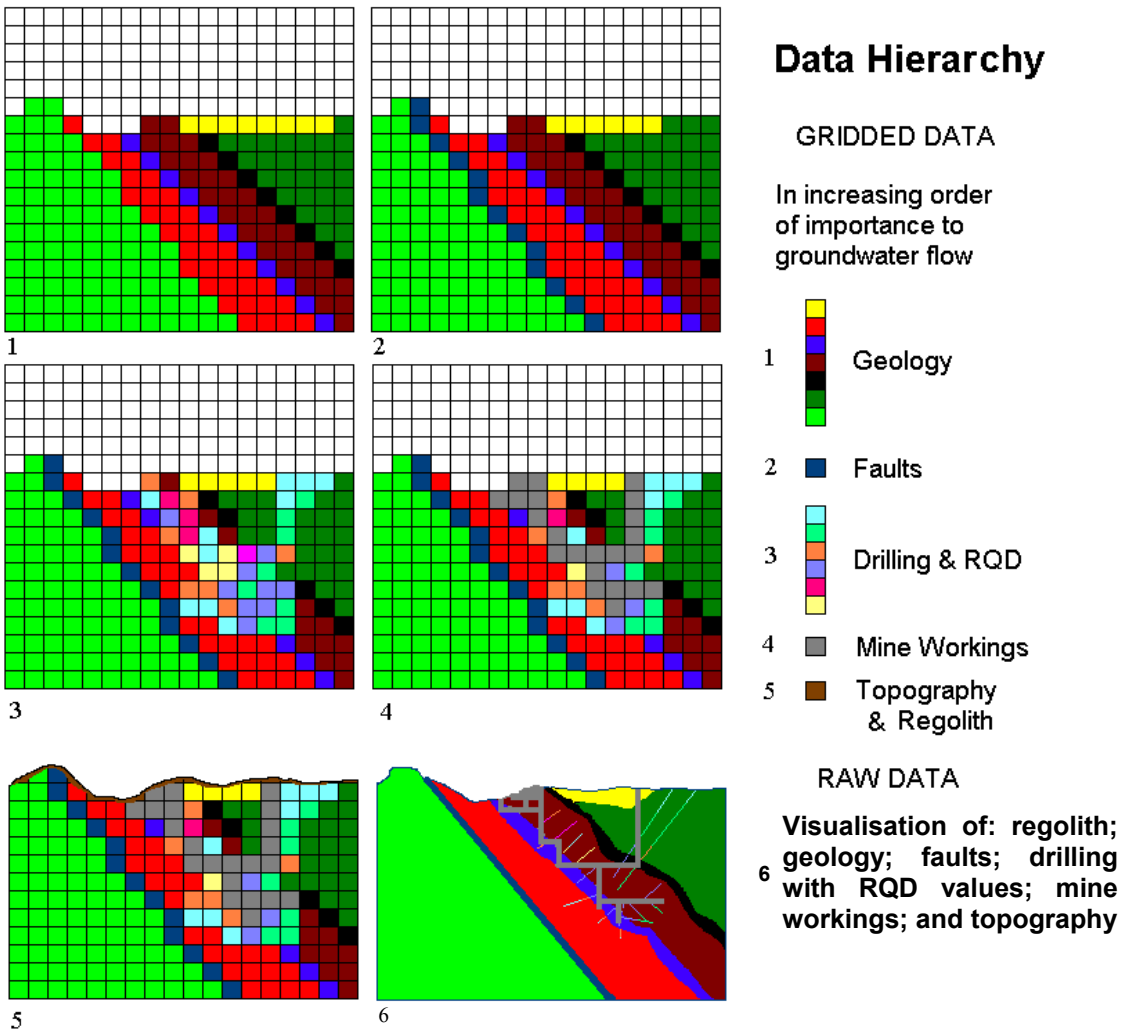

Figure 6.4 Data hierarchy at Rosebery showing the development of the conceptual numerical groundwater model. The model geometry was created to emphasise the features of dominant influence to groundwater flow. Initially the geology of the area was gridded, secondly faults were superimposed, thirdly the drilling (with RQD values) was imported, followed by the mine workings, and the topography and an inferred regolith were imposed over all the data. Topography and inferred regolith over writes all cells: mine workings overwrite drilling and RQD, faults and geology cells; drilling and RQD overwrite faults and geology cells; and faults overwrite geology cells.

Subsequent layers required an even 50 m grid for direct input from the block models (Figure 6.4). The glacial sediments were only ever represented by one block (50 m) in z direction, which corresponds to drilling data (PRM, 2003b) for maximum glacial thickness over the study area (Stratigraphy code FG, Fluvial Glacials). Thus, only layer 1 contains glacials.

Layers 3-25 were „compressed' to fit the grid to the topography using the GMS function „Fix layer' (Figure 6.5). Where no pre-existing material code existed, these layers were assigned the material code „Thinned Regolith'.

The complexity and extent of the drilling records hampered transferring geological data from Datamine Studio (MICL, 2003) into the GMS model. The sophisticated exploration and resource drilling information was unable to be adapted to the GMS v4.0, because the later only deals with vertical boreholes. The drilling records (PRM 2003b) were considered too detailed to be primary input for sub-surface layers of the groundwater model, however, like the 3D geology (Pasminco Exploration et al., 2002), visualisation with Datamine, provided insight into the subsurface geological distribution.

With the exception of the unconsolidated glacial sediments, surface geology was projected to a depth of 1700 m (RMG) using the surface geology block model, bedrock geology block model and the major fault block models as primary input, by creating a series of sections and plans in the MODFLOW grid. As part of the present study, some 195 W-E cross-sections or rows (i) were made manually and matched to 100 S-N long sections or columns (j); which in turn were matched to 54 „plan sections' or layers (k) (Appendix Twelve).

6.7.6.3 Geotechnical modelling input

Datamine (MICL, 2003) was used to create a very simple block model based on RQD data in much the same way resource geologists create block models for grade (e.g., Datamine, 1998). A cubic, inverse distance squared, search ellipse was used to calculate a RQD value for each block. Block models were refined by altering the search size, number of values examined and block size. Block models were also created to spatially represent areas where zero values were recorded and areas where 100 values were recorded (Appendix Six).

Block models were created with the same grid size as the groundwater model, primarily to aid in onerous data transfer between software packages. Such limitations in software compatibility complicated data transfer in all stages of the present study. The block model was exported as a text file, manipulated and reimported into GMS as geo-referenced grid centres assigned a material I.D. based on the RQD model. The RQD geotechnical block model was used to: (i) statistically analyse the hydraulic properties of the entire rock mass (Section 3.3); and (ii) model the influence of drilling on the flow field. Likewise, Hofrichter and Winkler (2006), GHD (2007) and Surrette et al. (2008) discuss the theoretical use of statistical analysis of fracture networks, in combination with hydraulic tests, as input for a continuum approach to numerical groundwater modelling.

The RQD block model was used as direct input to represent the drilling and degree of fracturing it intersects. Initially cells containing mine voids were assigned a conductivity two orders of magnitude higher than the surrounding rock mass. The concept was that cells containing drilling were assigned a hydraulic conductivity based on the RQD that the block model had calculated for that cell. If the RQD in the block model was 100, the same conductivity as the rock mass was assigned, assuming

little influence from the drilling, and limited connectivity. Conductivity was varied based on RQD in the block model varying linearly up to a conductivity an order of magnitude lower than the mine void if the RQD was zero (Table 6.2).

Such an approach was designed to replicate conditions observed in the field. Drillholes were observed to act as groundwater flow conduits in the underground mine in both the present study, and previously in Hale (2001). The potential for drill holes to act as flow paths has been discussed and modelled by other (e.g. Gass et al., 1977; Reily et al., 1989; Lacombe et al., 1995; Church and Granato, 1996; and Zinn and Konikow, 2007). Modelling flow within individual drill holes was considered beyond the scope of the present work, so the approach described above was developed as a substitute to represent the influence of flow within drillholes. Flow within individual drillholes was nevertheless considered extremely important in the present study, and provides scope for future work elsewhere within such environments.

	Mine	RQD 0-10	RQD 10-20	RQD 20-30	RQD 30-40	RQD 40-50	RQD 50-60	RQD 60-70	RQD 70-80	RQD 80-90	RQD 90+
K (m/day)	100	10	9	8	7	6	5	4	3	2	1

Table 6.2 Hydraulic Conductivity (K) variation associated with average RQD of drilling and mine voids.

6.7.6.4 Mine planning input

Datamine Studio (MICL, 2003), an orebody modelling and mine design package, was been used to provide three-dimensional insight into the geology and mine infrastructure. Both the geometry and spatial distribution of mine excavations are likely to greatly affect the groundwater flow regime. The high permeability of mine voids means that they will become the most important conduit during and after the filling of the mine. A three dimensional model of mine features had been generated by PRM (2003a). The mine features modelled include levels, declines, stopes, passes, vent rises, shafts, the open pit, and surface topography (Figure 2.2).

Each feature can be examined separately, and if complete, its volume may be calculated using the Datamine Studio (MICL, 2003) function „wireframe-volume'. This function also gives information on surface area that was important in determining the quantity of mine wall rock that is available for oxidation. A summary of mine void volumes is contained in Appendix Ten.

A mine block model was created at the 50 m block size to represent the geometry of the mine within the groundwater model. If a mine feature appears within a block, that entire block was deemed to be a groundwater conduit. The entire mine infrastructure was loaded into Datamine (MICL, 2003) and converted to a series of xyz points. These points were rounded to the nearest 50 m block centre and identical points removed. The mine input consisted 2629 125000 m^3 blocks (50 m, by 50 m, by 50 m) which were assigned the material code „Mine Void'.

In reality much of the 125000 m^3 sized blocks were not voids at all, as some drives were as small as 5 m^2 in cross section. It was assumed that either: (i) the cavity contributes to flow significantly enough that the average flow for such blocks was considerably higher than those without voids; or; (ii) the cavity's hydraulic influence could extend to much of the total block. Justification for the later assumption comes from Hoek and Brown (1980), who found that when underground workings are excavated, the stresses which previously existed in the rock are disturbed, and new stresses are induced in the immediate vicinity of the opening. The rule of thumb applied in geomechanics (Sidea, pers. comm., 2008) is that the stress influence is two times the void width. Thus, a standard 5.5 m wide drive could be expected to influence fractures over 27.5 m, i.e, a large proportion of a 50 m block. In underground mines, such mechanical unloading of fractures around open voids, in addition to blast damage, enhances this influence, thus providing further theoretical

justification for assignment of hydraulic conductivity at the 125000 m^3 block size. The actual decision to choose 125000 m^3 as the minimum block size was an arbitrary value based upon a block size that enabled the geometry of the mine to be represented, however, was still practically large enough to model given the computing limitations. Refinement at smaller scales was not computationally possible at the time, but could provide an avenue for future refinement of the model.

6.7.6.5 Topography and regolith

Layer one in the numerical model consisted of 50 m deep cells which were assigned an elevation from the DEM (Figure 6.5). This created a layer of a consistent 50 m thickness draped under the topography of the catchment, representing the surface geology mapped (Section 6.7.6.2) over the catchment (Corbett and McNeill, 1986). A second layer of „regolith' followed the same principle (Section 6.7.6.2) and where layers required „compacting' to fit the rigid vertical grid they were assigned the material code „thinned regolith'(Figure 6.6). Likewise, GHD (2007) applied a similar vertical model grid containing thinned layers in a wet, tropical, mountainous mining environment in Indonesia.

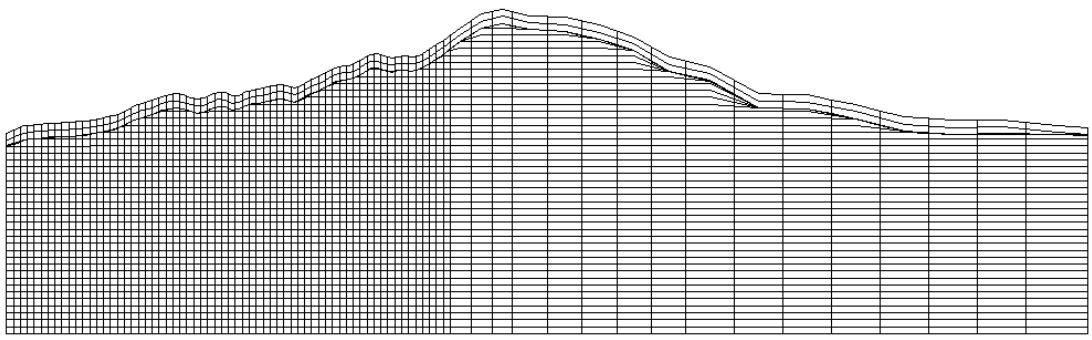

Figure 6.5 Example grid in cross section displaying the topography (upper most), regolith layer and subsequent uniform grid below

The justification for having a topography and regolith layer throughout the catchment was from the near-surface higher-value RQD data (Section 3.3). These

surface geology and regolith layers were assigned higher hydraulic conductivity values based on an increased fracture frequency. Likewise, Kahn et al. (2008) applied a similar approach with a multiple layer model and gradational regolith layers to represent a groundwater system in an alpine watershed in the United States of America.

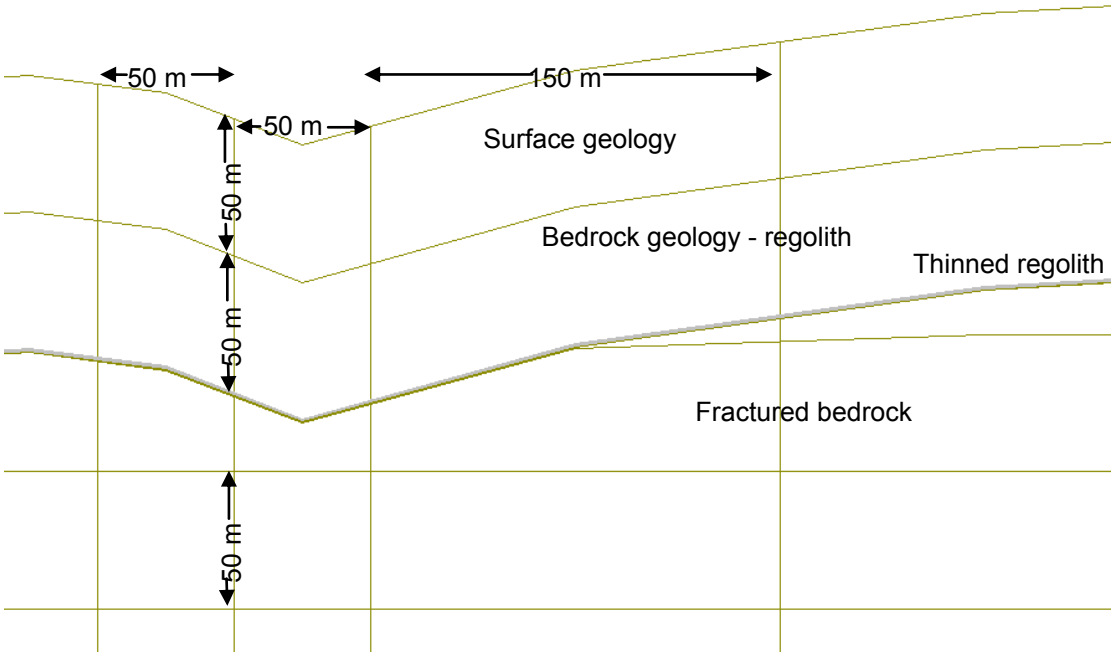

Figure 6.6 Example near surface grid configuration; Layer 1 (Surface Geology), Layer 2 (Bedrock Geology – Regolith), Thinned Regolith and Fractured Bedrock

6.7.6.6 Starting heads

Information about head distribution is always incomplete (Anderson and Woessner, 1992). Being required in every cell (layer data), starting heads could not be provided using observed heads unless: (i) a significantly larger monitoring network was established; or (ii) the grid sizes were changed to unrealistically large cells that would not adequately represent the natural system.

Starting heads for the initial modelling were set at the surface level of each of the block centres by creating a 50 m spaced DEM and applying it to the model grid. To ease convergence (Waterloo Hydrologic, 2003) starting heads were then set at a more realistic depth of h/10 (i.e., if the ground surface was at an elevation of 110 m

above sea level, the depth to groundwater would be 11 m, similarly at an elevation of 1200 m, the depth to groundwater would be 120 m). This broadly corresponded to observed heads (Section 2.3.3) and made an easy algorithm for starting head data allocation (remembering a value was required for every cell in the model).

6.7.6.7 Recharge RCH1

The recharge package simulates precipitation that percolates to the groundwater system (Brigham Young University, 2002). The recharge in (m^3/day) is applied to every single cell at the top of the vertical column of cells located at (i, j) as natural precipitation enters the groundwater system at the top. The water balance, defined in Chapter Five, outlines the calculation of the recharge to the groundwater system. Over the study area, precipitation and runoff, were functions of topography, and evapotranspiration (Chapter Five). Recharge varies spatially over the study area based on of these factors; however, an average value was applied over the entire area of the numerical model in the present study.

6.7.6.8 Evapotranspiration package EVT1

Evapotranspiration was accounted for within the water balance and was represented by the recharge package in the numerical model of the present study. Thus, the evapotranspiration package was disabled throughout modelling undertaken as part of the present study. The calculation of evapotranspiration has previously been discussed in Chapter Two, and its use in the water balance is discussed in Chapter Five.

6.7.7 List data

List data types include: (i) information on boundary cells that are used to create the boundary conditions; (ii) information on point sources and sinks throughout the

system; and (iii) actual observations throughout the system. List data inputs that were employed in the Rosebery study included: (i) well discharge rates; (ii) drain conductances; (iii) riverbed conductances; (iv) boundary elevations and flow conditions; and (v) observations of piezometric head.

6.7.7.1 Observations of piezometric head (OBS)

Chapter Three outlined the method for measuring the average piezometric head. Table 3.1 presents the average observations made throughout the catchment. These data were used as calibration targets for the numerical groundwater flow model. The observation process (OBS) calculates the simulated head values after a completed model run. OBS then compares the simulated heads with the observed heads by: (i) calculating the sum of squared weighted differences between model values and observations; and (ii) calculates the sensitivities related to the observations (Harbaugh et al., 2000).

6.7.7.2 Boundary conditions

The catchment boundaries of the Sterling and Stitt Rivers form the upper boundaries of the groundwater model. These „no-flow' boundaries represent the theoretical groundwater divide of the portion of the West Coast Range that traverses the Rosebery area. The lower boundaries of the groundwater model were the constant head hydro-electric lakes. Groundwater was assumed to discharge in to both Lake Rosebery and Pieman, the major topographic depressions in the area. „Specific head' values (i.e. those that remain constant in the model) were assigned along the boundaries of the lakes.

Although Lake Rosebery was subject to fluctuations due to climate differences and Hydro Tasmania electricity generating activities, for the purpose of modelling it

was given a constant head sloping from 3209 to 3205m (RMG). Likewise, Lake Pieman was assigned a constant sloping head from 3155 to 3151 m (RMG). The Bastyan Dam wall was given a ‚no-flow' boundary sloping from 3205 m to 3155 m (RMG). The 50 m difference is also the reality due to the dam wall. It is not unreasonable to assume that the lakes keep the rock mass fully saturated below each. Thus the sloping head represents the reality as best could be achieved at the scales of the model grid. The Time Variant Specific Head Boundary (CHD1) package was used to represent the lake boundary conditions.

6.7.7.3 The well package (WEL1)

Discharging or recharging wells can be simulated using the Well Package (WEL1). Wells were specified by assigning a pumping rate to a selected cell at the location of each well. Wells can be either injection wells (positive flow rate) or extraction (negative flow rate) wells.

The well package was utilised to represent mine pumping on a regional scale. Mine workings were represented by a number of cells that withdrew water from the aquifer at a rate Q (m^3/day). Negative values for Q were used to indicate well discharge. Mine pumping was simulated using a large number of wells pumping at a low flow rate.

MODFLOW, being based on Darcy's (1856) law, assumes laminar flow. Thus MODFLOW was inappropriate for modelling groundwater flow where flow was potentially turbulent in the underground mine voids. The possibility of potentially turbulent flow within these voids during pumping was overcome by the use of wells. Although turbulent flow was not modelled, groundwater was removed from the system by the wells; hence, whether its flow became turbulent was irrelevant to the system, as the removal rate was set for each well.

6.7.7.4 The drains package (DRN1)

The drains package was used to simulate the effect of drains on an aquifer and in this case the theoretical discharge level, both during and after mining. Drains only remove water from the aquifer if the water table was above the elevation of the drain. Drains were specified by assigning an elevation and a conductance to each cell at the location of each drain (Brigham Young University, 2002).

The decant point at the Rosebery mine was anticipated to be the level 8 mine adit. Lower decant points do exist, however, these were considered manageable conduits such as drill holes which could be capped or filled. The drains package was used to simulate the natural drainage of the mine at Level 8. Like the use of the wells package, the drains package was used to justify the approach of the excess potentially turbulent flow discharging at the mine adit.

6.7.7.5 The rivers package (RIV1)

Rivers differ from drains in that the river package can act as a source or a sink to the groundwater system. For each river cell, the rivers package requires: (i) river stage; (ii) conductance; and (iii) bottom elevation to be assigned where the river boundary occurs (Brigham Young University, 2002). If the cells' water table is above the river stage, the river acts as a sink, and if below, as a source to the groundwater system.

Both the Sterling and Lower Stitt Rivers were modelled using the rivers package. Although not officially named „rivers', Rosebery Creek and the tributaries flowing into Lake Pieman and Rosebery were also modelled using the rivers package. All rivers were assigned to layer 1 and the stage elevation data assigned from the DEM.

The geochemistry data provided in Chapter Four provided justification for: (i) groundwater contributing to rivers; and (ii) rivers discharging to the groundwater regime. This evidence of surface water - groundwater interaction provided justification for the use of the rivers package.

6.7.7.6 The general head package (GHB1)

Rather than using the river package to represent the Stitt River above Rosebery, the general head boundary package was used. This allowed for the specific calibration of the Stitt catchment data. The general head package is similar to the drain and river packages in that flow in or out of a cell is proportional to a difference in head (Brigham Young University, 2002). Assigning a head and a conductance to a selected set of cells specifies general head conditions. Like the rivers and drain package, flow rate is proportional to the head difference and the constant of proportionality is the conductance (Brigham Young University, 2002). As with the rivers, all general head boundaries were assigned to layer 1 and the elevation data was assigned from the DEM.

6.7.7.7 Horizontal flow barrier package (HFB1)

The horizontal flow barrier package is used to represent the low flow barriers of the tailings dam walls on a regional scale. The low conductance was set at 0.001 $(m^2/d)/m$ from layers 1 to 24 and the elevation was assigned from the DEM. It is stressed that representation of the tailings dams was on a regional scale. If there is a further need to understand the precise flow in and around the tailings dams, a more detailed analysis using a finer grid size and local calibration is recommended.

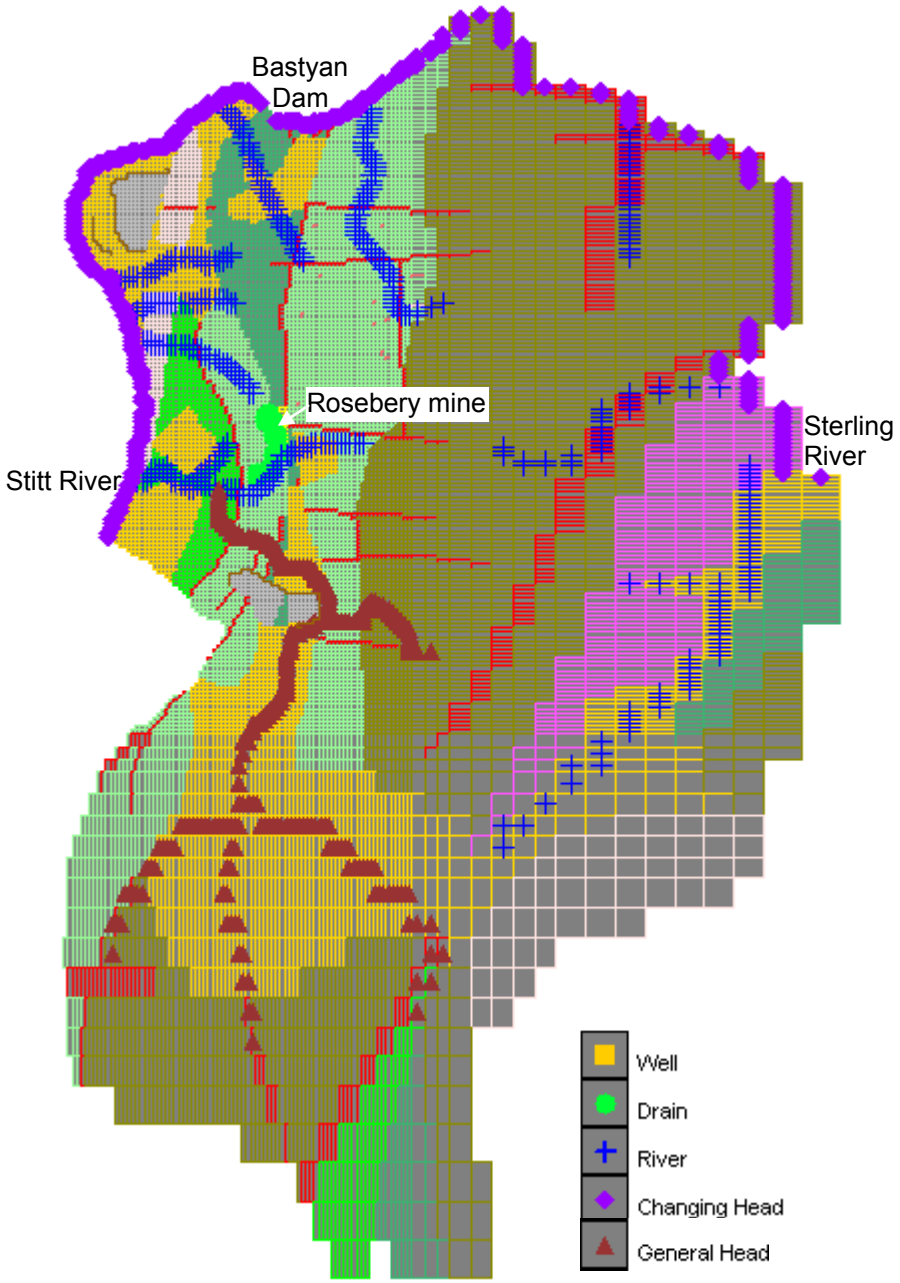

Figure 6.7 Layer 1 showing the distribution of MODFLOW packages throughout the Rosebery catchment model.

6.7.7.8 Graphical representation of the model

Graphical representation of the model is best provided in the GMS modelling package. Representing a digital 3D model in a hardcopy thesis is not ideal, however, some example plans, cross sections and long sections are provided in Appendix Twelve. The 3D GMS models presented digitally in Appendix Twelve provide the 195 cross sections (i), 100 long sections (j) and 54 layers (k) approach to the

modelling of the Rosebery catchment. Layer 1 is presented in Figure 6.7 as an example.

6.8 Model Calibration

To describe a groundwater system an understanding of both the distribution of the material properties of the rock mass, and the resultant hydraulic heads which depend on these properties is needed (Anderson and Woessner, 1992). Hassan (2003) defined calibration as "the process of tuning the model to identify the independent input parameters by fitting model results to some field or experimental data, which usually represents the dependent system parameters". Much information is known about the dependent variable (hydraulic head), but the independent variable (material hydraulic conductivity) is comparatively unknown. Where the dependent variable is the most well understood aspect of a groundwater system, it is referred to as „the inverse problem' (Anderson and Woessner, 1992; and Oreskes et al., 1994).

Model calibration is achieved by adjusting the unknown parameters in the numerical model to give a more realistic solution (Anderson and Woessner, 1992). In most numerical hydrogeological models, material hydraulic properties are adjusted until the simulation results closely match field measured hydraulic heads within a pre-established range of error (*ibid*.).

Calibration commonly comprises up to 50% of a modelling study effort (Middlemis, 2000). In the present study it was estimated that calibration and refinement of the numerical model was at the high end of this percentage.

6.8.1 Calibration approaches

Two calibration approaches were undertaken in this project: (i) automated parameter estimation; and (ii) manual, or trial and error, calibration. Manual calibration involves performing a series of forward run simulations and adjusting the

hydraulic conductivity until the most realistic solution is achieved. Defining a realistic solution for this stage of modelling in the wet, temperate, mountainous, mining environment is pivotal to assessing the success of the modelling effort. Due to the complexities involved in the present study a realistic solution, at this stage of hydrogeological research at Rosebery was simply one that appeared to qualitatively (Section 6.8.2) obey the conceptual model presented in Chapter Five.

6.8.1.1 Automated parameter estimation

Automated parameter estimation was attempted using the MF2K (Hill et al., 2000) and PEST (Doherty, 1994) codes. Automated parameter estimation is the process of using a code which changes parameter values in order to obtain a solution that is closer to pre-determined observed values. Doherty (1994) described the process thusly: "At the beginning of each iteration the relationship between model parameters and model-generated observations is linearised by formulating it as a Taylor expansion about the currently best parameter set; hence the derivatives of all observations with respect to all parameters must be calculated. This linearised problem is then solved for a better parameter set, and the new parameters tested by running the model again. By comparing parameter changes and objective function improvement achieved through the current iteration with those achieved in previous iterations, PEST can tell whether it is worth undertaking another optimisation iteration; if so the whole process is repeated."

In the early simulations, automated parameter estimation was unsuccessful due to problematic convergence or unrealistic solutions. Where parameters were successfully estimated, i.e. resulted in lower statistical errors than the starting values, the simulation results were unrealistic. The most common unrealistic simulation of this kind resulted in low hydraulic gradients such that all cells above lake level went

dry, or alternatively, all cells below the lake level dried out. Hydraulic head observations and the hydrogeological conceptual model discounted such unrealistic solutions.

Automated parameter estimation was abandoned in the early stages of the project until a more realistic manually calibrated model was created. Automated parameter estimation was then revisited and used to refine the „best fit' manual calibration. The experience indicated that automated parameter estimation was problematic at early stages in a modelling effort.

6.8.1.2 Manual parameter estimation

In order to achieve a more realistic solution, the laborious manual method was performed. When discussing manual calibration as being the standard accepted method of calibration of numerical groundwater models, Carrera and Neuman (1986), also refer to its drawbacks, summarising the process with "the method (of trial-and-error) is recognised to be labour intensive (therefore expensive), frustrating (therefore often left incomplete), and subjective (therefore biased and leading to results the quality of which is difficult to estimate)".

Manual calibration was partially performed on a 200x200x200 m spaced grid before being refined to a 50x50x50 m spaced grid. It was recognised that the mine geometry was too intricate to be represented in a 200x200x200 m grid. Calibration on the 200 m grid model was performed to a level at which the groundwater contours only vaguely represented the conceptual model. Subsequently, the initial coarse grid was used to obtain some broad material values, which could be used as starting values in the more complex computationally intensive 50x50x50 m grid model.

Much of the initial calibration was undertaken on models with low complexity, and the results used to construct and run more complex models, which better

represented the Rosebery catchment regime. Hence, the complexity of the model increased throughout the calibration process. Calibration of the simplest models (i.e. those involving too few parameters) could not provide an adequate solution, only broadly representing the conceptual model. This, along with the variation observed in the rock mass (Section 3.3), provided the justification for increasing the number of parameters to best provide a realistic solution whilst always applying parsimony to the issue of complexity.

The final model (Appendix Eleven) took around eight minutes for a forward run using a standard personal computer (AMD Athlon™ XP 2100+, 523,764 KB RAM). Thousands of trial and error calibrations were run, with the error continually being lowered until an adequate solution was found. For the present study an adequate calibration solution was defined as a solution which best represented: (i) the field observations made; and (ii) the data available on the Rosebery groundwater system.

In accordance with (Middlemis, 2000), water balance error was required to be below 1%. Residual head error at this early modelling stage was considered of less importance than general flow patterns, due to the potentially large errors involved in observed heads (Section 3.2) within the Rosebery catchment. An adequate solution was required to incorporate the Rosebery mine and its influence on the system. The complex nature of the groundwater system, and the significant number of material properties required to achieve an adequate solution, made this extremely laborious.

Justification for the calibration decisions made throughout the modelling process, include both qualitative and quantitative measures. Appendix Five provides an example of the modelling diary kept during this exercise, although not all diaries were digital, thus not all are provided in the appendix.

6.8.2 Qualitative measures of calibration

The initial evaluation of a model involved a number of qualitative assessments that indicate how well the model reproduces the system. Providing that a model was run successfully, the graphical interface of GMS provided a visual solution based on the model inputs. This visual output was compared to the observations and conceptual model of the system. Where the visual output did not match the anticipated solution, the conceptual model or the input was questioned.

The definition of an acceptable match in the case of qualitative evaluation of calibration is when the groundwater contours of the model best replicated those that would be expected of the field observations and conceptual model. The 3D visualisation capabilities of the GMS GUI enabled a comprehensive graphical review of model results (e.g. Appendices Ten and Eleven) and the qualitative measures of calibration provided the basis for much of the calibration effort.

In the case of calibration of the Rosebery model, it was usually the input (material hydraulic conductivities) rather than the conceptual model that was questioned and subsequently adjusted. Ongoing questioning of the conceptual model did, however, aid in the calibration decision-making process, ultimately resulting in a model that better represented the system.

6.8.2.1 Patterns of groundwater flow

The pattern of groundwater flow was the most visible of the qualitative measures. Using the contouring capabilities of the GMS GUI, the hydraulic head and resultant flow directions of the system could be displayed over the MODFLOW grid. Figure 6.8 shows the typical GMS graphical output used to evaluate patterns of groundwater flow represented by contours of the active hydraulic head dataset. Chapter 3 outlines the field observations and monitoring which helped to define the conceptual model for the catchments.

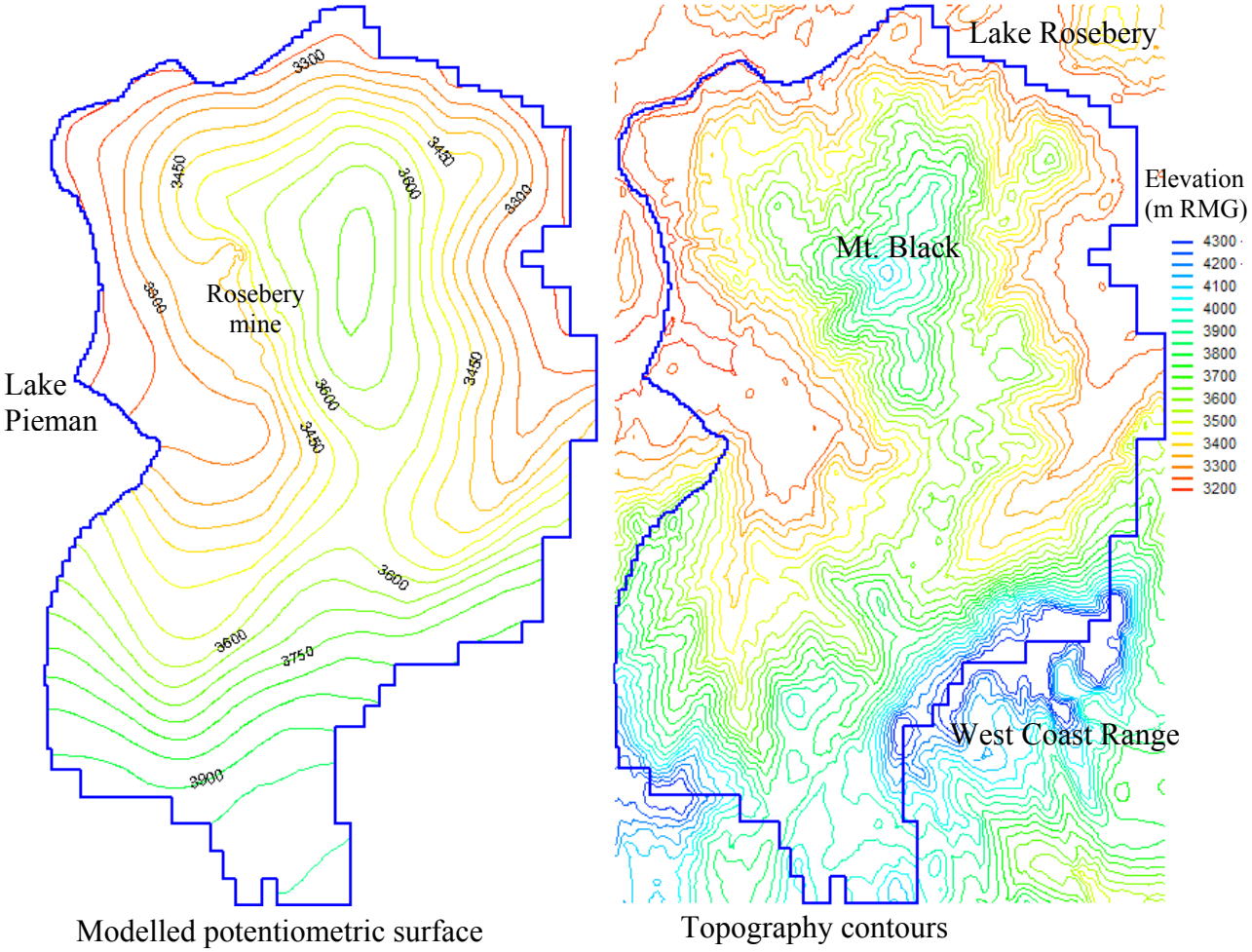

Figure 6.8 Topography and modelled potentiometric surface (m RMG) using the example of Layer 30 of the operation model. Note Layer 30 is modelled as isotropic in individual cells so modelled flow is truly perpendicular to the groundwater contours: (i) the general flow north off the West Coast Range; (ii) the radial flow from Mount Black; (iii) the influence of the Rosebery mine; and (iv) flow into Lake Pieman and Lake Rosebery

The conceptual model required that the groundwater regime of the study area was typified by a topographically controlled water table with the ultimate discharge occurring into low lying lakes and rivers (Chapter Five). A successfully calibrated model should produce a groundwater flow pattern that displays this, with the water table contours reflecting topography contours in a subdued fashion (Figure 6.8). The groundwater flow was essentially from the groundwater divides and topographic highs, towards the topographic lows and discharge features such as rivers and lakes.

6.8.2.2 Patterns of aquifer response

The pattern of aquifer response refers to how the aquifer responds to hydrological features. In this case it refers to not only the natural hydrological features, but also to anthropogenic features such as the mine workings and the drillhole network.

Assigning high hydraulic conductivity values to the mine workings and the drillhole network (Table 6.2), in combination with drains and wells to represent mine pumping and discharge, resulted in a realistic drainage pattern around the Rosebery mine (Figure 6.8). Cells containing drilling holes were successfully simulated as conduits, and the mine workings were simulated as behaving as the major anthropogenic sink within the catchment.

The numerous small ephemeral creeks over the study area were observed to act as both sources and sinks depending upon their altitude, flow rate, and the season. Only those that were considered to have a significant volumetric influence were represented within the model domain (Figure 6.7).

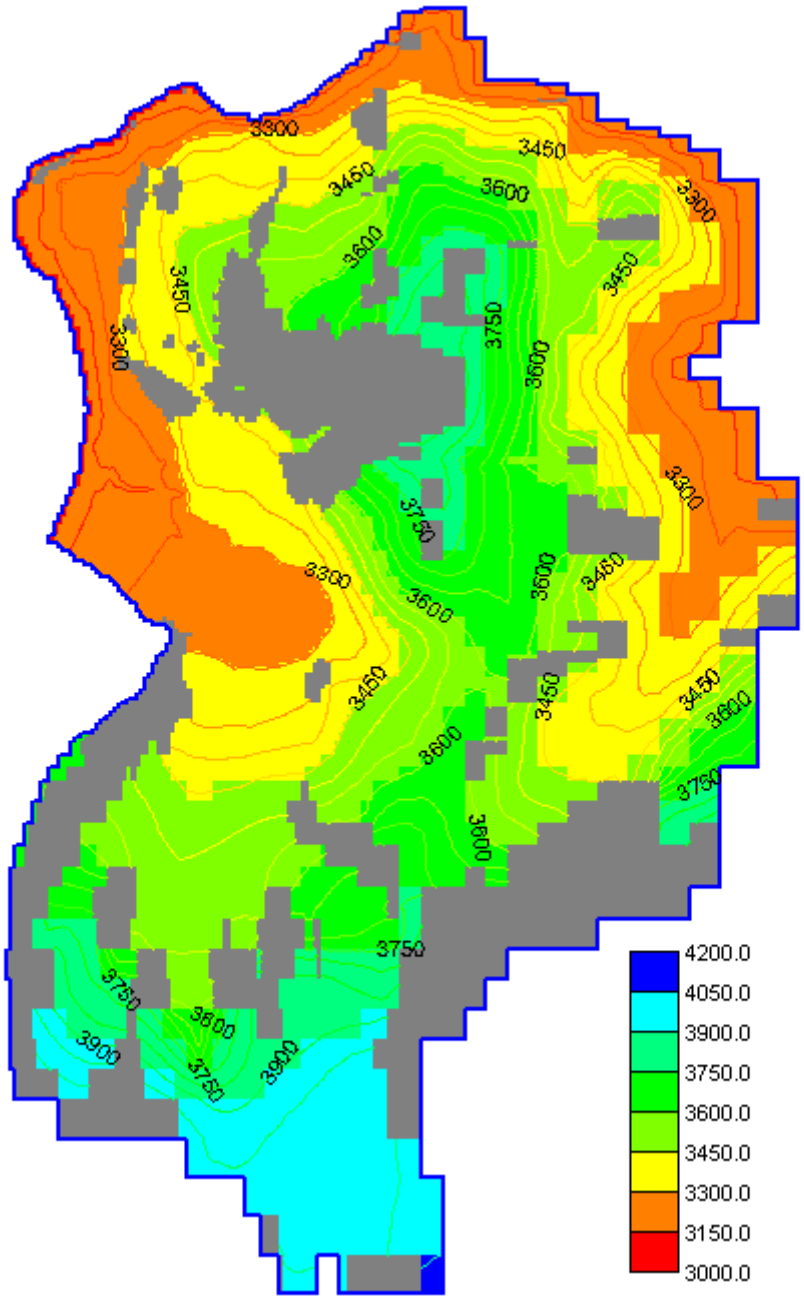

Figure 6.9 Layer 1 simulated heads. Note the dry cells (grey) in areas of high elevation representing water table depths of greater than 50 m. Head elevation displayed in Rosebery Mine Grid metres as both simulated head contours and simulated head elevation for individual cells.

6.8.2.3 Dry cells

The design of the grid to surface, with layers one and two having a uniform thickness of 50 m each, resulted in a significant number of dry cells within these layers. In the present study, this was neither problematic, nor erroneous. Unsaturated geology was modelled within the grid, however, if a cell finished as dry after the

model run it was excluded from the MODFLOW simulation (Figure 6.9; and Figure 6.10). Appropriately, MODFLOW excludes cells where the head is below the bottom elevation of the cell; partial saturation of a cell results in it being included in the model.

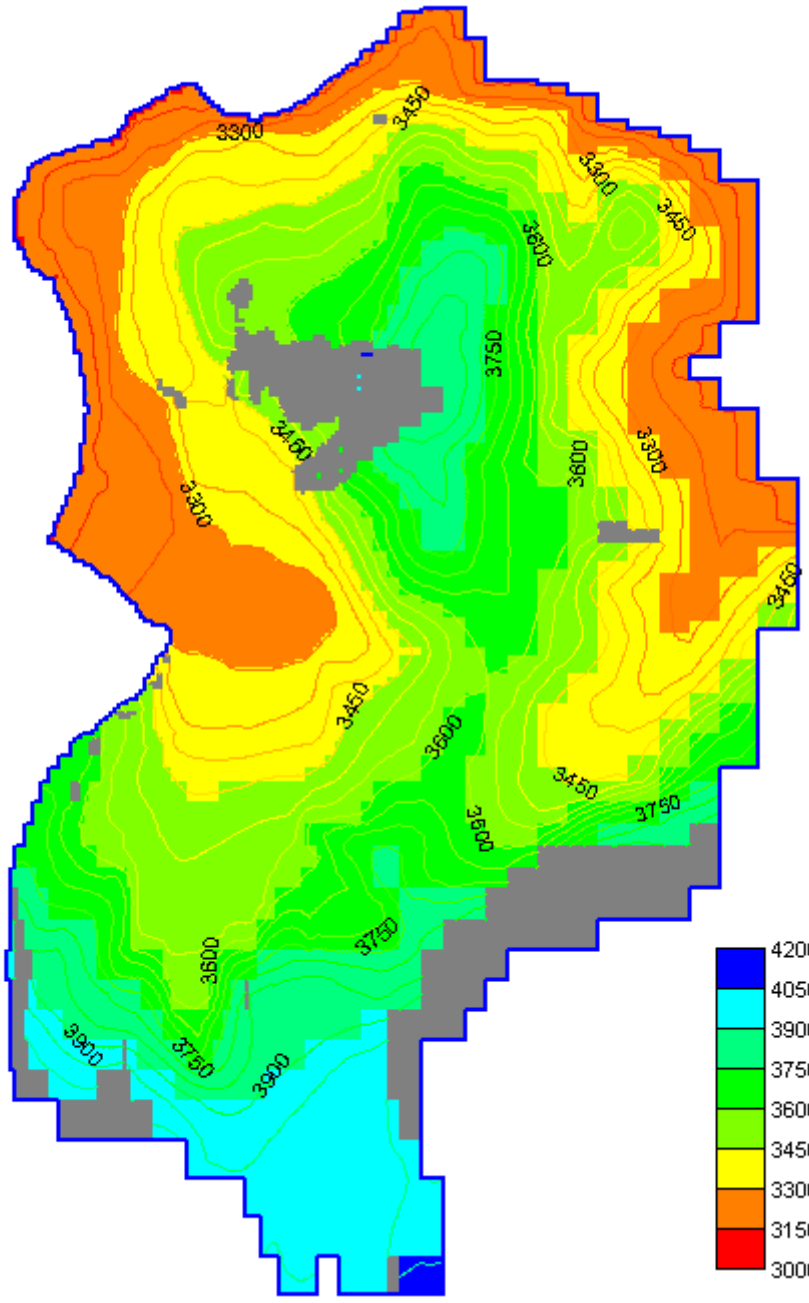

Figure 6.10 Layer 2 simulated heads. Note the dry cells (grey) in areas of high elevation representing water table depths of greater than 100 m. Head elevation displayed in Rosebery Mine Grid metres as both simulated head contours and simulated head elevation for individual cells.

This was more apparent in areas of dramatic changes in relief and in areas of high altitude. As discussed in Section 6.7.6.6, the water table in areas where the topography was > 1000 m above sea level (c. 4050 mRMG) would be expected to be greater than 100 m below the surface. Thus, in a well calibrated model, both layers 1 and 2 (Figure 6.9, Figure 6.10), and due to thinned layers (Section 6.6.7.5), potentially many down to layer 21 would be dry.

6.8.3 Quantitative measures of calibration

Quantitative measures of calibration are divided into two groups: (i) statistical; and (ii) graphical. Statistical measures include the differences between modelled and measured head data or system flow components. Graphical comparisons provide a quantitative measure of calibration by providing a plot of measured versus simulated aquifer heads.

6.8.3.1 Model water balance

The total model water balance error is calculated and provided in the output file after the forward model run and convergence is complete. The output for the operational model is presented in Figure 6.1. For the final model (Appendix Eleven) a total water balance error of 0.04% was achieved indicating that the model was well calibrated for flow components, and within the 1% proposed by Middlemis (2000).

	Cumulative volume in (m^3)	Cumulative volume out (m^3)	Cumulative volume in-out (m^3)
Storage	0	0	
Constant head	0	91974.02	
Wells	0	3943.5	
Drains	0	857.1099	
River leakage	2201.606	101656.1	
Head dependent bounds	9884.897	55066.71	
Recharge	241297.2	0	
Total	253383.7	253497.5	
			-113.797
Percent Discrepancy			-0.04

Table 6.3 Volumetric budget for entire operational model at the end of the time step (1 day)

6.8.3.2 Iteration convergence criterion

Iteration convergence criterion should be two (Anderson and Woesnner, 1992), or one to two (Middlemis, 2000) orders of magnitude smaller than the level of accuracy desired in the model head results. Iteration convergence criterion is commonly set in the order of millimetres or centimetres (Middlemis, 2000). The desired head accuracy within the Rosebery catchment model was on the 10 m scale (10 - 100 m) so a 0.1 m convergence criterion was justified. However, in fact 0.01 m was achieved.

Initially the convergence criteria was relaxed to as high as 1 m. This enabled convergence during the set-up stages of the model; once models were refined it was able to be reset at the GMS default of 0.01 m. The final models were run with the setting for iteration convergence at 0.01 m. At still lower values the model convergence became problematic and at higher values the accuracy of model convergence was questionable.

6.8.3.3 Observations and simulated heads

A standard observation coverage was created from the observed head values (Section 3.2). In addition, the starting head values (Section 6.7.6.6) were also used as a "complementary „observation' coverage". Unlike the limited standard observation (actual observations in the field), the complementary observation coverage (theoretical observations) provided an idealised calibration target covering the entire catchment. The quality of the model is measured using the differences between modelled heads and these two observation coverages; i.e., these differences are presented for both the actual and theoretical observation coverages. The operational model simulation was compared against the observations (Table 6.4).

Three statistical measures of the difference between measured (observed) and simulated were produced by the observation process within GMS: (i) mean error (ME); (ii) mean absolute error (MAE); and (iii) root mean squared (RMS) error. The mean error (ME) is the mean difference between measured heads (h_m) and simulated heads (h_s) (Anderson and Woessner, 1992).

$$ME = 1/n \sum_{i=1}^{n} (h_m - h_s)_i \tag{6.2}$$

The mean absolute error (MAE) is the mean of the absolute value of the differences in measured and simulated heads (*ibid*.).

$$MAE = 1/n \sum_{i=1}^{n} \left| (h_m - h_s)_i \right| \tag{6.3}$$

The root mean squared (RMS) error is the average of the squared differences in measured and simulated heads (*ibid*.).

$$RMS = \left[1/n \sum_{i=1}^{n} (h_m - h_s)_i^{\,2} \right]^{0.5} \tag{6.4}$$

	Observed heads (m)	Starting heads (m)
Mean error	64.295	12.593
Mean absolute error	65.89	15.526
Root mean squared error	83.879	37.153

Table 6.4 Error in simulations of observed heads and starting heads in the operational model

Table 6.4 shows the mean errors for both the observed heads and starting heads observation coverages for the final model. The large error in head was considered acceptable in the model at Rosebery due to: (i) the associated potential error of head observations throughout the catchment; (ii) the extremely large (2200 m) model extent of the model in the Z direction; (iii) the fact that calibrating the system for flows took precedence over precision in heads; (iv) the desired accuracy of heads was within the 10 to 100 m range; and (v) the general lack of coverage of *in-situ* hydraulic

property measurements and observations throughout the catchment. Modelling in such regimes as the Rosebery catchment, thus, differs significantly from modelling in other areas throughout Australia, such as the Murray Darling Basin, where desired accuracy is commonly in the 1 m range (Middlemis, 2000).

Four graphical measures of the difference between observed and measured heads were produced by the observation process within GMS: (i) simulated heads versus observed heads (Figure 6.11; and Figure 6.15); (ii) simulated heads versus observed heads (weighted) (Figure 6.12; and Figure 6.16); (iii) residual versus observed (Figure 6.13; and Figure 6.17); and (iv) residuals versus observed weighted (Figure 6.14; and Figure 6.18). Such plots were used throughout the calibration process. Progressive calibrations were plotted and compared with the aim of narrowing the residual between the observed heads and simulated heads.

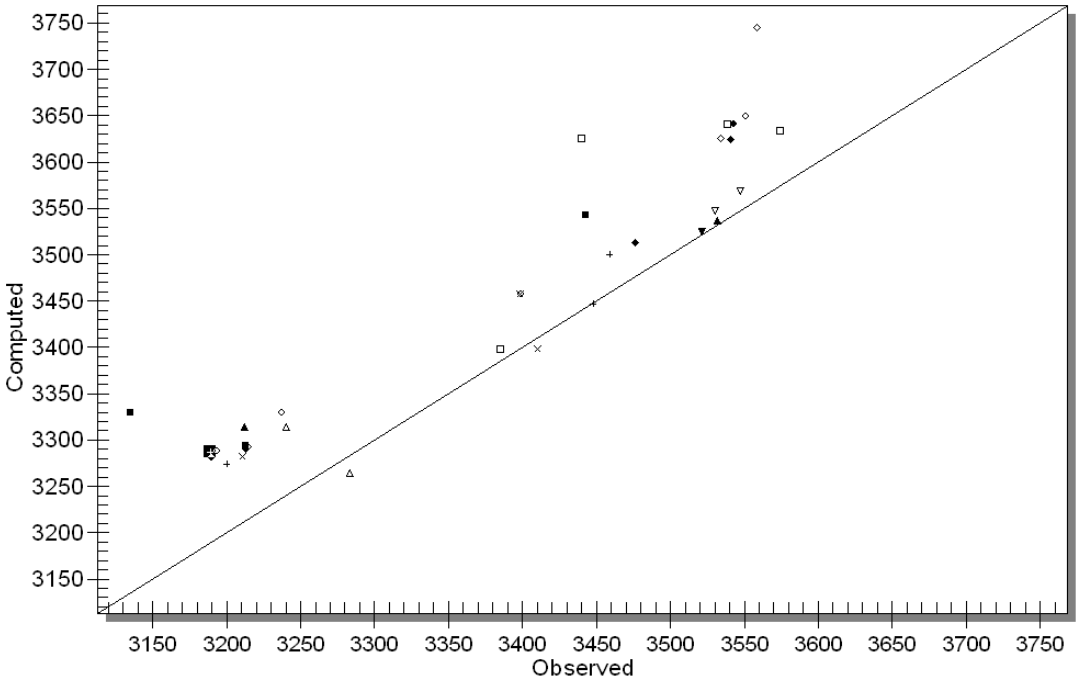

Figure 6.11 Simulated heads versus observed heads

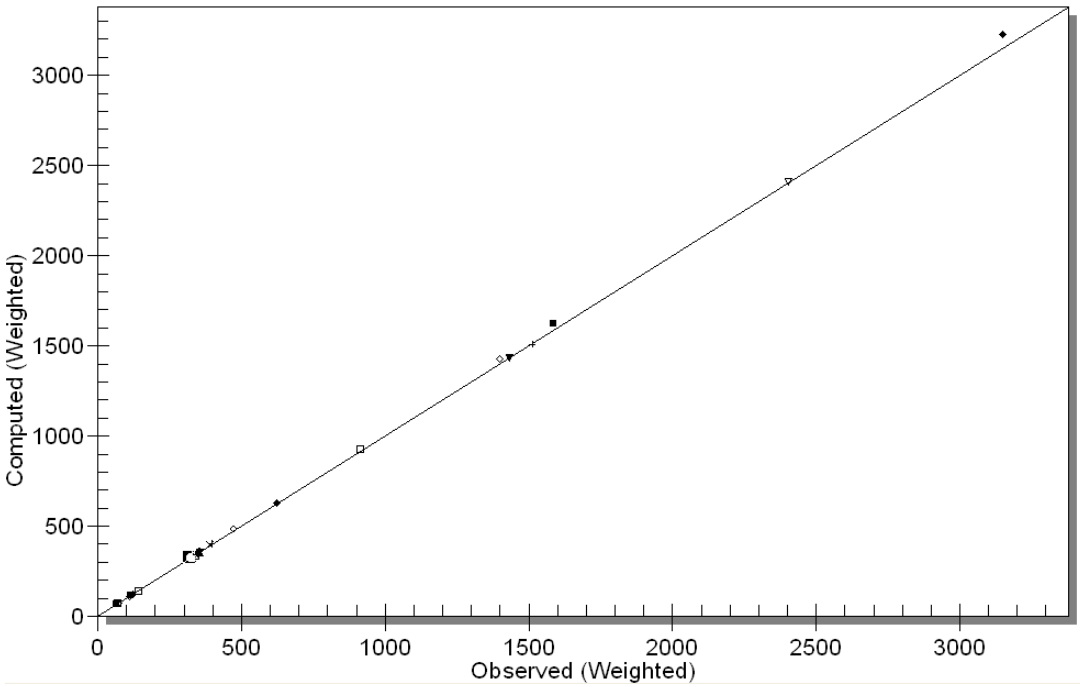

Figure 6.12 Simulated heads versus observed heads (weighted)

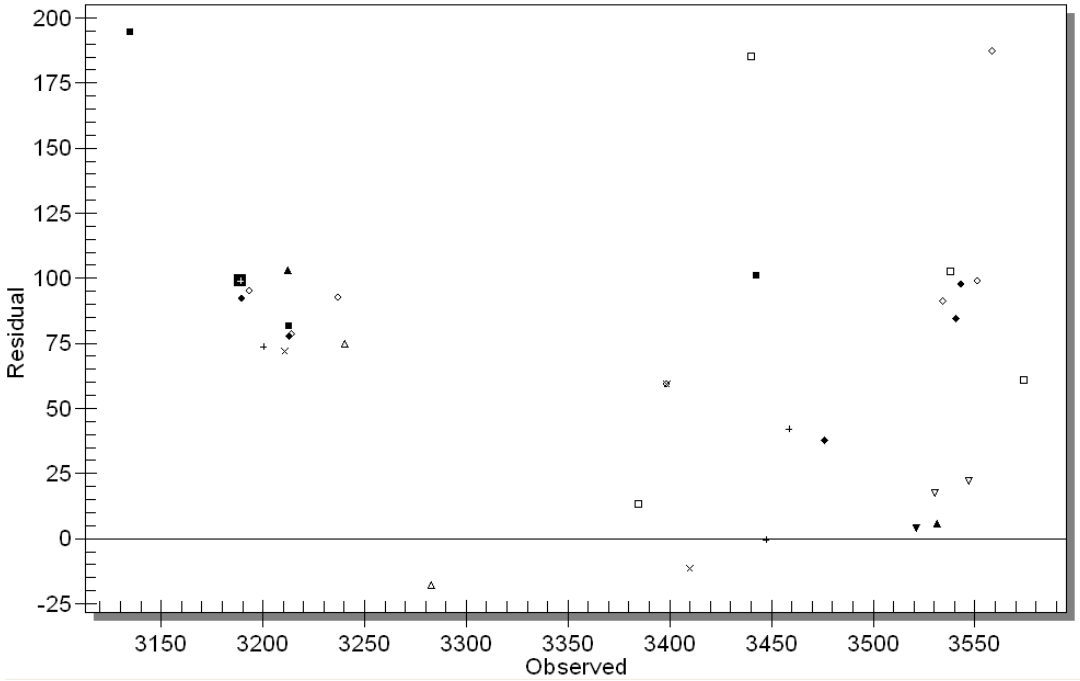

Figure 6.13 Residual versus observed heads (m)

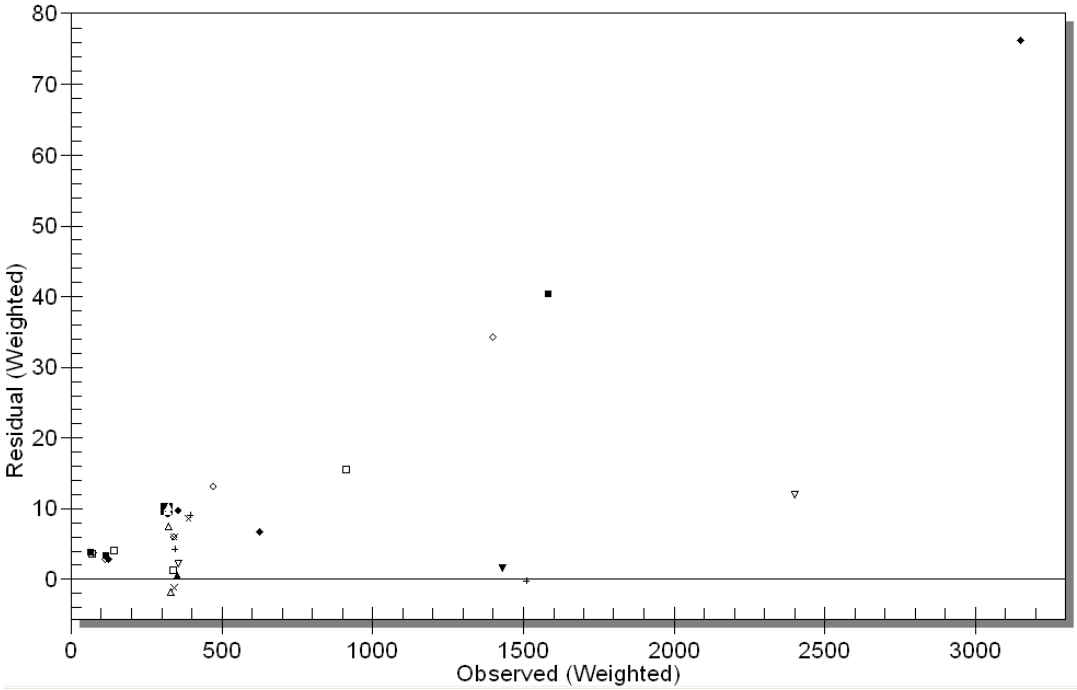

Figure 6.14 Residual versus observed heads (m) weighted

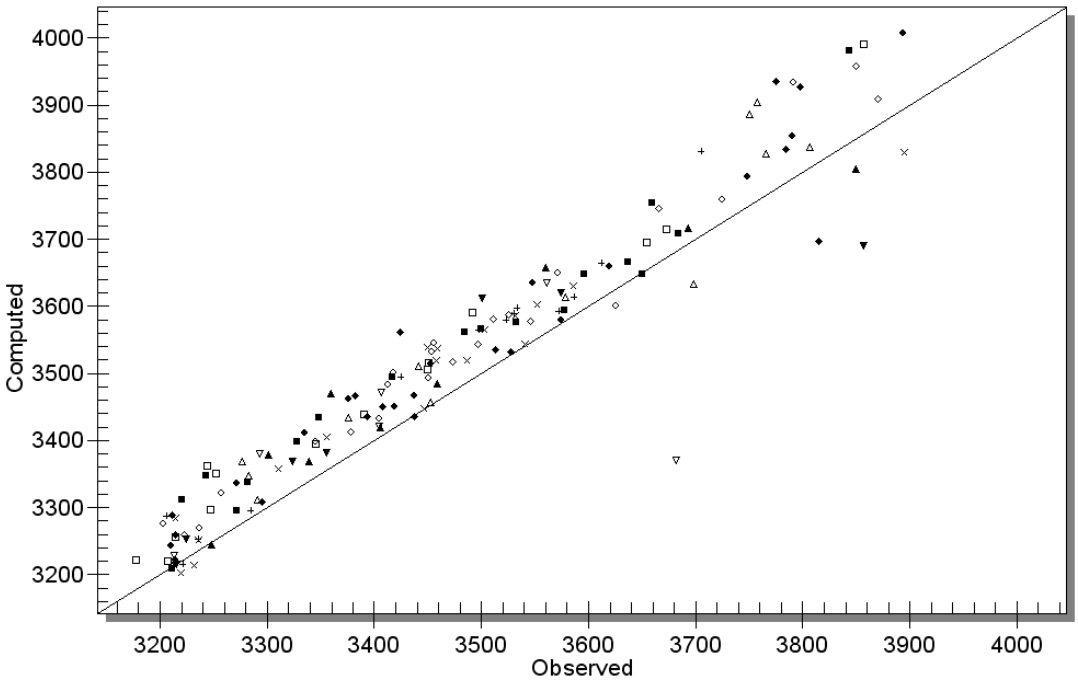

Figure 6.15 Simulated heads versus starting heads

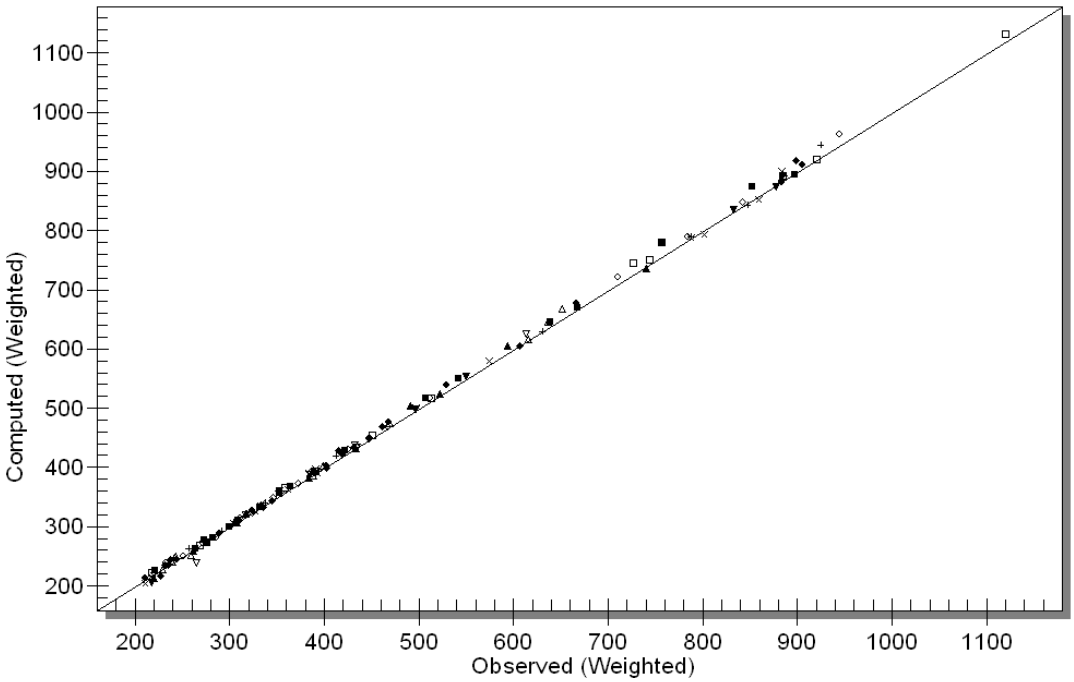

Figure 6.16 Simulated versus starting heads (weighted)

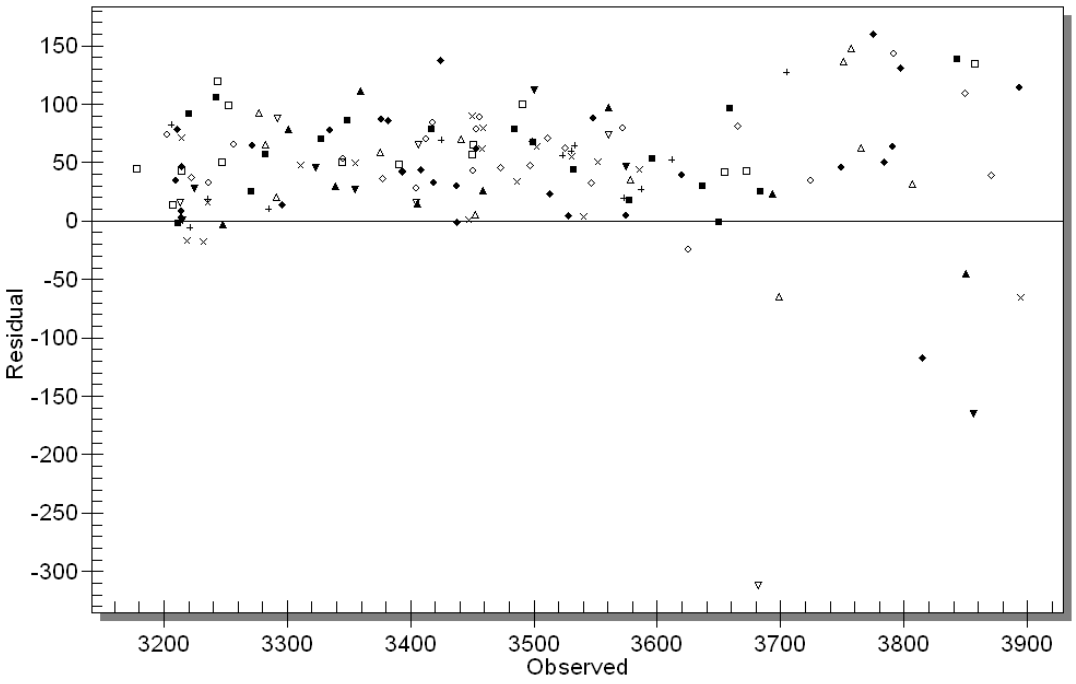

Figure 6.17 Residual versus starting heads (m)

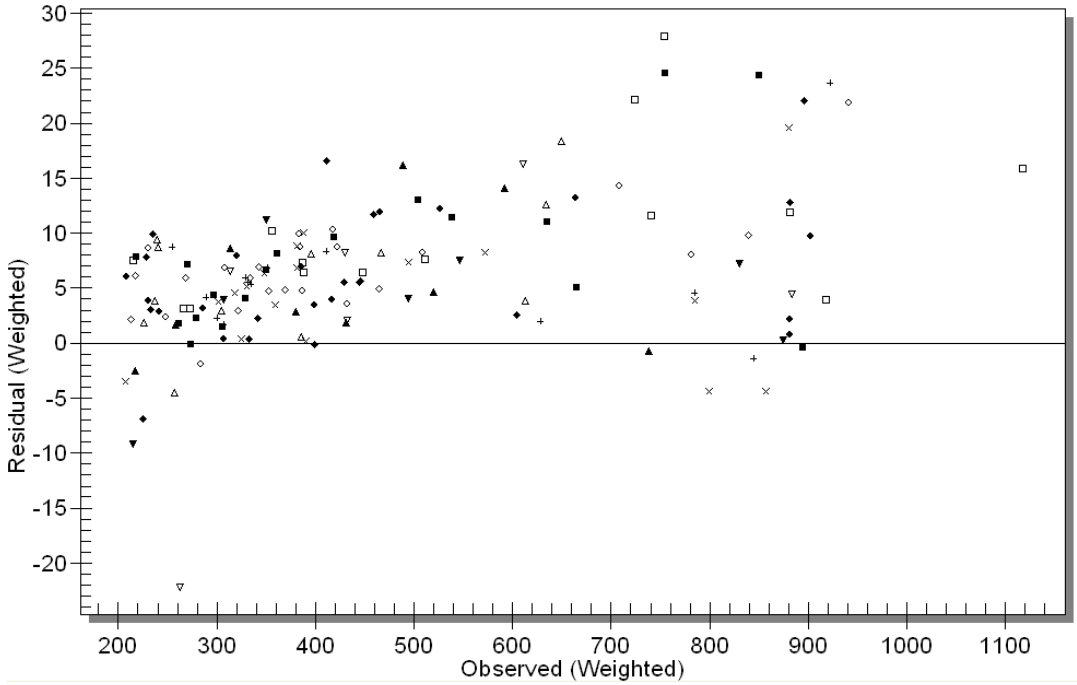

Figure 6.18 Residual versus starting heads (m) (weighted)

The weighting of the actual observation was related to observed variation in piezometers or a conceivable estimated variation where data was poor. Weighting in the theoretical dataset was based on an arbitrary estimated variation based upon the elevation (mAHD) divided by 50; i.e., an elevation of 500 m would have a theoretical groundwater elevation of 450 mAHD with a standard deviation of 10 m for weighting calculations.

Figure 6.11 to Figure 6.18 show that the simulation generally over-estimates head, however, the over-estimate was generally within the desired accuracy range of 10 to 100 m. Further calibration based on an increased longer term field-based dataset is justified but was considered beyond the scope of the present study. The simulation of heads that were generally too high, was problematic within the Rosebery catchment model, where it results in flooded cells at the surface level, however, this is consistent with wet, mountainous climate that experience frequent high volume recharge events. Within the Rosebery catchment model, flooded cells were especially associated with steep sided valleys. Such ‚errors' may be accounted

for by the presence of springs and seeps which were not always observable in the wet densely vegetated region.

Attempting to remove such flooding in cells through parameter adjustment often resulted in significant problems with model convergence. Using the starting heads algorithm (Section 6.7.6.6) results in no seeps being represented until the model theoretically reaches sea level, which was not the case within the Rosebery catchment. Seeps were observed throughout the catchment, however, due to the wet nature of the area, including them in the observation coverage as ‚zero depth to water values' was considered unwarranted. In hindsight, the inclusion of seeps in the observation dataset probably would have accounted for much of the over-prediction of head values with the model.

Further site investigation is needed to assess whether these predicted flooded cell regions correspond to actual locations of seeps or areas that would result in artesian conditions if they were drilled, as observed in many areas in the field (Chapter Three). Due to the widespread dense vegetation within the Rosebery catchment, such seepage faces cannot be easily observed from aerial photographs or remote sensing tools.

6.8.3.4 Mine pumping to wells

Each of the 2629 cells representing a mine void was pumped at the rate of -1.5 m^3/day to simulate the mine pumping rate of 3943.5 m^3/day (45.6 L/s). This correlates well to the observed average total mine pumping rate of 60 L/s (Hale, 2001) minus an estimated 12.5 L/s of water usage within the mine. For the post-pumping prediction simulation the wells were given a zero flow rate, and the theoretical discharge level was still modelled as a drain.

6.8.3.5 MIFIM to 8 level drains

The application of MIFIM coupled with MODFLOW was utilised by Banks et al. (2002). A similar approach was used in the present study. In the Rosebery catchment model, 8 level of the Rosebery mine was assigned as a drain at an elevation of 3225 mRMG. The conductance of the drain was assigned as 0.01 (m^2/d)/m. The MIFIM model presented in Chapter Five provided the justification for a discharge at 8 level. Seepage and runoff from the mine areas were taken into account with the use of the 8 level drain. The drains contributed to 9.9 L/s and 10 L/s of the water balance operational and predictive modelling scenarios, respectively.

6.8.3.6 Stream hydrograph to Stitt River

The lower sections in glacial sediments were given a conductivity of 0.05 (m^2/d)/m and upper sections and tributaries 0.01 (m^2/d)/m during initial manual calibration models. A PEST determined parameter value of 0.111 (m^2/d)/m was used in the final scenarios. The contribution of the Stitt River can be assessed through the head dependent bounds values in the volumetric budget (Table 6.3). As inputs from head dependent bounds were used to model the inputs from stream flow as well as outputs from baseflow, there was no direct correlation between this figure and the baseflow figure. This value, however, should fall between the total head dependent outputs and the difference between the inputs and outputs; these were 16.5 and 20.1 Mm^3/year in the Rosebery catchment operational simulation. The predetermined baseflow value of 18.3 Mm^3/year (Chapter Five) correlates well with these simulated data.

6.8.3.7 Rivers

The 0.2785 (m^2/d)/m PEST determined parameter for river conductance resulted in a model input of 0.8 Mm^3/year, and an output of 37.1 Mm^3/year for the remainder of the streams modelled within the Rosebery catchment.

6.8.3.8 Model parameters

Figure 6.19 and Table 6.5 display the estimated hydraulic conductivity values for the Rosebery catchment. Where applicable, parameters were created for each rock type to each of the nine depth classifications: (i) regolith; (ii) weathered; (iii) bedrock; (iv) depth; (v) depth 2; (vi) depth 3; (vii) depth 4; (iix) depth 5; and (ix) depth 6.

Due to the lack of detailed three dimensional geological interpretation to the west of the Rosebery mine (Pasminco Exploration et al., 2002), the Owen Group, Western Volcano-Sedimentary Sequence and the Tyndall Group were lumped for hydrogeological modelling at depth. The Sterling Valley Formation was not modelled at elevations less than 2950 m (RMG) due to lack of information. The Henty Fault Zone was modelled with the same parameters as other faults in the regolith and weathered layer, however, in bedrock, it was modelled as a separate parameter.

The predictive performance of the model depended upon how closely these automated porous flow parameter values reflected the equivalent fracture flow in the actual Rosebery catchment. The decrease with depth in modelled hydraulic conductivity values (Table 6.5 and Figure 6.19) corresponded to the range of published values for crystalline fractured rock aquifers elsewhere (e.g. Freeze and Cherry; 1979; Neuzil, 1986; Cripps et al., 1988; Pohll et al., 1999; Singal and Gupta, 1999; and Fitts, 2002), as well as the few local hydraulic properties calculated in the present study (Table 3.2). Further validation of the models performance is recommended.

	Depth (m) or elevation m (RMG)	Cleveland Waratah Association	Faults	Glacials	Henty Fault zone	Hercules Pumice Formation	Kershaw Pumice Formation	Mount Black Formation
Regolith	0-50 m deep	3.32E-01	3.41E-02	2.58E+00		3.04E+00	4.80E-01	2.64E-02
Weathered	50-100 m deep	1.10E-01	2.19E-01			4.13E-01	1.83E-01	2.36E-02
Bedrock	100 m deep-3200 mRMG	N/A	1.08E-01		3.87E-02	8.95E-03	9.34E-02	1.85E-02
Depth	3200 – 2950 mRMG	4.71E-03	6.38E-03		7.45E-02	1.63E-02	3.36E-02	6.06E-03
Depth 2	2950 – 2700 mRMG	4.12E-03	8.59E-03		1.43E-02	5.26E-03	2.35E-03	3.48E-03
Depth 3	2700 – 2450 mRMG	1.73E-04	4.07E-04		6.73E-04	9.14E-04	3.29E-04	6.75E-04
Depth 4	2450 – 2200 mRMG	1.05E-04	9.52E-05		4.78E-04	1.57E-04	1.06E-04	1.06E-04
Depth 5	2200 – 1950 mRMG	2.57E-05	1.33E-04		3.45E-05	1.08E-04	2.28E-04	1.56E-04
Depth 6	1950 – 1700 mRMG	1.02E-05	4.64E-05		2.80E-05	2.61E-05	2.48E-05	1.09E-05

	Depth (m) or elevation m (RMG)	Sterling Valley Formation	Owen Group	Tyndall Group	Tailings	Thinned regolith	Western volcano-sedimentary sequence
Regolith	0-50 m deep	6.03E-02	4.44E-01	3.67E-02	1.44E+01	1.15E-01	9.35E-02
Weathered	50-100 m deep	3.63E-01	9.89E-02	7.41E-01			1.66E+01
Bedrock	100 m deep 3200 m (RMG)	1.64E-02	2.98E-02				
Depth	3200 – 2950 m (RMG)	4.83E-02	1.20E-02				
Depth 2	2950 – 2700 m (RMG)		8.15E-03				
Depth 3	2700 – 2450 m (RMG)		3.12E-03				
Depth 4	2450 – 2200 m (RMG)		6.48E-04				
Depth 5	2200 – 1950 m (RMG)		1.24E-04				
Depth 6	1950 – 1700 m (RMG)		2.01E-04				

Table 6.5 Model calibrated hydraulic conductivity values for the Rosebery catchment (m/day)

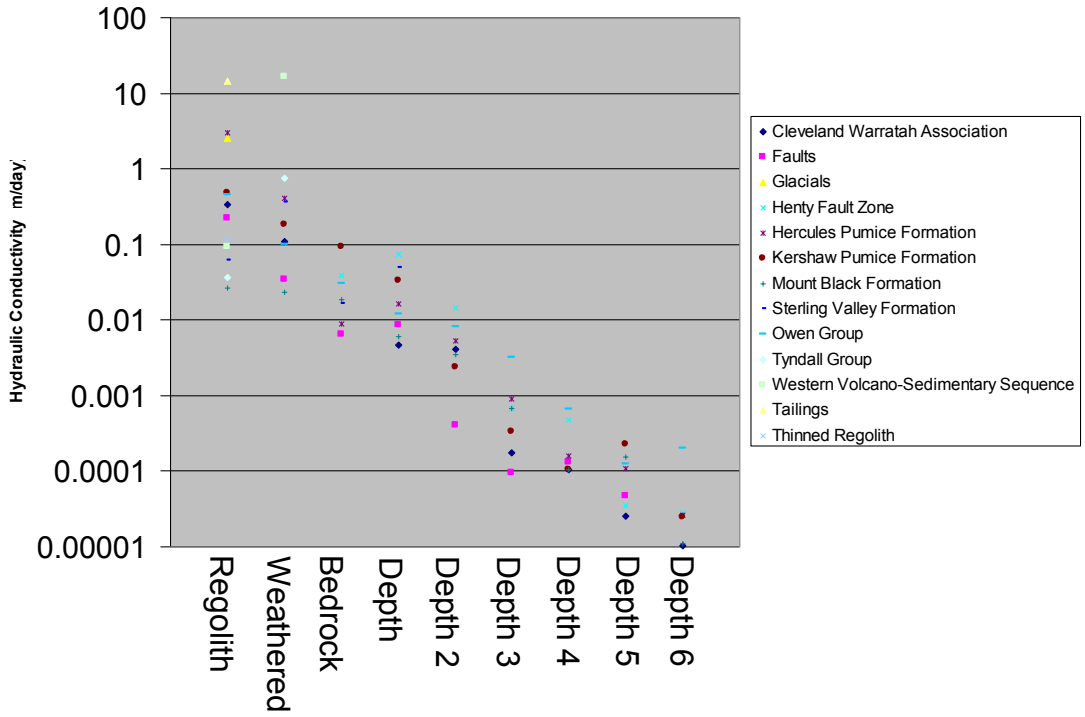

Figure 6.19 Model calibrated hydraulic conductivity values for the Rosebery catchment (m/day)

The aquifer is modelled as isotropic at depths greater than 100 m. In layers 1 and 2 the rock types were given a single vertical anisotropic value. The value for the bulk vertical anisotropy (Kh/Kv) was then calibrated to be 0.52 using the parameter estimation process. Application of this near surface vertical anisotropy value assisted in the subsequent overall calibration of the model.

6.9 Sensitivity Analysis

6.9.1 Is sensitivity analysis feasible in complex groundwater modelling?

Routinely in simple models, once calibration is achieved, individual parameter values are increased and decreased, usually by an order of magnitude either way (Middlemis, 2000), to determine how much each parameter influences output results. This sensitivity analysis defines the range of possible model outputs across a reasonable range of inputs. This approach has a number of problems, including: (i) analysing the number of parameters and possible outcomes is laborious and; (ii) the

validity of model runs is questionable once calibration conditions are breached by the alteration of parameter values.

To perform a valid sensitivity analysis of the final model would require more than simply altering each parameter by an order of magnitude. It would also involve the recalibration of every model once each parameter was changed. By changing any parameter, the calibrated model is no longer calibrated, so that any run is assessed against a model which no longer balances and which may contain a larger RMS error. Recalibrating will not give a solution with more validity and only highlights the problem of non-uniqueness. Middlemis (2000) refers to this problem, stating "a full sensitivity analysis is an unreasonable expectation when there are too many model parameters" and also, to paraphrase, that for a high complexity calibrated model, sensitivity analysis is best used by ranking parameters in order of their influence, and only testing the model sensitivity relative to the most influential parameters.

In reality, the entire manual calibration process was a type of sensitivity analysis, in terms of iteratively modifying the model as it was built to produce the most satisfactory conclusion. Where sensitivity analysis was valuable was in using the automated sensitivity package SENS that was incorporated into the GMS GUI for MODFLOW.

6.9.2 Sensitivity process (SENS)

Hill et al. (2000) defined the sensitivity calculation process as a function that determines the sensitivity of hydraulic heads throughout the model with respect to specified parameters using the accurate sensitivity-equation method. These values are called grid sensitivities (*ibid*.). The observation process uses the grid sensitivities to calculate sensitivities for the simulated values associated with the observations, producing observation sensitivities (*ibid*.). Observation sensitivities can be used to: (i)

diagnose inadequate data; (ii) identify potential additional parameters; and (iii) to evaluate the usefulness of proposed new data (*ibid*.).

The MODFLOW "Sensitivity Process" provided ongoing input on sensitivities throughout modelling. In addition, the manual sensitivity analysis undertaken within the extensive manual calibration provided justifications for the calibration decisions during the evolution of the model. Due to the number of parameters, performing a true manual sensitivity analysis on the calibrated final model was impractical, being too laborious for the purposes of the present study, and of little value at this early stage of the modelling effort. For example, to undertake a sensitivity analysis on hydraulic conductivity alone, would involving running the model an additional 142 times, presenting the model results and analysing the differences between these model runs. The same process can be investigated through the use the SENS package.

Table 6.6 presents the result for hydraulic conductivity parameter sensitivity values for the final model. Higher numbers correspond to parameters that have a high influence on the model result; they do not necessarily correspond to less accurate or reliable parameters. Hill et al. (2000) described how the observation sensitivities "can be scaled to obtain measures of such things as: (i) the relative importance of different observations to the estimation of the same parameters; (ii) the relative importance of an observation to the estimation of different parameters; and (iii) the total amount of information provided by the observations for estimating each parameter".

Using the automated technique (Table 6.6; and Table 6.1) the parameters that were found to be most sensitive towards heads were the hydraulic conductivity of: (i) the weathered Mount Black Formation; (ii) the weathered Western Volcano-Sedimentary Sequence; and (iii) the Henty Fault Zone between 2950 to 2700 m (RMG). The weathered Western Volcano-sedimentary sequence also produced the

most anomalous hydraulic conductivity through the use of PEST (Figure 6.19 and Table 6.5). This focussed the attention of manual calibration efforts upon the units mentioned above, and obtaining better physical estimates should be the focus of future field investigation.

	Cleveland Waratah Association	Faults	Glacials	Henty Fault zone	Hercules Pumice Formation	Kershaw Pumice Formation	Mount Black Formation
Regolith	0.58	4.94	1.89		12.44	6.75	6.70
Weathered	8.54	4.60			7.73	10.74	31.91
Bedrock	N/A	10.4		2.94	13.67	8.02	6.49
Depth	3.32	5.39		10.46	13.23	4.52	5.06
Depth 2	5.19	6.14		25.23	9.92	4.96	1.95
Depth 3	4.80	6.98		2.16	10.22	2.77	4.55
Depth 4	3.58	1.90		6.11	10.02	6.79	5.60
Depth 5	3.14	6.64		5.21	8.41	3.81	4.54
Depth 6	5.73	5.26		2.85	2.02	2.95	3.51

	Sterling Valley Formation	Owen Group	Tyndall Group	Tailings	Thinned regolith	Western volcano-sedimentary sequence
Regolith	3.39	3.46	1.35	10.90	8.30	5.54
Weathered	4.95	3.87	2.61			23.44
Bedrock	3.14	7.16				
Depth	5.87	1.61				
Depth 2		2.81				
Depth 3		6.13				
Depth 4		2.20				
Depth 5		0.39				
Depth 6		9.36				

Table 6.6 Parameter sensitivity values for the Rosebery catchment.

6.10 Limitations and uncertainties

There are limitations and uncertainties in any modelling study in regard to: (i) the hydrogeological understanding; (ii) the conceptual model design; (iii) the model calibration; (iv) prediction simulations; and (v) recharge and evapotranspiration estimation and simulation (Middlemis, 2000). Limitations and uncertainties exist at all stages of the modelling effort and this section seeks to address those relevant to the production of the simulation. The solution presented in this model is recognised as an output which has many limitations, contains numerous presumptions, and is not

assumed to be the only „correct and unique' possible representation of the Rosebery catchment groundwater system.

6.10.1 Non-uniqueness

Non-uniqueness refers to the situation in which more than one set of possible inputs can produce nearly identical model outputs (Andersen and Woessner, 1992; and Fetter, 2001). Multiple calibrations of the same groundwater system are possible using different combinations of stresses on the system. Unique solutions cannot be computed when many variables are involved in the calibration approach (Middlemis, 2000). Many combinations of groundwater flow rates and hydraulic conductivities in a model have the same ratio as the actual flow rates and hydraulic conductivities in the aquifer, will produce nearly identical hydraulic head distributions (Ritchey and Rumbaugh, 1996). The apparent matching of measured aquifer heads at a certain date by a „calibrated' model does not necessarily mean that the hydraulic properties used in the model are close to those actually found on site, although obtaining „correct' predictions does depend strongly upon using the correct properties.

To increase the probability of achieving a correct unique solution, the Rosebery model utilises measured groundwater flow rates (stream baseflow and mine pumping rates) as calibration targets. This restricted the water budget to values that were consistent with actual aquifer conditions. To further reduce the likelihood of multiple solutions to the model the input of actual values of the aquifer parameters from large scale test pumping are required. Although this was impractical within the present study, due to lack of infrastructure and funding (Chapter Three), it provides scope and direction for further work within the Rosebery catchment.

6.10.2 Conceptual

The conceptual model contains a number of assumptions including boundary properties, aquifer connectivity as well as inputs and outputs to the system. The conceptual model of groundwater flow largely limits the output of the model through the introduction of highly influential boundaries.

Prior to the present study, no information on the groundwater regime existed, so that the boundaries were assumptions based on the regional topography and standard hydrogeological interpretation. The West Coast Range was the major topographic high of the area and was a typical „no-flow' boundary for modelling purposes. The topographic lows of the Pieman and Rosebery Lakes also fit the criteria for a typical specific head flow model boundary for the lower end of the model.

6.10.3 Modelling approach

There is always a limitation in the extent that any modelling software package can depict a hydrogeologic environment in a hydrogeological model (Middlemis, 2000). The limits in accurate representation are particularly in regards to surface-groundwater interaction (Middlemis, 2000). The decision here to use MODFLOW was largely based on: (i) the surface-groundwater interaction packages it contained; as well as (ii) the widespread application of the software in groundwater research. GMS was initially chosen as a GUI for MODFLOW due to its advanced GIS and hydrogeological database functionality. Although this significantly aided the conceptual model development in the present study, inevitably, much of the data input was manipulated externally and altered in the MODFLOW source files. This placed a large limitation on the present study and would be likely to be the case with other hydrogeological modelling studies in mining environments. Future work could be directed at how the input of mine data would differ if FEFLOW or another finite element based modelling software was employed instead.

The existing approach did not consider modelling the unsaturated zone, nor did it consider important factors such as contaminant transport and dispersion or diffusion. Such considerations in fractured rocks are important, yet extremely complex to model at the catchment scale (Cook, 2003). This limitation is acknowledged, however, further exploration of the problem was considered to be beyond the scope of the present study.

6.10.4 Field scale heterogeneity modelling

The discretisation of the geologic regime into the hydrogeological model on a fifty metre grid inevitably resulted in limitations in representing field scale heterogeneity. It was an assumption, based on other fractured rock studies (e.g., Chen, 1987; Drogue, 1988; Min, 2002; Kulatilake and Panda, 2000; Jackson et al., 2000; and Wellman, 2006), that the Rosebery catchment was large enough that fractured rock and porous media could be modelled using an equivalent porous medium continuum approach.

6.10.5 Model geometry

Large hydraulic conductivity contrasts exist within the model due to the fact that mine voids and drill hole cells border competent rock cells. No „dampening', i.e., a gradual variation of hydraulic conductivity, was applied around these features. Such dampening may improve the model (Waterloo Hydrologic, 2003), and could be tested in future refinements of this model.

The thinned layer and two 50 m „skin' layers representing regolith and the weathered zone should also be reviewed as future models are refined. The 50 m division largely resulted from a computer processing limitation. Thus, refining the grid as computing power increases is a recommendation for future works.

6.10.6 Grid

Due to the nature of the data sources within the present study, the grid was somewhat predetermined (Section 6.7.5). Only one final grid discretisation was presented within the present study. Varying the grid or mesh may provide scope for enhancement of model run times. Futher work may wish to consider automating the grid generation to provide a grid which conforms to the Anderson and Woessner (1992) or Fetter (2001) spacing suggestions.

6.10.7 Time steps

A time step of one day attempts to represent the average heads and flows within the Rosebery catchment. Input data were in a number of scales, over varying length and time spans. The model does not attempt to vary flows over time, even though the seasonal fluctuations were apparent from observations. Transient modelling provides further scope for model validation and further calibration, however, due to the data requirements, was well beyond the scope of the present study. Such data could be obtained through an investment in water level loggers, as well as additional stream flow gauging, rainfall gauges and evapotranspiration measurement stations. A number of years of data, combined with large scale test pumping, would provide an ideal dataset for future work.

6.10.8 Water balance

The limitations of the water balance were that only one water balance scenario was attempted to be represented within the present study. Limitations of that particular water balance were addressed in Chapter Five. No attempt was made to vary the water balance to provide scenarios involving changes in climate. Altering the recharge values would not provide a climate change scenario and would grossly simplify a complex system.

6.10.9 Material hydraulic properties

The most significant limitation in the present study was the lack of a large database of locally measured hydraulic parameters: both (i) hydraulic conductivity measurements (using multiple methods and locations); and (ii) reliable representative hydraulic heads (over a longer period and with more frequent readings, and in more locations throughout the catchment). The installation of piezometers, and measurement of piezometric head and pump testing of the screened aquifers, are the most fundamental activities required for future hydrogeological works within the Rosebery catchment. The monitoring system was a reflection of the lack of historical investment made into such work at Rosebery. Although every attempt was made to substitute for such short-comings, future investment is required. Further correlation of RQD at Rosebery with hydraulic conductivity values using multilevel packer testing would make the parameterisation more powerful, since the RQD database at Rosebery, as in many mining environments, was very comprehensive. The conclusion that follows this is that the amount of near-mine drilling, although extensive, is not adequate to complete detailed flow modelling if hydraulic data is not intentionally obtained. Purpose specific drilling is also required to ensure representative knowledge of the flow field beyond the deposit area and a statistically valid database of hydraulic parameters.

6.10.10 Prediction scenarios

Two scenarios were explored within the scope of the present study: (i) an operational scenario; and (ii) a post-closure predictive scenario. The calibrated operational scenario was used as a predictive post-closure scenario by removing the wells package, thus, simulating a full mine without pumping. The predictive scenario was not considered to be a calibrated model, nor was any attempt made to calibrate

this model. Any further calibration would mean it could not reliably be used as a comparative tool to the operation simulation.

6.11 Economic considerations of modelling

Although it is difficult to gauge or compare the modelling effort of this PhD study to that of commissioning a professional study of a similar scale, should other mining operations approach modelling of this type in a similar manner, it will result in a significant cost. Consultancy rates for hydrogeological modelling within the mining industry are currently A$ 115 – 270 per hour. (Aquaterra, 2005; Cymod, 2005; Liquid Earth, 2005; and Coffey Mining, 2008). While the present study is recognised to be work of a very different nature, even at the lower end of these rates, the modelling effort of the present study would be in the order of millions of dollars.

Many mining operations at the closure stage are unlikely to pursue such studies on the basis of time and cost. These costs however, demonstrate the justification for detailed hydrogeological drilling and testing, which although unavailable in the present study, would remove a significant proportion of uncertainty in hydraulic properties and modelling results, thus streamlining the modelling effort as well as improving the accuracy and reliability of predictions for the impacts of the mining on the environment.

6.12 3D Model Outcomes

Comparisons of both scenarios modelled by the present study indicate that the regional flow regime is not expected to greatly differ from operation to decommissioning. There was a perception previously that the cessation of pumping would greatly alter the flow field. The flow field will differ from the original flow field in the area due to the introduction of artificial conduits. Flow paths from

contaminant point sources, identified through observation (Chapter Three) and geochemistry (Chapter Four), are tracked with the use of particle tracking.

The groundwater flow regime represented by the numerical model was generally only slightly sensitive to the hydraulic conductivities assigned. The groundwater flow regime was essentially driven by: (i) the topography in the mountainous terrain; and (ii) the large recharge in the wet temperate environment. The rate at which groundwater flows within the system was, however, more dependent on the hydraulic properties. A general over-estimation of head values broadly results in the model being poor at prediction in the upper layers (shallow groundwater), however, this should have little effect at depth throughout most of the model.

Rather than a simple sensitivity analysis, the parameters in which there was the least confidence, which have the largest influence on the model outcomes, are documented (Section 6.8.2). The parameters for which there was the most confidence in assigned relative hydraulic conductivities were those of the geology types which contain a significant amount of drilling with RQD measurements.

The parameters for which there was the least confidence within the catchment, were those to the west of the mine, due to the historical drilling strategy in delineating the orebody. Now that the flow regime has been delineated, it is apparent that this area is also significant in that flows from the mine report in a general westerly direction. This provides the justification for future works to focus on this area.

Although confidence in the parameter values to the west of the mine was low, basic manual sensitivity analysis of the parameters shows that to maintain a broadly calibrated solution within the current conceptual model, any reasonable variation of

the parameter values will not significantly alter the location or area of influence west of the mine.

The Rosebery groundwater model should be regarded as a computer model which was designed to best represent the limited conditions observed in the field. Much validation and further field analysis is required before the model can be considered to be an „end product'. The major outcome was the generation of a three-dimensional numerical groundwater flow model, which can be used as a predictive tool to aid monitoring and management of water from the Rosebery mine.

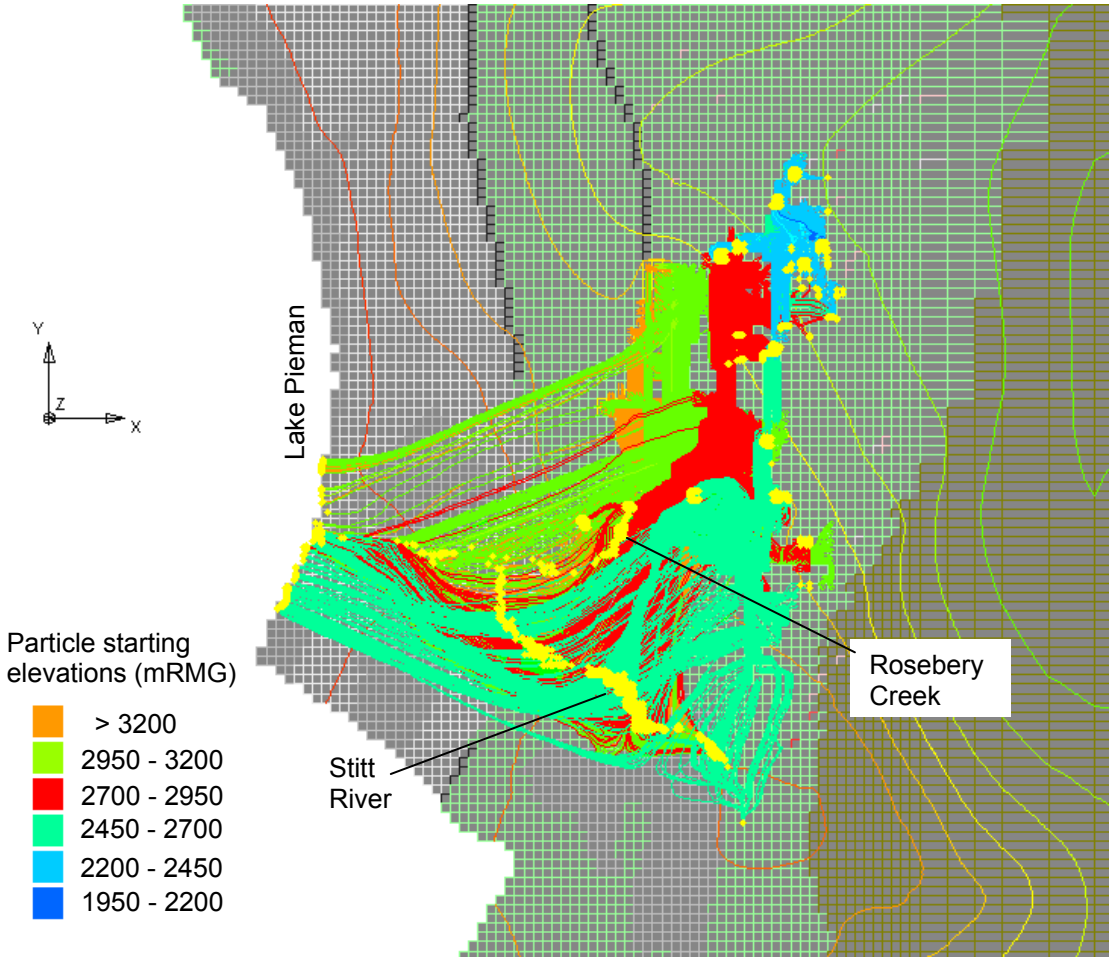

Figure 6.20 MODPATH representation of flow paths and final discharge points (yellow) of particles generated within the Rosebery mine. Contours displays piezometric head elevations, ranging from *c.* 3750 mRMG in the east, to *c.* 3150 mRMG in the west at Lake Pieman.

The most significant immediate finding, from analysis of the Rosebery catchment model, was the definition of an area of influence down gradient from the

Rosebery mine (Figure 6.20). This area is far smaller than initially thought by myself and environmental staff at the Rosebery mine (Staude, pers. comm., 2002b) based on our broad assumptions of topographic-driven flow at the onset of the present study. Figure 6.20 shows the end points for particles generated by MODPATH on the predictive model. It highlights the potential flow lines and discharge points for particles generated within the Rosebery mine in the Rosebery catchment numerical groundwater model.

The areas of potential discharge shown in Figure 6.20 were limited to: (i) areas along the Stitt River and Rosebery Creek, which were already experiencing significant AMD contamination (Chapter Four); and (ii) a very limited area south and north of the Pieman River's confluence with the Stitt River. Based on topography and mine geometry there was a perception, prior to the modelling study, that the latter area may have extended significantly further north along Lake Pieman, even possibly into Lake Rosebery near the Bastyan Dam area. In the field, the undulating nature of the mountainous terrain makes interpretation of hydrogeological and topographical information complex, further contributing to the above perception.

Prior to mining in the area, flow through the region containing the mine would have been expected to discharge further north along the Pieman River than it presently does today. This can be demonstrated using the groundwater model (Appendix Eleven) by removing mine voids and wells. Wether the pumps are operational or not, the mine voids now drive flow south and upwards, so in fact, the mine geometry itself is responsible for the limited area of influence on Lake Pieman. On the contrary, if the mine was totally backfilled with a low permeability waste material, the area if influence along the Pieman may increase.

6.13 Modelling Recommendations

The modelling effort should now be refined to focus specifically on the area displayed in Figure 6.20. The Bobadil tailings dam should be the focus of separate detailed work. The influence the tailings dams no. 1, 2 and 5, may still be influential in modelling near mine and this too requires further work. Future monitoring and *in situ* hydraulic measurements are required to both validate and further develop the current model.

The priority for such work should be in the vicinity of the Primrose area and Rosebery township (Figure 2.3), and within the deep fractured rock aquifer. Ideally multiple screens should be installed across areas of varying RQD or flow rates. Unlike much of the Rosebery catchment, the Primrose area and Rosebery township provides significant scope for access to undertake such drilling, although this may depend on community agreement. The area south of the Pieman's confluence with the Stitt River may be difficult to access, but should not be disregarded. Background monitoring should be extended both: (i) north, potentially along the Bobadil access road, and (ii) south beyond the modelled potential area of influence.

"We do not seek universal truth from models, simply engineering confidence" (de Marsily cited in Middlemis, 2000).

7 Summary, Discussion, Synthesis of Conclusions and Recommendations

7.1 Aims

The first chapter introduced the project, provided some key definitions, and outlined the significance of the study. The chapter also identified the aims of the study as: (i) to determine the modern existing hydrogeological flow field at and around the Rosebery mine; (ii) to assess the impact of AMD on the geochemistry of waters within the Rosebery catchment; (iii) to characterise the types and chemical signatures of waters within the Rosebery catchment; (iv) to develop a numerical groundwater flow model consistent with the existing conditions; (v) to use the numerical model to predict groundwater flow following cessation of mining; and (vi) to extrapolate the study findings to outline the challenges and benefits in monitoring and modelling sub-surface fluid behaviour in other wet, temperate, mountainous, sulphide-mining environments.

The modern existing hydrogeological flow field at and around the Rosebery mine was determined by defining the conceptual model outlined in Chapter Five. The conceptual model drew heavily on the observations of Chapter Three and Four as well as the physical setting defined in Chapter Two. The conceptual model was further refined through the process of creating the numerical model presented in Chapter Six. Flow paths from contaminant point sources, identified through observation (Chapter Three) and geochemistry (Chapter Four), were delineated with the use of particle tracking within the numerical groundwater flow model.

The impact of AMD on the geochemistry of waters within the greater Rosebery

catchment was examined in Chapter Four with support from observations presented in Chapter Three. The interpretation of the existing geochemical impact of AMD at Rosebery was further explored using the results of the particle tracking within the operational simulation of the numerical groundwater flow model presented in Chapter Six. The types and chemical signatures of waters within the Rosebery catchment were characterised in Chapter Four. End members for water groups were delineated and mixing trends interpreted. This interpretation provided justification for decisions in the conceptual and numerical models presented in Chapters Five and Six, respectively.

A numerical groundwater flow model was developed and is presented in Chapter Six. The numerical groundwater flow model was constructed and calibrated to be consistent with the existing conditions of: (i) the physical setting described in Chapter Two; (ii) the observations made within the catchment, documented in Chapters Three; (iii) the geochemical mixing trends discussed in Chapter Four; and (iv) the conceptual model and water balance created in Chapter Five. Once calibrated, the numerical model was then used to predict groundwater flow following cessation of mining and mine filling. The outcome of the numerical groundwater flow model was the generation of a calibrated three-dimensional numerical groundwater flow model, which can be used as a predictive tool to aid monitoring and water management decision at the Rosebery mine.

Potential application of the present study elsewhere is presented hereafter in Section 7.3. Following this, the final aim, to apply the study findings to improve monitoring and modelling sub-surface fluid behaviour in other wet, temperate, mountainous, sulphide-mining environments, is summarised in Section 7.4 and Section 7.6. Recommendations for Rosebery are made in Section 7.5.

7.2 Key Findings

Key findings included that although the area has been glaciated historically, mine data, particularly rock quality designator (RQD) values, provides clear evidence of: (i) a weathering induced increase in permeability within 100 m of the natural ground surface; (ii) an increased permeability associated with shear zones and faults; and (iii) beyond a depth of 100 m, a uniform decrease in permeability with depth below the ground surface. Insights into groundwater flow have been provided by qualitative and quantitative observations of piezometric level in 29 exploration drillholes, 8 piezometers, discharging groundwaters, and surface water flow monitoring points. Together, piezometric heads, flow rates, and calculated material properties have provided the framework for developing a conceptual model of the groundwater regime within the Rosebery catchment. The groundwater flow system is typified by a deep fractured aquifer (which contain the mine voids), overlain by surficial glacial deposits and weathered material. Significant interaction between surface waters and groundwater was observed throughout the catchment. Geochemistry provided support for conceptual flows and justification of the modelling approaches.

Key findings of the geochemistry are that potential acid-generating and neutralising minerals were identified by examining whole-rock geochemistry. The net acid generation and acid consuming potential of Rosebery materials was quantified. The results indicated that mined materials at Rosebery have the potential to produce a significant volume of acid mine drainage. At the Rosebery mine, metal contaminated waters originate from localised point sources of sulphides, such as tailings dams, waste rock, and mine workings. Waters are contaminated by AMD, resulting in elevated levels

of H_2SO_4 as well as the metals Pb, Zn, Cu, Fe, Mn, Mg Cd, Al, and Ca. The Mg content of AMD indicates that neutralisation is occurring, most likely through the dissolution of the hypogene minerals chlorite, ankerite, and dolomite. Although background surface waters and contaminated mine waters are acidic, regionally the groundwaters sampled are near-neutral.

Key findings of the modelling were that the quantification of the important flows in the conceptual model of the Rosebery catchment allows the construction of a water balance, which provides a reasonable estimation of annual flows. The average precipitation rate across the catchment is estimated at 8.4 m^3/s. The water budget for the Rosebery catchment is: (i) 42% of precipitation runs off to become true surface water flow (including interflow); (ii) 24% of precipitation is lost to evapotranspiration; (iii) 17% of precipitation becomes groundwater and is discharged as baseflow into creeks and rivers within the catchment; and (iv) 18% remains as groundwater discharging into the regional groundwater system outside of the catchment or into the Pieman River system. The water balance highlights the importance of groundwater in the catchment, with a groundwater to surface water flow rate ratio of 1:1.2. The water balance was applied to three scenarios: (i) a quantification of the contribution of the open pit to underground flows; (ii) the filling of the southern exploration decline; and (iii) the filling of the mine after decommissioning. This work indicated that the open cut makes only a minor contribution to underground water flow and that the mine is expected to fill to a decant point after six years.

Key findings of the numerical modelling were that modelling identified the potential hydrogeological area of influence of the mine was chiefly controlled by the topography

of the host catchment. The topographically-driven western flows off Mount Black are redirected south, primarily by the conduits of the mine workings. Conceptualisation of the groundwater regime improved using computer generated 3D visualisation, and through the numerical modelling exercise. The numerical modelling suggested that the potential area of discharge for contaminated mine waters is far more limited in extent than was previously believed by mine personnel. This area is limited to: (i) areas along the Stitt River and Rosebery Creeks, which are already experiencing significant acid mine drainage contamination; and (ii) a very limited area south and north of the Pieman River's confluence with the Stitt River. The implications of understanding the area of potential influence are: (i) resources for future monitoring investigations can be focussed in this discrete area; (ii) the scale of future modelling efforts can be restricted to this area, improving detail and limiting computational requirements; and (iii) background monitoring beyond this area can be used to further test the model and provide data for future model calibration and validation.

7.3 Application of the present study to regions of similar settings

The present study at the Rosebery mine has application to similar settings on both a local and global scale. Example regions of a similar setting to Rosebery were defined using global climate maps (Lieth, 1972; Leemans and Cramer, 1991; and FAO, 2008), combined with global maps of terrain (Google Earth, 2006) and mine information (Infomine, 2008). Figure 7.1 (FAO, 2008) displays climate information from Lieth (1972) and Leemans and Cramer (1991) using Koeppen's (1931) climate classification system. Although beyond the scope by definition, application of hydrogeological

methods presented in the current study might also extend to other rock settings involving excavation of sulphidic material such as: (i) tunnelling operations including civil, hydroelectric and nuclear storage; and (ii) coal or iron ore mining. In addition many of the hydrogeological methods presented in the current study might also be applicable in other environmental settings such as: (i) in dry climates; (ii) in tropical or polar latitudes; and (iii) in non-mountainous terrain.

Similarities between the present study area and several mining districts elsewhere in the world mean that the present study is relevant beyond the Rosebery district. The West Coast Region of the South Island of New Zealand contains a significant sulphide mining (gold) and coal mining district. The region is characterised by steep topography rising from sea level to 700 m and is cloaked in thick, protected, rainforest (Trumm, 2007). The area has a high rainfall climate with very low temperature seasonality (*ibid.*), and located at similar temperate latitudes to Tasmania. The topography and climate results in AMD with very high flow rates in locations with very little space for remediation (*ibid.*). This setting and circumstance is very similar to the Rosebery area with a key difference that AMD chemistry associated with sulphide mining are generally distinctive, elevated in particularly arsenic and antimony (Pope and Craw, 2008). Extensive AMD related to coal mining also occurs within the mining district of West Coast Region of the South Island of New Zealand (Trumm, 2007; and Pope and Craw, 2008).

Another analogous area is the Myra Falls district of British Columbia, Canada. At Myra Falls, despite high rainfall and steep hydraulic gradients (related to the mountainous topography) which limit the water to mineral contact (Phipps et al., 2004), AMD conditions have developed (Desbarats and Dirom, 2005) with similar geology and

climate to Rosebery. Research relating the geochemistry to mine water flows has been presented in similar settings to Rosebery (e.g., Phipps et al., 2004; and Pope and Craw, 2008), however, up-scaling this to a catchment scale context is rarely undertaken.

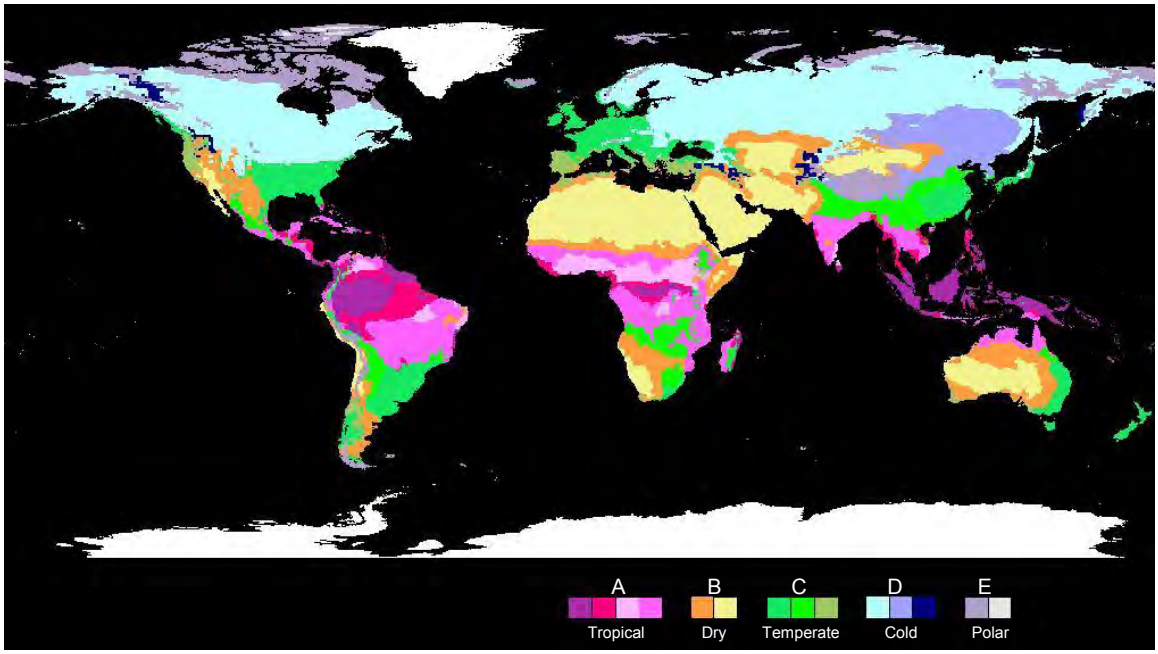

Figure 7.1 Koeppen's climate classification (FAO, 2008)

Additional mines that have a similar wet, temperate, mountainous sulphide-mining setting to the Rosebery mine (41°40'S, 145°50'E) include, but are not limited to, the operating mines of Renison (41°48'S, 145°25'E), and Henty (41°55'S, 145°50'E) Tasmania (Infomine, 2008). Globally, operating mines in wet, temperate, mountainous sulphide-mining districts include, but are not limited to, the examples of: Martha (37°23'S, 175°51'E), Waihi, New Zealand; Nkomati (25°40'S, 30°30'E), in western South Africa; El Toqui (44°32'S, 72°22'W), southern Chile; Myra Falls (49°33'N, 125°33'W) Eskay Creek (56°39'N, 130°27'W) and Huckleberry (53°41'N, 127°10'W), western Canada; Pogo (64°26'N, 144°56'W), Alaska and Pend Oreille (48°52'N, 117°22'W), in the north west of the United States of America ; Topia (25°13'N, 106°34'W), in central

temperate Mexico; Nalunaq (60°21'N, 44°50'W), of temperate coastal Greenland; Jianchaling (33°15'N, 106°22'E), in Shaanxi Province; and Dexing in Jiangxi Province, both in eastern China (Google Earth, 2007; FAO, 2008; and Infomine, 2008).

7.4 How does a wet, temperate, mountainous, sulphide-mining setting influence the approach to groundwater management and modelling?

7.4.1 Groundwater research in the Rosebery catchment

The wet, temperate, mountainous physical setting at Rosebery necessitated a different approach to groundwater research to that typically applied over much of the Australian continent. For instance, the high variable rainfall and low evaporation meant that traditional calculations of recharge, typically applied in arid and semi-arid environments, were difficult to apply in the wet environment. The Rosebery groundwater system provided an example of an area in which groundwater management is in its infancy. Literature review shows this neglect is widespread in similar settings.

The Rosebery area, being a mining district for over 100 years, contains a significant amount of spatial data that is not usually available in rural areas. The additional spatial information available at Rosebery, which might not have been otherwise available in the catchment if the mine did not exist, included: (i) rainfall data; (ii) stream flow data; (iii) drilling voids for water level and hydrochemistry monitoring; (iv) extensive geological investigations; (v) detailed geological mapping and cross sections; (vi) geotechnical data; (v) a 3D geological model; (v) a void model; (vi) water flow records within the mine; (vii) the opportunity to observe the rock mass at depth; and (viii) an extensive aqueous geochemistry dataset.

Data that are lacking at Rosebery include: (i) aquifer observations and characteristics;

and (ii) the infrastructure to make these observations and determine hydraulic characteristics (drilling rigs, packers, pumping bores and piezometers). To supplement the lack of these data at Rosebery, variations in research strategy were attempted and are elaborated on below.

7.4.2 Aquifer observations and characteristics at Rosebery

The third chapter described the field observations and aquifer characteristics. As the Rosebery mine was operational throughout the present study there was no saturated medium in the immediate vicinity of the mine which could be subjected to hydraulic testing. In addition, the ability to obtain extensive and representative aquifer property values in the field was limited by factors outlined below. This is also expected to be the case with many other groundwater studies in similar settings. The main limiting factors were lack of infrastructure, access, funds and field time (which also required funding). Plagued by a lack of traditional data, I found that the distinctive conditions and data that are available at such hard-rock mining operations could be employed to understand the aquifer characteristics.

7.4.2.1 Drillholes

Exploration drillholes provided a rudimentary substitute for piezometers. The east dipping attitude of the orebody influenced the location of drillholes, resulting in an abundance of information up-gradient of the mine (in the hangingwall) and little information down-gradient (in the footwall). Although gathering data from historical diamond drillholes proved problematic, it did provide coarse piezometric level information adequate for the conceptualisation and calibration of a steady-state numerical groundwater flow model. Piezometric level data were otherwise unobtainable in the

present study. The use of mineral exploration drill holes in groundwater studies is not widely referred to in the literature (e.g., it is not considered in the similar studies Banks et al., 2002; Morgan, 2003; and Rapantova et al., 2007), presumably due to the problems associated with them which were identified in the present study (Section 3.2.2).

Regionally, where test pumping proved impractical, slug tests were used as an alternative. Subtraction slug tests were considered relevant due to the low hydraulic conductivity of the material (Section 3.2.4.3). At Rosebery the hydraulic conductivity values provided by the Hvorslev test were applicable to modelling as they provided an average equivalent porous medium hydraulic conductivity for lengths of open or screened drillholes. Theses hydraulic conductivity values spanned 4 orders of magnitude, displaying the variability of hydraulic conductivity within the fractured rock mass. The great depth of exploration holes at Rosebery provided an advantage over shallow piezometers with discrete screened intervals that are typically used in classical groundwater studies. The resulting data were more appropriate when applied to modelling parameters at Rosebery, because data collection and modelling were applied at similar scales.

The exploration drilling also provided information concerning the geotechnical properties of the rock mass. The present study introduced the concept of using the analysis of mine geotechnical data as input for hydrogeological modelling (Evans et al., 2003). RQD data provided clear evidence of a weathering induced increase in permeability within 100 m of the natural ground surface, and an increased permeability associated with shear zones and faults. Beyond a depth of 100 m, RQD data also provided clear evidence for a uniform decrease in permeability with depth below the

ground surface.

Qualitative observation of discharging groundwaters and surface waters throughout the study area also provided insight into groundwater flow within the Rosebery catchment. Together with the quantitative data, these observations provided the framework for developing a conceptual model of the groundwater regime within the Rosebery catchment.

7.4.2.2 Aquifer observations

The dense rainforest and glacial cover over much of the catchment limited the direct observation of: (i) all groundwater presenting as seeps at surface; (ii) surface expression of geologic lineaments with the potential to act as groundwater conduits; and (iii) bedrock in outcrop at Rosebery. This is a problem faced elsewhere in such environments (e.g., Frohlich et al., 1996; Mayer and Sharp, 1998; and Tam et al., 2004). In the field, the undulating nature of the mountainous terrain makes interpretation of hydrogeological and topographical information complex. This contrasts with the fact that a great deal of sophisticated groundwater information (e.g., mapping; drillhole information; geotechnical data; and geochemical analyses) was available only due to the mining operation.

7.4.3 AMD and hydrogeochemistry at Rosebery

The geochemistry of acid mine drainage was the focus of the fourth chapter. The chapter examined both new and existing data on the chemistry of local waters and rocks within the study area.

At Rosebery the ANC method provided a best case scenario quantifying the volume of sulphuric acid that could be consumed per unit volume of material. Combined with

NAG, ANC provided a valuable tool for: (i) determining the potential that a material has to create acid; and (ii) the potential that surrounding materials have to neutralise that acid. Potential acid-generating and neutralising minerals were identified by using whole-rock geochemistry, and the acid-generating and neutralising capabilities of Rosebery materials were quantified using ABA. NAG and ANC classification provided a predictive management tool of the risk of AMD development at Rosebery. The results indicated that exposed materials at Rosebery have the potential to produce a significant volume of AMD.

Dissolved major ion concentrations in groundwater suggest that Mg containing lithologies react with AMD waters and consume some acid. The most likely reactions at Rosebery are the breakdown of chlorite, dolomite or ankerite. Volcanic hosted massive sulphide deposits elsewhere are typically enriched in alteration chlorite and less commonly enriched in alteration carbonate (e.g., Phipps et al., 2004; and Davidson, pers. comm. 2008). Mg containing lithologies at, for example Savage River (Kent, 2008), and MgO concentrates at Que River (e.g., Bass Metals, 2008) have also been investigated for their potential to neutralise AMD. Lithologies rich in these Mg minerals may prove useful in the long term management and neutralisation of AMD at Rosebery and potentially in other sulphide mining districts.

The present study confirmed previous work that mine waters were contaminated with H_2SO_4 as well as with the metals Pb, Zn, Cu, Fe, Mn and Mg. This new work also found that Rosebery waters are also highly enriched in Cd, Al, and Ca. Such contamination is typically related to AMD in Tasmania (Gurung, 2003) and elsewhere in similar settings (e.g., Desbarats and Dirom, 2005).

The severe impacts of AMD contamination are localised, occurring: (i) within close proximity to point sources of AMD; (ii) within the Rosebery mine workings; and (iii) within the surface waters draining the mining area. These locations included: (i) assay creek; (ii) the Rosebery open-cut mine; (iii) the Rosebery underground mine; (iv) Rosebery Creek; (v) the Stitt River; (vi) Primrose creek; (vii) filter plant creek; (viii) the tailings facilities; and (ix) shallow groundwaters within the mine area. Abandoned mine workings and the mine-waste material that has been used as construction materials throughout the catchment also provide small scale AMD contaminant sources. Although background surface waters and contaminated mine waters are acidic, regionally, deep groundwaters are near-neutral.

Mine water and groundwater flows have been quantified elsewhere for comparison with variations in water chemistry (e.g. Stapinsky et al., 1997; Wallace, 2002; and Pope and Craw, 2008). Using the water balance models and flows observed, in conjunction with water chemistry the relative ranking of contaminant point sources could be quantified to prioritise future management efforts at Rosebery. Along with the mine adit, Rosebery Creek and the Stitt River have been identified as the most significant potential long term, high volume, and high contaminant groundwater discharge locations within the catchment.

End members for water types at Rosebery were determined, and divided into: (i) creeks and rivers with significant interflow and deep groundwater input; (ii) surface waters that had compositions suggestive of them being recently emerged deep groundwater (seeps); (iii) surface water not influenced by groundwater and interflow interaction, suggesting that they had had little base flow contribution; (iv) groundwaters

with a contribution surface water suggesting leakage to aquifers from rivers and creeks, which provided justification for the use of stream, river or general head boundaries in the model; and (v) waters contaminated with AMD.

The role of geochemistry in the present study was to determine the extent of the AMD problem and to gain a better understanding of the existing flow field. The value of the identification of point sources of AMD was to locate particle starting points for MODPATH models, and this is a recommended validation strategy for modelling in mined areas. No contamination was encountered up gradient of obvious point sources, thus validating the conceptual and model flow directions, and the conceptual geological model of potential AMD sources. Although a considerable cost for a mine that is undertaking closure studies, metal and major element water chemistry has provided valuable information on the interaction and development of groundwaters, surface waters, and AMD in the Rosebery catchment, and is considered essential for similar studies in other areas.

7.4.4 Water balance at Rosebery

The water balance and the important environmental factors affecting the local Rosebery system were presented in Chapter Five. A mathematical model was created from local data, and used to outline the water budget for the important factors of the total water balance.

A key issue is the very large difference that was found to exist between precipitation measured at the top of the catchment compared to that measured at the Rosebery township. This variation was dealt with using an elevation-controlled function and the assumption of linear behaviour, however, this emerged to be the largest potential

source of error in the water balance. This model requires further validation, however, could be tested relatively cheaply through the installation of rain gauges at various elevations throughout the catchment. Determining a representative recharge value for a flow system is vital for any groundwater investigations (e.g., Daniel, 1976; and Marqinez et al., 2003) and emerges as a key difficulty in mountainous terrain due to a typical lack of measurement points, and large potential orographic effects on precipitation. At Rosebery a representative recharge was achieved by estimating the runoff baseflow components using stream gauging data and the estimate of precipitation discussed above. Modelling flows is especially important where total containment of mine site runoff is not feasible because rainfall exceeds evaporation (Meynink, 1996) as at Rosebery, and in other wet mining districts.

The average precipitation rate across the catchment was estimated at 8.4 m^3/s, of which 2.95 m^3/s is attributed to runoff (Table 5.3) giving an average runoff co-efficient of 0.44. Such a high runoff co-efficient (remembering that this does not include a baseflow component, which if included took the runoff co-efficient value to 0.59) is common in wet, mountainous Tasmanian settings (e.g., Atkinson, 1982; Edgar et al., 1999). Globally in wet mountainous terrain, runoff co-efficient values have a similar magnitude (e.g., Farina and Gaspari, 1990; and Wishart, 2000). In summary, the water budget for the Rosebery catchment (rounded to the nearest whole number percentage value) is: (i) 42% of precipitation runs off to becomes true surface water flow (including interflow); (ii) 24% of precipitation is lost to evapotranspiration; (iii) 17% of precipitation becomes groundwater and is discharged as baseflow into creeks and rivers within the catchment; and (iv) 18% remains as groundwater discharging into the regional groundwater system

outside of the catchment or into the Pieman River system.

The mine inflows were quantified as a percentage (1.6%) of the total estimated recharge to the Rosebery catchment, suggesting that the current mine-routed volumes are small on a regional scale. Water balance calculations adequately estimated flooding in the southern exploration decline and rebutted the theory that the open cut is the likely source for much of the water flowing into the underground workings. The estimated recharge value and mine inflows from the water balance were applied directly as numerical and mathematical model inputs.

The summary water balance highlights the importance of groundwater in the catchment, with a groundwater (those waters that have been groundwater at some stage i.e. inclusive of baseflow) to surface water (those that have been true surface waters including interflow) flow rate ratio of 1:1.2. The majority of hydrology research in Tasmania involves surface water. The relative amount of surface water to groundwater research ratio does not reflect this on the wet, temperate, mountainous west coast of Tasmania. If the high ratio of groundwater to surface water volume is similar in other wet, temperate, mountainous environments globally, the need for more research into hydrogeologic environments of such regions is apparent.

7.4.5 Predictive mine filling at Rosebery

The MIFIM model discussed in Chapter Five indicates that mine filling will occur within 5-10 years, most likely 6 years. The climate and geometry of the mine and surrounding topography indicate a constant supply of water to the underground workings and that discharge will continue indefinitely. The implications for such rate of filling of the Rosebery mine are: (i) that management options need to be in place within five years

of the cessation of pumping; and (ii) that as flooding is relatively slow, the oxidation of sulphidic waste rock placed underground will be increased compared to a rapid flooding, thus increasing environmental impact.

With the MIFIM results in mind, there was little benefit in attempting to numerically model the process of mine filling at the Rosebery mine within a package such as MODFLOW. Understanding that mine filling will occur naturally within a decade, or could be artificially filled (relatively instantaneously) was sufficient. The scope of numerical modelling was refined to represent: (i) operating conditions (an empty mine); and post decommission conditions (a full mine). This type and scope is expected to also be the case with other above-drainage mines in wet temperate mountainous conditions where the climate and geography result in mines filling to a decant point.

7.4.6 Numerical modelling at Rosebery

The design, construction and calibration of the numerical models were presented in Chapter Six. This chapter discussed the use of physical data to represent the hydrogeologic system in the numerical models. Chapter Six also analysed the simulation of the numerical groundwater flow model and the generation of particle flow paths. Generated in the Rosebery mine, these flow paths represent the mine's area of influence. Comparisons of both scenarios modelled by the present study (Section 6.12) indicated that the regional flow regime is not expected to greatly differ from operation to decommissioning. The areas of potential discharge (Figure 6.20) are limited to: (i) areas along the Stitt River and Rosebery Creeks, which are already experiencing significant AMD contamination (Chapter Four); and (ii) a very restricted area south and north of the Pieman River's confluence with the Stitt River.

Prior to mining in the area, flow through the region containing the mine would have been expected to discharge further north (towards the Bastyan Dam) along the Pieman River than it does today. Whether the pumps are in operation or not, the mine voids now drive flow south, so in fact, the mine geometry itself is responsible for the limited area of influence of mine derived groundwaters on Lake Pieman. In contrast, if the mine was totally backfilled with a low permeability waste material, the area of receipt of mine waters along the Pieman may increase, because this may return the flow regime closer to its original state. Mining on such scales in other areas may also change catchment scale flow regimes, and the present study displays that detailed flow modelling does provide a means of predicting the nature of that change.

MODFLOW proved to be a valuable tool in the wet temperate mountainous sulphide-mining environment due to its ability to represent the groundwater regime, especially surface water – groundwater interactions, in the Rosebery catchment.

7.5 Recommendations for Rosebery

Although the present study was limited, resulting in standard hydrogeological data being omitted, such data should not be excluded from future studies in the Rosebery area. For future groundwater investigations to be adequately resourced they should include the following elements.

7.5.1 Drilling investigations

A significant immediate finding from analysis of the Rosebery catchment groundwater flow model is the definition of an area of interest down gradient from the Rosebery mine (Figure 6.20), in the Primrose area (Figure 2.3) and downstream of the confluence of the Stitt River and Lake Pieman. Figure 6.20 highlights the potential flow

lines and discharge points for particles generated within the Rosebery mine in the Rosebery catchment numerical groundwater flow model, and Figure 7.1 displays the likely discharge locations for mine waters into the surface water system.

The focal areas for future investigation should be up-gradient of the modelled likely discharge locations (Figure 7.2). In addition to piezometers for monitoring, the installation of bores capable of being pumped for the purpose of pumping testing would greatly increase the confidence in hydraulic parameter estimation in this important area. Future hydrochemical monitoring of such bores could also determine whether these bores could be used as a mine water affected groundwater interception scheme.

In the present study the location of the available monitoring sites was dependent on exploration drillhole locations. Using existing up-gradient exploration drilling at Rosebery to monitor groundwater contamination is inadequate and is further justification for the installation of a purpose-built monitoring network of piezometers at Rosebery. Although no contamination is currently observed in the subsurface flow field distal from obvious point sources, it is not conclusive that no contamination is occurring.

Based on the fact that most drilling is in the hangingwall and up-gradient of the mine, the preliminary recommendation that piezometers should be installed down-gradient of the Rosebery mine and sources of AMD was made in the early stages of the present study (Evans and Davidson, pers. comm., 2002). The financial constraints of Pasminco being under administration at the time restricted the investment in such infrastructure.

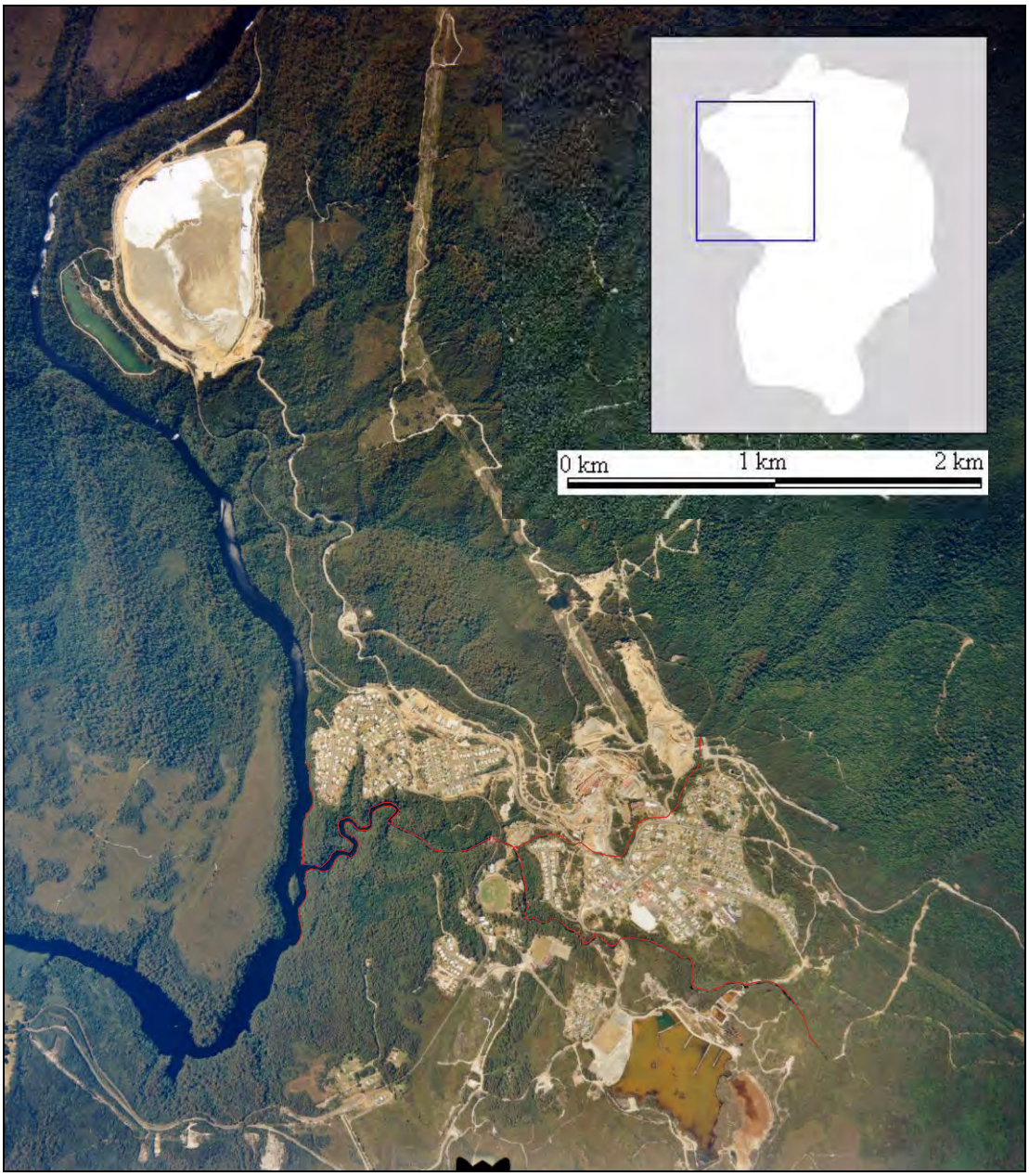

Figure 7.2 Modelled likely discharge locations (red) of mine waters into Lake Pieman, Stitt River and Rosebery Creek (after Figure 6.20 and Figure 2.3)

Subsequently, the recommendation has been partially accepted by Zinifex, who have: (i) contracted an engineering consultant (GHD) to quote upon the planning and installation of three piezometers down gradient of the mine and Bobadil tailings dam at a cost of $68646 (pers. comm., Morgan, 2004); and (ii) contracted Morrison and Blake (2006) to construct eight environmental monitoring water bores at the Bobadil and

No.2/5 tailings dams, the chemistry of which was summarised by Koehnken (2006). These recent studies focus on the potential contamination from tailings dams with no similar work yet being undertaken in the area of interest identified by the present study.

7.5.2 Stream flow measurements

Expansion of the stream flow measurement stations from the existing stations (Stitt River above Rosebery, and Bobadil outflow stations) could provide greater confidence and precision into the surface and baseflow regimes across the entire Rosebery catchment. The Sterling River, Rosebery Creek, and Mount Black tributaries are the initial station location recommendations. Linking these with a network of weather stations across the catchment could provide the data to test the water balance assumptions from the current study. Such validation could provide more confidence in the model solution proposed in the present study.

7.5.3 Hydraulic property investigations

In the present study the biannual (winter and summer) piezometric level monitoring that was undertaken over two years was considered in hindsight too limited for definition of seasonal variation, or the development of reliable temporal trends. The use of year-round down-hole pressure loggers would greatly improve the temporal definition of piezometric level fluctuation. Such logging instruments are recommended to obtain a future dataset for use as input data to a future transient groundwater model.

Pumping tests should be further investigated. Given adequate investment, pumping tests in appropriately designed bores, and analysis of water levels in adjacent monitoring piezometers, will greatly increase the confidence in hydraulic parameter estimation.

Multi-level packer tests within individual drillholes can provide information on the

vertical distribution of horizontal hydraulic conductivity (Widdowson et al., 1990). Multi-level packer tests as part of the exploration process could provide a powerful dataset of hydraulic parameters to achieve for example, a comparative analysis of RQD data and the direct estimates of hydraulic properties.

7.5.4 Geochemical investigations

Further aqueous geochemical work could involve the pursuit in the aqueous medium of trace metals known to reside in sulphides (Martin, 2004). For instance little is known about concentrations of Ag, Pd, Te and Tl within Rosebery waters. In the present study, due to the potential for toxicity at low levels, As, Bi, Cd, Co, Ni, Sb, and Sn analysis would have benefited from using more precise methods. In some cases analyses displayed results below detection but detection limits were above toxicity levels. Likewise, methods with lower detection limits (i.e., well below toxicity limits) could provide additional information on the potential contamination from Ag, As, Bi, Cd, Co, Cu, Fe, Ni, Mn, Pb, Pd, Sb, Sn, Te, Tl and Zn within the high volume receiving waters such as the Pieman. The extent of the influence of Rosebery mine waters on the Pieman are yet to be determined.

Using end member compositions relative to sample chemistry to indicate mixing extents may have application to future modelling efforts, especially in validating environmental tracer mixing estimates. Whilst beyond the scope of the current studies budget there is a significant scope for using environmental tracers to assist in groundwater model validation.

Given the large volumes of exposed material and the significant time period of exposure, AMD generation is expected to continue substantially beyond

decommissioning. The longevity and severity of AMD at Rosebery could be more precisely established through the use of further kinetic and column leach ABA analysis.

Future water quality monitoring should in future routinely incorporate major minor and trace elements including anions, turbidity and organic matter. Otherwise, interpretation of the data is limited, for both scientific purposes as well as environmental management for management purposes.

7.5.5 Mine flooding

Although flooding is relatively slow, and the environmental impact of sulphidic waste rock placed underground is thus increased, rapid mine flooding through artificial reinjection of water is not recommended. The benefits of rapid flooding need to be further justified given that the Rosebery mine has been exposed to oxygenated conditions for over 100 years and will not ever be fully flooded above 8 level.

The design of mine adit plugs needs to be considered for controlling and managing the discharge of AMD at Rosebery. Managing a single discharge point may prove advantageous. The present study has assumed that all points of egress below the 8 level adit would be plugged. Discharge of mine water at the site is likely as plugging of all points of water egress (including those at and above 8 level) is not recommended due to the geometry of the groundwater system and the resultant pressure head such plugs could be exposed to.

7.5.6 Modelling review

It is recommended that the modelling effort should now be refined to focus specifically on the area displayed in Figure 7.2. The Bobadil tailings dam should be the focus of separate detailed work. The influence of the tailings dams numbers 1, 2 and 5,

may still be influential in modelling near-mine flow, and this too requires further work. Future monitoring and in-situ hydraulic measurements are required to both validate and further develop the current model. Further site investigation is needed to assess whether the predicted flooded cell regions correspond to actual locations of seeps, or to areas that would result in artesian conditions if they were drilled. The 50 m grid size was considered a lower limit at Rosebery, largely due to a computer processing limitation. Thus, refining the grid as computing power increases is a recommendation for future works that employ finite difference modelling.

A transient groundwater flow model capable of accurately representing seasonal fluctuations would provide greater engineering confidence for closure management decisions. The enhanced monitoring network and hydraulic property investigations recommended herein (Sections 6.10.7 and 7.4.3) are required to provide the input data for such transient modelling.

7.5.7 Remediation

Given the findings of the present study, options for remediation of post decommissioning waters need to be investigated. Depending upon the fate of the Rosebery community beyond the mine life, some residential areas of the Primrose and Rosebery townships could provide a large area for a monitoring or groundwater interception network, and even a potential location for an AMD treatment facility (i.e. a passive wetland facility, or an active treatment plant) prior to discharge into the receiving environments. Relatively level, pre-disturbed areas such as these can be otherwise uncommon in wet, temperate, mountainous, sulphide-mining environments.

7.6 Recommendations for other wet, temperate, mountainous, sulphide-mining environments

The present study has highlighted the extensive data suite that is potentially available to groundwater investigations as a result of hard-rock sulphide-mining operations. In contrast, these mining districts also present unique challenges to the hydrogeologist. The potential for the mining of sulphides to generate AMD has promoted the study of the hydrogeological regime as a potential contaminant pathway at Rosebery. Coupled with the complexity of groundwater investigations in high rainfall and high relief environments, this makes the Rosebery catchment a particularly difficult hydrogeological environment to investigate. These issues are not unique to Rosebery, so that the present study has application to similar mining districts in similar topographic and climatic regions.

The characteristic feature of wet, temperate, mountainous environments is the local spatial variation in precipitation, evapotranspiration, and therefore recharge. Estimating a representative recharge value remains a pivotal quantification for undertaking groundwater investigations in such settings. Additional weather stations through study areas could assist in understanding local variations. The significant exchange between surface waters and groundwaters in wet, temperate, mountainous environments requires the use of code that is capable of accounting for this exchange.

The trade off between representing complex geometries using finite element methods and using a code with multiple modular packages resulted in MODFLOW being chosen in the present study. To maintain a representative complex geometry, a finite difference model with an unusually large number (52) of layers was constructed. This

approach would also be required elsewhere, if finite difference modelling is to be applied in mountainous terrain.

Surface water and groundwater exchange sites presented an opportunity to investigate the groundwater regime at the surface and near surface in shallow bores. Gauging stream flow for baseflow contribution provided important quantification of groundwater flow where bore flow data is scarce. Mine outflows also provided an important quantification of groundwater flow on a large scale. The present study proposed a method for amalgamating these data. Such an approach has potential application in other mining settings.

The present study has displayed how RQD, and other geotechnical parameters collected in the mining process, can provide valuable insight into the hydrogeologic regime. As rock quality (Q) values are widely used in the mining and tunnelling industry (Hoek and Brown, 1980; and DME, 1999), the routine conversion of these into hydro-potential (HP) values using the Gates (1997) method, could prove valuable in characterising the spatial variation in hydraulic properties of mined or tunnelled material. The modelling undertaken in the present study demonstrates that a valid 3D numerical groundwater flow model can be constructed and used to aid future closure decisions despite a lack of standard hydrogeological data.

Further correlation of RQD at Rosebery with hydraulic conductivity values using multilevel packer testing would make the parameterisation more powerful, since the RQD database at Rosebery, as in many mining environments, is very comprehensive. The conclusion that follows this is that the amount of near-mine drilling, although extensive, is not typically adequate to complete detailed flow modelling if hydraulic data

are not intentionally obtained. Purpose specific drilling is also required to ensure representative knowledge of the flow field beyond the deposit area and a statistically valid database of hydraulic parameters.

Flow within individual drillholes was considered extremely important in the present study, and provides scope for future work elsewhere within such environments. The extensive network of underground workings that typically exist in sulphide mines provides scope for detailed fracture mapping and research to be undertaken. Using existing geological mapping as a base, fracture information in other mining environments could also provide direct input to dual porosity or discrete fracture network modelling.

The effort needed to step up to a comprehensive discrete fracture network or dual porosity model would be large at Rosebery, however, it should be encouraged if data are sufficient elsewhere, as it may be in some mining environments. As in the study of Rapantova et al. (2007), the present study recognised the value and future widespread application of finite element groundwater flow modelling to represent complex geometries in the mining environment. Although not pursued at Rosebery, due to the lack data and lack of finite element modelling surface water interaction options, it should be recognised that the finite element technique also has particular application to mining data, particularly those in mountainous terrain, that may not be readily converted into finite difference grids.

Although the present study attempted to endure without some standard hydrogeological data, there remains a significant gap in the confidence of the modelling. The lack of resources had serious consequences for the present study, however, it did produce a situation synonymous with that facing most mines nearing closure, when cash

flow is likely to be reduced. A lack of time-series piezometric levels, and the need for a larger local material hydraulic property dataset, were the key gaps identified in the present study. In consequence, budgeting for the acquisition of such information should be considered a priority for groundwater investigations of wet, temperate, sulphide-mining districts elsewhere.

References

ABM (1996) Savage River Mine Development Proposal and Environmental Management Plan. NSR Environmental Consultants Pty Ltd, Victoria, Australia.

ABM (1997) Environmental Management Plan: Savage River Mine, Port Latta Pelletising Plant, Slurry Pipeline. Australian Bulk Minerals Tasmanian Operations.

ABS (2004) Australian Bureau of Statistics 1384.6 - Statistics - Tasmania, Latest Issue Released at 11:30 AM (Canberra Time) 22/04/2004 Contents >> Climate >> Rainfall.

Adams, M. (2006) Tasmanian vegetation evapotranspiration discussion. pers. comm.

Adams, R. and P. L. Younger (2001) A strategy for modeling ground water rebound in abandoned deep mine systems. Ground Water 39 (2):249-261

Aerden, D. G. A. M. (1990) Formation of a massive sulphide orebody by syn-deformational host rock replacement in a ductile shear zone, Rosebery, Tasmania. Geological Society of Australia, Abstracts 25 174-175

Aerden, D. G. A. M. (1991) Foliation-boudinage control on the formation of the Rosebery Pb-Zn orebody. Tasmania. Journal of Structural Geology 13 (7):759-775

Aerden, D. G. A. M. (1992) Macro- and Microstructural Controls on the Genesis of the Rosebery and Hercules Massive-Sulphide Deposits, Tasmania. James Cook University, Townsville PhD thesis: 260

Aerden, D. G. A. M. (1994) Formation of the Rosebery and Hercules ore deposits, Tasmania by syntectonic mobilization of metals and wallrock replacement about structural traps. Contentious issues in Tasmanian geology. 83-88

Agricola, G. (1556) De Re Metallica. translated by Hoover, H.C., and Hoover, L.H., 1950 Dover Publications New York: 638

Aiken, J. S. (2003) New Index Method for Logging Sonic Drill Core Samples in Carbonate Bedrock and Correlative Study of Secondary Permeability (Fracture) Distribution in the Shakopee Formation of the Prairie du Chien Group. McCain and Associates, Inc. Engineering and Environmental Services

Allen (1992) Construction of geological cross-sections at the Rosebery Mine, Tasmania. Pasminco Exploration and Pasminco Mining Rosebery 22

Allen (1993) Geological cross section and interpretation, 1320 mN, Rosebery Mine north end. Pasminco Limited 9

Allen, D. and F. Michel (1999) Characterizing a Faulted Aquifer by Field Testing and Numerical Simulation. Ground Water 37 (5):718-728

Allison, G. B. and C. J. Barnes (1985) Estimation of Evaporation from the Normally 'Dry' Lake Frome in South Australia. Journal of Hydrology 78 (3/4):229-242

Alpers, C. N. and D. N. Nordstrom (1990) Stoichiometry of mineral reactions from mass balance computations of acid mine waters, Iron Mountain, California. Acid Mine Drainage-designing for closure. 23-33

AMIRA (2002) ARD Test Handbook, Project P387A Prediction & Kinetic Control of Acid Mine Drainage. Ian Wark Research Institute 42

Anderson, M. P. and W. W. Woessner (1992) Applied Groundwater Modelling; Simulation of Flow and Advective Transport. Academic Press 381

Andrews, D. P. and J. E. Reid (2006) Geophysical monitoring of acid mine drainage at Savage River Mine, Tasmania. AESC2006

Andrews, J. N., W. Balderer, A. H. Bath, H. B. Clausen, G. V. Evans, T. Florkowski, J. Goldbrunner, H. Zojer, M. Ivanovich and H. H. Loosli (1984) Environmental isotope studies in two aquifer systems: A comparison of groundwater dating methods. Isotope Hydrology 535-576

ANZECC (2000) Australian and New Zealand Environment and Conservation Council, Australian and New Zealand Guidelines for fresh and marine water quality.

ANZMEC and MCA (2000) Australian and New Zealand Minerals and Energy Council and Minerals Council of Australia, Strategic Framework for Mine Closure. Commonwealth of Australia Canberra: 27

Appleyard, S. (1995) The Impact Of Urban Development On Recharge And Groundwater Quality In A Coastal Aquifer Near Perth, Western Australia. Hydrogeology Journal 3 (2):65-75

Aquaterra (2005) Quote on groundwater modelling. pers. comm.

Arnold, J. G. and P. M. Allen (1999) Automated methods for estimating baseflow and groundwater recharge from streamflow records. Journal of the American Water Resources Association 35 (2):411-424

Arnold, J. G., P. M. Allen, R. Muttiah and G. Bernhardt (1995) Automated base flow separation and recession analysis techniques. Ground Water 33 (6):1010-1018

Atkins, S. (1998) No. 2 Tailings Dam Seepage Assessment. University of Tasmania Hobart: 23

Atkinson, B. (1982). Mine Dewatering at Mt Lyell, the 1980's and Beyond. Underground Operators Conference, West Coast Tasmania Branch, The Australian Institute of Mining and Metallurgy.

Attanayake, P. and M. Waterman (2006) Identifying environmental impacts of underground construction. Hydrogeology Journal 14 (7):1160-1170

Augustinus, P. (1982) The Glacial Geomorphology of the Middle Pieman-Bulgobac Area. University of Tasmania, Hobart unpublished Hons thesis

Augustinus, P. and E. A. Colhourn (1986) Glacial history of the upper Pieman and Boco valleys, western Tasmania. Australian Journal of Earth Sciences 33 181-191

Australian Government (2009) Predictive Models - Connected Water Website, http://www.connectedwater.gov.au/framework/predictive_models.html

Australian Standards (1990) AS 2368-1990 Test pumping of water wells. 43

Baba, A. and T. Grungor (2002) Influence of Gold Mine on Groundwater Quality (Efemcukuru, Izmir, Turkey). Environmental Geology 41 621-627

Banks, D. (2001) A variable-Volume, Head-Dependent Mine Water Filling Model. Ground Water 39 (3):362-365

Banks, D., W. Holden, E. Aguilar, C. Mendez, D. Koller, Z. Andia, J. Rodriguez, O. Saether, A. Torrico, R. Veneros and J. Flores (2002) Contaminant source charactization of the San Jose Mine, Oruro, Bolivia. Mine Water Hydrogeology and Geochemistry 198 215-239

Banks, D. and N. Robins (2002) An introduction to groundwater in crystalline bedrock. Geological Survey of Norway Trondheim, Norway

Banks, D., P. L. Younger, R. T. Arensen, E. R. Inerson and S. B. Banks (1997) Mine Water Chemistry - The Good the bad and the Ugly. Environmental Geology 32 (3):

Banks, M. R. and J. B. Kirkpatrick (1977) Landscape and Man. The interaction between Man and Environment in Western Tasmania. The Proceedings of a Symposium organised by the Royal Soceity of Tasmanaia

Barenblatt, G. E., I.P. Zheltov and I. N. Kochina (1960) Basic Concepts in the Theory of Seepage of Homogeneous Liquids in Fissured Rocks. Journal of Applied Mathematics (USSR) 24 (5):1286-1303

Barton, N., R. Lien and J. Lunde (1974) Engineering classification of rock masses for design of tunnel support. Rock Mechanics 6 (4):189-236

Bath, A. H., W. M. Edmunds and J. N. Andrews (1979) Paleoclimate trends deduced from hydrochemistry of a Triassic sandstone aquifer, UK. Isotope Hydrology 545-568

Bass Metals (2008) Bass Metals Ltd. Mancala Que River Water Management Plan Review, 5th March 2008: 16

Bear, J., M. Beljin and R. Ross (1992) Fundamentals of Ground-Water Modeling EPA/540/S-92/005. EPA 11

Bell, F., T. Stacey and D. Genske (2000) Mining subsidence and its effect on the environment: some differing examples. Environmental Geology 40 (1-2):135-151

Bell, F. G. and S. E. T. Bullock (1996) The problems of acid mine drainage, with an illustrative case history. Environmental & Engineering Geoscience II: 369-392

Bell, L. C. (2004) Addressing the Environmental impact of mining in Australia - The role of Research and Development. Australian Centre for Minesite Rehabilitation Research

Benlahcen, A. (2003) A study of the Chimio-hydro-mechanical processes in fractured rock masses disturbed by mining operations: Example of the Bouchard-Hébert Mine, Abitibi, Québec. University of Québec (UQAC), Chicoutimi, Québec, Canada. unpublished PhD thesis: 473

Bense, V. F. and M. A. Person (2006) Faults as conduit-barrier systems to fluid flow in siliciclastic sedimentary aquifers. Water Resources Research 42 (5)

Berry, K. and D. Armstrong (1995) Olympic Dam operations Hydrogeological investigation and numerical modelling Lake Eyre region, Great Artesian Basin, HYD T044. Western Mining Corporation Limited, Belmont, WA.

Berry, M. V., P. W. Edwards, H. T. Georgi, C. C. Graves, C. W. A. Carnie, R. J. Fare, C. T. Hale, S. W. Helm, D. J. Hobby and R. D. Willis (1998) Rosebery lead-zinc-gold-silver-copper deposit. Geology of Australian and Papua New Guinean mineral deposits. 22 481-486

Berry, R. (1993) Rosebery Section, AMIRA Project Report P291: Structure and Mineralisation of Western Tasmania. Centre for Ore Deposit and Exploration Studies, University of Tasmania Hobart:

BHP (1996) Orebody 18, Consultative Environmental Review (unpublished).

Bieniawski, Z. T. (1973) Engineering classification of jointed rock masses. Trans S Afr Inst Civil Eng 15 335-344

Blainey, G. (1954) The Peaks of Lyell. Melbourne University Press 341

Blake, F. (1939) Underground Water in Tasmania. Mineral Resources Tasmania Hobart: 2

Blake, M. D. (1998) P349 geochemical whole-rock and mineral database. Hobart: 69-71

Bochenska, T., J. Fiszer and M. Kalisz (2004) Prediction of groundwater inflow into copper mines of the Lubin Glogów Copper District. Environmental Geology 39 (6):587-594

BOM (2002) Bureau of Meteorology www.bom.gov.au. Bureau of Meteorology

BOM (2004) Bureau of Meteorology www.bom.gov.au. Bureau of Meteorology

BOM (2008) Bureau of Meteorology http://www.bom.gov.au/climate/cdo/about/sitedata. Bureau of Meteorology

Bouwer, H. and R. Rice (1976) A slug test for determining hydraulic conductivity of unconfined aquifers with completely or partially penetrating wells. Water Resources Research 12 (3):423-428

Boyle, D. P., G. Lamorey, S. Bassett, G. Pohll and J. Chapman (2006) Development and Testing of a Groundwater Management Model for the Faultless Underground Nuclear Test, Central Nevada Test Area. Desert Research Institute, Nevada System of Higher Education

Bradd, J. M., W. A. Milne-Home and G. Gates (1997) Overview of factors leading to dry land salinity and its potential hazard in New South Wales, Australia. Hydrogeology Journal 5 (1):51-67

Brady, N. J. R. (1997) Open cut soil sampling and NAG analysis. Pasminco Mining Rosebery

Brassington, R. (1988) Field hydrogeology. John Wiley

Brathwaite, R. L. (1969) The Geology of the Rosebery Ore Deposit. University of Tasmania, Hobart PhD thesis: 193

Brathwaite, R. L. (1972) The structure of the Rosebery ore deposit, Tasmania. Proceedings - Australasian Institute of Mining and Metallurgy 241 1-13

Brigham Young University (2002) Groundwater Modelling System.

Briz-Krishore, B. and V. Bhimasankaram (1982) A comprehensive study and analysis of groundwater in a typical fractured environment. Groundwater in fractured rock 13-24

Brown (2003) Water for a Sustainable Minerals Industry - a Review. Water in Mining 3-14

Brown, L. (2006) Geophysical Characterisation of Bobadil Tailings Dam, Rosebery, Tasmania, University of Tasmania, Honours thesis.

Bull, L. R. (1977) Environmental effluent control at Rosebery. The AusIMM Conference

Cacas, M., E. Ledoux, G. D. Marsily, A. Barbeau, P. Calmes, B. Gaillard and R. Margritta (1990) Modelling Fracture Flow With a Stochastic Discrete Fracture Network: Calibration and Validation 2. The Transport Model. Water Resources Research 26 (3):491-500

Cacas, M., E. Ledoux, G. D. Marsily, A. Barbeau, P. Calmes, B. Gaillard and R. Margritta (1990) Modelling Fracture Flow With a Stochastic Discrete Fracture Network: Calibration and Validation 1. The Flow Model. Water Resources Research 26 (3):491-500

Cameron, M. (1996) A Guide to Flowers & Plants of Tasmania. Launceston Field Naturalists Club Launceston:

Campana, B. and D. King (1963) Palaeozoic tectonism, sedimentation and mineralization in west Tasmania. Journal of the Geological Society of Australia. 10 (Part 1):1-53

Campbell, I., T. McDougall and J. Turner (1984) A note on fluid dynamics processes which can influence the deposition of massive sulphides. Economic Geology 79 1905-1913

Carnie, C. (2003) Environmental Decommissioning and Rehabilitation Plan; Rosebery Open Cut. University of Technology Sydney, Sydney Masters thesis: 34

Carnie, C. (2002) Expected rebound times. pers. comm.

Carrera, J. and S. P. Neuman (1986) Estimation of aquifer parameters under transient and steady state conditions: 1. Maximum likelihood method incorporating prior information. Water Resources Research 22 (2):199-210

Carson, R. (1962) Silent Spring, Houghton Mifflin: 356

Cartwright, I. and T. R. Weaver (2004) Hydrogeology of the Golburn Valley, Murray Basin, Australia. Water - Rock Interaction: 383-388

Cartwright, I. and T. R. Weaver (2005) Hydrogeochemistry of the Goulburn Valley region of the Murray Basin, Australia: implications for flow paths and resource vulnerability. Hydrogeology Journal 13 (5-6):752-770

Chapman, D. (1992) Water quality assessments: a guide to the use of biota, sediments and water in environmental monitoring. Chapman & Hall London

Chen, E. (1987) A Computational Model for Jointed Media with Orthogonal Sets of Joints. SAND86-1122 Sandia National Laboratories, NNA.891020.0180 Albuquerque, New Mexico

Chen, J., C. Lee, T. Yeh and J. Yu (2005) A water budget model for the Yun-Lin plain, Taiwan. Water Resources Management 19 483–504

Chiang, W. and W. Kinzelbach (1991) Processing Modflow (PM), Pre- and postprocessors for the simulation of flow and contaminant transport in groundwater system with MODFLOW, MODPATH and MT3D. Distributed by Scientific Software Group Washington, DC

Chiang, W. and W. Kinzelbach (2001) 3D-Groundwater Modeling with PMWIN. Springer Berlin Heidelberg . New York: 346

Chillcott, S. J., H. Maxwell and P. E. Davies (1991) A study on the effects of the Hellyer Mine discharges on the aquatic fauna of the Southwell and Que rivers. Inland Fisheries Commission, Tasmania.

Choi, Y. S. and H. D. Park (2004) Variation of rock quality designation (RQD) with scanline orientation and length: a case study in Korea. International Journal of Rock Mechanics and Mining Sciences 41 (2):207-221

Church, P. and G. Granato (1996) Bias in ground-water data caused by well-bore flow in long-screen wells. Ground Water 34 262-273

Clarke, I. D. and P. Fritz (1997) Environmental Isotopes in Hydrogeology. Lewis New York: 328

CMT (1998) Revised Environmental Management Plan. Volumes 1 and 2. Copper Mines of Tasmania Limited.

Coastech Research (1989) Acid Rock Drainage Prediction Manual. MEND Ottawa, Ontario:

Coffey Partners (1995) Coffey Partners International P/L, E Lens subsidence and water management audit. Pasminco Mining Rosebery Hobart: 10

Coffey Mining (2008) Senior Hydrogeologist and GMS modelling software charge out rate.

Cook, N. G. W. (1982) Ground-water problems in open-pit and underground mines. In: Recent Trends in Hydrogeology. Geological Society of America Special Paper (189):397-405

Cook, P. G. (2003) A guide to regional groundwater flow in fractured rock aquifers. CSIRO Land and Water, Seaview Press, Glen Osmond, Australia: 108

Cook, P. G., T. Stieglitz and J. Clarke (2004) Groundwater Discharge from the Burdekin Floodplain Aquifer, North Queensland. CSIRO

Cooper, H. H., J. D. Bredehoeft and I. S. Papadopulos (1967) A Solution Is Presented For The Change In Water Level In A Well Of Finite Diameter After A Known Volume Of Water Is Suddenly Injected Or Withdrawn. A Set Of Type Curves Computed From This Solution Permits A Determination Of The Transmissibility Of The Aquifer. (Knapp-Usgs). Water Resources Research 3 (1):263-269

Corbett, K. D. (2002a) Bedrock Geology of the Mt Read Volcanics belt and adjacent areas South Darwin Peak to Hellyer.

Corbett, K. D. (2002b) Western Tasmanian Regional Minerals Program. Mount Read Volcanics Compilation. Updating the geology of the Mt Read Volcanics belt. Record, Tasmanian Geological Survey 2002/19.

Corbett, K. D. (2004) Updating and revision of the 1:25 000 scale series geological maps covering the Mt Read Volcanics belt in western and north-western Tasmania. Mineral Resources Tasmania Hobart: 10

Corbett, K. D. and T. C. Lees (1987) Stratigraphic and structural relationships and evidence for Cambrian deformation at the western margin of the Mt Read Volcanics, Tasmania. Australian Journal of Earth Sciences 34 45-67

Corbett, K. D. and A. W. McNeill (1986) Map 2: Geology of Rosebery Mt Block Area, Mt Read Volcanics Project.

Corbett, K. D., M. Solomon, M. P. McClenaghan, J. T. Carswell, G. R. Green, G. Iliff, H. J.W., M. G.J. and W. D.B. (1989) Cambrian Mt Read Volcanics and associated mineral deposits. Special Publication - Geological Society of Australia. Hobart: 84-153

Cox, M. E., J. Hillier, L. Foster and R. Ellis (1996) Effects Of A Rapidly Urbanising Environment On Groundwater, Brisbane, Queensland, Australia. Hydrogeology Journal, 4 (1):30-47

CPSMA (1990) Ground Water Models: Scientific and Regulatory Applications. Commission on Physical Sciences, Mathematics, and Applications, The National Academy of Sciences

Craig, H. (1961) Standard for Reporting Concentrations of Deuterium and Oxygen-18 in Natural Waters. Science 9 (133):1833-1834

Cripps, J., A. Deaves, F. Bell and M. Culshaw (1988) Geological controls on the flow of groundwater into underground excavations. 3rd Mine Water Conference 77-86

Critchley, W., K. Siegert and C. Chapman (1991) Water harvesting (AGL/MISC/17/91) A Manual for the Design and Construction of Water Harvesting Schemes for Plant Production. Food and Agriculture Organization of the United Nations Rome:

CSIRO (1998) Isotope Analysis Service. CSIRO Land and Water

Cymod (2005) Hamersley Iron Assessment of Dewatering Requirements Nammuldi Iron Ore Mine 2004. Perth:

Dames and Moore (1996) Environmental Assessment Rosebery Mine, Rosebery, Tasmania. Pasminco Limited Rosebery: 8

Daniel, J. F. (1976) Estimating Groundwater Evapotranpiration From Streamflow Records. Water Resources Research 12 (3):360-364

Dansgaard, W. (1964) Stable isotopes in precipitation. Tellus 16 435-468

Darcey, H. (1856) Les Fontaines Publiques de la Ville de Dijon, Dalmont. Paris:

Datamine (1998) Datamine Reference Manuals. Mineral Industries Computing Limited Digital

Davidson, G. J. (2006) Ore deposits of Tasmania. pers. comm.

Davidson, G. J. (2008) Greenhouse gas implications of AMD CO_2 release and alteration of VHMS deposits. pers. comm.

Davidson, G. J., D. Cooke and J. Yang (2000) SPIRT Application: Groundwaters in sulphide mining districts: understanding modern and post-closure water chemistry and fluid flow patterns. University of Tasmania Hobart:

Dawes, W., G. Walker, L. Zhang and C. Smitt (2004) Flow Regime, Salt Load and Salinity Changes in Unregulated Catchments. Interpretation for Modelling the Effects of Land-use Change. CSIRO

de Caritat, P., D. Kirste, G. Carr and M. McCulloch (2005) Groundwater in the Broken Hill region, Australia: recognising the interaction with bedrock and mineralisation using S, Sr and Pb isotopes. Applied Geochemistry 20 767-787

Deere, D. U. and D. W. Deere (1964) Rock Quality Designation (RQD). US Army Corps of Engineers, Vicksburg, Virginia

Deere, D. U. and D. W. Deere (1988) The Rock Quality Designation (RQD) Index in Practice, Rock Classification Systems for Engineering Purposes. ASTM Special Publication 984 91-101

Dellar, M. (1998) Acid mine drainage in the Rosebery mineral field. University of Tasmania, unpublished Honours thesis: 123

DeNicola, D. M. and M. G. Stapleton (2002) Impact of acid mine drainage on benthic communities in streams: the relative roles of substratum vs. aqueous effects. Environmental Pollution 119 303-315

Denney, S. (2000) Trace metal speciation in the Pieman River catchment, Western Tasmania. Deakin University, Warrnambool, unpublished PhD thesis: 200

Desbarats, A. J. and G. C. Dirom (2005) Temporal variation in discharge chemistry and portal flow from the 8-Level adit, Lynx Mine, Myra Falls Operations, Vancouver Island, British Columbia, Environmental Geology 47 (3):445-456

Dickson, H. (1997) Monitoring of No.2 Tailings Dam. Pasminco Rosebery Mine Rosebery: 16

Diersch, H. J. G. (1998) FEFLOW – Reference Manual. Release 4.7. WASY Ltd Berlin.

Diodato, D. M. (1994) A Compendium of Fracture Flow Models - 1994. Center for Environmental Restoration Systems, Energy Systems Division, Argonne National Laboratory 94

DME (1999) The ‘Q System’ Geotechnical Design Method was Updated in 1994. Department of Minerals and Energy - Mining Operations Division 4

Doble, R., C. Simmon, I. Jolly and G. Walker (2004) Spatial modelling of groundwater discharge patterns to predict floodplain salinisation and impacts on vegetation health. CSIRO Land and Water Technical Report No. 1/04

Doherty, G. (2004) Mine Inflows. pers. comm.

Doherty, J. (1994) PEST.

Dold, B. and L. Fontbote (2002) A mineralogical and geochemical study of element mobility in sulphide mine tailings of Fe oxide Cu-Au deposits from the Punta del Cobre belt, northern Chile. Chemical Geology 189 135-139

Domenico, P. A. and F. W. Schwartz. (1990) Physical and chemical hydrogeology. Wiley

Donovan, J. J., B. R. Leavitt and E. Werner (2003) Long-Term Changes in Water Chemistry as a Result of Mine Flooding in Closed Mines of the Pittsburgh Coal Basin, USA. 6th ICARD International Conference on Acid Rock Drainage 869-875

Donovan, J. J. and A. W. Rose (2001) Evolution and remediation of acid sulphate water associated with mining. Geochemistry: Exploration, Environment, Analysis 1 2

DPIWE (2005) TASVEG, the Tasmanian Vegetation Map, Tasmanian Spatial Data Dirrectory. DPIWE, Resource Management and Conservation

Driscoll, F. G. (1986) Groundwater and Wells. Johnson Division, St Paul, MN 1108

Drogue, C. (1998) Scale Effect on Rock Fissuration Porosity. Environmental Geology 11 (2):135-140

Dumpleton, S., N. S. Robins, J. A. Walker and P. D. Merrin (2001) Mine water rebound in South Nottinghamshire: risk evaluation using 3-D visualization and predictive modelling. Quarterly Journal of Engineering Geology and Hydrogeology 34 307-319

Dundon, P. J. (2000) Water in mining - where will it come from and where will it go to. After 2000 - The Future of Mining AusIMM Annual Conference 103-105

Durov, S. (1948) Natural Waters and graphical representation of their compositions. Dokl Akad Nauk SSSR 59 87-90

Dutrizac, J. S. and R. J. C. MacDonald (1974) Ferric iron as a leaching medium. Min.Sci.Eng 6 59-100

Dutton, A. R. and W. W. Simpkins (1989) Isotopic evidence for palaeohydrologic evolution of ground-water flow paths, Southern Great Plains, United States. Geology 17 (7):653-656

Earth Systems (1999) Remediation investigations and pilot works in the Zeehan mineral field. Earth Systems Pty Ltd.

East, S. (1999) Acid drainage and hydrogeology at the TME smelter site. University of Tasmania, Honours thesis: 195

ECGL (1998) Engineering Computer Graphics Laboratory , Groundwater modelling system reference manual (GMS v2.1). Brigham Young University, Provo, Utah, USA.

Edgar, G., N. Barrett and D. J. Graddon (1999) A classification of Tasmanian estuaries and assessment of their conservation significance using ecological and physical attributes, population and land use. Technical report series / Tasmanian Aquaculture & Fisheries Institute, University of Tasmania Taroona:

Edwards, P. (2003) Rosebery Tonnes and Grade. pers. comm.

Eggert, R. G. (1994) Mining and the environment: an introduction and overview. Mining and the environment : international perspectives on public policy. Resources for the Future (REF). 1-20

EGI (1996) Environmental Geochemistry International Geochemistry and acid forming potential of ore and waste rock in proposed mine extension. Australian Bulk Minerals Savage River Project. Environmental Geochemistry International Pty Ltd.

Eichinger, L., W. Rault, W. Stichler, B. Bertleff and R. Egger (1984) Comparative study of different aquifer types in Central Europe using environmental isotopes. Isotope Hydrology 271-289

Einstein, A.(1934) On the Method of Theoretical Physics Philosophy of Science. 1 (2):163

Eldridge, C., J. P. B. Barton and H. Ohomoto (1983) Mineral textures and their bearing on formation of the Kuroko orebodies. The Kuroko and Realted Volcanogenic Massive Sulphide Deposits, Economic Geology Monograph 241-281

El-Naqa, A. (2001) The hydraulic conductivity of the fractures intersecting Cambrain sandstone rock masses, central Jordan. Environmental Geology 40 973-982

Environment Agency (2002) Groundwater Resources Modelling: Guidance Notes & Template Project Brief. R&D Technical Report W213. Environment Agency (England & Wales).

Environment Australia (1997) Managing Sulphidic Mine Wastes and Acid Drainage. Environment Australia 79

Eriksson (1965) Deuterium and O18 in precipitation and other natural water: Some theoretical considerations. Tellus

EPA (1995) Environmental Protection Agency, Tailings Containment. Environmental Protection Agency 35

ESI (1997) Environmental Simulations Inc., Groundwater Vistas. Guide to Using.

ETS (1996a) Environmental & Technical Services, Pasminco Mining Rosebery environmental management plan. Rosebery Mine 178

ETS (1996b) Environmental & Tecnical Services Preliminary assessment of shallow groundwater quality. Rosebery Mine 25

ETS (2001) Environmental & Technical Services, Pasminco Mining Rosebery Environmental Management Plan for the calendar year October 1999 to September 2000. Rosebery Mine 57

Evangelou, V. P. (1995) Pyrite Oxidation and its Control. CRC Press New York

Evans, L. R. (2003) Mine inflow estimations provided complimentary to Pasminco Rosebery Mine. pers. comm.

Evans, L. R. (2005) Brockman BS2 Lower Hydrogeological Report. Pilbara Iron Tom Price:

Evans, L. R., D. Cooke, G. J. Davidson and G. Doherty (2004a) Regional and mine based hydrogeochemistry at the Pasminco Rosebery mine, western Tasmania, Australia. Water - Rock Interaction 1489-1492

Evans, L. R., G. J. Davidson and D. Cooke (2004b) Hydrogeochemistry at the Pasminco Rosebery mine, Tasmania. 17th Australian Geologic Convention Dynamic Earth: Past Present and Future Abstracts 73 13

Evans, L. R. and G. J. Davidson (2002) Recommendations for monitoring network at the Pasminco Rosebery Mine. pers. comm.

Evans, L. R., G. J. Davidson, D. Cooke and R. Willis (2003) Optimising Mining Data, With Emphasis on Rock Quality Designation, to Improve Groundwater Modelling of Fractured Rock Aquifers (Pasminco Rosebery Mine, Tasmania). Water in Mining 349-354

Ezzy, A. (1999) Groundwater resources within Tasmanian Jurassic dolerites. University of Tasmania, thesis:

Ezzy, A. (2006) MRT statewide groundwater monitoring network: Preliminary results for data collected between December 2003 and September 2005. Mineral Resources Tasmania Hobart: 44

Ezzy, A. R. and M. Latinovic (2005) MRT statewide groundwater monitoring network: Data collection - September 2004. Mineral Resources Tasmania Hobart: 58

FAO (2008) Sustainable Development Department, Food and Agriculture of the United Nations www.fao.org/sd/EIdirect/climate/EIsp0002.htm

Farina D. and A. Gaspari (1990) Application of the Kennessey method for the determination of the runoff coefficient and evaluation of aquifer recharge in mountain regions Hydrology in Mountainous Regions, Measurements; the Water Cycle (Proceedings of two Lausanne Symposia)

Feasby, D. G. and G. A. Tremblay (1995) New technologies to reduce environmental liability from acid generating mine waste. Sudbury '95 Mining and the Environment. 2 643-647

Ferguson, K. D. and P. M. Erickson (1988) Pre-mine prediction of acid mine drainage. Environmental Management of Solid Waste and Dredged Material and Mine Tailings 24-43

Ferris, J. G., D. B. Knowles, R. H. Brown and R. W. Stallman (1962) Theory of Aquifer Tests. United States Department of the Interior 69-174

Fetter, C. W. (2001) Applied Hydrogeology. Macmillan

Ficklin, W. H., G. S. Plumlee, K. S. Smith and J. B. McHugh (1992) Geochemical classification of mine drainages and natural drainages in mineralized areas. 7th International Symposium on Water-Rock Interactions

Finch, J. W. (1998) Direct groundwater recharge using a simple water-balance model-sensitivity to land surface parameters. Journal of Hydrology 211 (112-125):

Finucane, K. J. (1932) The Geology and Ore Depoists of the Rosebery District. University of Western Australia, Masters thesis: 123

Fitts, C., R. (2002) Groundwater Science. Academic Press London:

Forster, C. and L. Smith (1988) Groundwater flow system in mountainous terrain 2. Controlling factors. Water Resources Research 24 (7):1011-1023

Freeze, R. A. and J. A. Cherry (1979) Groundwater.

Freeze, R. A., J. Massmann, L. Smith, T. Sperling and B. James (1990) Hydrogeological decision analysis. 1. A framework. Ground Water 28 (55):738-766

French, P. (1986) The speciation and solubility of copper and cadmium in natural waters. Environmental Report 1226-M. Water Research Centre — Environment, Medmedham, UK

Frohlich, R.K., J.J. Fisher, and E. Summerly (1996) Electric-hydraulic conductivity correlation in fractured crystalline bedrock: Central Landfill, Rhode Island, USA. Journal of Applied Geophysics, 35 (11):249-259

GABCC (2002) Great Artesian Basin Consultative Council, Annual Report 2001-2002. 31

Gabler, H. E. and J. Scheidler (2000) Assessment of heavy-metal contamination of flooding soils due to mining and mineral processing in the Harz Mountains, Germany. Environmental Geology 39 (7):774-782

Gabr, M. A., B. JJ and R. MS (1994) Assessment of acid mine drainage remediation schemes on groundwater flow regimes at a reclaimed mine site. International Land Reclamination and

Mine Drainage Conference and Third International Conference on the Abatement of Acidic Drainage 168-177

Galileo Galilei (1610) Sidereus Nuncius: Venice, Italy, Thomas Baglionus.

Gallagher, M. R. and I. D. Hair (2003) Simulating the Interaction of Heavy Mineral Sands Mining With the North Stradbroke Island Groundwater System (Mining in Water). Water in Mining

Gandy, C. (2007) Dear Readers, Category Introduction. Mine Water and the Environment 26 (2):59

Gass, T., J. Lehr and H. J. Heiss (1977) Impact of abandoned wells on groundwater EPA-600/3-77-095. US Environmental Protection Agencey Washington DC:

Gat, J. R. (1971) Comments on the stable isotope method in regional groundwater investigations. Water Resources Research 7 980-983

Gat, J. R. (1996) Oxygen and hydrogen isotopes in the hydrological cycle. Annu. Rev. Earth Planet Sci. 24 225-62

Gates, W. C. B. (1997) The Hydro-Potential (HP) Value: A Rock Classification Technique for Evaluation of the Ground-Water Potential in Fractured Bedrock. Environmental and Engineering Geoscience 3 (2):251-267

Gburek, W. J., G. J. Folmar and J. B. Urban (1999) Field data and ground water modeling in a layered fractured aquifer. Ground Water 37 (2):175-184

Gemcom (2008) Gemcom Supac^{TM}, Gemcom Software International.

GHD (2001a) Gutteridge Haskins & Davey Pty Ltd, Tailings Dams and Water Retaining Structures. Pasminco Rosebery Mine Rosebery: 25

GHD (2001b) Gutteridge Haskins & Davey Pty Ltd, Pasminco Rosebery Dam Spillways. pers. comm.

GHD (2003) Gutteridge Haskins & Davey Pty Ltd, Info on Piezometers at Bobadil. pers. comm.

GHD (2007) Gutteridge Haskins & Davey Pty Ltd, K2 Nusa Halmahea, Kencana 2, Hydrogeological Site Assessment: 22

Gifkins, C. C. (2001) Submarine volcanism and alteration in the Cambrian, northern Central Volcanic Complex, western Tasmania. University of Tasmania, Hobart PhD thesis:

Gifkins, C. C. and R. L. Allen (2001) Textural and chemical characteristics of diagenetic and hydrothermal alteration in glassy volcanic rocks: example from the Mount Read Volcanics, Tasmania. Economic Geology 96 973-1002

Gilbert, L. and C. Fenton (2003) Water Refrom, Tradability and Understanding the Value of Water for Large-Scale Resource Projects. Water in Mining 67-70

Gilbert, S., D. Cooke and P. Hollings (2003) The effects of hardpan layers on the water chemistry from the leaching of pyrrhotite-rich tailings material. Environmental Geology 44 687–697

Giudici, C., A. Scanlon, J. Miedecke, T. Duckett, P. Burgess, A. Love, I. Irvine, J. Canterford and P. Waggitt (1996) Remediation options for tailings deposits in the King River and Macquarie Harbour. Mount Lyell Remediation Research and Demonstration Program, Supervising Scientist Report 119 Supervising Scientist Canberra: 74

Google (2006) Google Earth. www.earth.google.com

Gray, N. (1997) Environmental impact and remediation of acid mine drainage: a management problem. Environmental Geology 30 62-71

GRC (1985) Groundwater Resource Consultants, Preliminary Evaluation Groundwater Regime - Mine Dewatering North Bassett Area. Renison Limited Renison: 21

Green, G. (1990) Alteration mineralogy, whole rock geochemistry and oxygen isotope zonation in the area north of the Grand Centre Prospect, Rosebery Mine Leases-A report for Pasminco Mining Rosebery. Mines Consultancy Services Hobart

Green, G. R. (1983) The geological setting and formation of the Rosebery volcanic-hosted massive sulphide orebody, Tasmania. University of Tasmania, Hobart thesis

Green, G. R., M. Solomon and J. L. Walshe (1981) The formation of the volcanic-hosted massive sulfide ore deposit at Rosebery, Tasmania. A special issue on the geology and mineral deposits of Tasmania. 76 (2):304-338

Groves, D. I. and G. Loftus-Hills (1968) Cadmium in Tasmanian Sphalerites. Proceedings - Australasian Institute of Mining and Metallurgy 228: 43-51

Gurung, S. (2002) Tasmanian Acid Drainage Reconnaissance. 1. Acid drainage from abandoned mines in Tasmania. Mineral Resources Tasmania Hobart: 99

Gurung, S. (2003) Tasmanian Acid Drainage Reconnaissance — Acid Drainage From Abandoned Mines in Tasmania. ICARD 1035-1038

Gutmanis, J. C., G. W. Lanyon, T. J. Wynn and C. R. Watson (1998) Fluid flow in faults: a study of fault hydrogeology in Triassic sandstone and Ordovician volcaniclastic rocks at Sellafield, north-west England. Proceedings of the Yorkshire Geological Society 52 159-175

Hair (2003) Groundwater Issues in the Mining Industry. Water in Mining 173-178

Hale, C. T. (2001) Acid mine drainage at Rosebery Pb-Zn mine, Tasmania. University of Melbourne, Melbourne Master of Environmental Science and Hydrogeology thesis: 110

Halford, K. J. (1997) Effects of unsaturated zone on aquifer test analysis in a shallow-aquifer system. Ground Water 35 (3):512-522

Hall, G., V. M. Cottle, P. B. Rosenhain and R. R. McGhie (1953) The lead-zinc deposits of Read-Rosebery and Mount Farrell. Geology of Australian Ore Deposits 1145-1159

Hall, G., V. M. Cottle, P. B. Rosenhain, R. R. McGhie and J. G. Druett (1965) Lead-zinc deposits of Read-Rosebery. Geology of Australian Ore Deposits 1: 8th Commonwealth Mining & Metallurgical Congress

Hall, G. and M. Solomon (1962) Metallic mineral deposits. The Geology of Tasmania. Journal of the Geological Society of Australia 9 (285-309):

Hammarstrom, J. M., P. L. Sibrell and H. E. Belkin (2003) Characterization of limestone reacted with acid-mine drainage in a pulsed limestone bed treatment system at the Friendship Hill National Historical Site, Pennsylvania, USA. Applied Geochemistry 18 1705-1721

Hanna, G., R. Lucas, E. Randles, R. Smith and A. Brant (1963) Acid mine drainage research potentialities. J. Water Pollution Control Fed. 35 275

Harbaugh, A., B. Edward, M. C. Hill and M. McDonald (2000) MODFLOW-2000, The U.S. Geological Survey Modular Ground-Water Model - User Guide to Modularization Concepts and the Ground-Water Flow Process, Open-File Report 00-92. Reston-Virginia: 121

Harcourt Smith (1898) Report on the Mineral Fields in the Neighbourhood of Mt Black, Ringville, Mt Read and Lake Dore.

Harris, D. L., B. G. Lottermoser and J. Duchesne (2003) Ephemeral acid mine drainage at the Montalbion silver mine, north Queensland. Australian Journal of Earth Sciences 50 797–809

Hassan, A. E. (2003) A Validation Process for the Groundwater Flow and Transport Model of the Faultless Nuclear Test at Central Nevada Test Area. National Nuclear Security Administration Las Vegas: 86

Hatton, T. and R. Evans (1998) Dependence of Ecosystems on Groundwater and its Significance to Australia. Land and Water Resources Research and Development Corporation 81

HDMS (2000) Hope Downs Management Services Pty Ltd, Hope Downs Iron Ore Project – Public Environmental Review, August 2000 (unpublished).

HDMS (2001) Hope Downs Management Services Pty Ltd, Report and recommendations of the Environmental Protection Authority.

Heathcote, J. A., M. A. Jones and A. W. Herbert (1996) Modelling groundwater flow in the Sellafield area. Quarterly Journal of Engineering Geology 29 S59-S81

Hekman, A. (2000) solvers. http://www.bossintl.com/forums

Henley, K. J. and B. G. Stevenson (1978) The nature and position of precious metals in Rosbery ore. Geology and mineralization of Northwest Tasmania 14-15

Henton (1981) The problem of ground water table rebound after mining activity and its effects of ground and surface water quality. Quality of Groundwater

HGM (1997) Henty Gold Mine Environmental Management Plan. NSR Environmental Consultants Pty Ltd.

Hill, M. C. (1990) Solving Groundwater Flow Problems by Conjugate-Gradient Methods and the Strongly Implicit Process. Water Resources Research WRERAQ 26 (9):1961-1969

Hill, M. C. (1998) Methods and Guidelines for Effective Model Calibration. USGS Water-Resources Investigations Report 98-4005. 90

Hill, M. C., E. R. Banta, A. W. Harbuagh and E. R. Anderman (2000) MODFLOW-2000, The U.S. Geological Survey modular ground-water model-user guide to the observation, sensitivity, and parameter-estination process and three post-processing programs. The U.S. Geological Survey Denver, Colorado, 219

Hillier, J. R., J. R. Kellett, L. M. Foster and G. A. McMahon (2003) The Great Artesian Basin — Use and Sustainability. Water in Mining 71-80

Hoefs, J. (1997) Stable Isotope Geochemistry. Springer 201

Hoek, E. and E. T. Brown (1980) Underground Excavation in Rock. The Institution of Mining and Metallurgy

Hofrichter, J. and G. Winkler (2006) Statistical analysis for the hydrogeological evaluation of the fracture networks in hard rocks, Environmental Geology 49 (6):821-827

Hsieh, P. and S. P. Neuman (1985) Field determination of the three-dimensional hydraulic conductivity tensor of anisotropic media 1. Theory. Water Resources Research 21 (11):1655-1665

Huston, D. L. (1988) Aspects of the Geology of Massive Sulphide Deposits from Balcooma District, Northern Queensland and Rosebery, Tasmania: Implications for Ore Genesis. University of Tasmania, thesis: 380

Huston, D. L. and R. Large Ross (1989) A chemical model for the concentration of gold in volcanogenic massive sulphide deposits. Ore Geology Reviews 4 171-200

Huston, D. L. and R. R. Large (1988) Distribution, mineralogy, and geochemistry of gold and silver in the north end orebody, Rosebery, Tasmania. Economic Geology and the Bulletin of the Society of Economic Geologists 83 (6):1181-1192

Huston, D. L., S. H. Sie, G. F. Suter, D. Cooke and R. A. Both (1995) Trace elements in sulphide minerals from eastern Australian volcanic-hosted massive sulphide deposits. Economic Geology 90 1167-1196

Huston, D. L., S. H. Sie, G. F. Suter and C. G. Ryan (1993) The concentrations of pyrite in vulcanogenic massive sulphide deposits as determined with the proton microprobe. Nuclear Instruments and Methods in Physics Research B75 531-534

Hvilshoj, S. (1998) Estimation of Ground Water Hydraulic Parameters. Technical University of Denmark, PhD thesis: 108

Hvorslev, M. J. (1951) Time lag and soil permeability in groundwater observations. U.S. Army Coprs of Engineers Waterway Experimentation Station, Bulletin 26

Hydrogeologic Inc. (1996) MODFLOW-Surfact software (Version 2.2): Overview, Installation, Registration and Running Procedures. Hydrogeologic Inc, Herndon, VA, USA:

Hydstra (2004) Hydstra Database. Hydro Tasmania

IEAust (1987) Institution of Engineers Australia, Australian Rainfall and Runoff, A Guide to Flood Estimation (Revised Edition) 2 volumes.

Infomine (2008) Map.Infomine viewer. http://www.infomine.com/maps/

Jackson, C., A. Hoch and S. Todman (2000) Self-consistency of a heterogeneous continuum porous medium representation of fractured media. Water Resources Research 36 (1):189-202

Jaeger, J. C. and J. H. Sass (1963) Lee's Topographic Corrections in Heat Flow and the Geothermal Flux in Tasmania, Pure and Applied Geophysics 54 (1):53-63

Jakubick, A. T., U. Jenk and R. Kahnt (2002) Modelling of mine flooding and consequences in the mine hydrogeological environment: flooding of the Koenigstein mine, Germany. Environmental Geology 42 (2-3):222-234

Jamieson, G. and R. A. Freeze (1983) Determining Hydraulic Conductivity Distributions in a Mountainous Area Using Mathematical Modelling. Ground Water 21 (2):168-177

Johnson, S. L. and D. P. Commander (2003) Groundwater utilisation by the mining industry in arid Western Australia. Water in Mining 179-185

Johnson, S. L. and A. H. Wright (2003) Mine void water resource issues in Western Australia: Western Australia, Water and Rivers Commission, Hydrogeological Record Series, Report HG 9. 93

Jyrkama, M. I., J. F. Skyes and S. D. Normani (2002) Recharge Estimation for Transient Groundwater Modeling. Ground Water 40 (6):

Kahn, K.G., S. Ge, S. J. Caine and A. Manning (2008) Characterization of the shallow groundwater system in an alpine watershed: Handcart Gulch, Colorado, USA. Hydrogeology Journal 16 (1) 103-122

Kaufman, G. B. and C. A. Ferguson (1988) The endothermic dissolution of ammonium nitrate. Journal of Chemical Education 65 (2):267

Kent, S., D. Ray, B. Hutchison, and R. Dineen, (2008) Savage River Rehabilitation Project: Strategic Plan http://www.minerals.org.au/__data/assets/pdf_file/0008/5993/3A-2RayDaniel.pdf

Khan, S., T. Rana, J. Carroll, B. Wang and L. Best (2004) Managing Climate, Irrigation and Ground Water Interactions using a Numerical Model: A Case Study of the Murrumbidgee Irrigation Area. CSIRO Land and Water Technical Report

Khin Zaw (1991) Rosebery-Herclues. University of Tasmania, Hobart PhD thesis:

Khin Zaw and R. R. Large (1996) Petrology and Geochemistry of Sphalerite from the Cambrian VHMS deposits in the Rosebery-Hercules district, western Tasmania: implications for gold mineralisation and metamorphic-metosomatic processes. Mineralogy and Petrology 57 97-118

Kidd, C. H. (1997) Implementing an effective water management system for efficient mine production. Mine Water Management Conference

Kim, Y.Y. and K.K. Lee (2003) Disturbance of groundwater table by subway construction in the Seoul area, Korea. Geosciences Journal 7 (1):37-46

Kirkpatrick, J. B. (1997) The Alpine Flora and Vegetation of Tasmania. OUP Australia and New Zealand

Kirkpatrick, J. B. and S. Backhouse (1981) Native Trees of Tasmania. Hobart:

Kirkpatrick, J. B. and S. Backhouse (2004) Native Trees of Tasmania. Hobart:

Kitterod, N. O., H. Colleuille, W. K. Wong and T. S. Pedersen (2000) Simulation of groundwater drainage into a tunnel in fractured rock and numerical analysis of leakage remediation, Romeriksporten tunnel, Norway. Hydrogeology Journal 8 480-493

Klusman, R. W. and K. W. Edwards (1977) Toxic metals in ground water of the Front Range, Colorado. Ground Water 15 (2):160-169

Koehnken, L. (1992) Pieman River environmental monitoring programme technical report.

Koehnken, L. (1997) Final Report. Mount Lyell Remediation Research and Demonstration Program. Supervising Scientist Report 126 (Supervising Scientist: Canberra).

Koehnken, L. (2006) Ground water quality near 2 and 5 dams & Bobadil tailings dam, A report to ZRM. Technical Advice on Water 22

Koeppen W. (1931) Grundriss der Klimakunde. Berlin: De Gruyer.

Kostoglou, P. (2000) An archaeological survey of historic mine sites in the Pasminco Mineral Lease, Rosebery. 25

Kulatilake, P. H. S. W. and B. B. Panda (2000) Effect of Block Size and Joint Geometry on Jointed Rock Hydraulics and REV. Journal of Engineering Mechanics 126 (8):850-858

Lacombe, S., E. Sudicky, S. Frape and A. Unger (1995) Influence of leaky boreholes on cross-fotmational groundwater flow and contaminant transport. Water Resources Research 31 1871-1882

Ladiges, S. (1995) Heavy metal levels in stream waters, vegetation, soil and soil solutions in an evolving wetland, Zeehan, Tasmania. University of Tasmania, Hobart B.Sc. (Hons) Thesis:

Langmuir, D. (1997) Aqueous Environmental Geochemistry. Prentice Hall New Jersey: 600

Lapakko, K. A. (2002) Metal Mine Rock and Waste Characterization Tools: An Overview. Minesota Department of Natural Resources, US 31

Large, R. R. (1992) Australian volcanic-hosted massive sulphide deposits: features, styles, and genetic models. Economic Geology 87 471-510

Lawrence, J. S. (1996) Environmental geology of the Dundas drainage basin. University of Tasmania, Hobart B.Sc. (Hons.) Thesis:

Lawrence, R. W., S. Jaffe and L. M. Broughton (1988) In-House Development of the Net Acid Production Test Method. Coastech Research

Lawrence, R. W. and Y. Wang (1997) Determination of Neutralization Potential in the Prediction of Acid Rock Drainage. 4th International Conference on Acid Rock Drainage 449-464

Leaman, D. E. (1971) The Geology and Groundwater Resources of the Coal River Basin. Mineral Resources of Tasmania 1971: 88

Leaman, D. (2004) Issues of water management in Tasmania, Leaman Geophysics

Lee, C.-H., W.-P. Chen and R.-H. Lee (2006) Estimation of groundwater recharge using water balance coupled with base-flow-record estimation and stable-base-flow analysis. Environmental Geology 51 73-82

Lees, T., K. Zaw, R. R. Large and D. L. Huston (1990) Rosebery and Hercules copper-lead-zinc deposits. Geology of the mineral deposits of Australia and Papua New Guinea; Volume 2. 14 1241-1247

Leemans, R. and Cramer, W. (1991) The IIASA database for mean monthly values of temperature, precipitation and cloudiness on a global terrestrial grid. Research Report RR-91-18 International Institute of Applied Systems Analyses. 61

Lett, R., W. Jackaman and S. Sibbick (1996) Spring water and spring sediment geochemistry of the Gataga Mountain Area. B.C. Ministry of Energy, Mines and Petroleum Resources.

Lieth, H., 1972. Modelling the primary productivity of the earth. Nature and resources, UNESCO, 8 (2):5-10.

Liquid Earth (2005) Marandoo Hydrogeological Investigation Report, Pilbara Iron Pty. Limited, unpublished consultant report.

Loftus Hills (1915) The zinc lead sulphide deposits of the Read-Rosebery District. Part 2 Rosebery Group. Geological Survey Bulletin, Tasmanian Department of Mines. 23

Loftus Hills, G. (1968) Copper, nickel and selenium in Tasmanian ore minerals. University of Tasmania, thesis:

Loftus Hills, G., M. Solomon and R. J. Hall (1967) The structure of the bedded rocks west of Rosebery, Tasmania. Journal of the Geological Society of Australia 14 Part 2 333-337

Logan, A. S. and D. O'Toole (1996) Shaft Assessment and Excavation Lessons from Rosebery Mine Southern Upcast Shaft. IX Australian Tunneling Conference, 437-446

Long, J., P. Gilmor and P. Witherspoon (1985) A model for steady fluid flow in random 3-D network of disc shaped fractues. Water Resources Research 21 (8):1105-1115

Long, J. C. S., J. Remer, C. Wilson and P. Witherspoon (1982) Porous Media Equivalents for Networks of Discontinuous Fractures. Water Resources Research 18 645-658

Lottermoser, B. (2003) Mine Wastes: Charcterisation, Treatment and Environmental Impacts. Springer Heidelberg, Germany: 277

Lottermoser, B., P. M. Ashley and D. C. Lawrie (1999) Environmental Geochemistry of the Gulf Creek copper mine area north-eastern New South Wales, Australia. Environmental Geology 39 (1):61-74

Lui, J., D. Elsworth and B. Brady (1999) A coupled hydromechanical system defined through rock mass classification schemes. Int. J. Numer. Anal. Meth. Geomech. 23 1945-1960

Marquínez, J., J. Lastra and P. García (2003) Estimation models for precipitation in mountainous regions: the use of GIS and multivariate analysis, Journal of Hydrology 270 (1-2):1-11

Marszalek, H. and H. Wasik (2000) Influence of arsenic-bearing gold deposits on water quality in Zloty Stok mining area (SW Poland). Environmental Geology 39 (8):888-892

Martin, N. K. (2004) Genesis of the Rosebery massive sulphide deposit, western Tasmania, Australia. University of Tasmania, unpublished Hobart thesis: 273

Mathews, W. L. (1983) Geology and Groundwater Resources of the Longford Tertiary. Mineral Resources Tasmania Hobart: 151

Mayo, A. L., P. J. Nielsen, M. Loucks and W. H. Brimhall (1992) The Use of Solute and Isotopic Chemistry to Identify Flow Patterns and Factors Which Limit Acid Mine Drainage in the Wasatch Range, Utah. Ground Water 30 (2):243-249

Mayer, J. R. and J. M. J. Sharp (1998). Fracture control of regional ground-water flow in a carbonate aquifer in a semi-arid region. GSA Bulletin 110 (2): 269-283.

MCA (2000) Minerals Council of Australia, Mine Closure Guidance Note. Commonwealth of Australia Canberra: 5

McDonald, I. R. (1984) Orientation sampling of the Rosebery open cut. Mineral exploration and tectonic processes in Tasmania; abstract volume and excursion guide. 39

McDonald, M. and A. Harbaugh (1984) MODFLOW, A modular three dimensional finite difference ground-water flow model, U. S. Geological Survey, Open-file report 83- 875.

McDonald, M. and A. Harbaugh (1988) MODFLOW, A modular three dimensional finite difference ground-water flow model, U. S. Geological Survey Techniques of Water-Resource investigations. Book 6, Chapter A2 586

McDonald, M. and A. Harbaugh (2003) The history of MODFLOW. Ground Water 41 280–283

McDougall, T. (1984) Fluid dynamic implications for massive sulphide deposits of hot saline fluid flowing into a submarine depression from below. Deep Sea Research 31 (2):145-170

McHaina, D. M. (2001) Environmental planning considerations for the decommissioning, closure and reclamation of a mine site. International Journal of Surface Mining Reclamation and Environment 15 (3):163-176

McNeill, A. (2006) Rosebery geological advice. pers. comm.

Mehl, S. and M. Hill (2001) User Guide to the Link-AMG (LMG) Package for Solving Matrix Equations Using an Algebraic Multigrid. US Dept. of the Interior, US Geological Survey: US Geological

Merrick, N. P. (1997) Modelling of the groundwater impacts of a new underground railway through an urban area. Groundwater in the Urban Environment : Problems and Management 249

Meskanen, U. (1998) Acid Mine Drainage at the Comstock Ag-Pb-Zn Mine, Western Tasmania. University of Tasmania, Hobart Hons thesis:

Meyboom, P. (1961) Estimating groundwater recharge from stream hydrographs. Journal of Geophysical Research 66 1203-14

Meynink, W. J. C. (1996) Integrated Modelling of Minesite Runoff and River flows. 3rd International 21st Annual Minerals Council of Australia Environmental Workshop 17-25

MICL (2003) Datamine Studio Version 2.0.1313.0 © Mineral Industries Computing Limited 1983 – 2003

Middlemis, H. (1997) Century Mine Dewatering - Groundwater flow modelling to reduce capital cost. Mine Water Management Conference

Middlemis, H. (2000) Groundwater Flow Modelling Guideline. Murray-Darling Commission, Aquaterra Consulting Pty Ltd Perth: 72

Miedecke, J. (1996) Mount Lyell remediation: Remedial options to reduce acid drainage from historical mining operations at Mount Lyell, Western Tasmania. Supervising Scientist, Canberra:

Miedecke, J. (2002) Storys Creek Acid Drainage Remediation. Anoxic Limestone Drain Construction Report. Mineral Resources Tasmania Hobart: 7

Miller, S., J. Andrina and D. Richards (2003) Overburden Geochemistry and Acid Rock Drainage Scale-Up Investigations at the Grasberg Mine, Papua Province, Indonesia. ICARD

Miller, S., A. Robertson and T. Donahue (1997) Advances in Acid Drainage Prediction using the Net Acid Generation (NAG) Test. 4th International Conference on Acid Rock Drainage 533-549

Milligan, I. G., W. J. Huxley and M. Roche (2003) A Mine and its Neighbours — Delivering Sustainable Water Resource Management. Water in Mining 81-84

Mills, C. (1993) Intermin and final report technical review of interim policy for for acid rock drainage at minestites. Ministry of Energy, Mines and Petroleum Resources, West Coast Environmental Law Association. Vancouver, B.C.:

Mills, C. (1995) A Introduction to Acid Rock Drainage.

Milnes, A. R. (2002) A review of the key issues in mine environmental management, decommissioning and rehabilitation: case studies at Ranger and Jabiluka. The AusIMM Bulletin (5):

Min, K.-B. (2002) Determination of equivalent hydraulic and mechanical properties of fractured rock masses using the Distinct Element Method. Stockholm thesis:

Modflow (2006) www.Modflow.com.

Molinerio, J., J. Samper, and R. Juanes (2002) Numerical modeling of the transient hydrogeological response produced by tunnel construction in fractured bedrocks, Engineering Geology 64 (4): 369-386

Montgomery, A. (1895) Report on the progress of the mineral field in the neighbourhood of Zeehan. Report for the Secretary of Mines 1984-5.

Moore, W. R. (1977) The groundwater potential of north-eatern Tasmania. Mineral Resources Tasmania Hobart: 3

Morgan (2004) Quote on the installation of piezometers at Rosebery. pers. comm.

Morgan, K. H. (2003) Recording and Usage of Groundwater Data for a Mining Operation. 5th International Mining Geology Conference

Morin, K. and N. Hutt (1997) Environmental geochemistry of mine drainage. MDAG Publishing Vancouver:

Morrison, K. C. (1992) Trace Element Geochemistry of some Tasmanian Stream Waters: Using ICPMS (SEMI-QUANTITATIVE MODE). University of Tasmania, Hobart Matser of Economic Geology thesis: 56

Morrison, K. C. (1993) Stream Water Geochemistry Trial Mt Read Area Janurary - June 1993. Pasminco Exploration 17

Morrison, K. C. and M. Blake (2006) Report on Environmental Water Bore Drilling Project. Zinifex Ltd Rosebery Mine. 2/5 Bobadil Tailings Dams

Morton, F. I. (1983) Operational estimates of areal evapotranspiration and their significance to the science and practice of hydrology. Journal of Hydrology 66 1-76

Maptek (2004) Maptek Proprietary Limited, Vulcan 5.0 © Maptek Proprietary Limited

MRT (2002a) Mineral Resources Tasmania, MIRLOCH (Mineral deposits database). Mineral Resources Tasmania

MRT (2002b) Mineral Resources Tasmania TASGEOL (Rock Unit Database). Mineral Resources Tasmania

MRT (2002 c) Mineral Resources Tasmania, ROCKCHEM (Whole-Rock and Mineral Chemistry Database). Mineral Resources Tasmania

MRT (2002 d) Mineral Resources Tasmania, BORIS (Groundwater Quality and Borehole Database). Mineral Resources Tasmania

MRT (2002e) Mineral Resources Tasmania http://www.mrt.tas.gov.au/portal/page?_pageid=33,38234&_dad=portal&_schema=PORTAL. Mineral Resources Tasmania

MRT (2002f) Mineral Resources Tasmania, www.mrt.gov.tas.au. Mineral Resources Tasmania

MWH (2006) Marandoo Model Development 2006, Pilbara Iron, unpublished consultant report prepared by Youngs, J. and Milligan N..

NASA (2006) NASA Worldwind 1.3. Landsat Image, www.worldwind.arc.nasa.gov

Naschwitz, W. (1985) Geochemistry of Rosebery Ore Deposit. University of Tasmania, PhD thesis: 276

Naschwitz, W. and J. C. van Moort (1991) Geochemistry of wallrock alteration, Rosebery, Tasmania, Australia. Applied Geochemistry 6 (3):267-278

Neuzil, C.E. (1986) Groundwater Flow in Low-Permeability Environments, Water Resources Research WRERAO 22 (8) 1163-1195

NGC (2004) National Groundwater Committee, Improved management and protection of groundwater dependent ecosystems, Issue paper 2, National Groundwater Committee, Department of the Environment and Heritage, 2004 http://www.environment.gov.au/water/groundwater/committee/issue-2/index.html Cited 12 Feb 2007.

Nix, H. (1986) A biogeographic analysis of Australian Elapid Snakes. Atlas of Elapid Snakes of Australia Australian Flora and Fauna Series Number 7 415

NLWRA (2001) National Land and Water Resources Audit 2001, Australian Natural Resource Atlas, http://audit.ea.gov.au

Nordstrom, D. K., E. A. Jenne and J. W. Ball (1979) Chemical Modeling in Aqueous Systems. Chemical Modeling in Aqueous Systems 51-79

Novakowski, K. (1990) Analysis of aquifer tests conducted in fractured rock: A review of the physical background and design of a computer program for generating type curves. Ground Water 28 (1):99-107

Nunez, M., J. B. Kirkpatrick and C. Nilsson (1996) Rainfall estimation in south-west Tasmania using satellite images and phytosociological calibration. International journal of remote sensing 17 (8):1583-1600

Nye, P. B. (1921) The Undeground Water Resources of the Midlands. Mineral Resources Tasmania Hobart: 139

Oosting, N. L. (1998) Rehabilitation of abandoned mine sites in the Zeehan area. University of Tasmania, Hobart B.Sc. (Hons) Thesis thesis:

Oreskes, N., K. Shrader-Freshette and K. Belitz (1994) Verification, validation, and confirmation of numerical models in the earth sciences. Science (263):641–646

Osborne, P. S. (1993) Suggested Operating Procedures for Aquifer Pumping Tests. Ground Water Issue (EPA/540/S-93/503):

Osiensky, J. L. and R. E. Williams (1997) Potential inaccuracies in MODFLOW simulations involving the SIP and SSOR methods for matrix solution. Ground Water 35 (2):229-232

O'Toole, D. (2008) Comment on water inflows at Rosebery. pers. comm.

OZ Minerals, (2008) OZ Minerals, Home. www.ozminerals.com

Pankow, J., R. Johnson, J. Heweston and J. A. Cherry (1986) An evaluation of Contaminant Migration Patterns at Two Waste Disposal Sites on Fractured Porous Media in Terms of the Eqivalent Porous Media (EPM) Model. Journal of Contaminant Hydrology 1 (65-76):

Parks and Wildlife (1990) Climate grids of Tasmania.

Parr, T. (1997) Acid mine drainage in the Zeehan District. University of Tasmania, Hobart B.Sc. (Hons) Thesis thesis:

Pasminco (2003) Aerial photograph of the Rosebery mine.

Pasminco Exploration, University of Melbourne and Fractal Graphics (2002) Pasminco-Fractal Graphics western Tasmanian modeling. PRM

Pasminco Limited (2003) Environemental Management Plan. Pasminco Rosebery Mine Rosebery:

PRM (1996) Environmental improvement program for the Hercules mine. Pasminco Rosebery Mine

PRM (1998) Pasminco Rosebery Mine, Draft environmental improvement program for the Hercules mine, Williamsford, Tasmania. Pasminco Rosebery Mine

PRM (2002) Pasminco Rosebery Mine, Access Geochemical Database. PRM

PRM (2003a) Pasminco Rosebery Mine, Datamine Mine Model. PRM

PRM (2003b) Pasminco Rosebery Mine, Datamine Drillhole Database. PRM

PRM (2003c) Pasminco Rosebery Mine, Datamine Geology Cross Sections. PRM

PRM (2003d) Pasminco Rosebery Mine, Catastrophic Risk Management Program Inrush Risk Assessment.

PRM (2004) Pasminco Rosebery Mine, Access Geochemical Database. PRM

Paulson, A. J. and L. Balisrieri (1999) Modelling Removal of Cd, Cu, Pb, and Zn in Acidic Groundwater during Neutralization by Ambient Surface Waters and Groundwaters. Environmental Science & Technology 33 (21):3850-3856

Perkins, E. H., H. W. Nesbitt, W. D. Grunter, L. C. St-Arnaud and J. R. Mycroft (1995) Critical review of geochemical processes and geotechnical models adaptable for prediction of acidic drainage waste rock. Mine Environment Neutral Drainage (MEND) Program Prediction Committee

Petrides, B., I. Cartwright and T. R. Weaver (2004) The evolution of groundwater in the Tyrrell region, south-central Murray Basin, Victoria, Australia. Water - Rock Interaction 481-484

Phipps, G. C., D.R. Boyle, I.D. Clark (2004) Groundwater geochemistry and exploration methods: Myra Falls volcanogenic massive-sulphide deposits, Vancouver Island, British Columbia, Canada. Geochemistry: Exploration, Environment, Analysis, 4 (4):329-340

Piper, A. M. (1944) A graphical procedure in the geochemical interpretation of water anlyses. Trans. Amer. Geophys. Union 25 914-923

Plumlee, G. S. (1995) The environmental geology of mineral deposits. The Environmental Geochemistry of Mineral Deposits-Part A; Processes, methods, and health issues 6A

Pohll, G., A. E. Hassan, J. B. Chapman, C. Papelis and R. Andricevic (1999) Modeling ground water flow and radioactive transport in a fractured aquifer. Ground Water 37 (5):770-784

Pollock, D. W. (1994) User's guide for MODPATH/MODPATH-PLOT, version 3: A particle tracking post processing package for MODFLOW, the U.S. Geological Survey finite-difference ground-water flow model, Open-File Report 94-464. U.S. Geological Survey 249

Polya, D. A., M. Solomon, C. J. Eastoe and J. L. Walshe (1986) The Murchison Gorge, a possible cross section the a Cambrian massive sulphide system. Economic Geology 81 1341-1355

Pope, J. and Craw, D. (2008) CRL Energy LTD. Mine Drainage (AMD) Objective 1: Geochemistry http://www.crl.co.nz/research/MDObjective1.asp

Price, W. A., K. Morin and N. Hutt (1997) Guidelines for the Prediction of Acid Rock Drainage and Metal Leaching for Mines in British Columbia: Part II - Recommended Procedures for Static and Kinetic Testing. 4th International Conference on Acid Rock Drainage 15-30

Pulles, W. (1992) Water pollution: its management and control in the South African gold mining industry. Journal of the Mine Ventilation Society of South Africa 45 (2):18-36

Punthakey, J. F., S. A. Prathapar, N. M. Somaratne, N. P. Merrick, S. Lawson and R. M. Williams (1995) Modelling impacts of regional development and environmental change in the Lower Murrumbidgee River Basin. Water Resources and Ecology 3 29-34

Pwa, A., W. Naschwitz, M. Hotckins and J. C. van Moort (1992) Exploration rock geochemistry in the Rosebery mine area, western Tasmania. Tasmanian Department of Mines, Geological Survey Bulletin 70 (7-16):

Rapantova, N., A. Grmela, D. Vojtek, J. Halir and B. Michalek (2007) Ground Water Flow Modelling Applications in Mining Hydrogeology. Mine Water and the Environment Online First October: 7

RPDC (2003)Resource Planning and Development Commission, State of the Environment (SoE) Tasmania 2003, http://soer.justice.tas.gov.au/2003/index.php

Rehfeldt, K., J. Boggs and L. Gelhar (1992) Field study of dispersion in heterogeneous aquifer, 3. Geostatistical analysis of hydraulic conductivity. Water Resources Research 28 (12):3309-3324

Reid, E. I. (1998) Some key equations of ground water modelling simply explained. Tailings and mine waste '98; proceedings of the Fifth international conference. 5 481-490

Reid, J. (2004) Rosebery tailings dam geophysics projects. pers. comm.

Reid, J. B. and et al. (1988) Vegetation of Tasmania. Australian Biological Resources Study, 1999 Canberra:

Reid, K. and R. Meares (1981) Exploration for volcanic-hosted sulfide deposits in western Tasmania. Economic Geology 76 (2):350-364

Reilly, T., O. Franke and G. Bennett (1989) Bias in groundwater flow caused by wellbore flow. Journal of Hydraulic Engineering 115 270-276

Reilly, T. E. (2001) System and Boundary Conceptualization in Ground-Water Flow Simulation Chapter B8. Techniques of Water-Resources Investigations of the United States Geological Survey Book 3 Applications of Hydraulics

Renison (1995) Environmental Management Plan. NSR Environmental Consultants Pty Ltd.

Ripley, E. A., R. E. Redmann and A. A. Crowder (1996) Environmental effects of mining. St. Lucie Press Delray Beach, Florida:

Ritchey, J. and J. Rumbaugh (1996) Subsurface fluid flow (ground-water and vadose zone) modeling. ASTM Special Technical Publication1288.

Rio Tinto (2007) Closure and Legacy http://www.riotinto.com/ourapproach/5204_closure_legacy.asp.

Robertson, A. (1999) An investigation of stratergies used overseas for the environmental management of sulphidic mine wastes. Acid Drainage

Roche, M. (2002) Stewardship and the Great Artesian Basin: the Cannington perspective. GAB FEST 2000

Röhrich, T. and Waterloo Hydrologic Inc (2001) User's Guide for AquiferTest, The intuitive aquifer test analysis package.

Rojstaczer, S. (1987) The local effects of groundwater pumpage within a fault-influenced groundwater basin, Ash Meadows, Nye County, Nevada U.S.A. Journal of Hydrology 91 (3-4):319-337

Rorabaugh, M. I. (1964) Estimating changes in bank storage and ground-water contribution of stream flow. International Association of Scientific Hydrology 63 432-41

RPDC (2003) Resource Planning and Development Commission 2003, State of the Environment Tasmania 2003, http//www.rpdc.tas.gov.au/soer

Russell, D. W. and J. C. Van Moort (1981) Biogeochemistry and pedogeochemistry of the White Spur area, near Rosebery, Tasmania. Economic Geology 76 (2):339-349

RUST PPK (1994) Regional simulation of cumulative impacts arising from groundwater abstractions in the Great Artesian Basin. RUST PPK Consultants, Rhodes, NSW.

Sainty, R. A. (1986) Volcanic stratigraphy and a speculative model for the Rosebery Deposit. The Mount Read volcanics and associated ore deposits. 75-80

Sandford, W. (2002) Recharge and groundwater models: an overview. Hydrogeology Journal 2002 (10):110-120

Sansom, P. W. (1978) The glacial geomorphology of the Tullah area. University of Tasmania, Hobart Honours thesis:

Scanlon (1990) Behind the Scenery, Tasmania's landforms and geology. Department of Education and The Arts 163

Scanlon, B. R., R. W. Healy and P. G. Cook (2002) Choosing appropriate techniques for quantifying groundwater recharge. Hydrogeology Journal (10):18-39 347

Schmelling, S. and R. R. Ross (1989) Contaminant Transport in Fractured Media: models for Decision Makers. Ground Water Issue 8

Schoeenfeld, E. and T. Pfaff (1990) Methods of testing and developing the results of hydrogeological field work by mathematic modelling at the Asse II Saltmine. Water resources in mountainous regions. 22 Part 1-2 1344-1354

Schwartz, F. and L. Smith (1988) A continuum approach for modelling mass transport in fractured media. Water Resources Research 24 (8):1360-1372

Scott, C. (2008) Comments on the calculation of RQD pers. comm.

Seal, R. R. (2003) Stable-isotope geochemistry of mine waters and related solids. Environmental Aspects of Mine Wastes 31 303 - 334

Seal, R. R. and J. M. Hammarstrom (2003) Geoenvironmental Models. Environmental Aspects of Mine Wastes

Selley, D. (1997) Structure and Sedimentology of the Dundas Group, Western Tasmania. University of Tasmania, Hobart thesis: 188

SEMF (1998a) Final reviews report on the environmental improvement program. Pasminco Rosebery mine. EPI Final reviews report, June 1996. Hercules mine site, Williamsford. SEMF Holdings Pty Ltd.

SEMF (1998b) The rehabilitation of abandoned tin mines in north eastern Tasmania. SEMF Holdings Pty Ltd.

Sen, Z. (1996) Theoretical RQD-porosity-conductivity-aperture charts. International Journal of Rock Mechanics and Mining Sciences & Geomechanics Abstracts 33 (2):173-177

Shapiro, A. and J. Anderson (1989) Simulation of steady-state flow in three dimensional fracture networks using the boundary element method. Advances in Water Resources 8 (3):110

Shaw, S. and C. Mills (1998) Petrology and Mineralogy in ARD Prediction.

Sherlock, E., R. Lawrence and R. Poulin (1995) On the neutralization of acid rock drainage by carbonate and silicate minerals. Environmental Geology 25 43-54

Sherwood, J. (1993) A lumped parameter model of the groundwater rebound associated with the imminent closure of mines in the Durham Coalfield. Univ. of Newcastle, Newcastle MSc thesis: 73

Sherwood, J. and P. L. Younger (1994) Modelling groundwater rebound after coalfield closure: an example from County Durham, UK. 5th International Mine Water Congress 769-777

Sherwood, J. and P. L. Younger (1997) Modelling groundwater rebound after coalfield closure. Groundwater in the urban environment. Volume 1: Problems, processes and management, Proc. XXVIIth Congress of the International Association of Hydrogeologists 165-170

Shevenell, L. A. (2000) Water quality in pit lakes in disseminated compared to two natural, terminal lakes in Nevada. Environmental Geology 39 (7):807-815

Sidea, D. (2008) Comments on the extent of stress distributions around workings in hard rock mining. pers. comm.

Simmons, C. and P. Meyer (2000) A simplified model for the transient water budget of a shallow unsaturated zone. Water Resources Research 32 2835–2844

Singer, P. C. and W. Stumm (1970) Acid Mine Drainage: The Rate-Determining Step. Science 167 1121-1123

Singhal, B. B. S. and R. P. Gupta (1999) Applied hydrogeology of fractured rocks. Kluwer Academic Publishers Dordrecht:

SKM (2001) Sinclair Knight Merz Pty Ltd, Environmental Water Requirements of Groundwater Dependent Ecosystems, Sinclair Knight Merz Pty Ltd, Technical Report Number 2, Environment Australia, November 2001, Australian Government, Department of the Environment and Water Resources ISBN 0 642547696 http://www.environment.gov.au/water/rivers/nrhp/groundwater/chapter2.html#mining Cited 12 Feb 2007.

Skousen, J., J. Demchak and L. McDonald (2003) Discharge Chemistry From Above-Drainage Underground Mines in 1968 and 2000. 6th ICARD International Conference on Acid Mine Drainage

Smart, R. and S. Miller (2005) Developments in ARD Prediction. Fifth Australian Workshop on Acid Drainage Fremantle, Western Australia 22

Smith, R. N. (1975) Precious and volatile metal distributions in the ores and host rocks of the Rosebery sulfide deposit. University of Melbourne, Melbourne thesis: 171

Smith, R. N. and D. L. Huston (1992) Distribution and association of selected trace elements at the Rosebery Deposit, Tasmania. A special issue devoted to Australian volcanic-hosted massive sulfide (VHMS) deposits and their volcanic environment. 87; 3 706-719

Smith, S. (1998) Acid mine drainage in the Bakers Creek Dump, Hercules, Western Tasmania. University of Tasmania, Honours thesis: 95

Smith, S. R. and A. A. Sobek (1978) Physical and chemical properties of overburdens, spoils, wastes and new soils. Reclamation of Drastically Disturbed Lands 192-208

Sobek, A. A., W. A. Schuller, F. J.R. and R. M. Smith (1978) Field and laboratory methods applicable to overburden and mine soils. EPA 600/2-78-054.

Solomon, M. (1981) An introduction to the geology and metallic mineral resources of Tasmania. Economic Geology 76 (2):194-208

Solomon, M. and D. I. Groves (1994) Volcanic-Hosted Massive Sulphide Deposits of the Tasman Fold Belt System. The Geology and Origin of Australia's Mineral Deposits 580-647

Solomon, M. and J. Walsh (1979) The formation of massive sulphide deposits on the sea floor. Economic Geology 74 797-813

Solomon, M., J. L. Walshe and C. A. Heinrich (1990) The formation of Rosebery-type, volcanogenic massive sulphide deposits. Geological Society of Australia, Abstracts 25 6

SS&B (1993) Smith Sale & Burbury, Residue Dams No. 1, 2 and 5 Monitoring of Underground Seepage. pers. comm.

Stace, H., G. Hubble, R. Brewer, G. D. Hubble, K. H. Northcote, J. Sleeman, M. Mulcahy and E. Hallsworth (1968) A Handbook of Australian Soils. 435

Stahl, W., H. Aust and A. Dounas (1974) Origin of artesian and thermal waters determined by oxygen, hydrogen, and carbon isotope analyses of water samples from the Sperkhios Valley, Greece. Symposium on isotope techniques in groundwater hydrology; 11 Mar 1974; Isotope techniques in groundwater hydrology.

Stallman, R. W. (1971) Aquifer test design observation and data analysis Chapter B1. Techniques of Water-Resources Investigations of the United States Geological Survey, Applications of Hydraulics

Stapinsky, M., A. Desbarats, D. Boyle and M. Robin (1997) Response to rainfall of groundwater discharge from underground mine workings at Myra Falls mining camp, Vancouver Island, B.C. Fourth International Conference on Acid Mine Drainage 1779-1795

Staude, L. (2002a) Historical discharge into the Stitt River. pers. comm.

Staude, L. (2002b) Extent of mine influence. pers. comm.

Stephenson EMF Consultants (1997) Preliminary Review Acid Drainage Control And Treatment. Pasminco Rosebery, Tasmania: 9

Stevenson, P. C. (1982) A review of groundwater in fractured rock. Groundwater in fractured rock 199-215

Stewart, W., S. Miller, J. Thomas and R. Smart (2003) Evalutaion of the Effects of Organic Matter on the Net Acid Generation (NAG) Test. 6th ICARD

Stillwell, F. L. (1934) Observations on the zinc-lead lode at Rosebery, Tasmania. Australasian Inst. Min. and Met., Pr. n. s. 94 43-67

Struthers, S. (1996) Tailings Management Project, Characterisation Report, Pasminco Mining, Rosebery Tasmania. RMIT University Melbourne: 21

Stumm, W. and J. Morgan (1970) Aquatic chemistry, an introduction emphasizing chemical equilibrium in natural waters. J. Wiley New York:

Surrette, M., D. M. Allen and M. Journeay (2008) Regional evaluation of hydraulic properties in variably fractured rock using a hydrostructural domain approach. Hydrogeology Journal 16 (1):11-30

SWAT (2004) Baseflow Filter Program, bflow.exe www.brc.tamus.edu/swat/soft_baseflow.html.

Tam, V. T., F. De Smedt, O. Batelaan1 and A. Dassargues (2004) Study on the relationship between lineaments and borehole specific capacity in a fractured and karstified limestone area in Vietnam. Hydrogeology Journal 12 (6)

Tasmap (1986a) Rosebery 3637 Tasmania 1:25000 Series.

Tasmap (1986b) Tullah 3837 Tasmania 1:25000 Series.

Tasmap (1986c) Selina 3836 Tasmania 1:25000 Series.

Tasmap (1986d) Dundas 3636 Tasmania 1:25000 Series.

Taylor, K. (1998) Acid drainage abatement from an abandoned smelter site, Zeehan. University of Tasmania, Hobart Honours thesis:

Theophrastus (ca. 315 BC) Pyrite, acids and salts.

Thompson, A. (2001) A hydrogeological and hydrochemical investigation of acid mine drainage in the South Centre Pit and B-Dump areas of the Savage River Mine. University of Tasmania, B.Sc. (Hons) thesis:

Thompson and Brett (1998) Storage of Acid Generating Mine Waste. Pasminco Rosebery Mine,Thompson and Brett PTY LTD Consulting Engineers Hobart: 16

Tolman (1937) Ground Water. Mc-Graw Hill Book Company Inc. New York:

Toran, L. and K. R. Brdabury (1988) Ground-Water Flow Model of Drawdown and Recovery Near an Underground Mine. Ground Water 26 (6):724-733

Trescott, P. C., G. F. Pinder and S. P. Larson (1976) Finite-difference Model for Aquifer Simulation in Two Dimensions With Results of Numerical Experiments. U.S. Geological Survey, Techniques of Water-Resources Investigations, Book 7, Chapter C1

Trumm, D. (2007) Acid Mine Drainage in New Zealand. Reclamation Matters 3 (2):23-28

Tsang, Y., F. Tsang, F. Hale and B. Dverstorp (1996) Tracer transport in a stochastic continuum model of fractured media. Water Resources Research 32 (10):3077-3092

Turner, N. J. and R. S. Bottrill (2001) Blue amphibole, Arthur Metamorphic Complex, Tasmania: composition and regional tectonic setting. Australian Journal of Earth Sciences 48 167-181

Tweed, S. O., T. R. Weaver and I. Cartwright (2005) Distinguishing groundwater flow paths in different fractured-rock aquifers using groundwater chemistry: Dandenong Ranges, southeast Australia. Hydrogeology Journal 13 (5-6):771-778

Twelvetrees, W. (1901) Report of the Secretary of Mines for 1900-01 Parliment of Tasmania.

Tyler, P., and Bowling, L. (1990) The wax and wane of meromixis in estuarine lakes in Tasmania. Vehr. Int. Ver. Limnol. 24 (242-254):

USGS (2005) GWM--a ground-water management process for the U.S. Geological Survey Modular Ground-Water Model. USGS Open File 2005-1072.

Usher, B. H., A. Havenga, J. Hough, R. Grobbelaar and F. D. I. Hodgson (2003) The Challenges of Determining Intermine Flow in the Witbank Coalfield of South Africa. Water in Mining 349-354

Vallerine, B. (2000) The Precious Metal Distribution in K Lens, Rosebery Deposit, Tasmania. University of Tasmania, Hobart thesis:

Vartanyan, G. S. (1989) The impact of mining on environment, parts 1 and 2. Proceedings of an Workshop ,

Vatnaskil Consulting Engineers (1994) AQUA—Groundwater flow and contaminant transport model. AQUA user's manual. Reykjavý´k, Iceland:

Voss, C. I. and A. M. Provost. (2002) SUTRA, a model for saturated-unsaturated variable-density ground-water flow with solute or energy transport. Report 02-4231. Water-Resources Investigations USGS. Reston, Virginia:

Walker, J. A. (1998) The environmental effects of minewater discharge due to progressive abandonment of the North Derbyshire - North Nottinghamshire Coalfield. University of Sheffield, thesis:

Wallace, L. (2002) Aqueous Geochemistry of Constructed Wetlands treating Acid Mine Drainage, Rosebery, Tasmania. University of Tasmania, Hobart thesis: 155

Waller, G. (1902) Report on the Ore Deposits (other than Tin) of North Dundas: Report for the Secretary of Mines for 1902. 1-66

Wang, Q. J., F. L. N. McConachy, F. H. S. Chiew, R. James, G. C. d. Hoedt and W. J. Wright (2002) Climatic Atlas of Australia, Maps of Evapotranspiration. Bureau of Meteorology, Cooperative Research Centre for Catchment Hydrology, University of Melbourne, Cooperative Research Centre for Catchment Hydrology

Ward, L. R. I. (1909) The Mt. Farrell Mining Field. Report of the Secretary of Mines for Tasmania for 1908 1-120

Warren, J. E. and P.J. Root (1963) The Behavior of Naturally Fractured Reservoirs. Society of Petroleum Engineers Journal 245-255

Waterloo Hydrologic (2000) Visual Modflow Pro Version 3.0 Tutorial Guide. Melbourne Australia November 18-21: 82

Waterloo Hydrologic (2003) 3D Groundwater Flow and Transport Modelling, Course Notes. Melbourne Australia November 18-21:

Weiss, J. S. and A. C. Razem (1984) Simulation of ground-water flow in a mined watershed in eastern Ohio. Ground Water 22 (5):549-560

Wellman, T. (2006) Rethinking the Meaning of "REV" in Modeling Fractured Rock Aquifers. U.S. Geological Survey, Water Resources Discipline, Branch Of Regional Research,

White, M. J. and J. McPhie (1996) Stratigraphy and paleovolcanology of the Tyndall Group, Mount Read Volcanics, Western Tasmania. Australian Journal of Earth Sciences 43 147-159

White, W. W., K. A. Lapakko and R. L. Cox (1999) Static-test methods most commonly used to predict acid mine drainage: Practical guidelines for use and interpretation, in: The environmental geochemistry of mineral deposits. Part A: Processes, techniques, and health issues. Plumlee, G. S.; Logsdon, M. J. (ed.). Reviews in Economic Geology 6A 325-338

Widdowson, M. A., F. J. Molz and J. G. Melville (1990) An analysis technique for multilevel and partially penetrating slug test data. Ground Water 28 (6):937-945

Williams, K. L. (1960) Some less common minerals in the Rosebery and Hercules zinc-lead ores. Proceedings - Australasian Institute of Mining and Metallurgy 196 51-59

Williams, P. R. (1989) Areas north and south of Mt Bischoff. Geological Atlas 1:50 000 Series Sheet 36 (8015N), St Valentines 12-13

Willis, R., P. Edwards, A. McNeill and C. Carnie (2003) RQD Classification at Rosebery. pers. comm.

Willis, R. D. (1999) Bulk Density Determinations. pers. comm.

Wilson, J. L., L. R. Townley and A. Sa da Costa (1979) Mathematical Development and Verification of a Finite Element Aquifer Flow Model AQUIFEM-1, Technical Report No. 248. Ralph M. Parsons Laboratory for Water Resources and Hydrodynamics, M.I.T., 114

Winter, G. V., G. L. Bloomsburg and R. E. Williams (1984) Underground mine water inflow prediction. Abstracts from the 13th annual Rocky Mountain ground-water conference. 91 21-22

Wishart, D. N. (2000) Hydrogeology and Simulated Water Budget of the Rio Cobre and Rio Minho-Milk River Basins, Jamaica, West Indies. Department of Geological Sciences, Virginia Polytechnic Institute & State University Blacksburg, Virginia. Masters Thesis, 183

WMRL (1999) Environmental Management Plan (Hellyer Mine). 9th Annual and Third Three Year Consolidated Report to The Minister for Environment. Western Metal Resources Limited, Hellyer Operations.

WMRL (2000) Environmental Decommissioning and Rehabilitation Plan (Hellyer Mine). Western Metal Resources Limited

Wood, S. C., P. L. Younger and N. S. Robins (1999) Long-term changes in the quality of polluted minewater discharges from abandoned underground coal workings in Scotland. Quarterly Journal of Engineering Geology 32 69-79

Woodward-Clyde (1995) Ernest Henry Mine dewatering review. AGC Woodward-Clyde Pty Limited Perth:

Yeh, G. T. and D. S. Ward (1980) FEMWATER: A Finite Element Model of WATER Flow through Saturated-Unsaturated Porous Media. ORNL-5567. Oak Ridge National Laboratory Oak Ridge, TN.:

Younger, P. L. (1994) Minewater Madness. New Scientist 141 (1918):51

Younger, P. L. (1998) Environmental implications of the closure of Frazer's Grove fluorspar, County Durham, Report to the Environment Agency, Northumbria Area. Department of Civil Engineering, University of Newcastle

Younger, P. L. and M. Adams (1999) Predicting mine water rebound. Environment Agency R&D Technical Report Bristol, UK:

Youngs, J. and N. Milligan (2006) Pilbara Iron Marandoo Model Development 2006. MWH

Zhang, B. Y. and D. N. Lerner (2000) Modeling of ground water flow to adits. Ground Water 38 (1):99-105

Zinifex Limited (2004) www.zinifex.com.au Rosebery Home / Operations / Mines / Rosebery Mine / Geology.

Zinifex Limited (2005) www.zinifex.com.au Rosebery ASX - Zinifex Expands Exploration at Rosebery Mine.

Zinifex Limited (2006) www.zinifex.com.au Rosebery.

Zinifex Limited (2007) www.zinifex.com.au Rosebery Rosebery Mine Resource Grows by 65% ASX Release.

Zinn, B. A. and L. F. Konikow (2007) Effects of intraborehole flow on groundwater age distribution. Hydrogeology Journal 15 (4):633-644

Digital Appendices

Index of Files in Digital Appendices

Index of Files in Digital Appendices

Appendix 1 Field Data
- Drillhole survey.pdf
- pHCond Surv.pdf
- Reliable Driilholes.PDF

Slug Test Raw Data
- 114R.pdf
- 128R.pdf
- 210R Slug Test.pdf
- Feb03_P1.pdf
- Feb03_P7.pdf
- Feb03_P13.pdf
- Feb03_P14.pdf
- Feb03_P14_2.pdf
- Feb03_P15.pdf
- P1.pdf
- P7.pdf
- P13.pdf
- P14.pdf
- P15.pdf
- P15_2.pdf

Appendix 2 Geochemical Analayses
- 574361 report.pdf
- 593603 Cover.pdf
- 593603 Report.pdf
- Adelaide Laboratory CSIRO.pdf
- DIER.pdf
- Gurung, 2003.pdf
- GW Chemistry Survey.pdf
- Metals via ICPMS.pdf
- NAG and ACP.pdf
- nag test work job env00104.pdf
- NAG_Survey.pdf
- Pasmico Labs.pdf
- Sampling_dataset.pdf

Appendix 3 Geochemical Proceedures
- Aqueous Geochemistry Detection Limits.pdf
- Environmental Monitoring - Water, Air, Noise.pdf
- Groundwater monitoring proceedure.pdf
- Major Cations via ICPAES.pdf
- Sulphate via Photometer.pdf

Appendix 4 Computer Programs
- Appendix 4 Computer Programs.pdf

Appendix 5 Example Modelling and Calibration Diaries
- Calibration Diary.xls
- GMS Modelling Report.xls

Appendix 6 RQD Modelling Data
- comp01.dm
- compdh3d.dm
- Datamine Strat Stats.xls
- rqd0.dm
- rqd1.dm
- rqd12.dm
- RQD Modelling Diary.pdf

rqdmod1.dm
rqdmod2.dm
rqdmod3.dm
rqdmod4.dm
rqdmod5.dm
rqdmod6.dm
rqdmod7.dm
rqdmod8.dm
rqdmod9.dm
rqdmod10.dm
rqdmod11.dm
rqdmod12.dm
rqdmod13.dm
rqdmod14.dm
rqdmod15.dm
RQDMODEL STATS.pdf

Appendix 7 SWAT Analysis
SWAT.xls

Appendix 8 BOM and Hydtsra Data
BOM, 2002.csv
Hydrstra_2004.xls
Hydstra, 2004.xls

BOM, 2003
IainA.2913.3.csv
IainA.2913.ReadMe.txt
IainA.2913.Stations.csv
IainA.2913.1.csv
IainA.2913.2.csv

Appendix 9 Selected Piezometer Schematics
Bobadil Piezo1.jpg
Dam 2 Piezo13.jpg
Dam 2 Piezo14.bmp
Dam 2 Piezo15.jpg
Piezodesign bobadil.xls

Appendix 10 MIFIM Analysis
Appendix 10 Minevoids.xls
MIFIM_Rosebery.xls
Banks, 2001.pdf

Appendix 11 GMS Analysis
GMS Operation Calibration Plots
Computed vs Observed (weighted) cropped.bmp
Computed vs Observed (weighted).bmp
Computed vs Observed cropped.bmp
Computed vs Observed.bmp
Obs Computed vs Observed (weighted).bmp
Obs Computed vs Observed cropped.bmp
Obs Computed vs Observed.bmp
Obs Residual vs Observed (weighted).bmp
Obs Residual vs Observed.bmp
Obs Summary.bmp

GMS Model Output Files
Operation_Complete_Output.txt
Operation_Volumetric Budget.txt
Prediction_Complete_Output.txt

Prediction_Volumetric Budget.txt

GMS Model Files
Operation
GPCLAB01.asp
GPCLAB01.ba6
GPCLAB01.ccf
GPCLAB01.chd
GPCLAB01.chob
GPCLAB01.dis
GPCLAB01.drn
GPCLAB01.drob
GPCLAB01.gbob
GPCLAB01.ghb
GPCLAB01.glo
GPCLAB01.gpr
GPCLAB01.hed
GPCLAB01.hfb
GPCLAB01.hff
GPCLAB01.hob
GPCLAB01.ini
GPCLAB01.lmt
GPCLAB01.lpf
GPCLAB01.map
GPCLAB01.mfn
GPCLAB01.mfr
GPCLAB01.mfs
GPCLAB01.mlt
GPCLAB01.mst
GPCLAB01.obs
GPCLAB01.oc
GPCLAB01.out
GPCLAB01.param
GPCLAB01.pcg
GPCLAB01.ptk
GPCLAB01.rch
GPCLAB01.riv
GPCLAB01.rvob
GPCLAB01.tin
GPCLAB01.wel
GPCLAB01.xy
GPCLAB01.xyz
GPCLAB01.zon
GPCLAB01._b
GPCLAB01._nm
GPCLAB01._os
GPCLAB01._r
GPCLAB01._w
GPCLAB01._ws
GPCLAB01._ww
GPCLAB012s.dat
GPCLAB013g.dat
GPCLAB013s.dat
mf2kerr.p00
GPCLAB01.mat

Prediction
GPCLAB01.asp
GPCLAB01.avi
GPCLAB01.ba6
GPCLAB01.ccf

GPCLAB01.chd
GPCLAB01.chob
GPCLAB01.dis
GPCLAB01.drn
GPCLAB01.drob
GPCLAB01.gbob
GPCLAB01.ghb
GPCLAB01.glo
GPCLAB01.gpr
GPCLAB01.hed
GPCLAB01.hfb
GPCLAB01.hff
GPCLAB01.hob
GPCLAB01.ini
GPCLAB01.lmt
GPCLAB01.lpf
GPCLAB01.map
GPCLAB01.mfn
GPCLAB01.mfr
GPCLAB01.mfs
GPCLAB01.mlt
GPCLAB01.mst
GPCLAB01.obs
GPCLAB01.oc
GPCLAB01.out
GPCLAB01.param
GPCLAB01.pcg
GPCLAB01.ptk
GPCLAB01.rch
GPCLAB01.riv
GPCLAB01.rvob
GPCLAB01.tin
GPCLAB01.wel
GPCLAB01.xy
GPCLAB01.xyz
GPCLAB01.zon
GPCLAB01._b
GPCLAB01._nm
GPCLAB01._os
GPCLAB01._r
GPCLAB01._w
GPCLAB01._ws
GPCLAB01._ww
GPCLAB012s.dat
GPCLAB013g.dat
GPCLAB013s.dat
GPCLAB01.mat
fort.51

GMS40

adinit.dat
CHECK32.DLL
gms.ico
gms40.chm
GMS40.exe
gms40.ini
gmsquery.ini
mcmod.dll
netenble.001
NSLMS32.DLL
NSLMS324.DLL

pavia.exe
PEGRP32B.DLL
Readme.txt
Uninst.isu
gmsmats.mat
tutfiles

Appendix 12 GMS Model Views
4 MODPATH Prediction
Modpath Mine Ortho 1 day.bmp
Modpath Mine Ortho 1 months 30 days.bmp
Modpath Mine Ortho 1 years.bmp
Modpath Mine Ortho 100 years a.bmp
Modpath Mine Ortho 100 years.bmp

Modpath Mine Ortho 10000 years.bmp
Modpath Mine Ortho 6 months.bmp
Modpath Mine Ortho To End 2.bmp
Modpath Mine Ortho To End.bmp

3 Prediction
All Layers Above Orth.bmp
All Layers Above Orth2.bmp
All Layers Above Orth3.bmp
All Layers Above.bmp
i 10.bmp
i 100.bmp
i 105.bmp
J 80.bmp
J 85.bmp
Layer 01.bmp
Layer 02.bmp
Layer 03.bmp
Layer 04.bmp
Layer 05.bmp
Layer 10.bmp
Layer 15.bmp
Layer 20.bmp
Layer 21.bmp
Layer 22.bmp
Layer 23.bmp
Layer 24.bmp
Layer 25.bmp
Layer 30.bmp
Layer 35.bmp
Layer 40.bmp
Layer 45.bmp
Layer 50.bmp
Layer 54.bmp
Mine Layer 20.bmp
Mine Layer 21.bmp
Mine Layer 22.bmp
Mine Layer 23.bmp
Mine Layer 24.bmp
Mine Layer 25.bmp
Mine Layer 30.bmp
Mine Layer 35.bmp
Mine Layer 40.bmp
Mine Layer 45.bmp
Mine Layer 50.bmp
Mine Layer 54.bmp

i 110.bmp
i 115.bmp
i 120.bmp
i 125.bmp
i 130.bmp
i 135.bmp
i 140.bmp
i 145.bmp
i 150.bmp
i 155.bmp
i 160.bmp
i 165.bmp
i 170.bmp
i 175.bmp
i 180.bmp
i 185.bmp
i 190.bmp
i 20.bmp
i 30.bmp
i 40.bmp
i 50.bmp
i 60.bmp
i 70.bmp
i 75.bmp
i 80.bmp
i 85.bmp
i 90.bmp
i 95.bmp
J 15.bmp
J 30.bmp
J 45.bmp
J 47.bmp
J 50.bmp
J 51.bmp
J 52.bmp
J 53.bmp
J 54.bmp
J 55.bmp
J 56.bmp
J 57.bmp
J 58.bmp
J 59.bmp
J 60.bmp
J 65.bmp
J 70.bmp
J 75.bmp

2 Operation
All Layers Ortho Materials.bmp
All Layers Ortho.bmp
Layer 35.bmp
Layer 4.bmp
Layer 40.bmp
Layer 1.bmp
Layer 10.bmp
Layer 15.bmp
Layer 2.bmp
Layer 20.bmp
Layer 21.bmp
Layer 22.bmp
Layer 23.bmp

Layer 24.bmp
Layer 25.bmp
Layer 3.bmp
Layer 30.bmp
Layer 45.bmp
Layer 5.bmp
Layer 50.bmp
Layer 54.bmp
Mine Layer 20.bmp
Mine Layer 21.bmp
Mine Layer 22.bmp
Mine Layer 23.bmp
Mine Layer 24.bmp
Mine Layer 25.bmp
Mine Layer 30.bmp
Mine Layer 35.bmp
Mine Layer 40.bmp
Mine Layer 45.bmp
Mine Layer 50.bmp
Mine Layer 54.bmp

1 Model Geometry
Field Observations.bmp
GIS Inputs.bmp
Layer 1 Regolith.bmp
Layer 10 Bedrock, Mine, Drilling and Thinned Regolith.bmp
Layer 11 Bedrock, Mine, Drilling and Thinned Regolith.bmp
Layer 12 Bedrock, Mine, Drilling and Thinned Regolith.bmp
Layer 13 Bedrock, Mine, Drilling and Thinned Regolith.bmp
Layer 14 Bedrock, Mine, Drilling and Thinned Regolith.bmp
Layer 15 Bedrock, Mine, Drilling and Thinned Regolith.bmp
Layer 16 Bedrock, Mine, Drilling and Thinned Regolith.bmp
Layer 17 Bedrock, Mine, Drilling and Thinned Regolith.bmp
Layer 18 Bedrock, Mine, Drilling and Thinned Regolith.bmp
Layer 19 Bedrock, Mine, Drilling and Thinned Regolith.bmp
Layer 2 Weathered Material.bmp
Layer 20 Bedrock, Mine, Drilling and Thinned Regolith.bmp
Layer 21 Bedrock, Mine, Drilling and Thinned Regolith.bmp
Layer 22 Bedrock, Mine, Drilling and Thinned Regolith.bmp
Layer 23 Bedrock, Mine, Drilling and Thinned Regolith.bmp
Layer 24 Bedrock, Mine, Drilling and Thinned Regolith.bmp
Layer 25 Deep Bedrock, Mine and Drilling.bmp
Layer 26 Deep Bedrock, Mine and Drilling.bmp
Layer 27 Deep Bedrock, Mine and Drilling.bmp
Layer 28 Deep Bedrock, Mine and Drilling.bmp
Layer 29 Deep Bedrock, Mine and Drilling.bmp
Layer 3 Bedrock, Mine, Drilling and Thinned Regolith.bmp
Layer 30 Deep 2 Bedrock, Mine and Drilling.bmp
Layer 31 Deep 2 Bedrock, Mine and Drilling.bmp
Layer 32 Deep 2 Bedrock, Mine and Drilling.bmp
Layer 33 Deep 2 Bedrock, Mine and Drilling.bmp
Layer 34 Deep 2 Bedrock, Mine and Drilling.bmp
Layer 35 Deep 3 Bedrock, Mine and Drilling.bmp
Layer 36 Deep 3 Bedrock, Mine and Drilling.bmp
Layer 37 Deep 3 Bedrock, Mine and Drilling.bmp
Layer 38 Deep 3 Bedrock, Mine and Drilling.bmp
Layer 39 Deep 3 Bedrock, Mine and Drilling.bmp
Layer 4 Bedrock, Mine, Drilling and Thinned Regolith.bmp
Layer 40 Deep 4 Bedrock, Mine and Drilling.bmp

Layer 41 Deep 4 Bedrock, Mine and Drilling.bmp

Layer 42 Deep 4 Bedrock, Mine and Drilling.bmp
Layer 43 Deep 4 Bedrock, Mine and Drilling.bmp
Layer 44 Deep 4 Bedrock, Mine and Drilling.bmp
Layer 45 Deep 5 Bedrock, Mine and Drilling.bmp
Layer 46 Deep 5 Bedrock and Drilling.bmp
Layer 47 Deep 5 Bedrock and Drilling.bmp
Layer 48 Deep 5 Bedrock and Drilling.bmp
Layer 49 Deep 5 Bedrock and Drilling.bmp
Layer 5 Bedrock, Mine, Drilling and Thinned Regolith.bmp
Layer 50 Deep 6 Bedrock and Drilling.bmp
Layer 51 Deep 6 Bedrock and Drilling.bmp
Layer 52 Deep 6 Bedrock and Drilling.bmp
Layer 53 Deep 6 Bedrock and Drilling.bmp
Layer 54 Deep 6 Bedrock and Drilling.bmp
Layer 6 Bedrock, Mine, Drilling and Thinned Regolith.bmp
Layer 7 Bedrock, Mine, Drilling and Thinned Regolith.bmp
Layer 8 Bedrock, Mine, Drilling and Thinned Regolith.bmp
Layer 9 Bedrock, Mine, Drilling and Thinned Regolith.bmp
Observations Coverage.bmp

Explanatary Views
Layer 20.bmp
Layer 25.bmp
Layer 3.bmp
Layer 1.bmp
Layer 2.bmp
Layer 3 Explained.bmp
Layer 3 Explained2.bmp
Layer 30.bmp
Layer 35.bmp
Layer 40.bmp
Layer 45.bmp
Layer 50.bmp
Layer 54.bmp
Long 100.bmp
Long 25.bmp
Long 50.bmp
Long 75.bmp
Long 85.bmp
Long 95.bmp
Xsect 100.bmp
Xsect 110.bmp
Xsect 120.bmp
Xsect 125.bmp
Xsect 150.bmp
Xsect 175.bmp
Xsect 25.bmp
Xsect 50.bmp
Xsect 75.bmp
Xsect 90.bmp
Long 65.bmp

Orthogonal Views
All Layers Ortho Drilling Above yx.bmp
All Layers Ortho Drilling zx.bmp
All Layers Ortho Drilling zy.bmp
All Layers Ortho Drilling.bmp
All Layers Ortho Materials 1.bmp
All Layers Ortho Materials 2.bmp
All Layers Ortho Materials 3.bmp
All L ayers Ortho Materials.bmp

Appendix 13 Tasmania Mineral Deposits Database
MIRLOCH_MRT2002a.pdf

Appendix 14 Model Review Document
Middlemis, 2000 Model Review.pdf

Appendix 15 Site Visit Notes
Rosebery 9 Sept Visit Plan.pdf
Rosebery 14 Oct Site Visit Plan.pdf
28 Jan 03 Site Visit Plan.pdf
Enviro Geology Trip Rosebery Summary.pdf
April 03 Site Visit.pdf
Drilling Trip.pdf
Field Trip 7.pdf
Geochem Trip 8.pdf
Initial Site Inspection Trip 1.pdf
Jan04.pdf
Sept Field Trip Plan.pdf
Oct Site Visit.pdf
Progress Field Trip.pdf
Sep03 Site Visit.pdf
Sept Visit.pdf
Site Reconnaissance.pdf

Appendix 16 Publications
AUSIMM Water in Mining, Brisbane, 2003
Evans et al 2003.pdf
Evans et al 2003a.pdf

Water-Rock Interaction, New York, 2004
Evans et al 2004.pdf
Evans et al 2004a.pdf
Evans et al 2004b.pdf

Australian Geological Conference, Hobart, 2004
Evans et al, 2004a.pdf